# Investigation of Adsorptive Removal of Chromium (VI) from Aquatic System Using Dust Black Tea Leaves

**Ph. D Thesis**

*Submitted by*

**Md. Abdul Hannan**

Registration No.: 86
Session: 2014-2015

Physical Chemistry Research Laboratory
Department of Chemistry
University of Dhaka
Bangladesh

January 02, 2019

# Investigation of Adsorptive Removal of Chromium (VI) from Aquatic System Using Dust Black Tea Leaves

Ph. D Thesis


*Submitted by*

**Md. Abdul Hannan**

Registration No.: 86
Session: 2014-2015
January 02, 2019

*Supervisor*

**Dr. Mohammad Abul Hossain**
Professor
Department of Chemistry
University of Dhaka
Bangladesh

*Co-supervisors*

**Dr. Tajmeri S. A. Islam**
Professor (Retd.)
Department of Chemistry
University of Dhaka
Bangladesh

**Dr. Abu Jafor Mahmood**
Professor (Retd.)
Department of Chemistry
University of Dhaka
Bangladesh

# Declaration

The work described in this thesis was conducted to the Physical Chemistry Research Laboratory of the Department of Chemistry, University of Dhaka, Dhaka-1000, Bangladesh. Unless otherwise stated it is the work of the author and has not been submitted to any other University or Institute for any degree or diploma or any other award.

**Md. Abdul Hannan**
(Author)
Registration No.: 86
Session: 2014-2015
Date: January 02, 2019

# Acknowledgment

First of all, I would like to express my profound sense of gratitude to almighty Allah (SWT) for His kind bless that enabled me to complete this research work at the advanced level of education.

I am grateful to my reverent supervisor Professor Mohammad Abul Hossain, Ph. D (Env. Sci. & Chem. Technol., Kanazawa University, Japan), MS (Chem. Engr., Kanazawa University, Japan), M. Sc. (Phy. Chem., Dhaka University, Bangladesh), Professor, Department of Chemistry, University of Dhaka; Co-supervisors Professor Abu Jafar Mahmood, Ph. D (University of Cambridge, UK.), M. Sc. (Phy. Chem., Dhaka University, Bangladesh), Professor (Retd.), University of Dhaka, and Professor Tajmeri S. A. Islam, Ph. D, (University of Aberdeen, Scotland, UK, Postdoctoral Fellow , University of Southern California, Los Angeles, USA), M. Sc. (Phy. Chem., Dhaka University, Bangladesh), Professor (Retd.), University of Dhaka for their academic guidance with their depth of knowledge in every stage of this study.

It is my pleasure to thank Professor Qamrul Ehsan, D. Sc. (Japan), Department of Chemistry, University of Dhaka; Professor Omar Ahmed, Ph.D (Japan), Department of Chemistry, University of Dhaka and Professor Md. Mufazzal Hossain, Ph. D (Japan), Professor, Department of Chemistry, University of Dhaka for their continuous suggestion and inspiration during my research work.

I am especially grateful to Mr. Azam J. Chowdhury, Chairman, East Coast Group, Mr. Mezbahuddin, Senior Secretary, Mr. Ratan Chandra Pandit, Additional Secretary, Mr. Ehsan-E-Elahi, Additional Secretary, Mr. A. T. M. Mostafa Kamal, Joint Secretary to Government of Bangladesh and Mr. Ali Asgor, Commissioner of Taxes, Government of Bangladesh for their encouragement and appreciation to pursue this course of study.

I am delighted to thank Mr. Samsul Alam, Chief Inspector of Explosives in Bangladesh, Department of Explosives, Energy and Mineral Resources Division, Government of Bangladesh for his liberal cooperation in favour of completing this study.

Few words of acknowledge will never be sufficient anyway to express my thoughtful-sense of gratitude to my wife Ms. Shamima Aziz, B.Sc. (Hon's, First Class), M.Sc. (First Class), University of Dhaka, Faculty Member of Sunnydale, affectionate sons ***Sadat Ayman Hannan***, a junior Sunnydalian and ***Sahib Ayman Hannan***, BBA, Batch 27, IBA, University of Dhaka co-operated me as per their capacity and showed patience during my long-time involvement in this research activities.

**Md. Abdul Hannan**

Fazlul Huq Muslim Hall
University of Dhaka, Bangladesh

02 January, 2019

**CONTENTS**

# ABSTRACT

Some heavy metals are highly toxic as ions or in form of compounds. Ions or compounds of heavy metals, which are soluble in water, can be readily absorbed into living organisms. Chromium (VI) is a harmful heavy metal ion which is indiscriminately discharged to aquatic-body through the effluents of process-plants of leather tanning, metallurgy, electroplating, textile dyeing, paints, ink, etc. and thus aquatic environment is being severely polluted. These industrial effluents contain chromium (VI), which is much higher than the tolerance limit; 0.5 $mg \cdot L^{-1}$ in industrial wastewater (EPA). So, the removal of Cr(VI) from wastewater is prerequisite prior to discharge of the toxic ion into aquatic environment. The present study was undertaken to investigate the efficiency of Dust Black Tea leaves (DBTL), a waste of tea process plant, as an adsorbent to remove chromium (VI) from aqueous solution. Dust black tea leaves (DBTL) was collected and washed repeatedly with hot water until the color materials of the leaves were entirely eliminated. Small surface area, heterogeneous surface morphology and some functional groups were observed in dried DBTL using BET surface analyzer, SEM-EDX and ATR-IR.Chromium (VI) in aqueous solution was analyzed colorimetrically by forming a violet complex of Cr(VI) with 1,5-Diphenylcarbazide using UV-visible Spectrophotometric method.

In this process, Cr (VI), due to its contact with DBTL, was reduced to Cr(III) along with adsorption of Cr(VI) on DBTL. Concentration of Cr(VI) and Cr(III) in solution were quantitatively determined by the colorimetric method. Both adsorption and reduction were found to be dependent on pH of chromium (VI) solution. Since the minimum reduction of Cr(VI) to Cr(III) and insignificant quantity of adsorption of Cr(III) on DBTL were found at pH 2.0 of the solution, the pH 2.0 was considered as an optimum condition to obtain the maximum removal capacity of DBTL. In each experiment, reduced amount of Cr (VI) to Cr(III) was deducted from the total removal to receive the amount adsorbed only.

Batch adsorption kinetic experiments were conducted to investigate the effects of initial concentration of Cr(VI), pH of Cr(VI) solution, process temperature and particle-size of DBTL. Related-experimental data were verified by applying to different models of kinetic equations, such as, simple first order rate equation, second order rate equation , pseudo first order rate equation, pseudo second order rate equation and Elovich equation. The highest value of regression co-efficient, $R^2$ (0.999) supported that pseudo second kinetic equation is best-fitted for different initial concentrations, solution pH, temperatures and particle-size of DBTL. The equilibrium amount of Cr(VI) adsorbed ($q_e$), equilibrium concentration ($C_e$) of Cr (VI) solution and the pseudo-second order rate constant, $k_{2p}$ were calculated from the best-fitted pseudo-second order kinetic plots for different initial concentrations at pH 2.0. The maximum adsorption capacity, $q_m$ = 303.03 $mg \cdot g^{-1}$, was calculated from the above kinetic data ($q_e$ and $C_e$), using best fitted Langmuir equation. For a fixed concentration of Cr(VI), the equilibrium amount adsorbed ($q_e$), equilibrium concentration ($C_e$) and rate constant ($k_{2p}$) were calculated from the best-fitted pseudo-second order kinetic plots for different (i) temperatures at pH 2.0, (ii) pH at 30 $^{o}$C and (iii) sizes of DBTL at pH 2.0 and 30 $^{o}$C.

The effect of temperature on adsorption kinetics showed that the equilibrium amount of Cr(VI) adsorbed decreased with increase of temperature. This behavior indicated

exothermic nature of the adsorption at pH 2.0. Using the pseudo-second order rate constant, the activation energy $E_a$. of adsorption was determined from Arrhenius plot and the value was found to be 7.37 kJ·mol$^{-1}$ which is very small compared to that ($E_a$ = 65 - 250 kJ·mol$^{-1}$) of chemical adsorption.

Thermodynamic parameters: $\Delta G^o$, $\Delta H^o$ and $\Delta S^o$ for Cr(VI) adsorption on DBTL were determined from the equilibrium adsorption constant ($K_c$). The negative value (-27.38 kJ·mol$^{-1}$) of $\Delta H^o$ indicated the adsorption of chromium (VI) on DBTL was exothermic, spontaneous and physical in nature. The positive values from + 2.03 to + 5.60 kJ·mol$^{-1}$ of $\Delta G^o$ increased with increase of temperatures from 15 to 50 $^o$C which indicated the process was slow and less feasible due to the enhancement of the reduction of Cr(VI) at high temperature. The negative value of $\Delta S^o$ (-0.102 kJ·mol$^{-1}$·K$^{-1}$) predicted the decreased randomness through the adsorption of chromium (VI) on DBTL.

The effect of pH of solution showed that the equilibrium amount of Cr (VI) adsorbed linearly decreased with increase of pH from 2.0 to 6.0 and then became slow to the pH 8.0 indicating electrostatic interaction between anionic Cr(VI) and positively charged protonated-DBTL-surface at low pH. The effect of particle-size shown that the equilibrium amount of chromium (VI) adsorbed on DBTL decreased with increase of particle-sizes of DBTL due to the lowering of surface area. The rate of adsorption decreased with increase of particle-size of DBTL from 106 to 450 µm. The higher rate of Cr(VI) uptake by smaller size of particle is due to the greater accessibility to pores and greater surface area per unit mass of small sizes of DBTL.

The transfer mechanism of the adsorption of Cr (VI) on DBTL was investigated using Weber and Morris's intraparticle diffusion model equation towards the kinetic data for different concentrations, temperatures, pH and sizes of DBTL.The effects of concentration and temperature have shown that the film diffusion is dominative for the adsorption of chromium (VI) on DBTL at pH 2.0 for all concentrations. Again, the effects of solution pH and particle-size revealed that the intraparticle diffusion is favorable at high pH of the solution and large size of DBTL-particle, but at low pH and small particle-size, the adsorption is dominated by film diffusion.

Equilibrium adsorption isotherms at different temperatures were constructed using 6 hours as predetermined equilibrium time at pH 2.0. Different equations for adsorption isotherm, such as Langmuir, Freundlich, Temkin and Dubinin-Radushkevich **(**D-R) equations were applied to the equilibrium adsorption data obtained experimentally to evaluate the feasibility of the process. The results indicated that the Langmuir equation fits the data better than any other of the above isotherm equations. The maximum monolayer adsorption capacity, $q_m$ was calculated and found to be 303.03 mg·g$^{-1}$ at 30 $^o$C which decreased with increase of temperature. The Langmuir constant, *b* was used to determine the separation factor, $R_b$ and thermodynamic parameters to understand the mechanism of the process. At low concentration and low temperature, values of $R_b$ were found to be near to 1. These results indicated that the adsorption was favorable at this condition. The negative value of $\Delta G^o$ (-19.79 kJ·mol$^{-1}$) indicated the uptake of chromium (VI) on DBTL was spontaneous and the positive value of $\Delta H^o$ (15.3 kJ·mol$^{-1}$) which is too insufficient to that required for occurring chemical adsorption and the value of $\Delta S^o$ (+ 0.11 kJ·mol$^{-1}$·K$^{-1}$) might be due to small amount of reduction of chromium (VI) to chromium (III), during the adsorption of chromium (VI) on DBTL.

The mean adsorption energy, *E* at different temperatures were also calculated from the Dubinin-Radushkevich isotherm and the values were limited within the range of – 8.8 to -12.7 $kJ \cdot mol^{-1}$ which indicated that the adsorption of Cr(VI) on DBTL might be controlled by physical in nature.

The effects of pH and particle-size of DBTL on the adsorption isotherm were also investigated by applying different isotherms model equations. The maximum monolayer adsorption capacity was calculated using well fitted Langmuir isotherm equation. The results showed that the values were decreased with increase of both of solution pH and particle-size, like the same as the results obtained from kinetic study.

A comparison of the Attenuated Total Reflectance Infra-red (ATR-IR) spectra of un-adsorbed and Cr(VI) adsorbed DBTL shown that -OH, C=C, C-O and aromatic =C-H groups of DBTL were interacted (by shifted their positions) with Cr and a new peak appeared at 717.52 $cm^{-1}$ for –C-Cr interaction.

Scanning Electron Microscopic (SEM) microgram of Cr(VI) adsorbed DBTL shown some spherical chromium particles on the surface which were confirmed by Energy Dispersive X-ray (EDX) spectrum. Again, the deposition of chromium on DBTL surface are not homogeneously distributed which was determined by EDX point analysis of Cr(VI) adsorbed DBTL surface.

By treating with 2M sodium hydroxide solution, adsorbed chromium (VI) was fully recovered from the Cr(VI)-adsorbed-DBTL surface in order to eliminate the creation of secondary pollutant.

# List of Publication

1. **Md. Abdul Hannan**, Mohammad Abul Hossain*, Tajmeri S. A. Islam and Abu Jafor Mahmood; Kinetic Study of the Adsorption of Cr(VI) from Aqueous Solution on Dust Black Tea Leaves (Under Publication)
2. **Md. Abdul Hannan**, Mohammad Abul Hossain*, Tajmeri S. A. Islam and Abu Jafor Mahmood; Equilibrium Adsorption of Cr(VI) on Dust Black Tea Leaves from Aqueous Solution (Under Publication)
3. **Md. Abdul Hannan**, Mohammad Abul Hossain*, Tajmeri S. A. Islam and Abu Jafor Mahmood, ATR-IR and SEM/EDX Characterization of Cr(VI) Adsorbed Dust Black Tea Leaves (Under Publication)

# List of Figures

# List of Tables

# *Chapter 1*

# INTRODUCTION

# 1. INTRODUCTION

## 1.1 Background

### 1.1.1 Environment and Environmental Chemistry

Environment means the sum total of all surroundings of a living creature, including natural forces and other living things, which provide conditions for development and growth as well as of danger and damage. Environmental Chemistry is an interdisciplinary science involving atmospheric chemistry, aquatic chemistry, soil chemistry, physics, public health, sanitary engineering, etc. It refers to study of the chemical and biochemical phenomena that occur in nature. It can be defined as the study of the sources, reactions, transport, effects, and fates of chemical species in the environments of air, soil and water. Environmental chemistry deals with chemical processes occurring in the environment affected by human and biological activities.

Thus, environmental chemistry deals with sources, reactions, transport, effect and fate of chemical species in the air, water and soil and the effect of human and biological activities on these and finally application of various processes to make the environment free from pollution. So, environmental chemistry is an important subject that provides knowledge for the protection and conservation of environment. This subject is also important to anthropogenic activities leading to indiscriminate release of pollutants into the environment.

Environment consists of three major components are - Living components, e.g. flora and fauna, Non-living components and Energy components. e. g. solar energy, hydro-electric energy, wind energy etc. The non-living components, also called physical components, are sub-divided into three categories:

- Lithosphere or solid earth
- Aquatic environment or hydrosphere
- Atmosphere

## 1.1.2 Impact of Chemistry on Environment

Chemistry plays important role in understanding environment and preserving its quality. The present decade is at the height of science and technology. Although different modern inventions make our daily life easier and safer, it also causes threats on our environment gradually. It is proved that industrialization, galloping demand for energy and reckless explosion of nature resources during the last $21^{st}$ century are mainly responsible for environmental pollution. Wastes from chemical industries are being discarded by the cheapest and most convenient routes which are usually meant up the stack down the drain or onto the ground. These practices result in killing fishes, polluting river water, declining bird population and deforming the shape of animal. Increasingly, chemists have become familiar with chemical processes occurring in the environment and have developed means of directing chemical science toward environment improvement.

## 1.1.3 Pollutants

Pollutants are substances which add to the environment in amount which is sufficient to cause harmful effects on the environment to cause threat to the lives of human, other animals, vegetation etc. These pollutants pollute the air, water and soil. These are classified into (a) Inorganic pollutants and (b) Organic pollutants. Based on the medium where pollution occurs frequently, environmental pollution can be classified as follows:

i) Water pollution: It occurs in aquatic medium.

ii) Air pollution: It occurs in atmosphere.

iii) Soil pollution: It occurs in Lithosphere.

### 1.1.4 Pollution in Aquatic Environment

It is proverb that "another name of water is life". Life cannot be imagined without water. Unfortunately, the quality of these natural resources is deteriorating at an alarming pace due to ever increasing population, industrialization and many anthropogenic activities. Water in Bangladesh, especially river water is severely polluted. Population explosion coupled with increasing industrialization is mostly responsible in populating rivers, canals, lakes aquifers, estuaries and other natural bodies around the globe. Surface water contamination occurs when a body of water is adversely affected due to addition of any unwanted material to it. Due to any of such reasons, if water becomes unfit for its desired use, it is then considered to be contaminated.

Surface water can be contaminated by both direct and indirect ways. Water body is directly contaminated when effluents and outfalls from chemical factories, tanneries, refineries, water treatment plants etc are emitted indiscriminately due carelessness of concerned authorities. On the other hand, water is indirectly polluted due to environmental changes. Contaminants from soil, atmospheres via rainwater contaminate surface water. Soil and ground water contains residues of fertilizers pesticides, insecticides, and fungicides etc. that are extensively used for agricultural purposes.

### 1.1.5 Sources of Pollution of Aquatic Environment

The main sources of pollution of aquatic environment are:

(a) Industrial effluents

(b) Sewage and domestic waste

(c) Agricultural discharges
(d) Fertilizers and pesticides
(e) Soap and detergents.
(f) Mining activities
(g) Marine dumping
(h) Accidental Oil and other chemical leakage
(i) Chemical fertilizers and pesticides.

#### 1.1.5.1 Aquatic environment polluted by industrial effluents

Industries produce huge amount of waste which contains toxic chemicals that pollute aquatic environment severely. Industrial waste contains heavy metals, dyes, sulphur, asbestos, nitrates and many other harmful chemicals (Zhonghua *et al.* 1987). These substances are harmful to human and aquatic lives. Most of the industries do not have proper waste management systems and they drain the waste containing such detrimental chemicals in the fresh water, which goes into rivers, canals and later to sea. These toxic chemicals cause change in natural colour, ambient temperature of pure water as well as increase in amount of minerals in naturally pure water also. As a result, aquatic lives became victims of these harmful effects toxic chemicals. Pollution of aquatic environment, especially caused by industrial effluents containing heavy metals is an anxiety to environment-scientists in recent years. Chromium, in hexavalent form as a typical heavy metal, has been recognized as the most harmful substance to aquatic body, particularly in tannery waste water. **Figure 1.1** shows waste water containing chromium flowing to the Burhigonga, a life-line of Dhaka, the capital of Bangladesh from tannery industries at Hazaribag area in Dhaka city.

**Figure 1.1:** Flow of wastewater from tannery industries at Hazaribag in Dhaka City, Bangladesh.

### 1.1.5.2 Aquatic environment polluted by sewage and wastewater

The sewage and waste water that is produced by each household is chemically treated and released in to sea with fresh water. The sewage water carries harmful bacteria and chemicals that can cause serious health problems. Pathogens are known as a common water pollutant. Microorganisms in water are known to cause dreadful diseases and become the breeding grounds for other creatures that act like carriers. These carriers inflict these diseases via various forms of contact onto individuals. A very common example of such a process is Malaria.

### 1.1.5.3 Aquatic environment polluted by effluents by of mining industries

Mining is the process of crushing the rock and extracting coal and other minerals from underground. These elements, when extracted in the raw form, contain harmful chemicals and can increase the amount of toxic elements when mixed up with water to cause harmful effects in human health as well as aquatic lives. Mining activities emit several metal-waste and sulfides from the rocks and thus contaminate aquatic environment.

### 1.1.5.4 Aquatic environment polluted by the effluents of marine-dumping

In some countries, especially in some developing-countries in Asia the garbage produced by household in form of paper, aluminum, rubber, glass, plastic, waste-food etc are collected and dumped into the sea. These items take 2 weeks to 200 years to decompose. Sea water is contaminated by these items to cause threat to aquatic lives in sea.

#### 1.1.5.5 Aquatic environment polluted by accidental oil leakage

Oil spill pose a huge concern as large amount of oil enters into the sea and does not dissolve in water to cause problem for local marine wild-lives, such as fish, birds and sea otters. As for example, a ship, carrying large quantity of oil, may spill oil, if it faces an accident. Due to discharge of oil-spill caused by the accident can damage to various species in the ocean.

#### 1.1.5.6 Aquatic environment polluted by chemical fertilizers and pesticides

Chemical fertilizers and pesticides are used by farmers to protect crops from insects and bacteria. They are useful for the plants growth. However, when these chemicals are mixed up with water, the water is contaminated to cause harmful effect on aquatic lives.

### 1.1.6 Heavy Metals and Toxicity of Heavy Metals

Metals and metalloids having relatively high density ranging from 3.5 to 7.0 g $cm^{-3}$ are referred to as heavy metals. Small number heavy metals have an essential role in the metabolism of humans and animals in very trace amounts but their higher concentration may cause toxicity and health hazards. Some heavy metals includes mercury (Hg), cadmium (Cd), arsenic(As), chromium (Cr), thallium (Tl), nickel (Ni) and lead (Pb) are toxic even at low concentration.

Heavy metals are widely documented as widespread-pollutants of soils and water bodies (Dudus, 2002). Heavy metals and organic wastes from leaking sewage systems of various industries can accumulate in aquatic bodies. These metals are non-biodegradable in nature. They enter into the human body via air, water and food. Bioaccumulation of metals in fish, crabs and other edible aquatic species, may cause health problems to enter the food chain. Also, this can destroy the water aeration system, the self-purifying process of rivers.

Toxic heavy metals can bid to vital cellular components, such as structural proteins, enzymes and nucleic acids and interfere with their functioning (Lanids, *et al*., 2000). Symptoms and effect vary according to the metal or metal compound and the dose involved. Long-term exposure to toxic heavy metals can have carcinogenic, central and peripheral nervous system and circulatory effects.

The toxicity and carcinogenic properties of chromium (VI) have been known since at least the late 19th century (Barceloux, 1999). In 1890, Newman described the elevated cancer risk of workers in a chromate dye company. Chromate-induced dermatitis was reported in aircraft workers during World War II.

## 1.1.7 Sources of Chromium (VI) in Aquatic Environment

Tanneries are the major source of chromium (VI) in aquatic environment in Bangladesh. Chromium sulphate is used as a mordant in tanning leather. Untreated wastes from tanneries are being dumped into the canals that subsequently add to water of the river linked to the canals. Spent chrome liquors and wastes from tanneries contain chromium in the range of 2900 to 4500 $mg.L^{-1}$ and 10 to 15 $mg \cdot L^{-1}$ respectively (Sarkar, 1994 and Hossain, 1997). But environment safety regulations do not allow >2.00 $mg.L^{-1}$ chromium in any industrial waste.

Hexavalent chromium in ground water has generally be assumed to anthropogenic contamination, since it is used in numerous industrial applications, including electroplating, tanning, paper pulp production, industrial water cooling, petroleum refining etc. Anthropogenically, chromium is released into the environment through sewage and fertilizers (Ghani, 2011). Chromium is extensively used in the industries, such as – metallurgy, electroplating, production of paints and pigment, tanning, wood preservation, chemical production, pulp and paper production in Bangladesh are shown in Table 1.1. These industries play a vital in chromium pollution with adverse effects on biological and ecological species (Ghani, 2011).

Table 1.1: Industries from which chromium adds to aquatic environment in Bangladesh.

| Industry | Location of industry | Chemicals used |
|---|---|---|
| Leather | Bengal Leather Tanning Limited, Dhaka<br>Apex Tanning Limited, Hazaribag, Dhaka<br>Tanneries in Savar, Rupgonj, Dhamrai, Jessore. | $Cr_2O_3$, $Cr(OH)SO_4$, $K_2Cr_2O_7$, $Na_2Cr_2O_7$, $CrCl_3$, $Cr_2(C_2D_4)_3$ |
| Textiles | Padma Textile Damra, Narayanganj, Bangladesh<br>Ashraf Textile Tongi, Gazipur, Bangladesh<br>Pakiza Dyeing & Printing Ind. Savar<br>Dhaka, Bangladesh<br>Sonya Printing Industries Savar<br>Dhaka, Bangladesh | $Cr_2(SO_4)_3$, $PbCrO_2$, $PbCrO_3.PbO$, $ZnCrO_4.Zn(OH)_2$ $KrCrO_4.3ZnCrO_4$. $Zn(OH)_2$, $H_2SO_4$ |
| Pulp, Paper and Rubber | Karnaphuli Paper Mill, Chandrogona,<br>Chittagong, Bangladesh<br>North Bengal Paper Mill Ltd. Pabna, Bangladesh,<br>Khulna Newsprint Khulna, Bangladesh<br>Ibrahim Rubber Industry Tongi, Gazipur<br>Bangladesh. | $Cr_2O_3$, $CrCl_3$ |
| Glass | Osmania Glass Sheet Factory Kalurghat, Chittagong, Bengal Glass Workers Damra, Dhaka, Ali Glass Workers Ltd. Tongi, Gazipur. | $Cr_2O_3$<br>Ni-Cr alloy $CrKSO_4$ |
| Ceramic | Monno Ceramic, Dhamrai, Savar; Peoples Ceramic Tongi, Gazipur; National Ceramic Industry, Tongi, Gazipur; Tajma Ceramic Industry, Bogra. | $Cr_2O_3$ $Cr_2(SO_4)_2$ |
| Dyes & Varnish | Eastern Paint Industry Tongi, Gazipur;<br>Elite Paint Bangladesh Ltd, Bayejeed Bustami, Chittagong<br>Berger Paint Bangladesh Ltd, Kalurghat, | $Cr_2O_3$, $K_2Cr_2O_7$, $PbCrO_4$, $Cr_2(SO_4)_3$, $Cr(COOCH_3)_3$, $K_2CrO_4$, |

| | | |
|---|---|---|
| | Chittagong; Dhaka Dying, Tongi, Gazipur. | $Cr_2(C_2O_4)_3$ |
| Steel mill | Chattagram Steel Mill Ltd. Potenga, Chittagong.<br>Dhaka Steel Mill Ltd., Tongi, Gazipur. | Metallic<br>Chromium and $Cr_4C_3$ |
| Refinery | Eastern Refinery, Potenga, Chittagong. | Metallic Cr. |
| Fertilizer | Chittagong Urea Fertilizer Ltd, Chittagong<br>Zia Fertilizer Company Ltd, Ashugonj<br>Kharnaphuly Fertilizer Company Ltd (KAFCo), Chittagong;<br>Chittagong T.S.P. Fertilizer, Chittagong. | Fe-Cr alloy used to prepare absorption.<br>Cr-impurities in<br>raw materials. |
| Chloro-alkali | Chittagong Chemical Complex, Chittagong | Cr-impurities in the raw materials |

In most of the industries of tanneries, metal finishing and electroplating, chromium (VI) is often supplied in form of $Cr_2O_7^{2-}$. Chromium (VI) is widely as an important species in such plants. As it is typically quite soluble over wide range of pH, it can easily be transported, both in natural aquatic body and into organisms exposed to the ions. In both dilute and moderately strong solutions, chromium predominantly exists as chromium (VI).

## 1.1.8 Chemistry of Chromium

Chromium is typical transition metal. Chromium is the first element in group 6 in the Periodic Table. The name of the element is derived from the Greek word *chrōma*, meaning color, because many of the chromium compounds are intensely colored. Naturally occurring isotopes of chromium are chromium-50 (4.3%), chromium-52 (83.8%), chromium-53 (9.6%), and chromium-54 (2.4%) and seven are man-made.

Chromium is a steely-grey, lustrous hard and brittle metal. Its atomic number is 24, relative atomic mass is 51.999 g, having high melting point (1900º C), boiling point (2642º C) and relative density is 7.14. It is of high value for its high corrosion resistance and hardness. A major development was the discovery that steel could be made highly resistant to corrosion by adding metallic chromium to form stainless steel. Stainless steel and chrome plating (electroplating with chromium) together comprise 85% of the commercial use. Chromium is remarkable for its magnetic properties: it is the only elemental solid which shows anti-ferromagnetic ordering at room temperature (and below). Above 38 °C, it changes to paramagnetic.

Elemental chromium is very stable, Cr (24): [Ar] $4s^2$, $3d^4$, but it is not usually found pure in nature. It exists in aqueous solution mainly in two oxidation states Cr (III), [Ar] $3d^3$ and Cr (VI), [Ar] $3d^o$. In addition to these states, it exists in other oxidation states, viz. Cr (IV) and Cr (V). Of these all, Cr (III) is the most stable state of chromium. Chromium (VI) compounds are powerful oxidants at low or neutral pH. Most important ions are chromate ($CrO^{2-}$) and dichromate ($Cr_2O_7^{2-}$) which exist in equilibrium. In aqueous solution, hexavalent chromium exists as oxoforms in a variety of species depending on its pH and concentration (Rumpa *et al*., 2011)**.** Under oxidizing conditions, chromium in aqueous state exists in anionic species under different pH of the solution. $CrO_4^{2-}$ in pH 6-10, $Cr_2O_7^{2-}$ and $HCrO_4^{-1}$ in pH 2-6 and $H_2CrO_4$ in pH < 1 are parent. The abundance of these forms depends on concentration.

The following equilibrium exists when anions are present in aqueous medium **(**Cotton and Wilkinson, 1974).

$$2[CrO_4]^{2-} + 2\,H^+ \rightleftharpoons [Cr_2O_7]^{2-} + H_2O$$

$$H_2CrO_4 \rightleftharpoons HCrO_4^- + H^+$$

$$HCrO_4^- \rightleftharpoons CrO_4^{2-} + H^+$$

$$Cr_2O_7^{2-} + H_2O \rightleftharpoons 2HCrO_4^-$$

$H^+$ $H^+$ $2H^+$

$$\text{i.e. } H_2CrO_4 \rightleftharpoons HCr_2O_7^- \rightleftharpoons Cr_2O_7^{2-} \rightleftharpoons 2CrO_4^{2-}$$
$$\text{pH} < 1 \qquad \text{pH 2 to 6} \qquad \text{pH} > 6$$

According to Werner's co-ordination theory, chromium atom possesses two types of valency, i.e. ordinary and auxiliary. The ordinary valency is 3 and auxiliary valency is 6. A chromium atom holds atoms, radicals or co-coordinated groups to form a complex ion which is known as chrome complex (Sarkar, 1994). Chromium occurred naturally and due to anthropogenic activities can exist in various environmental media including surface and ground water, sea water, soil and sediments, rocks and even in air. In ground water and soil, chromium exists in two major oxidation states: the oxidized chromium (VI) and less-oxidized chromium (III). Chromium (III) compounds are sparingly soluble in water; chromium (VI) compounds are quite soluble. The resulting chromium (VI) solutions are powerful oxidizing agents under acidic conditions, but less under basic conditions. Chromium (VI) is much more toxic and mobile in ground water than relatively immobile chromium (III). The common dissolved chromium species (all chromium (VI) are $HCrO_4^-$, $CrO_4^{2-}$ and $Cr_2O_7^{2-}$ (Rumpa *et al*., 2011). Depending on the physical and chemical state of chromium, same concentration of chromium has a wide variety of mobility and reactivity which result different effects of chromium (Steven, *et al.,* 1976). Chromium toxicity to aquatic biota is significantly affected by abiotic variables, such as hardness, temperature, pH, salinity of water, biological factors, such as species, life stage and potential differences in sensitivities of local populations (EAI, 1981).

In aquatic environment, the major sources of chromium are electroplating, metal finishing industries, publicly owned treatment plants, tanneries, textile manufacturing plants and runoff from urban and residential areas (Towill *et al.,* 1978). Due to anionic nature as polyatomic ions, adsorption of chromium (VI) in soil is limited to positively-charged surface exchange sites, the number of which decreases with increase of pH. The adsorbed chromium (VI) easily desorbs into uncontaminated ground water indicating non-specific adsorption (Rumpa *et al.,* 2011).

### 1.1.9 Toxicity of Chromium

Toxicity and carcinogenic properties of chromium (VI) have been identified since late 19$^{th}$ century (Barceloux *et al.*, 1999). According to the survey of literature, chromium (VI) has been found to be more dangerous than chromium (III) as chromium (VI) enters the cell more readily than chromium (III) does. Concentration of chromium like other heavy metals is known to cause physiological disorders in organisms and phytotoxicity. Chromium (VI) has been identified to cause harmful effects in human health including mutagenic and carcinogenic risks in humans (Park *et al.*, 2001**).** Chromium (VI) can be absorbed by lung and gastrointestinal tract and even to a certain extent by intact skin (Zheng *et al.*, 2013)**.** Because of carcinogenic and mutagenic properties, chromium (VI) has been categorized as a group 1 human carcinogen and mutagen by the International Agency for Research on Cancer (IARC) (Monisha, *et al.*, 2014).

Toxicity of chromium compounds depends on its oxidation state of chromium in the compound and solubility of the compound in water. In environment, chromium (III) is generally less harmful than chromium (VI) due to its weak permeability in membrane. Chromium (VI) compounds are strong oxidizing agents and thus tend to be irritating, corrosive and toxic systematically than chromium (III) compounds. The acute toxicity of chromium (VI) is due to its strong oxidative properties. When it reaches to bloodstream, it damages blood cells by oxidation. Hemolysis and subsequently kidney and liver failure are the common results of such damages. Chromium (VI) can pass through cell membranes readily and its subsequent intracellular reduction under physiological conditions to form short-lived reactive intermediates viz. chromium (V), chromium (IV), and ultimately chromium (III). The reduced chromium (III) is excreted immediately from the body leaving behind the other reactive intermediates. Any of these species attacks DNA, proteins and membrane lipids of human body to cause disruption in cellular integrity and functions (Atsdr, 2013).

Three mechanisms have been proposed to describe genotoxicity of chromium (VI). The first one includes the generation of short-lived highly reactive hydroxyl radicals and other short-lived reactive radicals which are byproducts of reduction of chromium (VI) to chromium (III). The second process is the direct binding of short-lived chromium (V), generated by reduction in the cell and chromium (IV) compounds to DNA. The last mechanism attributes the genotoxicity to binding to DNA of the end product of chromium (III) reduction (Cohen *et al*., 1993**).**

Environment chemists throughout the world are concerned regarding dreadful effects of chromium (VI) on human body and environment. World Health Organization (WHO) concerned US and European Regulatory Authorities have imposed stringent environmental regulations on the quantity of chromium (VI) in drinking water and wastewater. According to the recommendation of World Health Organization (WHO) and Environmental Protection Agency (EPA, 1998), the standard limits of concentration of chromium (VI) in drinking water and wastewater are 0.05 $mg.L^{-1}$ and 0.5 $mg.L^{-1}$, respectively (Atsdr, 2013).

# 1.2 Techniques for Removal of Cr(VI)

In recent years, pollution of aquatic environment caused by toxic heavy metals has become a reason of great concern to environment chemist. So, the researchers are relentlessly paying their utmost efforts to find out effective and cost-friendly techniques to relieve aquatic environment from harmful contamination caused by toxic heavy metals. Chromium is one of the most toxic metals widely-used in different industries particularly in tannery. Improper disposal of such industrial wastes causes chromium (VI) pollution in aquatic environment. The following methods have been used for removal of chromium (VI) from aquatic systems:

(i) Membrane process and Electro-chemical technique (Uosaki, 1975)
(ii) Précipitation (Zhan *et al*., 2001; Dhanakumar *et al.,* 2007)
(iii) Ion Exchange (Colella, 1996)
(iv) Coagulation (Cotton and Wilkinson., 1998)
(v) Filtration (Benjamin *et al.,* 1996)
(vi) Sedimentation (Richard and Bourg, 1991)
(vii) Evaporation (Dhanakumar *et al.,* 2007)
(viii) Sedimentation (Richard and Bourg, 1991)
(ix) Flotation (Richard and Bourg, 1991)
(x) Adsorption (Ho and McKay, 1999).

Application of these physiochemical methods is either economically prohibitive or too complicated for treatment of heavy metals (Jihyun *et al*., 2008). As a result, these methods are not viable for small and middle-categorized industries. Various

conventional methods with a series of limitations are available for removal of chromium (VI) from aqueous system.

Removal of toxic heavy metal ions at low concentration from aquatic system is a very important issue that is effectively possible by means of adsorption method using activated carbon (Tajmeri *et al*., 2009). Though, ion exchange methods and adsorption using resins and activated carbon are still popular for wastewater treatment. High financial investment in setting up of these processes and regeneration cost of activated carbon and resins used in these processes has resulted in resulted demand of cost-friendly adsorbent. Adsorption has shown several advantages over other physico-chemical processes. It has proved to be the most versatile, effective and a cost-friendly promising process for treatment of aquatic effluent of industries (Hossain *et al.,* 2013, Dhanakumar *et al*., 2007). Chromium (VI) can be removed from aquatic system by means of other conventional methods with an exceptional problem. Since chromium (VI) is an oxidizing agent, it is easily reduced to chromium (III) by organic or reducing agent. This reduction reaction is not suitable at low concentration of chromium (VI). An exceptional advantage of adsorption method is that it is an efficient method for removal of chromium (VI) at low concentration. In recent years, serious attention has been paid to develop adsorption method using a biomass which is available and cost-friendly for removal of chromium (VI) from aquatic system.

### 1.2.1 Use of Bio-sorbent

Most recently researchers are relentlessly paying the utmost attention to find a cost-friendly bio-sorbent which has environmental benefits to evaluate its potential for the treatment of heavy metals in aquatic system. In recent years, several studies have been reported about the sorption of chromium (VI) using different biomasses as low-cost sorbents such as Used Black Tea Leaves (Hossain *et al.,* 2005), algae (Yu *et al*., 1999), green algae Spyrogyra species (Gupta *et al*., 2001), bark (Alves *et a*l., 1993), hazelnut shell (Cimino *et al*., 2000), bagasse fly ash (Park *et al.,* 1999), red-mud (Gupta *et al*.,

2001), coconut waste (Selvi *et al.,* 2001), sawdust (Iqbal *et al*., 2002), mustard seed cakes (Saeed *et al.,* 2002), wool, rice husk, straw, coconut husk, peat, moss (Dakiky *et al.*, 2002), walnut skin, coconut fibre (Espinola *et al.,* 1999), Cotton seed hulls (Tarley *et al*, 2004).

### 1.2.2 Tea Leaves Dust as a Biosorbent

The word 'Tea' was originated from only one species of plant, *Camellia sinesis* (Mokgalaka *et al.,* 2004). Different types of teas, viz. Black Tea, Green Tea, Flavored Tea and Instant Tea are producing in worldwide. Among these, Black Tea is common in Bangladesh. Several studies have been reported about the application of used black tea leaves as a bio-sorbent for the removal of heavy metals and dyes from aqueous system and exhibited high removal capacity (Hossain 2000, 2005, 2006, 2011, 2012, 2013).

During the period of tea processing, a large amount of dust tea leaves are coming out as a waste material of tea industry as shown in Figure 1.2. Dust black tea leaves (DBTL) is a waste product of the tea plants that is a puzzling problem to the plant authority to destroy it, as it is also a pollutant to environment. From these consideration, Dust Black Tea Leaves (DBTL) has been selected as a potential cost-effective bio-sorbent in this study to develop an adsorptive removal process for the treatment of chromium (VI) from aquatic environment.


Figure 1.2: Dust Black Tea Leaves produces as a waste material of tea processing plant in Bangladesh Tea Research Institute (BTRI), Srimongal, Bangladesh.

# 1.3 Adsorption

Adsorption is a surface phenomenon. It is defined as accumulation or concentration of particular substance at the surface or interface of a solid phase or liquid phase due to inelastic collision suffered by molecules on the surface or interface. The substance (solid or liquid or gas) accumulated or concentrated at the surface or interface is called adsorbate and the material on which, the adorbate accumulates or concentrates is called adsorbent. The reason of this accumulation is either a long range van der Waals force of attraction of the un-saturation of the valance force on the surface i.e. the residual field of force.

It is, actually, an attraction of molecules of adsorbate to the surface of an adsorbent. It occurs due to adhesion of atoms, ions, or molecules from a gas, liquid, or dissolved solid to a surface or interface of particular adsorbent. This process creates a film of the

adsorbate on the surface or interface of the adsorbent. Similar to surface tension, adsorption is a consequence of surface energy. The preferential concentration of molecules in the proximity of a surface arises because the surface forces of an adsorbent solid are unsaturated. Both repulsive and attractive forces become balanced when adsorption occurs.

This process differs from absorption, in which a fluid called the *absorbate* is dissolved by or permeates a liquid or solid called absorbent respectively. The term *sorption* encompasses both processes: adsorption and absorption. While desorption is the reverse of adsorption.

## 1.3.1 Types of Adsorption

According to the nature of attractive forces between adsorbate and adsorbent, adsorption is of two types:

(a) Physical adsorption or Physisorption

(b) Chemical adsorption or Chemisorption

### 1.3.1.1 Physical adsorption

The adsorption which occurs due to attractive forces caused by the interaction of long-range van der Waals Force or London force holding the adsorbate species on the surface of adsorbent is referred to as physical adsorption or physisorption. This adsorption is also known as van der Waals adsorption. In case of such adsorption, no electronic interaction takes place. Since these types of forces are weak, the process of physisorption can be easily reversed by heating or decreasing the pressure of the adsorbate (as in case of gases). When a particle is physisorbed, the energy released is of the same order of magnitude as the enthalpy of condensation. Physical adsorption requires no activation energy and the typical values of enthalpy are in the region of 20

$kJ \cdot mol^{-1}$ **(**Parfitt and Rochester, 1983). This process is exothermic. Physical adsorption occurs when the inter-molecular attractive forces between molecules of the solid adsorbent and the gas are greater than those between molecules of the gas itself.

#### 1.3.1.2 Chemical adsorption

Chemical adsorption occurs due to attractive force that binds the adsorbate species in mono-layer on the surface of the adsorbent. This type of adsorption is also known as activated adsorption. In chemisorption, the attractive force arises from electronic interaction to form chemical bond between the adsorbent and adsorbate. As a result, molecules stick to the surface by forming chemical bond and tend to find sites that maximize their coordination number with the substrate during chemisorption, surface of adsorbent becomes unsaturated and adsorption occurs rapidly, even at low temperature. In chemisorption, adsorbate undergoes chemical change and consequently dissociates into independent fragments. The individual species may be ions, free radicals or atoms which are the units of layers of chemisorption. The existence of independent fragments on the surface of the adsorbent is the result of chemisorptions. The enthalpy of chemisorption is very much greater than that for physisorption and typical values are in the region of 200 $kJ \cdot mol^{-1}$. The distance between the surface and the closest adsorbate atom is shorter for chemisorption than that for physisorption. A chemisorbed molecule may be torn apart at the demand of the unsatisfied valences of the surface atoms.

### 1.3.2 Factors Affecting Adsorption

Adsorption depends on the following factors:

**(i)** ***Surface Area*** : Generally, the extent of adsorption is proportional to specific area i.e. larger the surface area of the adsorbent, greater is the extent of adsorption. Specific area can be defined as that portion of the total area that is available for adsorption.

**(ii)** ***Nature of the Adsorbate :*** Adsorption of a solute is inversely proportional to its solubility in the solvent. The greater the solubility, the stronger the solute-solvent bond and the smaller the extent of adsorption.

**(iii)** ***Concentration of adsorbate :*** The extent of adsorption is proportional to the concentration of adsorbate.

**(iv)** ***Solution pH :*** Because hydrogen and hydroxide ions are adsorbed quite strongly, the adsorption of other ions is influence by the pH of the solution. In general, adsorption of typical organic pollutant from water is increased with decreasing pH.

**(v)** ***Processing temperature:*** As adsorption is accompanied by evolution of heat, so according to the Le-Chatelier's principle**,** the magnitude of adsorption should decrease with rise in temperature.

Thus the extent of adsorption depends on the following factors

(a) The pressure of the adsorbate in case of gases
(b) The nature of the active sites on the surface
(c) The concentration of the liquid phase
(d) The nature of adsorbent or adsorbate
(e) The temperature of surroundings
(f) pH of the system in the case of liquid phase
(g) The ionic strength of liquid phase

## 1.3.3 Measurement of Adsorption

The extent of adsorption is normally expressed as fractional coverage ($\bar{\theta}$) where theta indicates the ratio of number of adsorption sites occupied and the number of adsorption sites available. The rate of adsorption, *v,* is the rate at which the fractional coverage is changed with time as shown in equation (1.1),

$$v = \frac{d\bar{\theta}}{dt} \qquad (1.1)$$

The concentration difference between the bulk phase and interface may be positive or negative, that is, the concentration of mobile molecules may be greater or less in interface than it is in bulk-phase. In case of positive adsorption, the interface is often called two-dimensional phase or adsorbed layer, which can be localized or mobile depending on magnitude of attractive force existing between the adsobate and adsorbent molecules.

Adsorption is a dynamic process. It can be characterized by investigating the kinetic parameters of adsorption. The overall process of adsorption can be quantitatively described by the adsorption isotherm, which, at constant temperature, provides measured data relating to the amount adsorbed ($q_e$) and the equilibrium pressure or concentration ($C_e$) measured in the bulk-phase after adsorption.

The average thickness of adsorbate is often expressed with the names: mono-and mulilayer-adsorption. In monolayer adsorption, every of the adsorbed molecules exists in contact with the surface of the adsorbent, while, in case of multilayer adsorption, the adsorption space accommodates more than one layer or molecules so that all adsorbed-molecules do not exist in direct contact with the molecules of the adsorbent.

The physical and mathematical explanation of adsorption and interpretation of monolayer adsorption isotherm measured on homogeneous surface were initially studied by Langmuir in 1916. At equilibrium, the number of adsorbed molecules and that of desorbed molecules in unit time on unit surface area are equal.

### 1.3.4 Adsorption Kinetics

Adsorption is a physicochemical process that involves mass transfer of a solute from liquid phase to the adsorbent surface. At the maximum agitation speed of 150 rpm, it was assumed that no mass transfer, both external and internal, resistance occurs to overall adsorption process. (Hossain *et al.,* 2015). Therefore, adsorption kinetics can be studied through the residual concentration of adsorbate solution. Kinetic study of adsorption process provides information about kinetic behavior of adsorbate on adsorbent. Adsorption kinetics deals, the rate at which adsorption occurs. It is one of the most important characteristics to define efficiency of an adsorbent. Rates of adsorption can be determined by monitoring the change in concentration of adsorbate solution with time. Different kinetic equations such as first order (Hosssain and Alam, 2012), second order (Hosssain and Alam, 2012), pseudo first order (Lagergren 1898), pseudo second order (Ho and McKay, 2000), can be used for characterization of adsorption kinetics.

### 1.3.5 Adsorption Equilibrium

Adsorption is considered as a reversible process. During the adsorption from solution as the adsorption continues, the adsorbed solute tends to desorbs into the solution. At one stage, equal amounts of solute is adsorbed and desorbed simultaneously. Eventually, the rates of adsorption and desorption will attain an equilibrium. This is called adsorption equilibrium and the corresponding time at which such equilibrium is achieved is known as the equilibrium time ($t_e$). The corresponding solute concentration is called equilibrium concentration.

The knowledge of equilibrium time is necessary for adsorption, which control the adsorption capacity. The position of equilibrium is the characteristics of the entire system, the adsorbate, adsorbent, solvent, temperature, pH etc. Equilibrium time may be chosen in such a position, where no significant removal of adsorbate occurs. This is

obtained from the plot of solute removal versus time and the time at which no apparent change in the concentration of the solute occurs. This method involves eye judgments. The decision of such equilibrium time depends on many factors; the dose of adsorbent, initial concentration, pH, particle size of adsorbents, temperature etc. Usually equilibrium time increases with increase of temperature for physisorption and decrease in case of chemisorption. But nature and dose of adsorbent, initial solute concentration and pH of the solution largely effect equilibrium time.

### 1.3.5.1 Adsorption Isotherm

Study of adsorption isotherm is the most favorable approach to investigate adsorption mechanism. The most important aspects are:

(a) Shape of the isotherm

(b) Significance of the plateau found in many isotherms

(c) Whether the adsorption is monomolecular or extends over several layers

(d) Orientation of the molecules adsorbed

(e) Effect of temperature etc.

In case of adsorption from solution of on solid surface, it has been established that the amount of adsorbate adsorbed depends on the specific nature of adsorbent, adsorbate, process temperature, pressure (in case of gaseous adsorbate), concentration of solution and also the nature of the solvent of adsobate solution. The adsorbare molecules have translational motion and they collide with solid surfaces that cause to be adsorbed. The amount adsorbed at equilibrium is a function of temperature and concentration. At constant temperature, the plot of amount of the substrate adsorbed against equilibrium concentration is called the adsorption isotherm which expressed by equation (1.2), i.e.

$$x/m = f(C_e), \quad \text{at constant } T \qquad (1.2)$$

$x/m$, $C_e$ and $T$ indicate amount of the substrate adsorbed per gram of adsorbent, equilibrium concentration and absolute temperature, respectively. Different model equations for adsorption such as Freundlich (Freundlich 1906), Langmuir (Langmuir, 2018), Temkin (Temkin and Pyzhev, 1940) and Dubinin-Radushkevich (Dubinin and Radushkevich, 1947) isotherms are commonly used for characterization of equilibrium adsorption data.

### 1.3.6 Techniques for Analysis of Adsorbent Surface

In adsorption study, surface analysis of adsorbent is one of the important investigations. Surface analysis provides information whether the surface of the adsorbent is homogenous or heterogeneous, nature of the surface topology, pore size of the surface and presence of different elements in surface can also be identified by surface analysis. Varieties techniques are available for characterization of solid surface of adsorbent. The following techniques are widely used:

(a) Attenuated Total Reflectance IR spectroscopy (ATR-IR)
(b) Scanning Electron Microscopy (SEM)
(c) Energy Dispersive X-ray Spectroscopy (EDX)
(d) Transmission Electron Microscopy (TEM)
(e) Field Emission Microscopy (FEM)
(f) Atomic Force Microscopy (AFM)
(g) Ultraviolet Photoelectron Spectroscopy (UPS)
(h) Powder X-ray Diffractometry (XRD)
(i) Low Energy Electron Diffraction (LEED)
(j) X-ray Photoelectron Spectroscopy (XPS)
(k) Auger Electron Spectroscopy (AES), etc.

Following three techniques Attenuated Total Reflectance IR spectroscopy (ATR-IR), Scanning Electron Microscopy (SEM) and Energy Dispersive X-ray Spectroscopy (EDS

or EDX) were used in the present study.

### 1.3.6.1 Attenuated Total Reflectance IR spectroscopy (ATR-IR)

ATR stands for Attenuated total reflectance which is a sampling technique used in conjunction with IR spectroscopy which enables samples to be examined directly in the solid or liquid state without further preparation.

ATR uses a property of total internal reflection resulting in an evanescent wave. A beam of infrared light is passed through the ATR crystal (Typical materials for ATR crystals are germanium, zinc selenide and KRS-5 while silicon is ideal for use in the Far-IR region of the electromagnetic spectrum) in such a way that light undergoes multiple internal reflections in the crystal of high refractive index surface in contact with the sample. This reflection forms the evanescent wave which extends into the sample. The penetration depth into the sample is typically between 0.5 and 2 µm, with the exact value being determined by the wavelength of light, the angle of incidence and the indices of refraction for the ATR crystal and the medium being probed. The number of reflections may be varied by varying the angle of incidence. The beam is then collected by a detector as it exits the crystal. Most modern infrared spectrometers can be converted to characterize samples via ATR by mounting the ATR accessory in the spectrometer's sample compartment (Goldstein, *et al.,* 2003).

- Infrared (IR) spectroscopy by ATR is applicable to the same chemical or biological systems as the transmission method. One advantage of ATR-IR over transmission-IR, is the limited path length into the sample. This avoids the problem of strong attenuation of the IR signal in highly absorbing media, such as aqueous solutions.

- The ability to passively characterize samples, with no sample preparation has lead to the use of ATR-FTIR in studying trace evidence in forensic science.

- Recently, ATR-IR has been applied to micro-fluidic flows of aqueous solutions by engineering micro-reactors with built-in apertures for the ATR crystal, allowing the flow within micro-channels to pass across the crystal surface for characterization.

### 1.3.6.2 Scanning Electron Microscopy (SEM)

The SEM is a microscope that uses electrons instead of light to form an image. Surface analyses, chemical analysis and imaging on a variety of materials are performed using a Scanning Electron Microscope (SEM).

The scanning electron microscope (SEM) is a type of electron microscope that images the sample surface by scanning it with a high-energy beam of electrons in a raster scan pattern. The electrons interact with the atoms that make up the sample producing signals that contain information about the sample's surface topography, composition and other properties such as electrical conductivity. The types of signals produced by an SEM include secondary electrons; back scattered electrons (BSE), characteristic X-rays, light (cathodoluminescence), specimen current and transmitted electrons. These types of signal all require specialized detectors that are not usually all present on a single machine. In the most common or standard detection mode, secondary electron imaging ( SEI), the SEM can produce very high-resolution images of a sample surface, revealing details about 1 to 5 nm in size. SEM micrographs have a very large depth of field yielding a characteristic three-dimensional appearance useful for understanding the surface structure of a sample (Goldstein, *et al.*, 2003).

A wide range of magnifications is possible, from about x 25 (about equivalent to that of a powerful hand-lens) to about ×5,00,000, about 500 times the magnification limit of the best light microscopes. Back-scattered electrons (BSE) are beam electrons that are reflected from the sample by elastic scattering. BSE are often used in analytical SEM

along with the spectra made from the characteristic X-rays. Because the intensity of the BSE signal is strongly related to the atomic number (Z) of the sample, BSE images can provide information about the distribution of different elements in the sample.

- The SEM also has much higher resolution, so closely spaced samples can be magnified at much higher levels. Because the SEM uses electromagnets rather than lenses, the researcher has much more control in the degree of magnification.

- The Scanning Electron Microscope is equipped with an Energy Dispersive Spectrometer (EDS). SEM/EDS provides chemical analysis of the field of view or spot analyses of minute particles.

- This micro-chemical analysis is also a non-destructive test.

All of these advantages, as well as the actual strikingly clear images, make the scanning electron microscope one of the most useful instruments in research today.

### 1.3.6.3 Energy Dispersive X-ray Spectroscopy (EDS or EDX)

The Energy Dispersive Spectroscopy (EDS) is an analytical technique used in concert with the SEM. The EDS is used for the chemical characterization of a sample used in concert with SEM for compositional microanalysis. Its characterization capabilities are due in large part to the fundamental principle that each element has a unique atomic structure allowing unique set of peaks on its X-ray spectrum (Joseph Goldstein, 2003). It is also useful for material characterization since it can perform qualitative and semi-quantitative microanalysis on a sample from a relatively low (~25×) to high magnification (~20,000×).

The EDS technique is based on the investigation of an interaction of some source of X-ray excitation and a sample. At rest, an atom within the sample contains ground state (unexcited) electrons in discrete energy levels or electron shells bound to the nucleus. When the sample is focused by the SEM's electron beam or high energy beam of charged particles, the incident beam may excite an electron in an inner shell, ejecting it from the shell while creating an electron hole where the electron was. An electron from an outer, higher-energy shell then fills the hole, and equal energy to the difference in energy between the higher-energy shell and the lower energy shell may be released in the form of X-ray. The EDS X-ray detector measures the relative abundance of emitted X-rays versus their energy. The detector is typically a Lithium-drifted silicon, solid-state device. When an incident X-ray strikes the detector, it creates a charge pulse that is proportional to the energy of the X-ray. The charge pulse is converted to a voltage pulse (which remains proportional to the X-ray energy) by a charge-sensitive preamplifier. The signal is then sent to a multichannel analyzer where the pulses are sorted by voltage. The energy as determined from the voltage measurement, for each incident X-ray is sent to a computer for display and further data evaluation. The spectrum of X-ray energy versus counts is evaluated to determine the elemental composition of the sampled volume (Goldstein, *et al.*, 2003).

- More than 90 elements can be detected with our low-atomic number detector using the SEM/EDS method.

# 1.4 Review of Literature

It was reported that chromium (VI) was a toxic heavy metal. It has carcinogenic, mutagenic and teratogenic properties. Since chromium (VI) is widely used in tanning leather, tannery effluents contain huge quantity of chromium (VI). Discharge of untreated or poorly treated tannery effluents into natural water bodies is a major environmental problem. Chromium (VI) is not only toxic heavy metal ion having

carcinogenic, mutagenic and teratogenic properties, it is also non-biodegradable. For this reason, development of the process for removal of chromium (VI) from tannery effluents has become an important issue to researchers in recent years. Adsorptive removal of chromium (VI) from tannery effluents is an economically viable method. Effects of different conditions, viz. concentration of adsorbate, temperature, pH of adsorbate and particle size of adsorbent on adsorption were studied. Review of literatures in recent decades provides updated information about adsorption of chromium (VI) from aquatic body on different adsorbents.

Timbo, *et al.,* (2017) studied on adsorptive removal from aqueous solution of Cr (VI) by Green Moringa Tea Leaves. The study was carried to test the use of Green Moringa Leaves biomass as an adsorbent for Cr (VI) from aqueous solutions. Batch adsorption method was used. The effects of contact time, adsorbent dosage, pH, initial adsorbate concentration and temperature on adsorption were studied. Results had shown that maximum removal capacity of 33.9 $mg \cdot g^{-1}$ at pH 2.0. The Langmuir and Freundlich adsorption isotherm models were used to fit the experimental data. The data showed that adsorption on Green Moringa Oleifera leaves tea biomass fitted well to Freundlich isotherm ($R^2 = 0.943$) compared to the Langmuir isotherm ($R^2 = 0.912$).

Dhanakumar *et al.,* (2007) conducted research on removal of Cr (VI) from aqueous solution by adsorption using cooked tea dust. Batch mode adsorptive removal was carried out at varying pH, agitation time, particle size and adsorbent dosage. The optimum pH for Cr (VI) adsorption on CTD was found to be 2.0. Results conformed to both Langmuir and Freundlich adsorption models for adsorption equilibrium of Cr (VI) onto CTD. The adsorption followed the pseudo second order kinetics. The Langmuir adsorption capacity was found to be 30.39 $mg \cdot g^{-1}$ while Freundlich constants $k_f$ and $n$ were 7.524 and 2.673, respectively.

Altun and Kar (2016) conducted a research on removal of Cr(VI) from aqueous solution by pyrolytic charcoals. Bio-chars produced by the pyrolytsis of walnut shells at 450 $^oC$ (BC 450) and the co-pyrolysis of walnut shells and 20 wt % tar sand (BCTS20) at the

same temperature, were investigated as potential adsorbents for the removal of Cr(VI) ions from aqueous solutions using batch experiments. The Cr (VI) removal percentages under optimal conditions were 80.47 % and 95.69 % for BC450 and BCTS20 respectively. Langmuir, Freundlich and D-R models were used to fit the adsorption isotherms and the Langmuir models described the adsorption isotherm best. The research revealed that the maximum Langmuir adsorption capacity of BCTS20 is comparable to that of some reported commercial activated carbons.

Mishra (2015) studied on Biosorption of chromium (VI) from aqueous solutions using waste plant biomass. Biosorption of chromium (VI) from aqueous solution onto waste plant biomass of portulaca Oleracea was studied in the present work, Batch studies were carried out to examine the effects of process parameters, Influence of altering various process parameters was studied, The biosorption process was fast, and equilibrium was achieved in 45 min of contact time, It was found that the biosorption capacity of Plant material depends on many factors mainly on solution pH, with a maximum biosorption capacity for chromium at pH 2. The biosorption kinetics was tested with pseudo-first-order and pseudo-second-order reaction, and results showed that biosorption followed pseudo-second-order rate expression, Experimental equilibrium data were applied to two different isotherm models, Isotherm tests showed that equilibrium sorption data were better represented by Langmuir model, and the sorption capacity of plant biomass was found to be 54.945mg/g.Thermody-namic parameters like $G^o$, $H^0$ and $S^0$ were also evaluated, and it was found that the biosorption was spontaneous and endothermic in nature. Plant biomass was found to be an effective adsorbent for chromium (VI) from aqueous solution. This study indicated that plant biomass could be used as an efficient , cost effective and environmentally safe biosorbent for the treatment of chromium containing aqueous solutions.

Jeyaseelan and Gupta (2016**)** contacted a research on green tea leaves as a natural adsorbent for the removal of chromium (VI) from aqueous solution. This study deals with removal of chromium (VI) using used green tea leaves. The sorption of chromium

(VI) was carried out by using batch method. The effects of different adsorption-parameters, such as contact time, concentration of adsorbate solution, pH of the solution, process temperature and mass of adsorbent were investigated in the study. Langmuir adsorption isotherm, Freundlich adsorption isotherm and adsorption kinetic were investigated. The values of aG, aH, and aS were calculated. The result of the thermodynamic parameters showed that the process was spontaneous and the extent of adsorption of the adsorbate decreases with increase in temperature. The kinetic study showed that the reaction followed pseudo-second order kinetics.

Agegnehu *et al.* (2018) studied on removal of chromium (VI) from aqueous solution using vesicular basalt: A potential low cost wastewater treatment system. A series of batch experiments were carried out to study the effects of experimental parameters, pH, ionic-strength and contact time on chromium (VI) adsorption. The study revealed that the removal efficiency of chromium (VI) decreased with increasing pH and ionic strength. Initial solution pH 2.0 was found to be the optimum pH of the adsorbate solution. The maximum adsorption capacity was 79.20 $mg.kg^{-1}$ at an initial concentration 5.0 $mg \cdot L^{-1}$ and adsorption dosage of 50 $g.L^{-1}$. Result of the study of equilibrium adsorption better described Freundlich isotherm model and that of kinetic study showed that the reaction was pseudo-second-order kinetic.

Ksakas *et al.* (2015) conducted a research on the adsorption of chromium (VI) from aqueous solution by natural materials from Morocco. The effects of initial concentration of Cr (VI) ion, temperature, amount of adsorbent and pH of the solution on adsorption have been investigated. Optimum conditions for adsorption were determined as initial concentration of 100 $mg \cdot L^{-1}$, adsorbent dose 2.0 g, and pH 2.0. Removal of chromium ion was found as highly dependent on pH and initial concentration of the aqueous solution of chromium (VI). The adsorption isotherm followed the Langmuir equation. The maximum adsorption capacity was found to be 15.67 $mg.g^{-1}$ and 14.43 $mg.L^{-1}$ for the materials KS and PN respectively.

Mohan *et al.* (2005) studied on removal of hexavalent chromium from aqueous solution using low-cost activated carbons derived from agricultural waste materials and activated carbon fabric cloth. Systematic studies on equilibrium adsorption of hexavalent chromium and kinetics using low-cost activated carbons as well as commercially available activated carbon fabric cloth was carried out at different temperatures, particle size, pH and adsorbent doses. Both Langmuir and Freundlich models of isotherms fitted the adsorption data reasonably. The results indicated that the Langmuir adsorption isotherm model fits the data better than the Freundlich adsorption isotherm model. The kinetic studies were conducted to describe the effects of temperature, initial adsorbate concentration, adsorbent particle size and solid-to-liquid ratio. The adsorption of chromium (VI) follows pseudo-second-order rate kinetics. Based on these studies various parameters, such as, effective diffusion co-efficient, activation energy and entropy were calculated and evaluated to establish the adsorption mechanisms. The adsorption capacities of the tested adsorbents were found to be comparable to those of the available adsorbents.

Mutongo *et al*. (2014) studied on **r**emoval of chromium (VI) from aqueous solutions using powder of potato peelings as a low cost sorbent**.** Batch experiments were carried out with an artificial effluent comprising of potassium dichromate in deionized water, The effects of the initial hexavalent chromium concentration, dose of biosorbent, and removal kinetics were explored. An adsorbent dosage of 4 $g \cdot L^{-1}$ was effective in complete removal of the metal ion, at pH 2.5 in 48 minutes. Kinetic process of Cr(VI) adsorption onto potato peel powder was tested by applying pseudo-first-order and pseudo-second-order models as well as the Elovich kinetic equation to correlate the experimental data and to determine the kinetic parameters, The adsorption data were correlated by the Langmuir and Freundlich isotherms. A maximum monolayer adsorption capacity of 3.28 $mg \cdot g^{-1}$ was calculated using the Langmuir adsorption isotherm, suggesting a functional group limited adsorption process. The results confirmed that potato peels are an effective biosorbent for the removal of hexavalent chromium from effluent**.**

Mozumder *et al.* (2008) studied on kinetics and mechanism of Cr(VI) adsorption onto tea-leaves waste. In that research, adsorption equilibrium and kinetic experiments have been conducted in batch mode to evaluate Cr(VI)-tea-leaves waste system. The equilibrium data followed the Langmuir adsorption isotherm and the adsorption was viewed as a physiochemical reversible process. The model satisfactorily described both kinetics and equilibrium data. The adsorption and desorption rate constants were evaluated from the best fitting of the isotherm model. It was found that the rate constants were not dependent on initial concentration and adsorbent doses. $pH_{zpc}$ of the adsorbent was evaluated as 4.2 ± 0.1, and below that pH, the adsorbent surface was found to be positively charged. Adsorption of Cr(VI) was found highly pH dependent, and the removal efficiency dropped sharply from 95% to 10% when pH of the system changed from 2 to 5. The surface functional groups of tea-leaves waste (before and after adsorption) were analyzed by Fourier Transform Infrared (FTIR) and the amine groups were found to take part in the adsorption of Cr(VI). The experimental result inferred that electrostatic attraction between the surface and species is one of the major adsorption mechanisms for binding metal ions to tea-leaves waste**.**

Dehghani *et al.* (2016) conducted a research on removal of chromium (VI) from aqueous solution using treated waste newspaper as a low-cost adsorbent: Kinetic modeling and isotherm studies. In that study, treated waste newspaper (TWNP) was used to remove chromium (VI) from aqueous solution using batch experiments. The adsorption parameters optimized were: initial Cr (VI) concentration (50 $mg \cdot L^{-1}$), contact time (60 min.) adsorbent dose (3.0 $g \cdot L^{-1}$), and solution pH (3.0). The experimental data fitted well to Langmuir isotherm ($R^2 = 0.98$); maximum adsorption capacity 59.88 $mg \cdot g^{-1}$) and pseudo-second-order kinetic model kinetic model. The rate constant $k_2$ varied from 0.0019 to 0.0068 at initial Cr (VI) concentration from 5 to 20 $mg \cdot L^{-1}$. It was observed that adsorption of Cr (VI) was pH dependent. The percentage removal of Cr (VI) was 59.88 $mg \cdot g^{-1}$ at pH 3.

Tejada-Tover *et al.* (2018) conducted a research on adsorption kinetics of Cr (VI) using modified residual biomass in batch and continuous system. The research focused on comparative study of adsorption capacity of cassava peel (CP), Lemon Peel (LP) and their chemical modification with citric acid (CA), (CP-CA and LP-CA). The adsorption process was carried out in batch and continuous systems in order to determine the effects of biosorbent particle-size and pH of the solution on Cr(VI) removal yield. The findings of the study were 54% and 56 % were the removal yields for unmodified cassava peel and citric acid-modified cassava peel respectively. Freundlich model was found to be the best to describe the adsorption process. The kinetic model was adjusted to the pseudo-second order model and Elovich model for both modified and unmodified biomasses regarding adsorption isotherms.

Park and Tavlarides (2008) studied on adsorption of chromium (VI) from aqueous solutions using an imidazole functinalized adsorbent. Removal of chromium from aqueous solutions was investigated using an imidazole functionalized sol-gel adsorbent. The adsorbent has been formed by the sol gel synthesis method. Batch adsorption equilibrium studies show a decrease in chromium uptake capacity with increase in pH in the range from 2 to 9, and the uptake capacity at pH 2.5 is found to be 2.93 $mmol \cdot g^{-1}$ (152 $mg \cdot g^{-1}$). The Langmuir adsorption isotherm gives a satisfactory fit of the adsorption date. A kinetic study conducted with different concentrations of chromium (VI) solution in batch reactor shows a rapid rate of adsorption. The adsorption shows a high selectivity toward Cr(VI) and negligible adsorption of Cu(II), Ni (II) and Zn (II).

Hossain *et al* (2005) conducted a research on optimization of parameters for Cr(VI) adsorption on used black tea leaves. Dynamic characteristics of Cr(VI) sorption on used black tea leaves (UBTLs) as a low-cost adsorbent were studied. Batch experiments were conducted to evaluate the effects of Cr(VI) concentration, solution pH and temperature on the removal process. Both adsorption and reduction, involved in the process, are affected by the process parameters. The adsorption kinetics is described successfully using pseudo-second order rate equation. Experimental and calculated kinetic data for

equilibrium were well expressed by Langmuir isotherm. The solution pH has a profound effect on the adsorption rate. The rate constant increases linearly with an increase in temperature, and the low value of activation energy of adsorption,16.30 $kJ \cdot mol^{-1}$ indicates that Cr (VI) is easily adsorbed on UBTLs.

Hossain *et al*. (2013) studied kinetic and thermodynamic studies of the adsorption of crystal violet onto used black tea leaves. The effects of concentration, solution pH and temperature on adsorption kinetics were carried out in batch process. Kinetic studies have shown that the adsorption data partially follow the simple first order, second order and pseudo-second order kinetic equations for different initial concentration at pH 2.0. The equilibrium amount adsorbed, equilibrium concentration and rate constant were calculated from better fitted pseudo-second order kinetic plots for different initial concentrations at pH 2.0. The equilibrium amount adsorbed, equilibrium concentration and rate constant were calculated from the pseudo-second order kinetic plots, which were fitted better, for different temperature. The equilibrium amount adsorbed increased with increase of temperature, indicated endothermic nature of adsorption. Using the pseudo-second order rate constant, the activation energy ($E_a$) of adsorption was determined and the value was found to be 83.1kJ/mol revealed the process is chemisorptions. The equilibrium amount adsorbed was found to be increased with increase of pH from 2.0 to 6.0 indicating electrostatic interaction between cationic CV with anionic surface of UBTL dominated at higher pH due to the low zero point charge pH of UBTL.

Hajira *et al*. (2009) conducted a research on remedial of azo dyes by using household used black tea as an adsorbent .In that study, used black tea and its impregnates were used as an adsorbents for the removal of textile dyes, such as methylene blue and malachite green. The study showed that used black tea and its impregnate exhibit have adsorption tendency for dyes used in textile. By applying batch method, the adsorption process were carried out at various temperatures ranging from 303 to 318 K under the optimized conditions of concentration, stay time and amount of adsorbent. The

researchers applied Langmuir adsorption isotherm, Freundlich adsorption isotherm and D-R adsorption isotherm to find the values of the constants of these different models of isotherms. Thermodynamic parameters like free energy, $G^o$, enthalpy, $H^o$ and entropy $S^o$ were also calculated.

Hossain (1997) studied on the removal of Cr (VI) from environment by adsorption on used tea leaves. The adsorption equilibrium and hence the equilibrium time was found to be affected by the dose of adsorbent, initial solute concentration and pH of the solution.

Ho and McKay (1999) studied on the pseudo-second order model for sorption process. They reported that many adsorbent having heterogeneous surface like tea leaves, peat, cypress leaves, rice husk, peanut hull carbon etc. follow pseudo second order kinetics.

Ozlen *et al*., (2003) studied on the adsorption of some textile dyes by hexadecyl trimethyl ammonium bentonite. The experimental results show that the brown alga *C.barbatula* could be used as alternative low cost adsorbent in the removal of MB. The adsorption kinetics and isotherm parameters were found from pseudo first order, pseudo second order, and Langmuir, Freundlich and Dubinin Radushkevich equations.

Gupta and Babu (2009) perform investigation on the adsorption of Chromium (VI) by a low cost adsorbent prepared from tamarind seeds. They reported that tamarind seeds had maximum adsorption capacities of 11.08 mg $g^{-1}$ at pH of 7 but the maximum adsorption took place on pH range 1-3.

Hossain *et al*., (2006) studied on the kinetics of Cr (VI) adsorption on used black tea leaves. He calculated the equilibrium concentration and equilibrium amount adsorbed by using pseudo second order kinetics and reported that the calculated and experimental values are nearly same.

Nevine *et al*., (2007) conducted a research on removal of reactive dye from aqueous solutions by adsorption onto activated carbons prepared from sugarcane baggase pith.

He successfully applied three adsorbent prepared from baggase pith for the removal of reactive orange dye from the aqueous solution. Adsorption was influenced by various parameters such as initial pH, initial dye concentrations and dose of the adsorbrnt. The data were in good agreement with both Langmuir and Freundlich isotherms and it is found to follow the pseudo second order kinetics model.

Xiu-Yan *et al*. (2008) performed investigation on the study on the adsorption kinetics of acid red 3B on expended graphite. They reported that the adsorption of the system can well described by the pseudo second order kinetic model, equilibrium time and half adsorption time $t^{1/2}$ decreases with the increase of temperature.

Vasu (2008) studied on the removal of Rhodamine B and Malachite Green from aqueous solutions by activated carbon. He shown that direct carbonization of tamarind fruit shells can be used as a means of preparation of activated carbon that can be successfully used for the removal of cationic dyes like rhodamine B and malachite green. He also pointed out that the kinetics of the pH dependant sorptions were found to be film-diffusion controlled at low dye concentrations and particle diffusion controlled at high dye concentrations. Temperature variation studies indicated that the sorptions were endothermic.

Maximova and Koumanova (2008) studied on the equilibrium and kinetics of adsorption of basic dyes onto perfil from aqueous solutions. They reported that the sorption amount increases with the increase of initial concentration .The agitation rate slighty influenced the kinetics and the adsorption kinetics was succesfully fit by a pseudo-second order kinetic model.

Alzaydien (2009) studied on the adsorption of methylene blue from aqueous solution onto a low-cost natural ripolin. They reported that the natural ripolin, abundant low-cost clay, can be used as sorbent for the removal of methylene blue dye from aqueous solution. The amount of dye sorbed was found to vary with initial pH, tripoli dose,

methylene blue concentration and contact time· the sorption equilibrium data were found to fit the Langmuir isotherm, Pseudo-second-order rate equation.

Khan *et al*., (2011) studied on Adsorption of Rhodamine B dye from aqueous solution onto acid activated mango (*Magnifera indica*) leaf powder: their Equilibrium, kinetic and thermodynamic studies showed that the mango leaf powder (MLP) adsorbent is capable for the removal of RB with high affinity and capacity indicating its potential use as a low cost adsorbent in near future.

Ansari *et al.* (2011) studied on the adsorption, bisorption and decolourization of Rhodamine-B and Basic Violet- 2 Using Fungi isolated (Aspergillus flavus, Fusarium sp. and Aspergillus niger.) form the soil of textile dye industry and waste water disposal sites .They shown that maximum decolourisation has occurred at 30 ppm. The efficiency of dead fungal biomass in removing the dye by biosorption was done. Aspergillus flavus was an efficient biosorbent among the three fungal isolates.

# 1.5 Objective of the Study

Medical science support that most of the diseases are borne by contaminated water. So it is quite pertinent to protect water from every possible source of contamination. Unfortunately, surface water is severely contaminated by anthropogenic activities. Chromium (VI) is highly toxic in biological systems. Contamination of environment, particularly aquatic environment by chromium (VI) has been identified as a severe problem throughout the world So, the presence of chromium (VI) as a heavy metal ion

in aquatic systems poses dreadful threat to the aquatic environment due to its acute toxicity to human life and other life-forms. Unlike organic pollutants, (the majority of which are susceptible to biological degradation) chromium (VI) ion does not degrade into harmless end-product like other heavy metal ions (Gupta, *et al*., 2001).

Chromium (VI) causes various life-spoiling diseases in human health. It is a carcinogenic tetragenic, mutagenic renal and kidney damaging metal ion, it is, therefore, quite urgent to remove it from aquatic body by means of a simple, efficient and eco-friendly technique to remove the harmful chromium (VI) from aquatic body.

In recent years, several techniques have been used to remove chromium (VI) from aquatic body. Of these, adsorption has proven to be a simple, cost-friendly and promising technique for removal of chromium (VI) from aquatic body using different biomass as adsorbents (Hossain *et al*. 2005 and Dhankumar *et al*., 2007).

Since the researchers have drawn their keen attention to tea leaves as potential adsorbents and by this period of time, Used Black Tea Leaves (UBTL) (Hossain *et al*. 2005) and Cooked Tea Leaves (CTL) (Dhankumar *et al*., 2007) have already been studied. Dust Black Tea Leaves are untreated waste materials of tea in the tea processing-plant in Bangladesh. It is an available and a cost-free biomass. The objective of this research work focuses on the evaluation of the efficiency of Dust Black Tea Leaves (DBTL) as an adsorbent for adsorptive removal of chromium (VI) from aquatic solution. To evaluate the efficiency the adsorbent the following investigations have been carried out:

1. Preparation and characterization of DBTL using different techniques.
2. Identification of the removal phenomena
3. Investigation of the kinetics of adsorption and its affecting parameters such as concentration, solution pH, temperature, particle size of adsorbent, etc.
4. Determination of thermodynamic parameters

5. Estimation of equilibrium for the adsorption
6. Evaluation of equilibrium adsorption and its affecting parameters such as temperature, solution pH, particle size of adsorbent, etc.
7. Analysis of the Cr(VI) adsorbed DBTL surface by ATR-IR, SEM and EDX to evaluate the surface morphology and the nature of interaction of the system to elucidate the adsorption mechanism.
8. Desorption and recovery of adsorbed chromium from adsorbed surface.

# *Chapter 2*

# EXPERIMENTAL

# 2. EXPERIMENTAL

## 2.1 Instruments

1. Attenuated Total Reflectance IR Spectrometer (ATR-IR) (Shimadzu, Japan).
2. Computerized UV Spectrophotometer: UV-1650A, Shimadzu, Japan
3. BET Surface Analyzer (BEL Japan, Inc., Belsorp Adsorption/Desorption Data Analysis Software – Version 6.1.0.8.
4. SEM (Scanning Electron Microscope), JSEM-6490, JEOL, Japan
5. EDX (Energy Dispersive X-ray), JED 2300, JEOL, Japan
6. Thermostat-controlled water-bath Shaker: NTS-4000A, Tokyo Rikakikai Co., Ltd., Japan.
7. Centrifuge Clipton: DSC- N158A, BS 4402, Nickel Electric Ltd., England.
8. pH meter (HANNA Instrument, pH 211, Romania)
9. Electronic Digital Beam Balance (FR-200, Shimadzu, Japan)
10. Teflon made volumetric flasks, agitation bottles and centrifuge tubes
11. Sieve (Endecotts Ltd., England)
14. Pipettes

## 2.2 Materials

### 2.2.1 Chemical Reagents

1. 1, 5-Diphenylcarbazide (DPC), Merck, Germany
2. Potassium dichromate (VI) ($K_2Cr_2O_7$), Merck, Germany
3. Buffer: pH 4.01 and pH 6.86
4. Sodium azide, ($NaN_3$), Merck, Germany
6. Amonia solution, ($NH_4OH$), Merck, Germany
7. Sulphuric acid, ($H_2SO_4$), BDH

8. Phosphoric acid, ($H_2PO_4$), BDH
9. Double distilled water
10. Dust Black Tea Leaves (DBTL), Tea Processing Plant in "Bangladesh Tea Research Institute (BTRI)", Srimongal, Banglades.

All chemical reagents used in this study were of analytical grade.

## 2.2.2 Adsorbent

Dust Black Tea Leaves (DBTL) collected from Tea Processing Plant in "Bangladesh Tea Research Institute (BTRI)", Srimongal, Bangladesh was used as adsorbent in this study.

### 2.2.2.1 Preparation of adsorbent

About 500 g. Dust Black Tea Leaves (DBTL) was added to about 1000 mL of double distilled water. The DBTL mixed with double distilled water was boiled for about 3 hours. After 3 hours, the boiled tea leaves was washed with hot distilled water followed by cold distilled water several times repeatedly until the colour of tea liquor was completely disappeared. After washing with cold double distilled water, the tea leaves were initially dried at room temperature and then dried in oven at 105$^{o}$C for 12 hours. Dried tea leaves were grinded and then sieved through metallic device of mesh-sizes 106 µm 150 µm 212 µm and 450 µm to obtain different particlesize of the adsorbent. Different particle-sizes of the DBTL were mentioned in Table 2.1. Different sizes of DBTL were kept in air-tight bottles in dessicator for using in adsorption experiments.

# 2.3 Characterization of Adsorbent

## 2.3.1 Physical Observation of DBTL

Dust Black Tea Leaves (DBTL) collected from the Tea Processing Plant was observed attentively and unwanted materials were separated manually. The optical views of collected DBTL, gruinded particles and hot water treated DBTL were captured with high-resolution digital camera and shown in Figure 3.1.

## 2.3.2 Determination of BET Surface Area and Pore Size Distribution

The specific surface area and pore size distribution of prepared Dust Black Tea Leaves (DBTL) was determined by BET Surface Analyzer (Belsorp mini-II, BEL Japan, Inc., Belsorp Adsorption/Desorption Data Analysis Software – Ver 6.1.0.8). Nitrogen adsorption-desorption isotherms on DBTL were measured at different relative pressures, $p/p_o$, ranging from 0.01-0.99, and used to determine the specific surface area and pore size distribution of DBTL. Experimental conditions and measured values are presented in table 3.1. Figures 3.2 show the adsorption and desorption isotherms and Figure 3.3 shows the BET plot of $N_2$ adsorption on DBTL.

The pore size and pore volume distribution of prepared DBTL was calculated from the $N_2$ desorption data using BJH (Barrett, Joyner and Halenda, 1951) method. The BJH pore size distribution of prepared DBTL (<106 μm in diameter) is presented in Figures 3.4.

## 2.3.3 ATR-IR Studies on Prepared Adsorbent

The ATR-IR spectrum of prepared DBTL was measuded directly, without making a pillets with potassium bromide, using a Attenuated Total Reflectance IR Spectrometer (ATR-IR, Shimadzu, Japan). The of ATR-IR spectrum is shown in Figure 3.6 and characteristic peaks with their positions are given in Table 3.2.

### 2.3.4 SEM and EDX Studies of Surface Morphology

To investigate the surface morphology and chemical composition of preapred DBTL, SEM and EDX analysis of prepared DBTL were performed. To take a SEM microgram, at first a conductive carbon tape was adhered to the SEM stub. Then a small amount of DBTL particles were spread on the conducting tape, which makes conduction between the sample and the stub. Then SEM micrograms of solid DBTL were taken at different magnification using voltage of 20 and 25 kV by a Scanning Electron Microscope (JSEM-6490, JEOL, Japan). The energy dispersive X-ray (EDX) spectra of DBTL under the same SEM were taken at ×2,000 magnification for chemical composition. The SEM and EDX spectra of prepared DBTL were presented in Figure 3.7 and 3.8, respectively. The composition of DBTL are presented in Table 3.3.

# 2.4 Analysis of Adsorbate

Potassium dichromate, $K_2Cr_2O_7$ of analytical grade was used as a source of chromium (VI). Chromium (VI), in form of dichromate ion, $Cr_2O_7^{2-}$ and $HCrO_4^{-1}$ was the adsorbate in this study (Cotton and Wilkinson, 1974).

### 2.4.1 Preparation of Chromium (VI) Solution

A stock solution of 1000 $mg \cdot L^{-1}$ chromium (VI) was prepared by dissolving appropriate amount of potassium chromate, $K_2Cr_2O_7$ (MW: 294.22 $g \cdot mol^{-1}$) in double-distilled water. Aqueous solutions of Cr(VI) of different concentration, as per requirement in this study, were prepared by diluting appropriately with double-distilled-water. In this study, accurate concentration of every solution of Cr(VI) was measured by colorimerically.

### 2.4.2 Absorption Spectrum Cr(VI)-1,5 DPC Complex Solution

In this colorimetric, 1,5-Diphenylcarbazide (DPC) is the suitable reagent which forms a red-violet complex of Cr(VI)-1,5-DPC at a suitable condition (Am. Pub. Health. Ass.,

1985 and Hossain, 1997). For the measurement of absorption maximum, 2 mL freshly prepared 0.5% of 1,5-DPC solution in acetone was added to 100 mL of 1.2 $mg \cdot L^{-1}$ of Cr(VI) aqueous acidic solution at 30 ± 0.2 °C. After 10 minutes, for complex formation, the absorption spectrum was measured using UV-visible Spectrophotometer (UV-1650A, Shimadzu, Japan). It should be mentioned that to make the acidic solution of Cr(VI) for complex formation with 1,5-DPC, proper amount of 1:1 $H_2SO_4$ was added to the Cr(VI) solution to maintain its acidity at 0.2 M. Before addition of $H_2SO_4$, 5 drops of 85% $H_2PO_4$ was added to the Cr(VI) solution for protecting the interferences of iron if present the source solution. Recorded absorption spectrum of Cr(VI)-1,5-DPC complex is presented in Figure 3.9.

## 2.4.3 Construction of Calibration Curve for Cr(VI)-1,5 DPC Complex

For construction of a calibration curve, 25 mL 5.0 $mg \cdot L^{-1}$ of Cr(VI) solution was prepared from freshly prepared 100 $mg \cdot L^{-1}$ potassium dichromate solution. A number of 100 mL standard solutions of concentration ranging from 0.1 to 1.2 $mg \cdot L^{-1}$ were prepared using micro-burette by diluting the appropriate volume taken from freshly prepared 5.0 $mg \cdot L^{-1}$ solution. Each of these standard-solutions was made suitable for formation of chromium (VI)-1,5-Diphenylcarbazide complex by adding the reagents as outlined in the clause 2.4.2 to each of the standard solutions. Then 2 mL of freshly prepared 0.5% 1, 5-Diphylcarbazide solution were added to each of the Cr(VI) solutions. Then, each of the solutions, in its term, was allowed to stand for 10 minutes for complete formation of Cr(VI)-1, 5-diphenylcarbazide complex (red-violet). Thus accurate concentrations of Cr(VI) solutions were measured at the predetermined $\lambda_{max}$= 543 nm and at temperature (30 ± 0.2 °C) using UV-visible Spectrophotometer (UV-1650A, Shimadzu, Japan). Measured absorbances were plotted against the known concentrations of Cr(VI) as shown in Figure 3.10, a calibration curve.

## 2.4.4 Determination of Cr(VI) and Cr(III) in $K_2Cr_2O_7$ Solution

The existence of hexavalent and trivalent chromium in aqueous solution of potassium dichromate were determined using the following method described elsewhere (Am. Pub. Health. Ass., 1985 and Hossain, 1997). 1.0 mL of about 100 $mg \cdot L^{-1}$ potassium dichromate solution was taken in a 100 mL volumetric flask. The solution was diluted up to the mark of the flask by double-distilled-water and acids ere added as described in last section. CrVI)-1,5-Diphenylcarbazide complex was formed by adding 2 mL of freshly prepared 0.5% 1,5-Diphylcarbazide solution to the acidic Cr(VI) solution. Absorbance of the solution was measured at the pre-determined $\lambda_{max}$= 543 nm by using the UV-visible spectrophotometer and thus the concentration of Cr(VI) in the potassium dichromate solution was calculated using the calibration curve and presented in Table 3.5.

For the determination of existence Cr(III) in the potassium dichromate ($K_2Cr_2O_7$) solution, 1.0 mL of the freshly prepared 101.333 $mg \cdot L^{-1}$ $K_2Cr_2O_7$ solution was taken in an 100 mL volumetric flask and it was initially diluted up to 50 mL with double-distilled-water. Then 2 drops of freshly prepared 4% potassium permanganate ($KMnO_4$) were added to the solution and the solution was boiled gently for 10 minutes to oxidize Cr(III) completely to Cr(VI), if the original sample of $K_2Cr_2O_7$ contained any Cr(III). Then 10 drops of freshly prepared 0.5% sodium azide ($NaN_3$) solution were added to decolorize the solution by reduction of excess sodium azide. The solution was cooled and then it was made suitable for formation of red-violet complex of Cr(VI)-1,5-Diphenylcarbazide by adding the aforesaid reagents. Double distilled water was added up to the mark of the 100 mL volumetric flask. 2.0 mL 0.5% 2 mL 0.5% 1, 5-Diphylcaebazide solution were added to the solution and allowed for 10 minutes for complete formation of the red-violet Cr(VI)-1, 5-Diphenylcarbazide complex. Absorbance of the solution was measured at the wave-length, $\lambda_{max}$ = 543 nm using the UV-visible spectrophotometer. The measured absorbance was for the total chromium [Cr(VI)+Cr(III)], calculated by using the calibration curve. Thus the content of Cr(III) in the source solution was determined from the subtraction of the content of Cr(VI) from the content of total chromium [Cr(VI) + Cr(III)]. These results are presented in Table 3.5.

# 2.5 Investigation of Removal Phenomena

To investigate the process involved in the removal of Cr(VI) by DBTL, a batch kinetic removal experiment was performed by suspending 2.5 mg of the DBTL in 25 mL of Cr(VI) solution at pH 2.0. The suspensions were mixed on a shaker with a constant speed of 150 rpm. The solutions were withdrawn at certain time intervals and separated solutions were analyzed for Cr(VI) and Cr(III) using a UV-visible spectrophotometer as described previously. The processes such as adsorption and reduction involved in this removal were calculated using equations 3.3-3.8. Experimental results are presented in Table 3.6 and Figure 3.11.

# 2.6 Experiments for Adsorption Kinetics

Adsorption kinetic experiments were carried out in batch process using different initial concentrations of Cr(VI) solution, different pH of the solution, different temperature and different particle-sizes of DBTL, considering the affecting factors for the adsorption of Cr(VI) on DBTL in this study.

## 2.6.1 Effect of Concentration

To determine the effect of concentration, 0.0025 g dry DBTL was taken in each of 6 bottles containing 25 mL of a fixed concentration of Cr(VI) solution at pH 2.0 as an optimum pH for DBTL (estimated by preliminary experiment) and was shaken in a thermostatic mechanical shaker (HAAKE SWB20, Fissions Ltd., Germany) at 30.0 ± 0.2°C. After shaking of different time of intervals, the mixtures were separated by centrifuge. Separated supernatants for different time intervals were analyzed for the remaining concentration of Cr(VI) and total chromium using UV-visible spectrophotometer at $\lambda_{max}$ 543 nm as described in 2.4.4 section. Initial concentrations of Cr(VI) and Cr(III) in source solution were also determined using same procedure described in section 2.4.4. From the analytical data, amount of Cr(VI) adsorbed on DBTL and the amount of Cr(VI) reduced to Cr(III), in presence of DBTL were

calculated by using equation 3.9. Similar kinetic experiments were carried out using different initial concentrations of Cr(VI) ranging from 25 to 250 $mg \cdot L^{-1}$ and presented in Table 3.7 – 3.9. In each case, by deduction of reduced amount of Cr(VI), variation of pure amount adsorbed of Cr(VI) on DBTL with time are presented in Figure 3.12.

## 2.6.2 Effect of Temperature

To investigate the effect of temperature on the adsorption kinetics, adsorption kinetic experiments as described last section were carried out at 15, 30 and 50 °C using same initial concentration of 100 $mg \cdot L^{-1}$ of Cr(VI) solution, pH 2.0 and remaining other parameters were fixed. Separated supernatants for different time intervals at different temperatures were analyzed for the remaining concentration of Cr(VI) and total chromium using UV-visible spectrophotometer at $\lambda_{max}$ 543 nm as described in 2.4.4 section. The variation of pure amount adsorbed of Cr(VI) with time for different temperatures are given in Tables 3.15-3.16 and Figure 3.23. .

## 2.6.3 Effect of pH

The effect of pH on the adsorption kinetic was investigated by performing kinetic experiment at different initial pH of solution using same initial concentration of 100 $mg \cdot L^{-1}$ Cr(VI) solution at 30.0 ± 0.2 °C, remaining other parameters fixed. After performing the kinetic experiments at different pH, supernatants for different time intervals at different pH were analyzed for the remaining concentration of Cr(VI) and total chromium using UV-visible spectrophotometer at $\lambda_{max}$ 543 nm as described in 2.4.4 section. The variation of pure amount adsorbed of Cr(VI) with time for different initial pH of solution are given in Tables 3.23-3.24 and Figure 3.33.

## 2.6.4 Effect of Particle Size of Adsorbent

To determine the effect of pH on the adsorption kinetic, adsorption kinetic experiments as described last section were carried out with <106, 150, 212 and 450 μm diameter particle sizes of DBTL using same initial concentration of 100 $mg \cdot L^{-1}$ of Cr(VI) solution

at 30.0 ± 0.2 °C, pH 2.0 and remaining other parameters were fixed. Separated supernatants at different time intervals for different particle sizes were analyzed for the remaining concentration of Cr(VI) and total chromium using UV-visible spectrophotometer at $\lambda_{max}$ 543 nm as described in 2.4.4 section. The variation of pure amount adsorbed of Cr(VI) with time for different particle sizes are given in Tables 3.25-3.26 and Figure 3.42. .

# 2.7 Experiments for Equilibrium Adsorption

## 2.7.1 Estimation of Equilibrium Time

Equilibrium time is important for adsorption study. To determine the equilibrium, 0.0025 g dry DBTL was taken in each of 6 bottles containing 25 mL of 100 $mg \cdot g^{-1}$ Cr(VI) solution at pH 2.0 and was shaken in a thermostatic mechanical shaker (HAAKE SWB20, Fissions Ltd., Germany) at 30.0 ± 0.2°C. After shaking of different time of intervals, the mixtures were separated by centrifuge. Separated supernatants for different time intervals were analyzed for the remaining concentration of Cr(VI) and total chromium using UV-visible spectrophotometer at $\lambda_{max}$ 543 nm as described in 2.4.4 section. Initial concentrations of Cr(VI) and Cr(III) in source solution were also determined using same procedure described in section 2.4.4. By deduction of reduced amount of Cr(VI), variation of pure amount adsorbed of Cr(VI) on DBTL with time are presented in Table 3.30 and Figure 3.50.

## 2.7.2 Effect of Temperature on Adsorption Isotherm

To evaluate the effect of temperature on adsorption isotherm, equilibrium adsorption experiments were performed at different temperatures. In this experiment, 0.0025 g dry DBTL was taken in each of 6 bottles containing 25 mL of 6 different concentrated solution of Cr(VI) at pH 2.0 and was shaken in a thermostatic mechanical shaker (HAAKE SWB20, Fissions Ltd., Germany) at 30.0 ± 0.2°C. After 6 hours of shaking as a pre-determined equilibrium time, the mixtures were separated by centrifuge. Separated

supernatants from each bottle were analyzed for the remaining concentration of Cr(VI) and total chromium using UV-visible spectrophotometer at $\lambda_{max}$ 543 nm as described in 2.4.4 section. Initial concentrations of Cr(VI) and Cr(III) in each of 6 different solutions were also determined using same procedure described in section 2.4.4. From the analytical data, equilibrium concentration of Cr(VI) and equilibrium amount adsorbed of Cr(VI) on DBTL for each of 6 bottles/initial concentration were calculated by using equation 3.9. Similar equilibrium experiments were carried out at 15 and 50 $^{o}$C keeping other conditions in same. The experimental and derived data are presented in Tables 3.31-3.33 and adsorption isotherms at different temperatures are shown in Figure 3.51.

## 2.7.3 Effect of pH on Adsorption Isotherm

The effect of pH of solution on adsorption isotherm was investigated by performing equilibrium adsorption experiments at solution pH 2.0, 4.0, 6.0 and 8.0, and temperature at 30.0 ± 0.2 °C, keeping other conditions in same as described in 2.6.2 section. From the analytical data for different pH, equilibrium concentration of Cr(VI) and equilibrium amount adsorbed of Cr(VI) on DBTL for each of 6 bottles/initial concentration were calculated by using equation 3.9. The experimental and derived data are given in Tables 3.39-3.41 and adsorption isotherms at different pH of solution are presented in Figure 3.61.

## 2.7.4 Effect of Particle Size Adsorption Isotherm

To investigate the effect of particle size of DBTL, equilibrium adsorption experiments were performed with <106, 150, 212 and 450 μm diameter particle sizes of DBTL using solution pH 2.0 and at 30.0 ± 0.2 °C, remaining other parameters were fixed as described in 2.6.2 section. From the analytical data for different particle size, equilibrium concentration of Cr(VI) and equilibrium amount adsorbed of Cr(VI) on DBTL for each of 6 bottles were calculated by using equation 3.9. The experimental and derived data are given in Tables 3.43-3.45 and adsorption isotherms at different pH of solution are presented in Figure 3.67.

# 2.8 Analysis of Cr(VI) Adsorbed DBTL

In equilibrium study, after 6 hours adsorption of Cr(VI) on DBTL at pH 2.0 and 30 °C, the residual DBTL was washed and dried in electric oven at 105 $^{o}$C. The dried DBTL was characterized by ATR-IR, SEM and EDX as follows:

## 2.8.1 ATR-IR Study on Cr(VI) Adsorbed DBTL

Required amount of dried DBTL sample was put in the ATR-IR sample holder (ATR-IR, Shimadzu, Japan) and spectrum was recorded from 600 to 4000 $cm^{-1}$. The ATR-IR spectrum of Cr(VI) adsorbed DBTL is presented in Figure 3.73 and its comparison with un-adsorbed DBTL is presented in Figure 3.74 and Table 3.47.

## 2.8.2 SEM and EDX Analysis of Cr(VI) Adsorbed DBTL

A small portion of Cr(VI) adsorbed dried DBTL was taken on a sample holder of Scanning Electron Microscope (SEM: JSEM-6490, JEOL, Japan) and micrograms were taken at 20 keV with 2,000, 5,000 and 20,000 Magnifications. Figure-3.75 shows the SEM micrograms with different magnifications. EDX spectrum of a specific point on SEM microgram in Figure 3.75 is recorded at 20 keV with 2,000 magnifications and shown in Figure 3.76. Elemental composition is presented in Table 3.48.

Again, the point analysis of SEM microgram was performed by EDX spectrum at 7 (A-G) different places on SEM microgram presented in Figure 3.79. Variation of composition at different places is presented in Table 3.50 and Figure 3.80.

# 2.9 Desorption and Recovery of Cr

For desorption study, 0.1 g DBTL was put in a 50 mL of 100 $mg \cdot L^{-1}$ Cr(VI) solution at pH 2.0 and shaken at 30 $^{o}$C. After 6 hours, Cr(VI) adsorbed DBTL was separated from the clear solution and 25 mL of 2M NaOH was added to the adsorbed DBTL. Within 2 hours, the DBTL was completely decomposed in solution and all adsorbed chromium back to the solution. The whole process is presented in Figure 3.81.

*Chapter 3*

# RESULTS AND DISCUSSION

# 3. RESULTS AND DISCUSSION

Hexavalent chromium exists in aqueous system as an anionic forms ($HCrO_4^-$, $Cr_2O_7^{2-}$ and $CrO_4^{2-}$) which can be removed either by reduction to chromium (III) or by adsorption on solid surface (Hossain, 2006). Adsorption is the accumulation of chemical species on solid surface. It is an easy technique for the separation of dissolved substances from their mixtures. Reduction is suitable for high concentration of chromium (VI) and further treatment of chromium (III) is required. But at low concentrations, removal is more effective by adsorption on solid adsorbents. Therefore, from the view point of environmental aspect to remove low concentration of chromium (VI), we have chosen the adsorption process and dust black tea leaves (DBTL) were selected as a low-cost adsorbent, prepared from west of black tea leaves.

## 3.1 Adsorbent

### 3.1.1 Preparation of the Adsorbent

The west of black tea leaves as a bi-product of tea industries was collected from the Tea Leaves Processing Plant of Bangladesh Tea Research Institute (BTRI), Srimongal, Sylhet, Bangladesh. An optical view of the waste black tea leaves, before preparation of adsorbent, is shown in **Figure 3.1(a, b & c)**. The waste black tea leaves was washed with boiling distilled water for several times to removed all colored materials and dried in air for 12 hours followed in oven dried at 110 $^oC$ for 6 hours. Dried leaves were grinded and sieved to received different particle sizes of dust black tea leaves (DBTL) of < 106, 106-150, 150 - 212 and 212 - 450 μm. The optical view of the prepared DBTL was shown in **Figure 3.1.**

### 3.2 Characterization of Adsorbent

The adsorption of solutes on solid is affected by the particular physical-chemical properties of the adsorbent. These properties include particle size, surface area and porosity, structural morphology, nature and quantities of surface sites, etc. These are

important properties that control the adsorptive characteristics of adsorbents were investigated. Dust Black tea Leaves was analyzed by the following techniques to investigate its characteristics that play active role in adsorbing chromium (VI) on it.

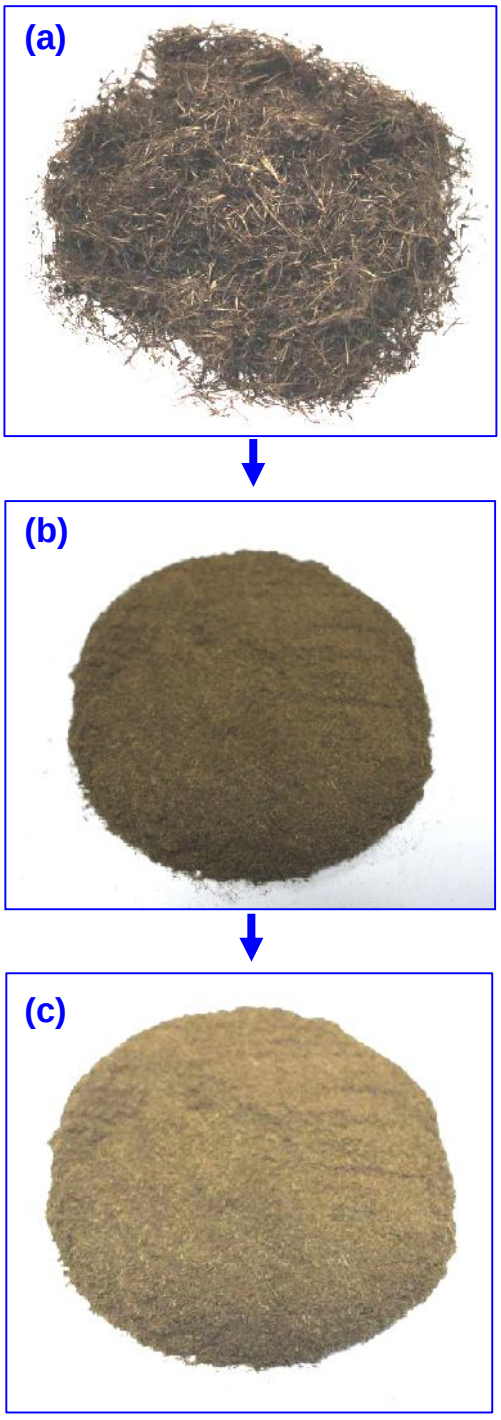


**Figure 3.1:** Optical view of the prepared adsorbent (DBTL) from waste of Black Tea Leaves: (a) Waste Black Tea Leaves, (b) Grounded Waste Black Tea Leaves and (c) Dust Black Tea Leaves (DBTL) as an adsorbent.

### 3.2.1 Determination of BET surface area

The specific surface area is the detectable area of solid surface per unit mass of material ($m^2 \cdot g^{-1}$). Surface area of a solid can be determined from the plot of the measurement of gas adsorption on respective solid. Its value depends on the method and experimental conditions employed, and on the molecular size of probe gas used. BET plot, based on BET equation (3.1), is widely used for determination of surface area (BET 1938).

$$\frac{p}{V_a(p_o - p)} = \frac{1}{V_m c} + \frac{c-1}{V_m c}\left(\frac{p}{p_o}\right) \qquad (3.1)$$

where, $V_a$ = volume of gas adsorbed by unit mass of solid, $V_m$ = gas volume at the monolayer coverage, $c$ = BET constant, $p$ = absolute pressure, $p_o$ = saturated pressure of gas. The specific surface area of prepared DBTL was determined from the $N_2$/77K adsorption method (BET Surface Analyzer: Belsorp mini-II, BEL Japan, Inc., Belsorp Adsorption/Desorption Data Analysis Software – Ver 6.1.0.8). Figures 3.2 show the adsorption and desorption isotherm of < 106 μm in diameter DBTL. Figures 3.3 shows the BET plot, ($p/V_a(p_o-p)$) as a function of ($p/p_o$), of prepared DBTL. The $N_2$ adsorption isotherm was then analyzed to determine the specific surface area using equation (3.2) (Hossain 2006).

$$S_m = X_m A_m N_A \times 10^{-18} \qquad (3.2)$$

where $S_m$ is the specific surface area ($m^2 \cdot g^{-1}$), $X_m$ is the amount adsorbed for monolayer coverage ($mol \cdot g^{-1}$), $A_m$ is the surface area of adsorbed ($N_2$) molecule ($nm^2$), $N_A$ is the Avogadro's number ($mole^{-1}$) and $10^{-18}$ is conversion factor between nm and $m^2$. The calculated value of BET specific surface area of DBTL is 1.7032 $m^2 \cdot g^{-1}$. The specific surface area of prepared DBTL is very small compare with activated carbon (200-1400 $m^2 \cdot g^{-1}$).

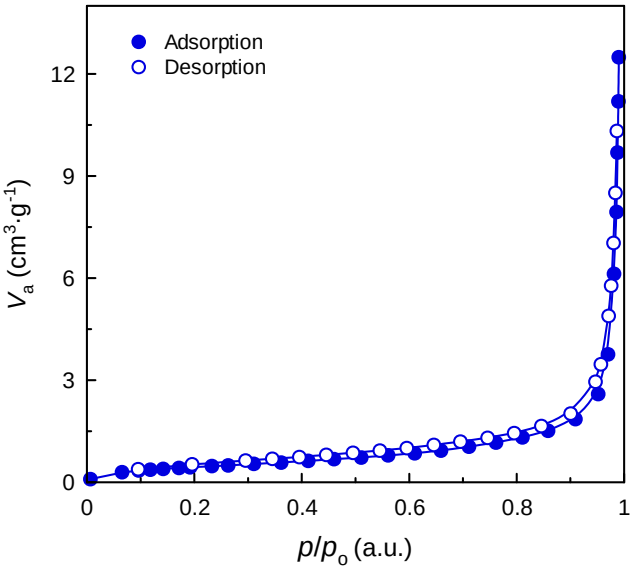


**Figure 3.2:** $N_2$ adsorption-desorption isotherms of prepared DBTL at 77K.

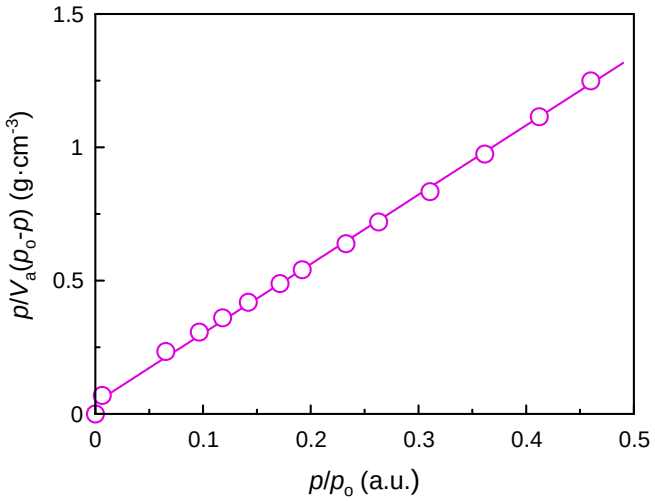


**Figure 3.3:** BET-plot of $N_2$ adsorption on prepared DBTL at 77 K.

### 3.2.2 Pore volume and pore size distribution

The pore volume and pore size distribution are presented by derivatives $dA_p/dr_p$ or $dV_p/dr_p$ as a function of $r_p$, where $A_p$, $V_p$ and $r_p$ are the wall area, volume and radius of the pores. The pore volume and pore size distribution can be determined from different plots constructed from gas adsorption-desorption measurements. Among those BJH plot is commonly used to represents the mesopore size distribution (Barrett, Joyner and Halenda, 1951). Here the pore size and pore volume distribution of prepared DBTL was

calculated from the $N_2$ desorption data using BJH (Barrett, Joyner and Halenda, 1951) method. Figures 3.4 shows the BJH pore size distribution of prepared DBTL (< 106 μm in diameter). The figure shows different sizes of pore are available in DBTL and the maximum pore volume is at 1 to 2 nm pore radius. Total pore volume ($1.9117\times10^{-2}$ $cm^3\cdot g^{-1}$), mean pore radius (22.448 nm) and radius of pore peak area (1.66 nm) were calculated and presented in Table 3.1.

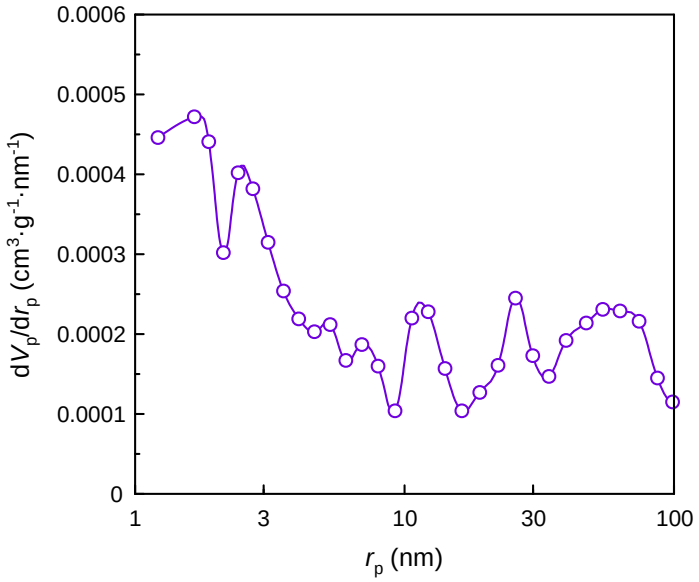


**Figure 3.4:** BJH plot from $N_2$ desorption isotherm for the pore size distribution of prepared DBTL (< 106 μm in diameter) (where $r_p$= mean pore radius).

**Table 3.1** BET surface area, pore volume and pore volume distribution of prepared DBTL.

| Experimental condition | | Parameter | Estimated values |
|---|---|---|---|
| Sample mass | : 0.1720 (g) | $S_{mBET}$ | : 1.7032 ($m^2\cdot g^{-1}$) |
| Adsorption temp. | : 77 (K) | Total pore volume | : $1.9117\times10^{-2}$ ($cm^3\cdot g^{-1}$) |
| Adsorbate | : $N_2$ | Mean pore diameter | : 44.896 (nm) |
| Leak amount | : 1.917 ($Pa\cdot min^{-1}$) | $V_p$ | : $1.9220\times10^{-2}$ ($cm^3\cdot g^{-1}$) |
| $V_m$ | : 0.3913 ($cm^3\cdot g^{-1}$) | $a_p$ | : 2.3459 ($m^2\cdot g^{-1}$) |
| $C$ | : 40.251 (a.u.) | $r_{p\text{-peak}}$ (Area) | : 1.66 (nm) |

### 3.2.3 Chemical composition of adsorbent

Tea leaves are basically of only one species of plant, *Camellia sinesis* (Mokgalaka *et al.*, 2004). Chemical composition of tea leaves depends on their type. Chemical analyses reported by Hurler (1972) shows that almost 80% of the composition of tea leaves is insoluble in water (Harler, 1972). Insoluble part of tea leaves consists of mainly cellulose (37%), polyphenols (25%) and hemi-cellulose and lignin (14%). The structure of unit-cell of cellulose and its molecular structure are shown Figures 3.5(a) and 3.5(b), respectively. The polar hydroxyl groups in cellulose and phenolic group of polyphenols, main constituent of tea leaves, work as the active site for the uptake of adsorbates.

**(i)**

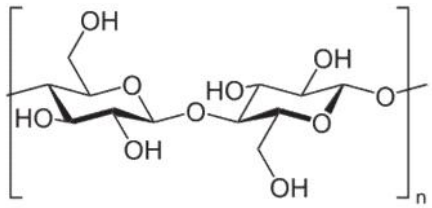

**(ii)**

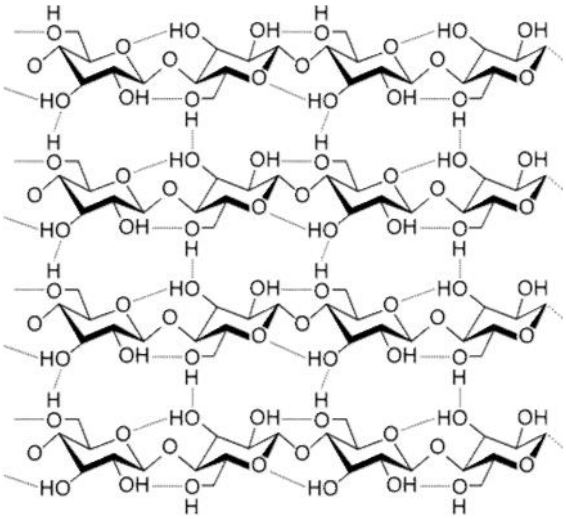

**Figure 3.5(a):** (i) Structure of unit-cell of Cellulose and (ii) Molecular structure of Cellulose.

**(i)**

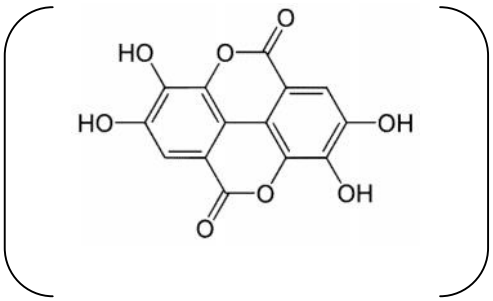

**(ii)**

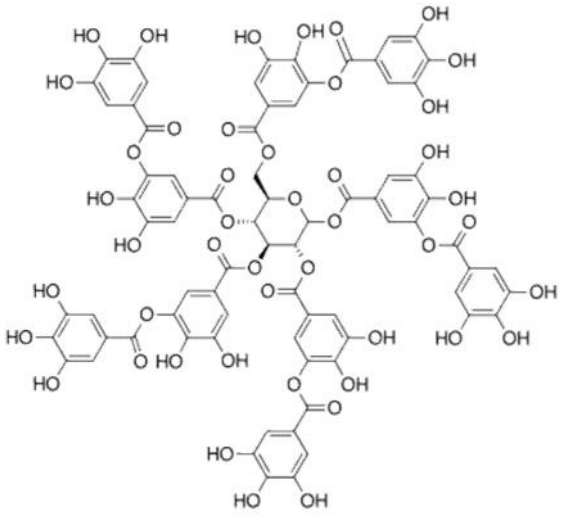

**Figure 3.5(b): (i)** Structure of unit-cell of Polyphenol and (**ii)** Molecular structure of Polyphenols.

## 3.2.4 ATR-IR Studies on Prepared Adsorbent

Attenuated Total Reflectance Infra-red (ATR-IR) spectroscopic study on prepared DBTL was performed to characterize the composition of prepared DBTL. Figure 3.6 shows the ATR-IR spectra of prepared DBTL using Attenuated Total Reflectance IR Spectrometer (ATR-IR, Shimadzu, Japan). The characteristic peaks with their positions are given in Table 3.2. The broad peak at 3342.64 $cm^{-1}$ indicates the presence of – OH groups in DBTL. Other peaks at 1624.06, 1379.10, 1265.30 and 1045.42 $cm^{-1}$ for C=C, -C-H, C-O-H and C-O, respectively shown in Table 3.2 with reference peaks of functional groups.

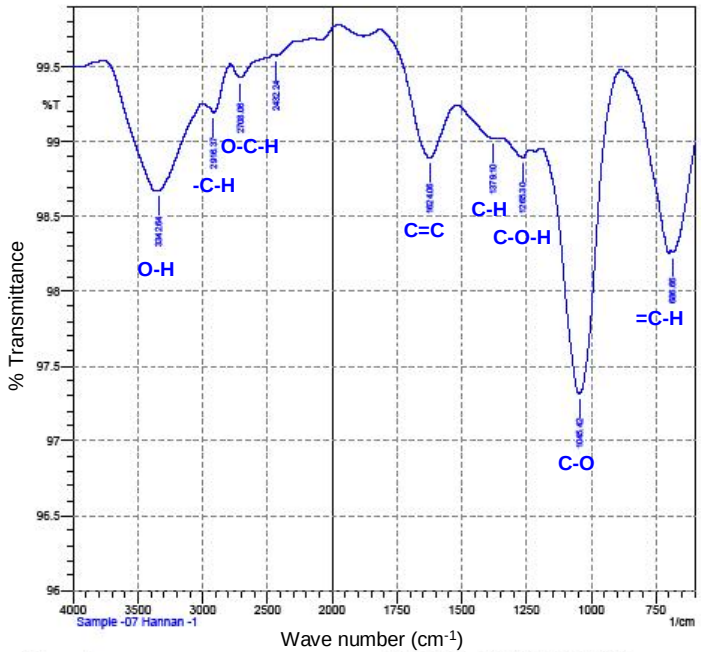


**Figure 3.6:** ATR-IR spectrum of prepared adsorbent, DBTL.

**Table 3.2** Peak positions in FTIR spectrum of prepared DBTL.

| **Peak positions ($cm^{-1}$)** | | **Characteristics Gr.** |
|---|---|---|
| **DBTL** | **Reference values** | |
| 3342.64 | 3400-3200 | -O-H (str) (H-bonded) |
| 2916.37 | 3000-2850 | -C-H (str) |
| 2708.06 | 2850.79 | -O-C-H (def) |
| 1624.06 | 1680-1620 | >C=C (aromatic) |
| 1379.10 | 1375 | -C-H (bending) |
| 1265.30 | 1440-1220 | C-O-H (bending) |
| 1045.42 | 1300-1000 | C-O-C (def) |
| 686.66 | 667 | =C-H |

### 3.2.5 SEM and EDX Studies of Surface Morphology

The surface morphology of the prepared Dust Black Tea Leaves (DBTL) was investigated by Scanning Electron Microscope (SEM) (JSEM-6490LA, JEOL, Japan). The SEM micrograph of prepared tea leaves is shown in Figure 3.7 which shows heterogeneous surface morphology of the prepared DBTL. The energy dispersive X-ray (EDX) spectra were taken at 2000 magnification for Dust Black Tea Leaves (DBTL) using the same scanning electron microscope. The EDX spectrum of DBTL is presented in Figure 3.8 and the composition of DBTL is given in Table 3.3. Carbon and oxygen are the main constituents of DBTL. A summery of the physico-chemical characteristics of Dust Black Tea Leaves (DBTL) is presented in Table 3.4.

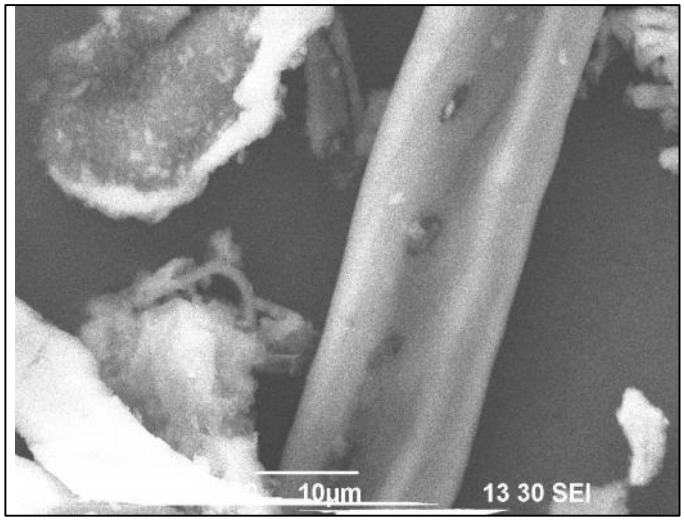


**Figure 3.7:** SEM micrograph of prepared DBTL (×2000).

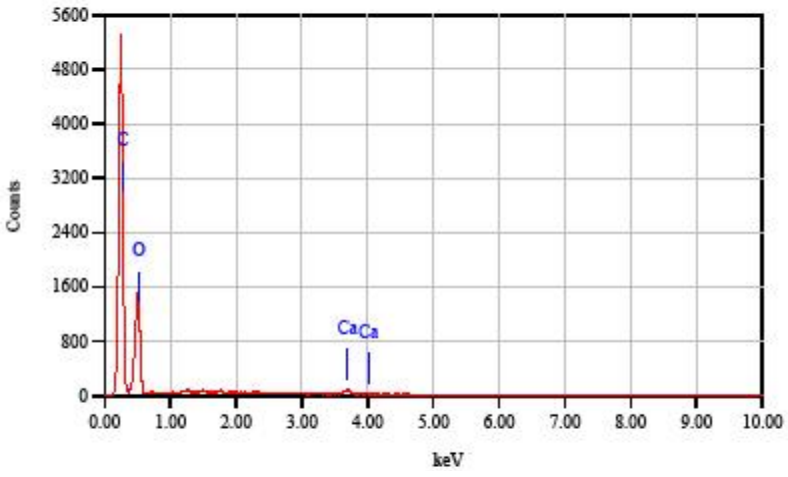


**Figure 3.8:** EDX spectrum of prepared DBTL (×2000).

**Table 3.3** Elemental composition of DBTL estimated by energy dispersive X-ray (EDX).

| Elements | Mass (%) | Atom (%) |
|---|---|---|
| **C** | 45.99 | 53.42 |
| **O** | 53.03 | 46.24 |
| **Ca** | 0.98 | 0.34 |

**Table 3.4:** Physico-chemical characteristics of Dust Black Tea Leaves (DBTL).

| No. | Parameters | Value |
|---|---|---|
| 1 | Cellulose (main composition) | 37 (%) |
| 2 | Particle size | < 106, 106-150, 150-212 and 212-450 µm |
| 3 | Specific surface area | 1.7032 ($m^2 \cdot g^{-1}$) |
| 4 | Total pore volume | $1.9117 \times 10^{-2}$ ($cm^3 \cdot g^{-1}$) |
| 5 | Mean pore diameter | 44.896 (nm) |
| 6 | Maximum pore size diameter | 1.66 (nm) |
| 7 | Nature of surface | Heterogeneous (SEM) |
| 8 | Elemental composition | C, O and Ca |

# 3.3 Analysis of Chromium in Aqueous Solution

Aqueous solution of potassium dichromate ($K_2Cr_2O_7$) prepared in this study was considered as an aquatic environment, contaminated with chromium (VI). In this study, chromium (VI) in aqueous solution of potassium dichromate is considered as an adsorbate. Since there is a possibility of existing some chromium (III) in aqueous solution of potassium dichromate, in addition to chromium (VI), it is essential to determine the percentage of chromium (VI) and chromium (III) in the potassium dichromate solution as well as its residual stages during the adsorption study.

Trace level of chromium both hexavalent and trivalent can not be determined directly by spectroscopic measurement. Hexavalent chromium in trace level can be determined by UV-visible spectroscopic method after complex formation with 1,5-Diphenylcarbazide in an acidic medium. Trivalent chromium can not reacts 1,5-Diphenylcarbazide. Therefore, trivalent chromium in trace level can be determined after oxidation to hexavalent chromium and complex forming with 1, 5-Diphenylcarbazide in an acidic medium (Hossain 1997).

## 3.3.1 Absorption Spectrum of Cr(VI)-1,5 DPC Complex

Colorimetric method (Am. PHA, 1985) using UV Spectrophotometer is a sophisticated method by which accurate concentration of chromium (VI) in trace level can be determined. In this colorimetric method, under a specific condition, an intense colour of Cr(VI)-1,5-Diphenylcarbazide complex was developed and measured the absorbance using UV Spectrophotometer. Absorption maximum ($\lambda_{max}$) is an important parameter for spectroscopic studies. Figure 3.9 shows the absorption spectrum of Cr(VI)-1,5-DPC complex where absorption maximum ($\lambda_{max}$) is 543 nm which was used for construction of calibration curve as well as the whole analysis.

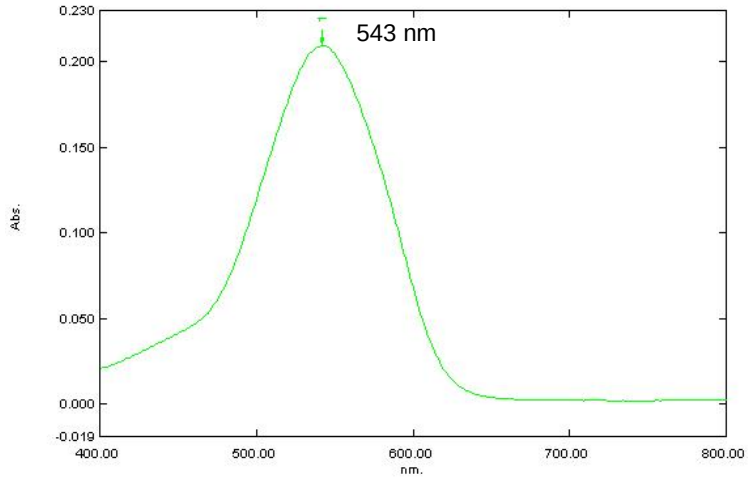


**Figure 3.9:** Absorption spectrum of 0.25 mg·$L^{-1}$ Cr(VI)-1,5 DPC complex.

## 3.3.2 Construction of Calibration Curve for Chromium (VI)-1,5 DPC Complex

Calibration curve is the representation of variation of absorbance with the respective concentration of an analyte. Figure 3.10 shows a straight line obtained from the plot of the absorbance *vs.* concentration of chromium (VI)-DPC complex in the range from 0.1 to 1.2 mg·$L^{-1}$. The straight line with $R^2$ = 0.9966, passing through the origin suggests the validity of the Beer-Lambert law. Using this law, molar absorption coefficient (£) of chromium (VI)-1,5-Diphenyl-carbazide complex was obtained. It was found to be 0.60 L·$mg^{-1}$·$cm^{-1}$ at the $\lambda_{max}$= 543 nm and at temperature (30 ± 0.2 °C). This value was used to calculate the concentration of chromium (VI) solutions in every experiment in this study.

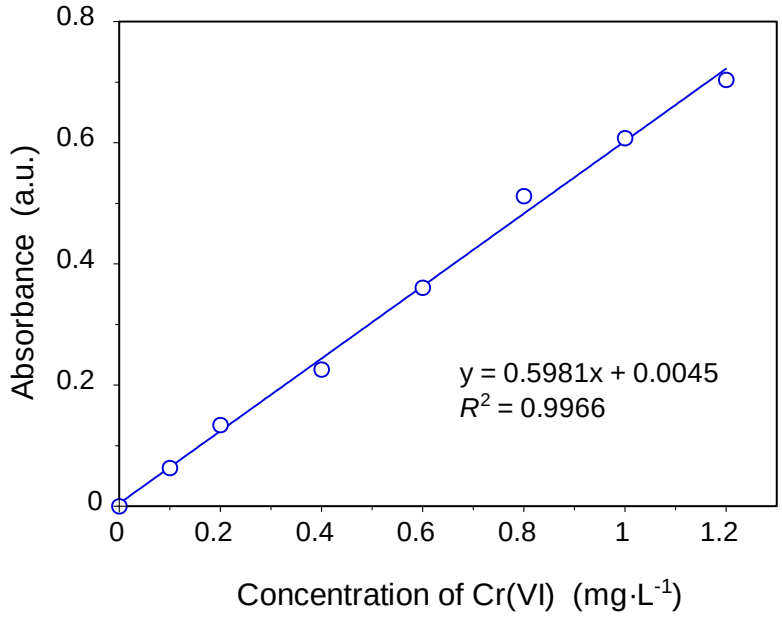


**Figure 3.10:** Calibration curve of chromium (VI)-1,5 DPC complex at $\lambda_{max}$= 543 nm and 30.0 ± 0.2 $^{o}$C.

## 3.4. Analysis of Chromium (VI) in $K_2Cr_2O_7$ Solution

Since objective of this study was to remove only Cr(VI) from aqueous solution in trace level using adsorptive method, existence of chromium (III) in the original source sample of $K_2Cr_2O_7$ was determined using the following conditions:

**Conditions of Analysis:**

| | |
|---|---|
| Sample | : Aqueous solution of $K_2Cr_2O_7$ |
| Reagent for complex formation | : 1,5 -diphenyle-carbazide (DPC) |
| Solution pH for complex formation | : 0.7 |
| Analysis temperature | : 30 ± 0.2 °C |
| Oxidizing agent for reduction of Cr(III) | : $KMnO_4$, $H_2SO_4$ |

The results in Table 3.5 show that the original sample of potassium dichromate, $K_2Cr_2O_7$ contains 98.848 % chromium (VI) and 1.152 % chromium (III) by concentration in $mg \cdot L^{-1}$. Such small amount of chromium (III) might be formed due to reduction of chromium (VI) by the dissolved oxygen in water. Similar result was reported for the removal of chromium (VI) by used black tea leaves (Hossain 1997).

**Table 3.5** Estimation of chromium (VI) reduced to chromium (III) in the sample of potassium dichromate, $K_2Cr_2O_7$.

| $C_o$, Cr(VI) ($mg \cdot L^{-1}$) | $C_{oxidation}$ ($mg \cdot L^{-1}$) | $C_{Cr(III)}$ ($mg \cdot L^{-1}$) | $C_{Cr(III)}$ (%) | $C_{Cr(VI)}$ (%) |
|---|---|---|---|---|
| 101.333 | 102.500 | 1.167 | 1.150 | 98.85 |

$C_o$ is the initial concentration of chromium (VI), $C_{oxidation}$ is the concentration of chromium (VI) after oxidation, $C_{Cr(III)}$ is the concentration chromium (III) oxidized to chromium (VI) and $C_{Cr(VI)}$ is the initial concentration of chromium (VI).

# 3.5 Investigation of Removal Phenomena

The phenomena involved in the removal of chromium (VI) from aqueous solution in presence of Dust Black Tea Leaves (DBTL) were investigated. Preliminary experiments showed that both adsorption and reduction were involved in the process and minimum reduction was observed at pH 2.0. Thus a kinetic experiment was performed to investigate the effect of contact time on adsorption as well as reduction using the following experimental conditions.

**Experimental Conditions**

| | |
|---|---|
| Volume of chromium (VI) solution | : 25 mL |
| Solution pH | : 2.0 |
| Amount of DBTL | : 0.0025 g |
| Particle size of DBTL | : < 106 µm |
| Adsorption temperature | : 30 ± 0.2 °C |
| Agitation rate | : 150 rpm |

**Table 3.6** Estimation of chromium (VI) adsorbed and reduced to chromium (III) during the removal process using DBTL.

| $t$ (min) | $C_{Cr(III)}$ ($mg \cdot L^{-1}$) | $C_o$ ($mg \cdot L^{-1}$) | $C_t$ ($mg \cdot L^{-1}$) | $C_T$ ($mg \cdot L^{-1}$) | $C_R$ ($mg \cdot L^{-1}$) | $q_R$ ($mg \cdot g^{-1}$) | $q_{ad.}$ ($mg \cdot g^{-1}$) | $q_T$ ($mg \cdot g^{-1}$) |
|---|---|---|---|---|---|---|---|---|
| 15 | 1.167 | 101.333 | 90.500 | 92.833 | 2.333 | 11.51 | 85.00 | 96.50 |
| 30 | | | 86.500 | 89.667 | 3.167 | 19.74 | 116.66 | 136.40 |
| 60 | | | 83.500 | 87.167 | 3.667 | 24.67 | 141.66 | 166.33 |
| 120 | | | 81.000 | 85.333 | 4.333 | 31.24 | 160.00 | 191.24 |
| 240 | | | 78.500 | 83.500 | 5.000 | 37.83 | 178.33 | 216.16 |
| 360 | | | 77.500 | 83.333 | 5.833 | 46.05 | 180.00 | 226.05 |

where, $t$ is the time for agitation of chromium (VI) solution in contact with 0.0025 g of DBTL, $C_{Cr(III)}$, is the concentration of chromium (III) existing in the sample of potassium dichromate (VI), $C_o$ is the initial concentration of chromium (VI) and $C_t$ is the concentration of chromium (VI) after agitation time $t$.

The total concentration ($C_T$) of chromium(VI), {Cr(VI) + Cr(III)} existing in the solution after agitation ($mg \cdot L^{-1}$), the concentration of reduced ($C_R$) chromium (VI) to chromium (III) during the removal process ($mg \cdot L^{-1}$), the equilibrium amount ($q_R$) of chromium (VI) reduced to chromium (III) during agitation, the equilibrium amount ($q_{ad}$) of chromium (VI) adsorbed on DBTL during agitation, and the total amount ($q_T$) of chromium (VI) removed from chromium (VI) solution during the removal process were calculated using following equations (3.3-3.8) and presented in Table 3.6 and Figure 3.11.

$$C_T = \mathrm{Cr(VI)} + \mathrm{Cr(III)} \tag{3.3}$$

$$C_R = (C_o - C_t - C_{Cr(III)}) \tag{3.4}$$

$$q_R = \frac{C_R \times V}{W_{DBTL}} \tag{3.5}$$

$$q_{ad} = \frac{(C_o - C_t - C_R) \times V}{W_{DBTL}} \tag{3.6}$$

$$q_T = q_R + q_{ad} \tag{3.7}$$

$$\mathrm{Removal \cdot efficiency} = \frac{C_o - C_t - C_R}{C_o} \times 100 \tag{3.8}$$

where $V$ is the volume of chromium (VI) agitated in contact with DBTL (L) and $W$ is the amount of DBTL agitated in contact with chromium (VI) solution (g). The Figure 3.11 shows that the adsorption as well as total removal rapidly increased with increase in contact time and reached to the steady value. Where as the reduction increased slowly but not more than 20% of total removal. The values of percent removal of chromium (VI) by the DBTL, may be referred to as the sorption efficiency was also calculated. The result showed that 82.31%, by mass, of the total removal of chromium (VI) during the process is due to the pure adsorption on DBTL and 17.69 %, by mass, is removed due to reduction to chromium (III).

The reduction of chromium (VI) to chromium (III) during the removal process, in presence of DBTL, may be due to the presence of active sites of DBTL surface. They are reduced to chromium (III) by the available lone-pair of electrons of OH groups of

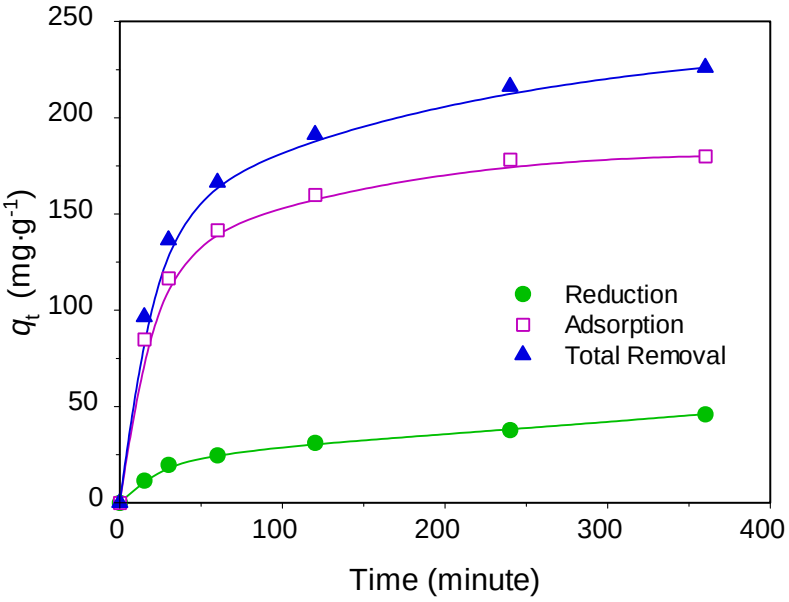


**Figure 3.11:** Variation of removal phenomena (adsorption, reduction and total removal) of chromium (VI) with time for the uptake of chromium (VI) on DBTL from aqueous solution at pH 2.0 and 30.0 ± 0.2 $^{o}$C.

cellulose, a major constituent of tea leaves and phenolic groups of polyphenols. As the objective of this study was to investigate only adsorptive removal of chromium (VI), the amount of chromium (VI) reduced to chromium (III) was estimated in case of every experiment in the removal process, and the reduced amount of chromium (VI) was deducted from the total amount of chromium removed in every case to find out the actual amount of chromium (VI) adsorbed.

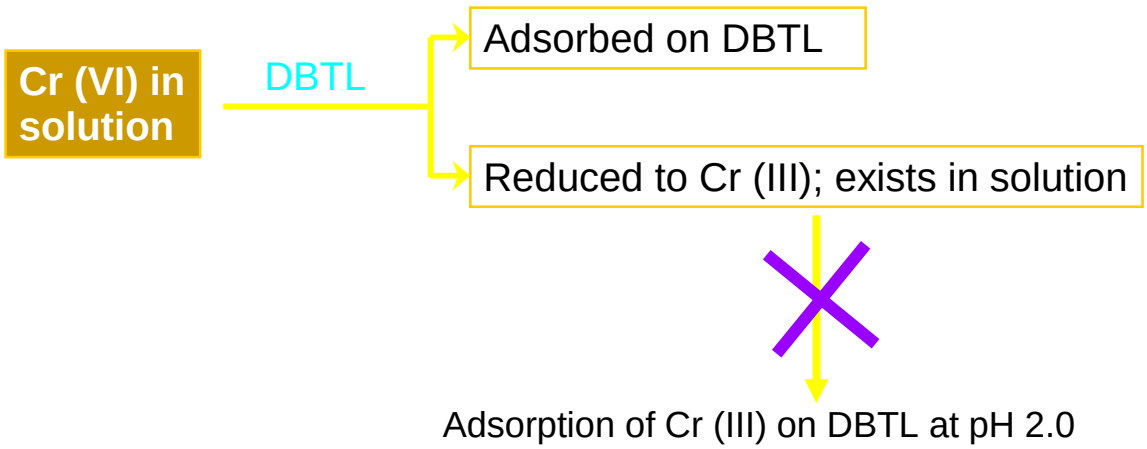

# 3.6 Kinetics of Adsorption

## 3.6.1 Effect of Concentration on Adsorption Kinetics

The effect of concentration on the adsorption kinetics was investigated using the following experimental conditions:

**Experimental Conditions**

| | |
|---|---|
| Volume of chromium (VI) solution | : 25 mL |
| Concentration of chromium (VI) solution | : 25 – 250 $mg \cdot L^{-1}$ |
| Solution pH | : 2.0 |
| Amount of DBTL ($W_{DBTL}$) | : 0.0025 g |
| Particle size of DBTL | : < 106 µm |
| Adsorption temperature | : 30 ± 0.2 °C |
| Agitation rate | : 150 rpm |
| Agitation time ($t$) | : 0 to 6 hrs |

The amounts of chromium (VI) adsorbed on DBTL with different times were calculated using the following equation (3.9).

$$q_t = (C_o - C_t - C_R) \times \frac{V}{W_{DBTL}} \qquad (3.9)$$

where, $C_o$ stands for the initial concentration of chromium (VI) in solution, $t$ stands for agitation time, $C_t$ stands for concentration of chromium (VI) after time $t$ and before oxidation, $C_T$ stands for the total concentration of chromium (VI) {conc. of chromium (VI) + conc. of chromium (III) due to reduction} existing in the solution after time, $t$ and $C_R$ stands for the concentration of chromium (VI) reduced to chromium (III) after the time, $t$ and $q_t$ stands for the amount of chromium (VI) adsorbed on per gram DBTL at the time, $t$ and presented in Table 3.7 to 3.9.

The amounts of chromium (VI) adsorbed on DBTL as function of time for different initial concentrations were shown in Figure 3.12. It was evident that the maximum amount of chromium (VI), in case of each of different initial concentration of chromium

**Table 3.7** Effect of concentration on the adsorption kinetics of chromium (VI) on DBTL at pH 2.0 and 30 ± 0.2 $^{o}$C.

| $C_o$ (mg·L$^{-1}$) | $t$ (min.) | $C_t$ (mg·L$^{-1}$) | $C_T$ (mg·L$^{-1}$) | $C_R = C_T - C_e$ (mg·g$^{-1}$) | $q_t$ (mg·g$^{-1}$) |
|---|---|---|---|---|---|
| 25.417 | 15 | 22.667 | 23.250 | 0.583 | 21.67 |
| | 30 | 21.708 | 22.542 | 0.834 | 28.75 |
| | 60 | 20.958 | 22.000 | 1.042 | 34.17 |
| | 120 | 19.292 | 20.458 | 1.166 | 49.59 |
| | 240 | 16.875 | 17.625 | 1.583 | 77.92 |
| | 360 | 15.625 | 17.500 | 1.875 | 79.17 |
| 51.167 | 15 | 46.417 | 46.500 | 0.083 | 46.67 |
| | 30 | 44.500 | 44.667 | 0.167 | 65.00 |
| | 60 | 43.000 | 43.583 | 0.583 | 75.84 |
| | 120 | 39.833 | 40.667 | 0.834 | 105.00 |
| | 240 | 37.583 | 39.500 | 1.917 | 116.67 |
| | 360 | 36.250 | 39.417 | 3.167 | 117.50 |
| 101.333 | 15 | 90.50 | 92.833 | 2.333 | 85.00 |
| | 30 | 86.50 | 89.667 | 3.167 | 116.66 |
| | 60 | 83.500 | 87.167 | 3.667 | 141.66 |
| | 120 | 81.000 | 85.333 | 4.333 | 160.00 |
| | 240 | 79.000 | 83.500 | 4.500 | 178.33 |
| | 360 | 77.500 | 83.333 | 5.833 | 180.00 |
| 150.750 | 15 | 141.250 | 141.750 | 0.500 | 90.00 |
| | 30 | 137.000 | 138.250 | 1.250 | 125.00 |
| | 60 | 133.500 | 135.500 | 2.000 | 152.50 |
| | 120 | 130.250 | 134.000 | 3.750 | 167.50 |
| | 240 | 124.250 | 129.750 | 5.500 | 210.00 |
| | 360 | 122.500 | 129.500 | 7.000 | 212.50 |
| 201.667 | 15 | 192.00 | 192.333 | 0.333 | 93.34 |
| | 30 | 187.667 | 189.000 | 1.333 | 126.67 |
| | 60 | 182.667 | 186.000 | 3.333 | 156.67 |
| | 120 | 179.667 | 184.333 | 4.666 | 173.34 |
| | 240 | 171.000 | 178.333 | 7.333 | 233.34 |
| | 360 | 170.333 | 178.000 | 7.667 | 236.67 |
| 251.250 | 15 | 241.250 | 241.667 | 0.417 | 95.83 |
| | 30 | 236.667 | 238.333 | 1.666 | 129.17 |
| | 60 | 231.250 | 235.000 | 3.750 | 162.50 |
| | 120 | 227.083 | 232.500 | 5.417 | 187.50 |
| | 240 | 220.000 | 227.500 | 7.5000 | 237.50 |
| | 360 | 218.750 | 227.083 | 8.333 | 241.67 |

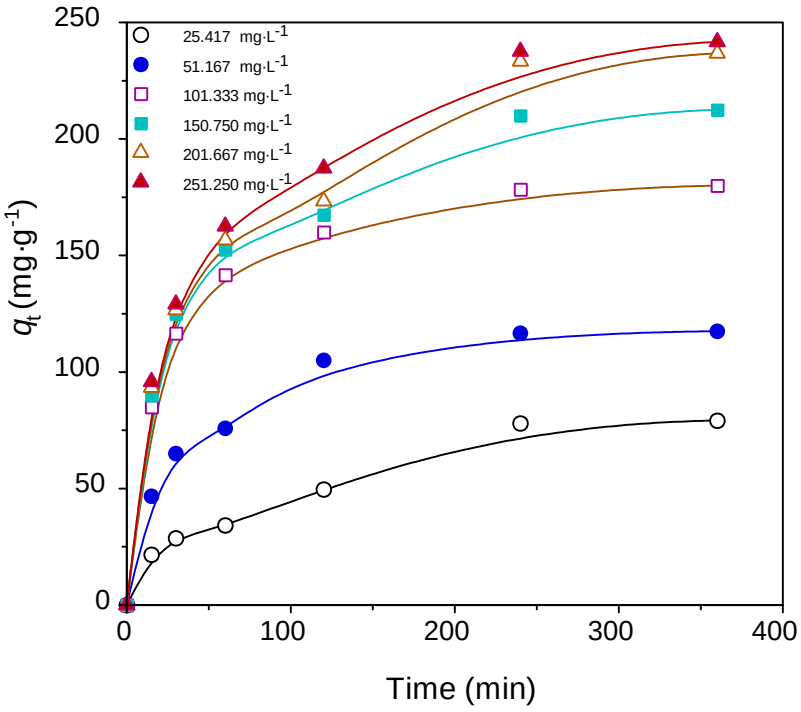


**Figure 3.12:** Effect of concentration on the variation of amount adsorbed of chromium (VI) on DBTL with time from aqueous solution at pH 2.0 and 30.0 ± 0.2 $^{o}$C.

(VI) was adsorbed on the DBTL and the equilibrium time was independent of initial concentrations. The rate of adsorption was rapid during the initial period of time and gradually became slow in the later stages and became almost steady at 360 minutes. This was may be due fact that the chromium (VI) ions occupied the active sites in random ways because of maximum availability of sites on the surface of DBTL. The active sites on DBTL surfaces were being blocked with increase of time and hence the rate of adsorption was being slowed and at stage it became almost steady.

The adsorption kinetic data for different concentration were investigated using different kinetic equations such as first order, second order, pseudo-first order, pseudo-second kinetic, intraparticle diffusion and Elovich equations, to evaluate the feasibility of the adsorption of chromium (VI) on DBTL. Applicability of the equations was justified based on the value of coefficient corelation ($R^2 > 0.99$) of data fitness.

**Table 3.8** Derived-data for the application of first order, second order, pseudo-first order and pseudo-second kinetic equations to the adsorption chromium (VI) on DBTL for different initial concentrations.

| $C_o$ (mg·L$^{-1}$) | $t$ (min) | $C_t$ (mg·L$^{-1}$) | $q_t$ (mg·g$^{-1}$) | $t/q_t$ (min·g·mg$^{-1}$)} | ln $C_t$ (mg·L$^{-1}$) | $1/C_t \times 10^2$ (L.mg$^{-1}$) | log ($q_e$- $q_t$) (mg·g$^{-1}$) |
|---|---|---|---|---|---|---|---|
| 25.417 | 15 | 22.667 | 21.67 | 0.692 | 3.121 | 4.412 | 1.760 |
| | 30 | 21.708 | 28.75 | 1.043 | 3.078 | 4.607 | 1.703 |
| | 60 | 20.958 | 34.17 | 1.756 | 3.043 | 4.771 | 1.653 |
| | 120 | 19.292 | 49.59 | 2.420 | 2.960 | 5.183 | 1.471 |
| | 240 | 16.042 | 77.92 | 3.080 | 2.775 | 6.234 | 0.097 |
| | 360 | 15.625 | 79.17 | 4.547 | 2.749 | 6.400 | undefined |
| 51.167 | 15 | 46.417 | 46.67 | 0.321 | 3.838 | 2.154 | 1.850 |
| | 30 | 44.500 | 65.00 | 0.462 | 3.795 | 2.247 | 1.720 |
| | 60 | 43.000 | 75.84 | 0.791 | 3.761 | 2.326 | 1.620 |
| | 120 | 39.833 | 105.00 | 1.143 | 3.685 | 2.510 | 1.097 |
| | 240 | 37.583 | 116.67 | 2.057 | 3.627 | 2.661 | -0.081 |
| | 360 | 36.250 | 117.50 | 3.064 | 3.590 | 2.759 | undefined |
| 101.333 | 15 | 90.500 | 85.00 | 0.176 | 4.505 | 1.105 | 1.978 |
| | 30 | 86.500 | 116.66 | 0.257 | 4.460 | 1.156 | 1.802 |
| | 60 | 83.500 | 141.66 | 0.424 | 4.425 | 1.198 | 1.584 |
| | 120 | 81.000 | 160.00 | 0.750 | 4.394 | 1.235 | 1.301 |
| | 240 | 79.000 | 178.33 | 1.346 | 4.369 | 1.266 | 0.223 |
| | 360 | 77.500 | 180.00 | 2.000 | 4.350 | 1.290 | undefined |
| 150.750 | 15 | 141.250 | 90.00 | 0.167 | 4.951 | 0.708 | 2.088 |
| | 30 | 137.000 | 125.00 | 0.240 | 4.920 | 0.730 | 1.942 |
| | 60 | 133.500 | 152.50 | 0.393 | 4.894 | 0.749 | 1.778 |
| | 120 | 130.250 | 167.50 | 0.716 | 4.869 | 0.768 | 1.653 |
| | 240 | 124.250 | 210.00 | 1.143 | 4.822 | 0.805 | 0.398 |
| | 360 | 122.500 | 212.50 | 1.694 | 4.808 | 0.816 | undefined |
| 201.667 | 15 | 192.000 | 93.34 | 0.161 | 5.257 | 0.521 | 2.156 |
| | 30 | 187.667 | 126.67 | 0.237 | 5.235 | 0.533 | 2.041 |
| | 60 | 182.667 | 156.67 | 0.383 | 5.208 | 0.547 | 1.903 |
| | 120 | 179.667 | 173.34 | 0.692 | 5.191 | 0.557 | 1.802 |
| | 240 | 171.000 | 233.34 | 1.029 | 5.142 | 0.585 | 0.522 |
| | 360 | 170.333 | 236.67 | 1.521 | 5.138 | 0.587 | undefined |
| 251.250 | 15 | 241.250 | 95.83 | 0.157 | 5.486 | 0.415 | 2.164 |
| | 30 | 236.667 | 129.17 | 0.232 | 5.467 | 0.423 | 2.051 |
| | 60 | 231.250 | 162.50 | 0.369 | 5.443 | 0.432 | 1.899 |
| | 120 | 227.083 | 187.50 | 0.640 | 5.425 | 0.440 | 1.734 |
| | 240 | 220.000 | 237.50 | 1.011 | 5.394 | 0.455 | 0.620 |
| | 360 | 218.750 | 241.67 | 1.490 | 5.388 | 0.457 | undefined |

**Table 3.9** Derived-data for the application of Elovich equation to the adsorption of chromium (VI) on DBTL at pH 2.0 and 30.0 ± 0.2 º C for different initial concentrations.

| $C_o$ (mg·L-$^{1}$) | $t$ (min) | ln$t$ (-) | $q_t$ (mg·g$^{-1}$) |
|---|---|---|---|
| 25.417 | 15 | 2.708 | 21.67 |
| | 30 | 3.401 | 28.75 |
| | 60 | 4.094 | 34.17 |
| | 120 | 4.787 | 49.59 |
| | 240 | 5.481 | 77.92 |
| | 360 | 5.886 | 79.17 |
| 51.167 | 15 | 2.708 | 46.67 |
| | 30 | 3.401 | 65.00 |
| | 60 | 4.094 | 75.84 |
| | 120 | 4.787 | 105.00 |
| | 240 | 5.481 | 116.67 |
| | 360 | 5.886 | 117.50 |
| 101.333 | 15 | 2.708 | 85.00 |
| | 30 | 3.401 | 116.66 |
| | 60 | 4.094 | 141.66 |
| | 120 | 4.787 | 160.00 |
| | 240 | 5.481 | 178.33 |
| | 360 | 5.886 | 180.00 |
| 150.75 | 15 | 2.708 | 90.00 |
| | 30 | 3.401 | 125.00 |
| | 60 | 4.094 | 152.50 |
| | 120 | 4.787 | 167.50 |
| | 240 | 5.481 | 210.00 |
| | 360 | 5.886 | 212.50 |
| 201.667 | 15 | 2.708 | 93.34 |
| | 30 | 3.401 | 126.67 |
| | 60 | 4.094 | 156.67 |
| | 120 | 4.787 | 173.34 |
| | 240 | 5.481 | 233.34 |
| | 360 | 5.886 | 236.67 |
| 251.250 | 15 | 2.708 | 95.83 |
| | 30 | 3.401 | 129.17 |
| | 60 | 4.094 | 162.50 |
| | 120 | 4.787 | 187.50 |
| | 240 | 5.481 | 237.50 |
| | 360 | 5.886 | 241.67 |

### 3.6.1.1 First order kinetic equation

The verification of the first order kinetic equation (Eq. 3.10) (Hossain *et al.*, 2005, 2011, 2012, 2013; Gupta *et al*., 2001; Cimino *et al*, 2000) was done by plotting $\ln C_t$ *vs*. time.

$$\ln C_t = k_1 t + \ln C_o \qquad (3.10)$$

where, $C_t$ is the final concentration of chromium(VI) after time $t$ ($mg \cdot L^{-1}$), $C_o$ is the initial concentration of chromium(VI) ($mg \cdot L^{-1}$) and $k_1$ is first order rate constant, which has units of time. Figure 3.13 as a plot of $\ln C_t$ vs. $t$ gave the straight line with a slope of $-k_1$ and intercept with $\ln C_o$. The figure shows the adsorption kinetics of chromium (VI) on DBTL follows the simple first order kinetics satisfactory at lower concentration but at higher concentration it starts to deviate. The value of the coefficient corelation of data fitness is given in Table 3.10.

### 3.6.1.2 Second order kinetic equation

Second order kinetic equation (Eq. 3.11) (Hossain *et al*., 2005, 2011, 2012, Gupta *et al*., 2001), was verified by plotting $1/C_t$ vs. $t$.

$$\frac{1}{C_t} = k_2 t + \frac{1}{C_o} \qquad (3.11)$$

where, $C_t$ is the final concentration ($mg \cdot L^{-1}$) after time $t$, $C_o$ is the initial concentration ($mg \cdot L^{-1}$), $k_2$ is second order rate constant. Figure 3.14 as a plot of $l/C_t$ vs. $t$ gave the straight line with a slope of $k_2$ and intercept of $1/C_o$. The experimental data follow second order kinetic equation satisfactory at lower concentration and its fitness is better than that of first order kinetics but at higher concentration it starts to deviate. The value of the coefficient corelation of data fitness is given in Table 3.10.

### 3.6.1.3 Pseudo first order kinetics

Lagergren pseudo-first order rate equation is commonly used to the adsorption of liquid/solid system based on adsorbent capacity (Lagergren 1898, Hossain *et al.*, 2005, 2011, 2013; Gupta *et al*., 2001 and Attia *et al*., 2004). According to this model, one adsorbate species reacts with one active site on surface. The linearized form of the

pseudo-first order kinetic equation is expressed as follows by Lagergren (Lagergren 1898):

$$\log(q_e - q_t) = \log q_e - \frac{k_{1p}}{2.303}t \qquad (3.12)$$

where, $q_e$ and $q_t$ are the adsorption capacity ($mg \cdot g^{-1}$) at equilibrium and at time $t$, respectively, $k_{p1}$ is the rate constant of pseudo first order equation ($L \cdot min^{-1}$). The values of $k_{p1}$ and $q_e$ can be determined from the slope and intercept of the plot, respectively **(**Gholami-Borujeni *et al*., 2011). The applicability of the pseudo-first order equation to experimental data generally differs in two ways; the parameter does not represent the number of available sites and the parameter $\log q_e$ is an adjustable parameter and often found not equal to the intercept of the plot $\log(q_e – q_t)$ versus $t$, whereas in true first order, $\log q_e$ should be equal to the intercept (Khan *et al*., 1994). Figure 3.15 shows the weak fitness of pseudo-first order plots at different initial concentrations of chromium (VI). Values of correlation coefficients for different initial concentrations of chromium (VI) are given in Table 3.10. The results showed that the pseudo first order rate constant, $k_{1p}$ is irregularly changes with concentration i.e. $k_{1p}$ independent of initial concentration as shown in Table 3.11. Similar result has been presented in literatures (Arami *et al*., 2005 and Poots *et al*., 1978).

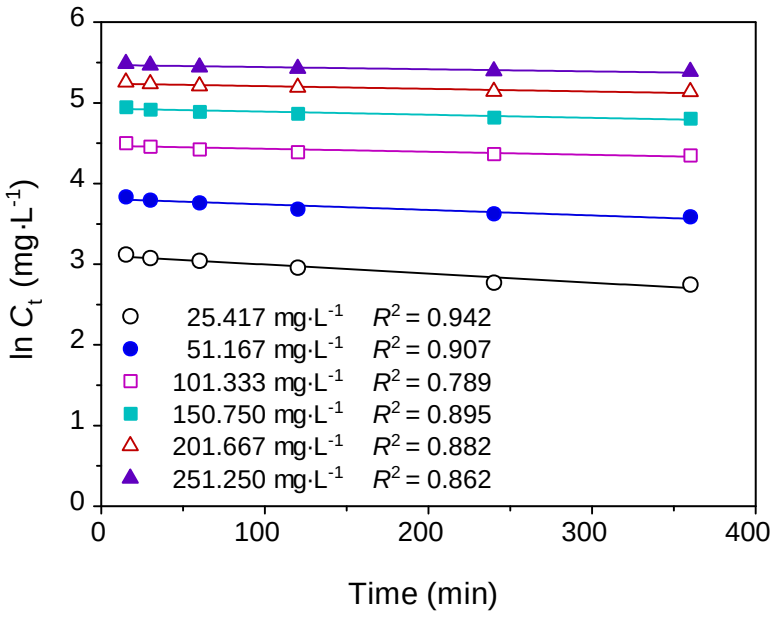


**Figure 3.13:** Application of the simple first order kinetic equation for the adsorption of chromium (VI) on DBTL with time from aqueous solution at pH 2.0 and 30.0 ± 0.2 $^{o}$C.

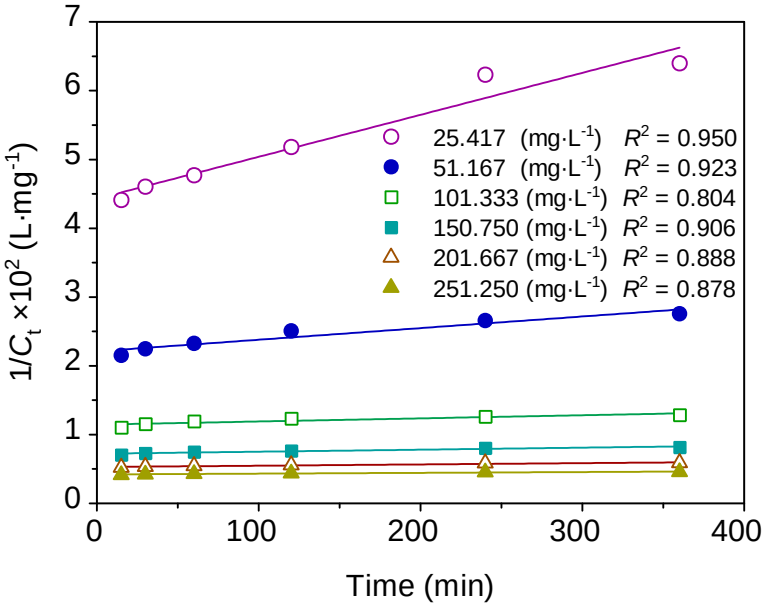


**Figure 3.14:** Application of the simple second order kinetic equation for the adsorption of chromium (VI) on DBTL with time from aqueous solution at pH 2.0 and 30.0 ± 0.2 $^{o}$C.

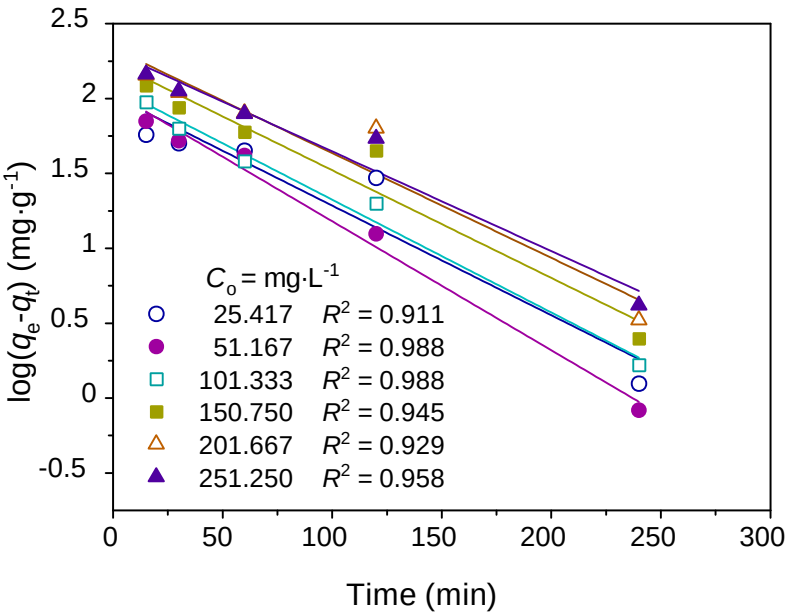


**Figure 3.15:** Application of the pseudo first order kinetic equation for the adsorption of chromium (VI) on DBTL with time from aqueous solution at pH 2.0 and 30.0 ± 0.2 $^{o}$C.

### 3.6.1.4 Pseudo-second order kinetics

Ho and McKay's (Ho and McKay, 2000; Sun and Xu, 1997; Hossain *et al*., 2012) pseudo second order rate equation was applied for the adsorption of chromium (VI) on UBTL at different initial concentrations. The linearized form of Ho and McKay's pseudo second order rate equation is shown in Eq. (3.13),

$$\frac{t}{q_t} = \frac{1}{k_{2p} q_e^2} + \frac{t}{q_e} \qquad (3.13)$$

where, $q_t$ is the amount adsorbed at time, $t$ (mg·g$^{-1}$), $q_e$ is equilibrium amount adsorbed (mg·g$^{-1}$) and $k_{2p}$ is pseudo second order rate constant (g·mg$^{-1}$·min$^{-1}$). The plot of $t/q_t$ *vs.* $t$ as shown in Figure 3.16 gives a straight line with a slope $1/q_e$. This figure shows that each plot gives straight line with the whole range of concentration indicating the best fitness of pseudo second order rate equation for the adsorption of chromium(VI) on DBTL in both at low and high concentration of Cr(VI). Hence from the slope and intercept of the plots for different initial concentrations, equilibrium amount adsorbed, equilibrium concentration and pseudo second order rate constant, $k_{2p}$ can be calculated from equation 3.13 and presented in Table 3.11 and 3.12. Therefore, it can be suggested that two active sites of chromium (VI) are interacted with the DBTL surface. Several

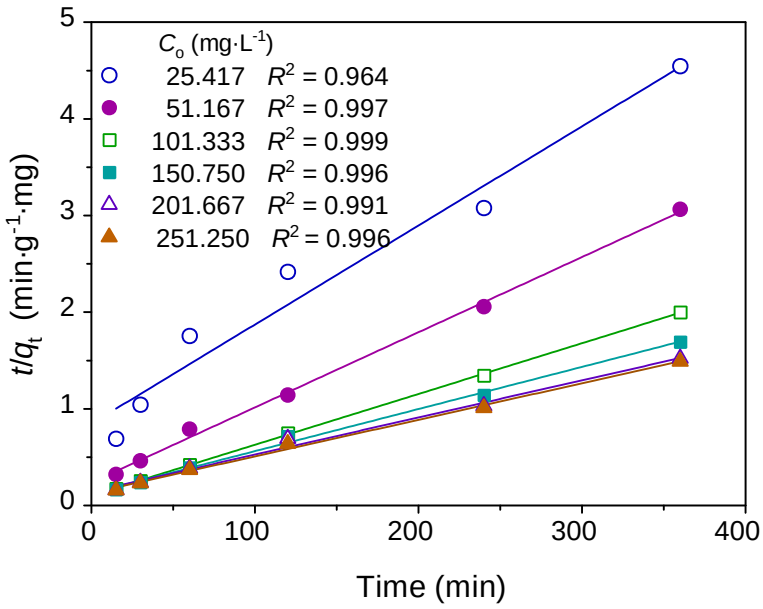


**Figure 3.16**: Application of the pseudo second order kinetic equation for the adsorption of chromium (VI) on DBTL with time from aqueous solution at pH 2.0 and 30.0 ± 0.2 $^{o}$C.

studies have been reported (Hossain *et al*., 2005; Suyamboo *et al*., 2012; Awala *et al*., 2011) that the adsorption of divalent ions follows pseudo second order kinetics.

### 3.6.1.5 Elovich Equation

Elovich equation (Theivarasu and Mylsamy 2010; Alzaydien and Manasreh 2009) was also verified for the adsorption of Cr(VI) on DBTL. General expression of the Elovich model equation is shown as equation (3.14)

$$\frac{dq_t}{dt} = \sim \exp(- \ q_t) \qquad (3.14)$$

where $dq_t/dt$ is the initial adsorption rate ($mg \cdot g^{-1} \cdot min^{-1}$), $\alpha$ is the initial adsorption rate ($mg \cdot g^{-1} \cdot min^{-1}$) and $\beta$ is the desorption constant ($g \cdot mg^{-1}$), related to the extent of surface coverage and the activation energy for chemisorption. To simplify Elovich equation, Chien and Clyton (1980) assumed $\alpha\beta t >> t$ and by applying boundary conditions $q_t = 0$ at $t = 0$ and $q_t = t$ at $t = t$, the equation becomes (3.15)

$$q_t = \frac{1}{} \ln(\sim \ ) + \frac{1}{} \ln t \qquad (3.15)$$

All the plots give straight line with the slope $1/\beta$ and an intercept of $\ln\alpha\beta/\beta$ indicating the validity of Elovich equation**.** The adsorption of chromium (VI) on DBTL for different initial concentrations were verified by using Eq. (3.15) and the plot of $q_t$ versus ln*t* in Figure 3.17 shown the adsorption of chromium (VI) on DBTL did not follow the Elovich equation for different initial concentrations of chromium (VI) at pH 2.0 and at 30 ± 0.2°C. As the concentration increases it starts to deviate. Several studies reported that the Elovich kinetic equation often valid for heterogeneous surface (Ho and McKay, 2000). Hence present adsorption system also provides good agreement with the previous study. Different parameters of Elovich model was calculated and given in Table 3.12. The increse of Elovich parameter, $\beta$ indicates that desorption increses with the increse of concentration.

A comparison of the data fitness based on the value of correlation coefficient, to the first order, second order, pseudo second order and Elovich model kinetics equations in Tables 3.11 and 3.12 show that the pseudo second order rate equation is well fitted over

other equations. Several studies have been reported that the adsorbents having heterogeneous surface like tea leaves (Hossain, 2005), moss peat (Ho and McKay, 2000), clay- wood sawdust (Yeddou and Bensmaili, 2005), rich husk (Allen and Koumanova, 2005), peanut hull carbon (Amin, 2008) follow pseudo second order kinetics.

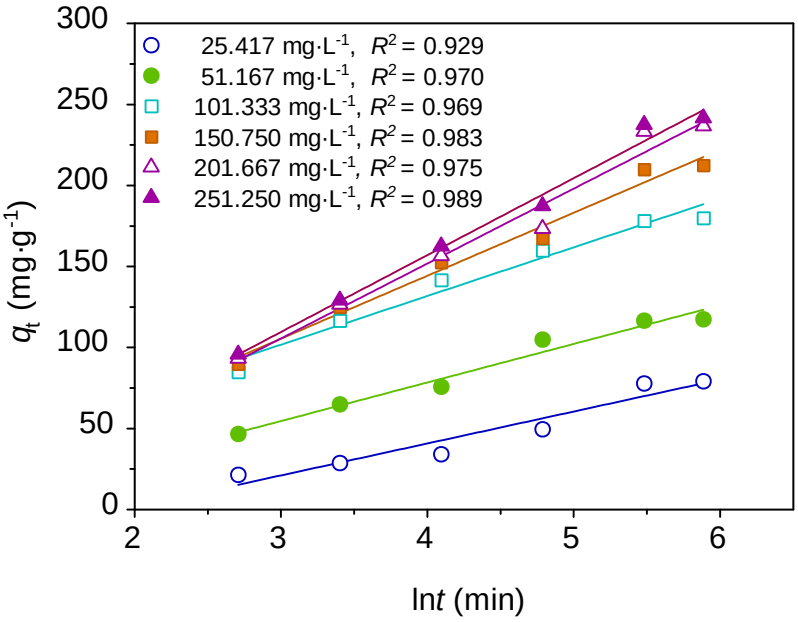


**Figure 3.17:** Application of the Elovich equation for the adsorption of chromium (VI) on DBTL with time from aqueous solution at pH 2.0 and 30.0 ± 0.2 $^{o}$C.

**Table 3.10** Comparison of the regression co-efficient ($R^2$) to justify the fitness of different kinetic equations for adsorption of chromium (VI) with different initial concentrations at pH 2.0 and temperature 30 ± 0.2$^{o}$ C.

| Initial Conc. $C_o$ (mg·L$^{-1}$) | $R^2$ First order kinetic equation (a.u.) | $R^2$ Second order kinetic equation (a.u.) | $R^2$ Pseudo first order kinetic equation (a.u.) | $R^2$ Pseudo second order kinetic equation (a.u.) | $R^2$ Elovich equation (a.u.) |
|---|---|---|---|---|---|
| 25.417 | 0.942 | 0.950 | 0.911 | 0.964 | 0.929 |
| 51.167 | 0.907 | 0.923 | 0.988 | 0.997 | 0.970 |
| 101.333 | 0.989 | 0.804 | 0.988 | 0.999 | 0.968 |
| 150.750 | 0.895 | 0.906 | 0.945 | 0.996 | 0.982 |
| 201.667 | 0.882 | 0.888 | 0.929 | 0.991 | 0.975 |
| 251.250 | 0.862 | 0.878 | 0.958 | 0.996 | 0.989 |

**Table 3.11** Comparison of the rate constants of different kinetic equations for adsorption of chromium (VI) at different initial concentrations at pH 2.0 and temperature 30 ± 0.2° C.

| Initial Conc. $C_o$ ($mg \cdot L^{-1}$) | $k_1$ First order kinetic equation ($min^{-1}$) | $k_2$ Second order kinetic equation ($L \cdot mg^{-1} \cdot min^{-1}$) | $k_{1p}$ Pseudo first order kinetic equation ($min^{-1}$) | $k_{2p} \times 10^4$ Pseudo second order kinetic equation ($L \cdot g^{-1} \cdot min^{-1}$) | $\alpha$ Elovich equation ($mg \cdot g^{-1} \cdot .min^{-1}$) |
|---|---|---|---|---|---|
| 25.417 | - 0.001 | $6.0 \times 10^{-5}$ | 0.016 | 1.181 | 2.83 |
| 51.167 | 0 | $1.0 \times 10^{-5}$ | 0.018 | 2.067 | 11.78 |
| 101.333 | 0 | 0 | 0.016 | 2.427 | 44.58 |
| 150.750 | 0 | 0 | 0.016 | 1.270 | 28.84 |
| 201.667 | 0 | 0 | 0.016 | 0.634 | 21.93 |
| 251.250 | 0 | 0 | 0.014 | 0.692 | 28.91 |

**Table 3.12** Parameters of different kinetic equation for adsorption of chromium (VI) at different initial concentrations at pH 2.0 and temperature 30 ± 0.2° C.

| Initial Conc. $C_o$ ($mg \cdot L^{-1}$) | Pseudo first order kinetics | | Pseudo second order kinetics | | $\beta$ Elovich equation ($g \cdot mg^{-1}$) |
|---|---|---|---|---|---|
| | $C_t$ ($mg \cdot L^{-1}$) | $q_t$ $mg \cdot g^{-1}$) | $C_t$ ($mg \cdot L^{-1}$) | $q_t$ ($mg \cdot g^{-1}$) | |
| 25.417 | 15.018 | 103.99 | 15.417 | 100.00 | 0.051 |
| 51.167 | 40.152 | 110.15 | 36.881 | 142.86 | 0.042 |
| 101.333 | 89.366 | 119.67 | 81.333 | 200.00 | 0.033 |
| 150.750 | 133.372 | 173.78 | 125.750 | 250.00 | 0.026 |
| 201.667 | 180.040 | 216.27 | 168.334 | 333.33 | 0.022 |
| 251.250 | 230.738 | 205.12 | 217.917 | 333.333 | 0.021 |

### 3.6.1.6 Adsorption isotherm from kinetic study

From the straight lines of each plot of $t/q_t$ vs $t$, pseudo second order rate constant and equilibrium amount adsorbed of chromium (VI) on DBTL were calculated for different initial concentrations of chromium (VI). The equilibrium concentrations for different initial concentration were also calculated from pseudo second order kinetic study as shown in Table 3.13. Using these data an adsorption isotherm as a function of equilibrium amount adsorbed ($q_e$) vs. equilibrium concentrations ($C_e$) was constructed as shown in Figure 3.18. The adsorption isotherm data was analyzed using Langmuir

(Langmuir 1918), Freundlich (Freundlich 1906) and Temkin (Tempkin and Pyzhev, 1940) equations (3.16-3.18) and presented in Figures 3.19, 3.20 and 3.21, respectively.

Langmuir equation: $$\frac{C_e}{q_e} = \frac{1}{q_m b} + \frac{C_e}{q_m} \quad (3.16)$$

Freundlich equation: $$\log q_e = \log k_f + \frac{1}{n} \log C_e \quad (3.17)$$

where, $q_e$ ($q_e = x/m$) indicates amount of adsorbed species ($mg \cdot g^{-1}$), $C_e$ indicates equilibrium concentration of the adsorbate in solution ($mg \cdot L^{-1}$), $q_m$ indicates amount of monolayer adsorbed species ($mg \cdot g^{-1}$), $b$ indicates the adsorption equilibrium constant or Langmuir constant ($L \cdot mg^{-1}$), $k_f$ indicates Freundlich constants related to adsorption capacity ($mg \cdot g^{-1}$) and $1/n$ indicates adsorption intensity, respectively (Voudarias, *et al.*, 2002). The values of $n$ in the equation indicate the following information: $n$ =1, indicates the partition between the two phases are independent of the concentration, value of $n$ less than 1 indicates a normal adsorption, whereas the value of $1/n$ greater than 1 indicates cooperative adsorption (Mohan, *et al.*, 1997). From Langmuir equation, the straight line of $C_e/q_e$ *vs* $C_e$ gives the slope $1/q_m$ and intercepts $1/q_m b$. Values of $q_m$ and $b$ can be calculated from the slope and intercept, respectively. From Freundlich equation, the straight line of $\log C_e$ *vs* $\log q_e$ gives the slope $1/n$ and intercepts $\log k_f$. Values of $n$ and $k_f$ can be calculated from the slope and intercept, respectively.

Temkin equation : $$q_e = B \ln A_T + B \ln C_e \quad (3.18)$$

where, $q_e$ indicates amount adsorbed per unit mass of adsorbent ($mg \cdot g^{-1}$) and $C_e$ indicates equilibrium concentration of the adsorbate ($mg \cdot L^{-1}$). $B$ ($B = RT/b_T$) indicates Temkin constant related to the heat of adsorption ($J \cdot mol^{-1}$), $A_T$ indicates the equilibrium binding constant corresponding to the maximum binding energy ($L \cdot g^{-1}$), $T$ indicates absolute temperature (K) and $R$ indicates universal gas constant (8.314 $J \cdot K^{-1} \cdot mol^{-1}$), $A_T$ indicates the equilibrium binding constant corresponding to the maximum binding energy ($L \cdot g^{-1}$) and $b_T$ is Temkin isotherm constant. The straight line of $\ln C_e$ *vs* $q_e$ give slope $B$ and intercept $B \ln A_T$. The value of $B$ can be calculated from the slope.

Calculated parameters of the above isotherms are given in Table 3.14. The adsorption isotherm is well expressed ($R^2$ = 0.996) by Langmuir equation (3.16) as shown in Figure 3.19 and the maximum adsorption capacity ($q_m$) and Langmuir constant ($b$) are 303.03 $mg \cdot g^{-1}$ and 0.018 $L \cdot mg^{-1}$, respectively as shown in Table 3.14. Thus the kinetic evaluation of an adsorption process is another method for determination of maximum adsorption capacity (Sultana, 2009).

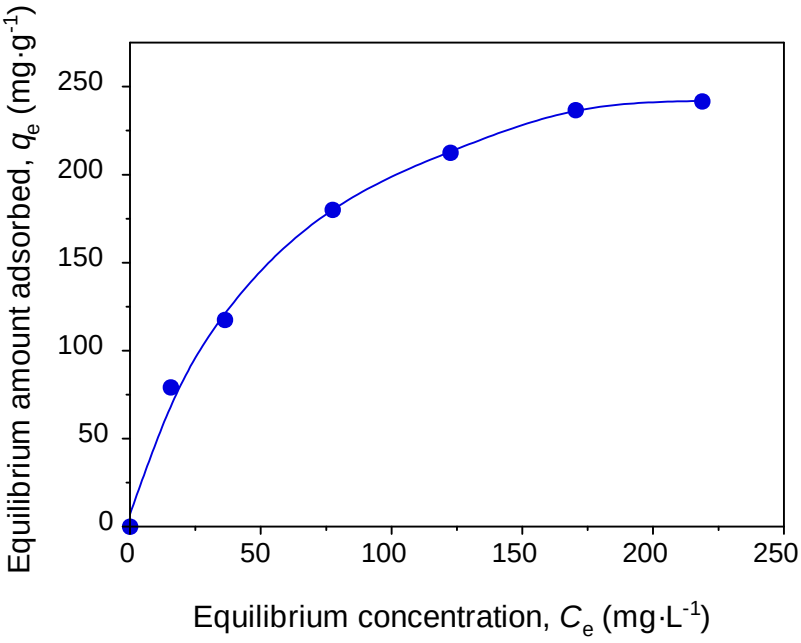


**Figure 3.18:** Adsorption isotherm of chromium (VI) adsorption on DBTL from aqueous solution at pH 2.0 and 30.0 ± 0.2 $^oC$, derived from pseudo second order kinetics.

**Table 3.13** Derived-data from kinetic study for construction of adsorption isotherm of chromium (VI) on DBTL at pH 2.0 and 30.0 ± 0.2 $^oC$.

| $C_o$ ($mg \cdot L^{-1}$) | Equilibrium Conc., $C_e$ | | Amount adsorbed, $q_e$ | | $C_e/q_e$ ($g \cdot L^{-1} \cdot$) | log$C_e$ ($mg \cdot L^{-1}$) | ln$C_e$ ($mol \cdot L^{-1}$) | log$q_e$ ($mg \cdot g^{-1}$) |
|---|---|---|---|---|---|---|---|---|
| | ($mg \cdot L^{-1}$) | ($mol \cdot L^{-1}$) $\times 10^3$ | ($mg \cdot g^{-1}$) | $q_t \times 10^3$ ($mol \cdot g^{-1}$) | | | | |
| 25.417 | 15.625 | 0.300 | 79.17 | 1.523 | 0.197 | 1.194 | -8.11 | 1.899 |
| 51.167 | 36.250 | 0.697 | 117.50 | 2.260 | 0.309 | 1.559 | -7.269 | 2.070 |
| 101.333 | 77.500 | 1.490 | 180.00 | 3.462 | 0.430 | 1.889 | -6.509 | 2.255 |
| 150.750 | 122.500 | 2.356 | 212.50 | 4.087 | 0.576 | 2.088 | -6.051 | 2.327 |
| 201.667 | 170.333 | 3.276 | 236.67 | 4.551 | 0.720 | 2.231 | -5.721 | 2.374 |
| 251.250 | 218.750 | 4.207 | 241.67 | 4.648 | 0.905 | 2.340 | -5.471 | 2.383 |

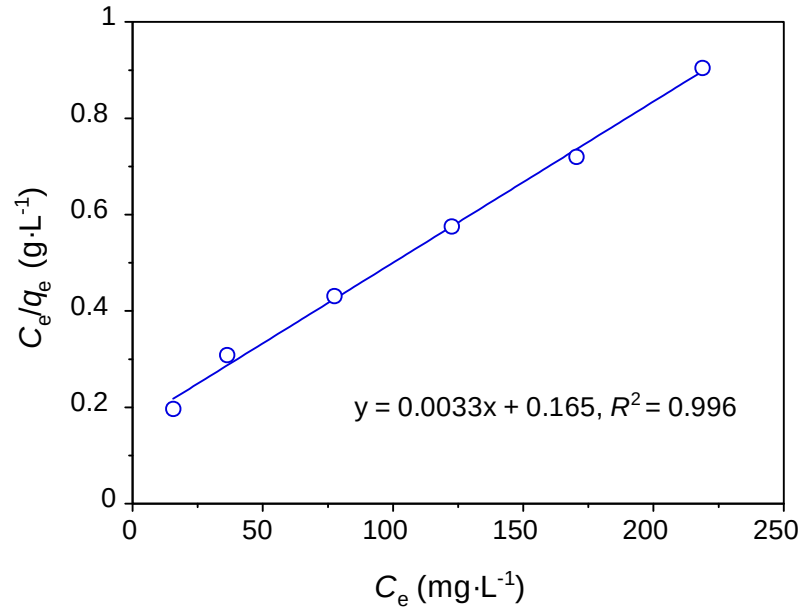


**Figure 3.19:** Langmuir adsorption isotherm derived from kinetic study for adsorption chromium (VI) on DBTL from aqueous solution at pH 2.0 and 30.0 ± 0.2 $^{o}$C.

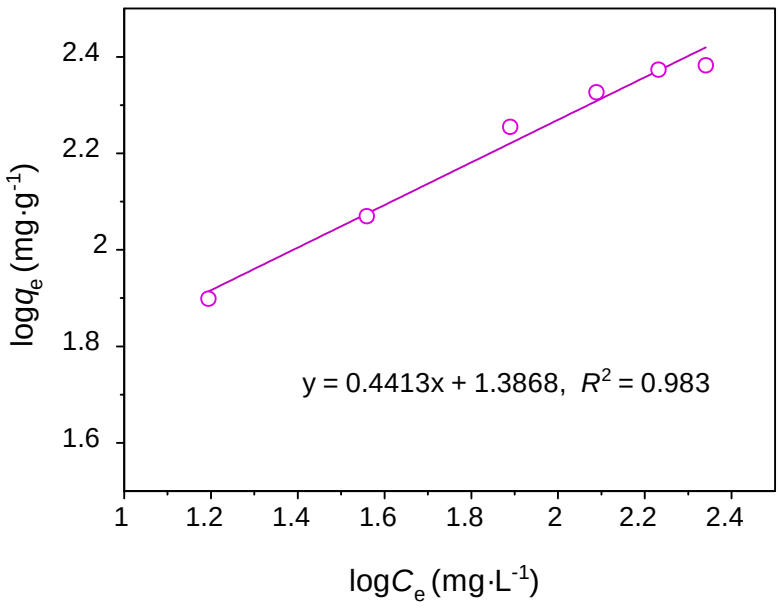


**Figure 3.20**: Freundlich adsorption isotherm derived from kinetic study for adsorption chromium (VI) on DBTL from aqueous solution at pH 2.0 and 30.0 ± 0.2 $^{o}$C.

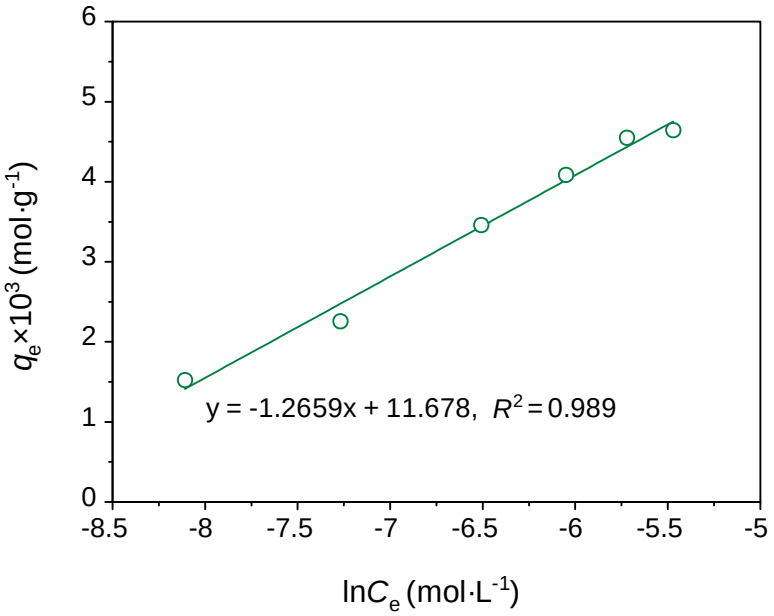


**Figure 3.21**: Temkin adsorption isotherm derived from kinetic study for the adsorption chromium (VI) on DBTL from aqueous solution at pH 2.0 and 30.0 ± 0.2 $^{o}$C.

**Table 3.14** Parameters of different isotherms derived from kinetic study for the adsorption chromium (VI) on DBTL from aqueous solution at pH 2.0 and 30.0 ± 0.2 $^{o}$C.

| Isotherms | Parameter | | $R^2$ |
|---|---|---|---|
| Langmuir isotherm | $q_m$ (mg·g$^{-1}$) | $b$ (L·mg$^{-1}$) | 0.996 |
| | 303.03 | 0.02 | |
| Freundlich isotherm | $k_f$ (mg·g$^{-1}$) | $n$ (a.u.) | 0.987 |
| | 24.56 | 2.262 | |
| Temkin isotherm | $A_T$ (L·mol$^{-1}$) | $B$ (J·mol$^{-1}$) | 0.991 |
| | 10.02×10$^{3}$ | 1.287×10$^{-3}$ | |

### 3.6.1.7 Investigation of the transfer mechanism

For porous adsorbents like as DBTL, diffusional effects may be quite important and the physical meaning of the evaluated rate constants has to be consequently determined in order to get insight into the transfer mechanism. Equation (3.19) is a general representation of the kinetics, where the intercept is related to the mass transfer across the boundary layer and the expected value of the exponent (*n*) is 0.5 (for Fickian diffusion and plate geometry).

$$q_t = k_{id} t^n + D \qquad (3.19)$$

where, $q_t$ is the mass transfer at time *t*, $k_{id}$ is the intraparticle diffusion rate constant and *D* is the intraparticle diffusion constant. The Weber and Morris model (Weber and Morris, 1963) or intraparticle diffusion model (Eq. 3.20) describes the time evolution of the concentration in adsorbed state, where the rate constant ($k_{in}$) is obtained from the plot of $q_t$ versus $t^{1/2}$ and is related to the respective intraparticle diffusion coefficient (*D*) according to equation (3.21). (Tsibranska and Hristova, 2011)

$$q_t = k_{id} t^{1/2} \qquad (3.20)$$

$$k_{id} = 6\frac{q_o}{R}\sqrt{\frac{D}{®}} \qquad (3.21)$$

The Weber and Morris model (Weber and Morris, 1963; Namasivayam and Ranganathan, 1995) or intraparticle diffusion model (Eq. 3.20) is of major interest because the internal diffusion determines the adsorption rate in most of the liquid systems. The transfer mechanism of the adsorption of Cr (VI) on DBTL was investigated using Weber and Morris's intraparticle diffusion model equation towards the kinetic data. The amount adsorbed ($q_t$) at time *t* for different initial concentrations were plotted against the square root of time ($t^{1/2}$) to verify the applicability of intra-particle diffusion model as shown in Figure 3.22. The plots for different initial concentrations have shown the deviation from linearity in Figure 3.22a and the values of $R^2$ are presented in Figure 3.22b, reveals that the film diffusion is dominative for the adsorption of chromium (VI) on DBTL.

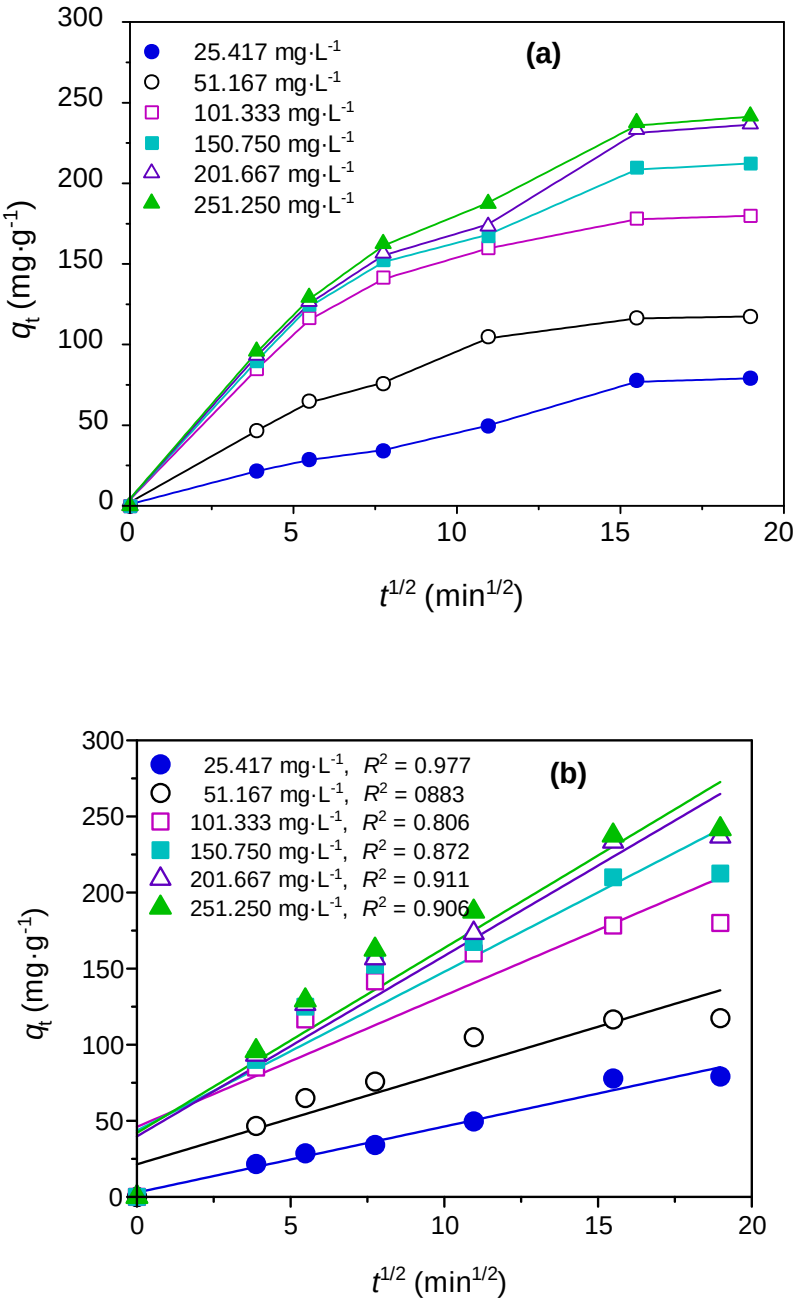


**Figure 3.22:** Application of the intra-particle diffusion model for the adsorption of chromium (VI) on DBTL from aqueous solution at pH 2.0 and 30.0 ± 0.2 $^{o}$C.

## 3.6.2 Effect of Temperature on Adsorption Kinetics

The effect of temperature on the adsorption kinetics was investigated using the following experimental conditions:

**Experimental Conditions**

| | |
|---|---|
| Volume of chromium (VI) solution | : 25 mL |
| Concentration of chromium (VI) solution | : ≈100 $mg \cdot L^{-1}$ |
| Solution pH | : 2.0 |
| Amount of DBTL ($W_{DBTL}$) | : 0.0025 g |
| Particle size of DBTL | : < 106 µm |
| Adsorption temperature | : 15, 30 and 50 ± 0.2 °C |
| Agitation rate | : 150 rpm |
| Agitation time ($t$) | : 0 to 6 hrs |

The amounts of chromium (VI) adsorbed on DBTL with different times were calculated using equation (3.9) and presented in Table 3.15 and 3.16. The amounts of chromium (VI) adsorbed on DBTL as a function of time for different temperatures were shown in Figure 3.23. The adsorption kinetic data for different temperatures were investigated using different kinetic equations such as first order (Eq. 3.10), second order (Eq. 3.11), pseudo-first order (Eq. 3.12), pseudo-second kinetic (Eq. 3.13) and Elovich equations (Eq. 3.15), and presented in Figure 3.24-3.28, respectively. Applicability of the equations was justified based on the value of coefficient corelation ($R^2 > 0.99$) of data fitness given in Table 3.18. Different parameters of the fitness of above equations are given in Table 3.19 and 3.20. Based on the values of coefficient of determination ($R^2$), experimental data of adsorption is well expressed by pseudo-second order kinetic equation. The equilibrium amount adsorbed and rate constants for different temperatures were determined from the well fitted plot of pseudo second order kinetics and given in Table 3.21. The Figure 3.29 shows that the equilibrium amount of chromium (VI) adsorbed on DBTL decreases with increase of temperature, i.e. the process is exothermic indicating physical interaction of the process.

**Table 3.15** Effect of temperature on the adsorption kinetics of 101.333 mg·L$^{-1}$ chromium (VI) on DBTL at pH 2.0.

| Temperature ± 0.2° (°C) | $t$ (min) | $C_t$ (mg·L$^{-1}$) | $C_T$ (mg·L$^{-1}$) | $C_R = C_T - C_t$ (mg·L$^{-1}$) | $q_t$ (mg·g$^{-1}$) |
|---|---|---|---|---|---|
| 15 | 15 | 92.167 | 92.667 | 0.500 | 86.66 |
| | 30 | 88.833 | 89.500 | 0.667 | 118.33 |
| | 60 | 82.500 | 83.333 | 1.333 | 175.00 |
| | 120 | 76.333 | 78.500 | 2.167 | 228.33 |
| | 240 | 68.333 | 72.667 | 4.334 | 286.66 |
| | 360 | 67.667 | 72.333 | 4.666 | 290.00 |
| 30 | 15 | 90.500 | 92.833 | 2.333 | 85.00 |
| | 30 | 86.500 | 89.667 | 3.167 | 116.66 |
| | 60 | 83.500 | 87.167 | 3.667 | 141.66 |
| | 120 | 81.00 | 85.333 | 4.333 | 160.00 |
| | 240 | 79.00 | 83.500 | 4.500 | 178.33 |
| | 360 | 77.50 | 83.333 | 5.833 | 180.00 |
| 50 | 15 | 96.667 | 99.167 | 2.500 | 21.66 |
| | 30 | 94.000 | 97.500 | 3.500 | 38.33 |
| | 60 | 90.500 | 94.333 | 3.833 | 70.00 |
| | 120 | 87.833 | 92.333 | 4.500 | 90.00 |
| | 240 | 86.167 | 91.000 | 4.833 | 103.33 |
| | 360 | 85.000 | 90.8333 | 5.833 | 105.00 |

**Table 3.16** Derive data for the application of pseudo second order kinetic equation and Elovich equation to the adsorption kinetics of chromium (VI) on DBTL for different temperatures at pH 2.0.

| Température ± 0.2° (°C) | *t* (min) | ln*t* (a.u) | $q_t$ ($mg \cdot g^{-1}$) | $t/q_t$ ($min \cdot g \cdot mg^{-1}$) |
|---|---|---|---|---|
| 15 | 15 | 2.708 | 86.66 | 0.173 |
| | 30 | 3.401 | 118.33 | 0.254 |
| | 60 | 4.094 | 175.00 | 0.343 |
| | 120 | 4.787 | 228.33 | 0.526 |
| | 240 | 5.481 | 286.66 | 0.837 |
| | 360 | 5.886 | 290.00 | 1.241 |
| 30 | 15 | 2.708 | 85.00 | 0.176 |
| | 30 | 3.401 | 116.66 | 0.257 |
| | 60 | 4.094 | 141.66 | 0.424 |
| | 120 | 4.787 | 160.00 | 0.750 |
| | 240 | 5.481 | 178.33 | 1.346 |
| | 360 | 5.886 | 180.00 | 2.000 |
| 50 | 15 | 2.708 | 21.66 | 0.693 |
| | 30 | 3.401 | 38.33 | 0.783 |
| | 60 | 4.094 | 70.00 | 0.857 |
| | 120 | 4.787 | 90.00 | 1.333 |
| | 240 | 5.481 | 103.33 | 2.323 |
| | 360 | 5.886 | 105.00 | 3.429 |

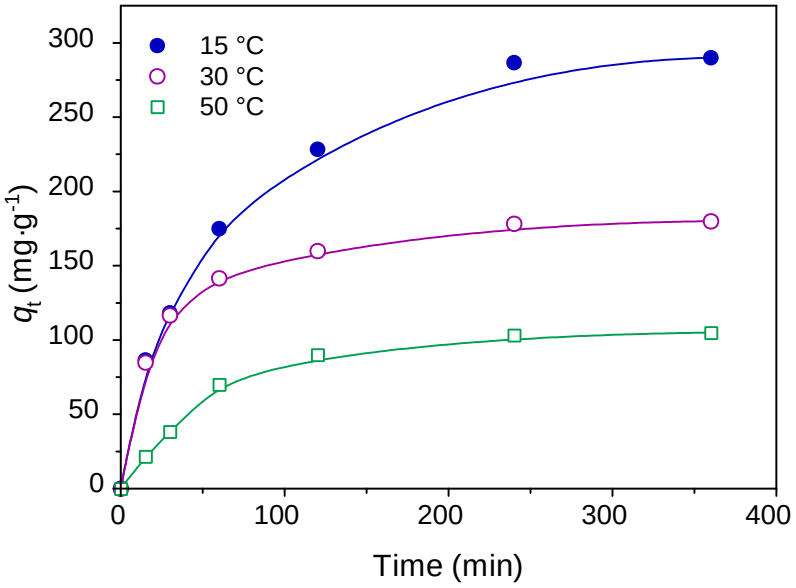


**Figure 3.23:** Variation of amount adsorbed of chromium (VI) on DBTL with time from aqueous solution at pH 2.0 for different temperatures.

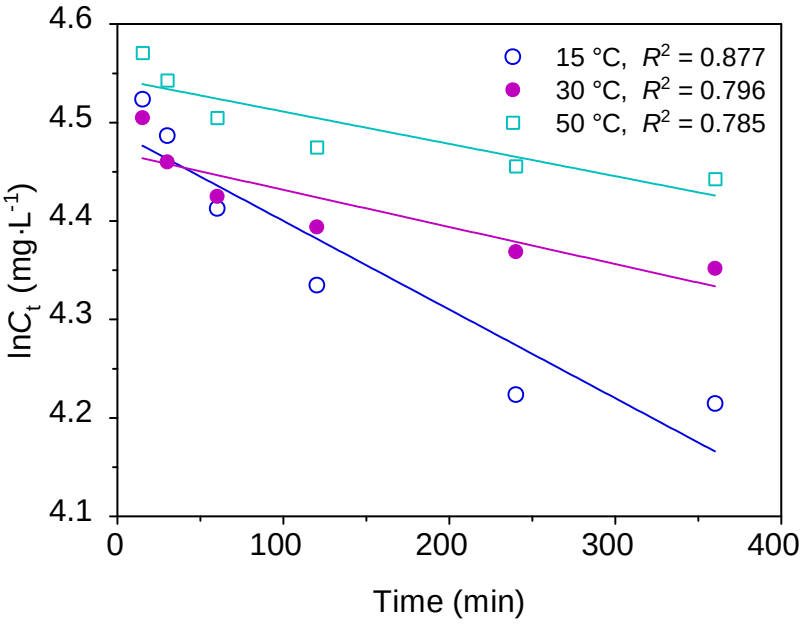


**Figure 3.24:** Application of the simple first order kinetic equation for the adsorption of chromium (VI) on DBTL at pH 2.0 for different temperatures.

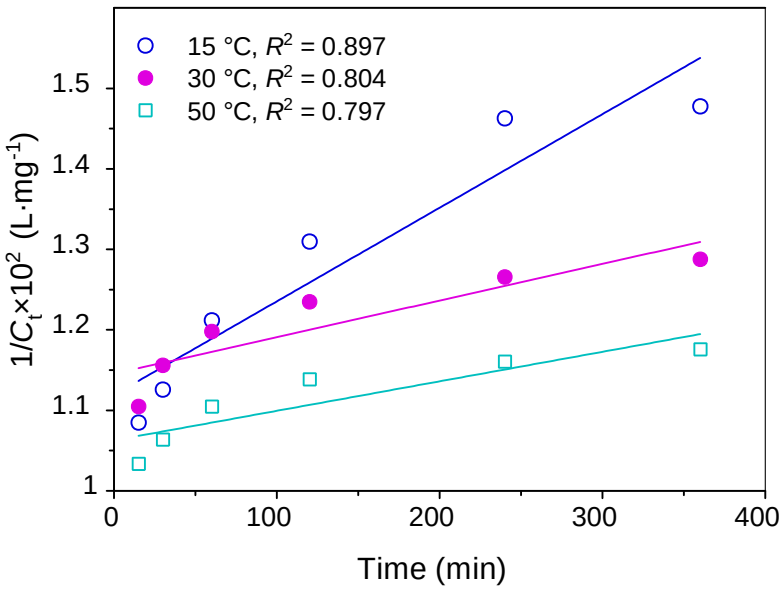


**Figure 3.25:** Application of the simple second order kinetic equation for the adsorption of chromium (VI) on DBTL at pH 2.0 for different temperatures.

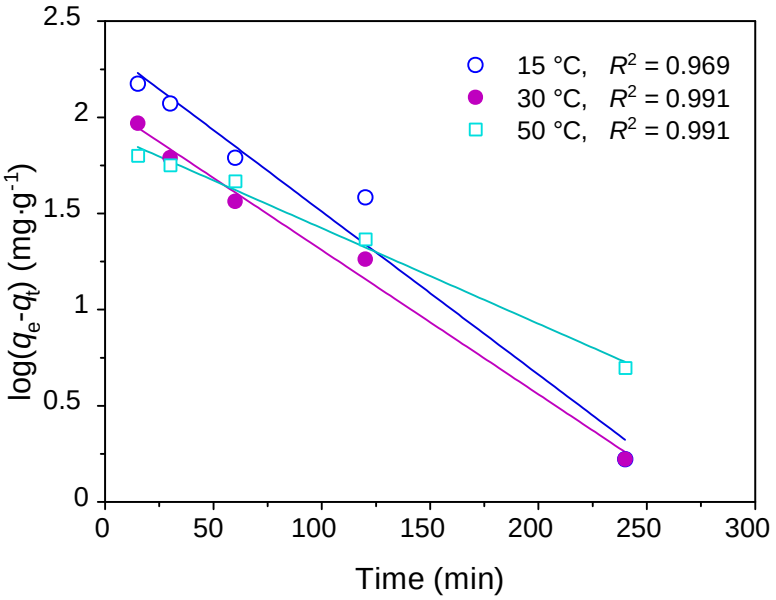


**Figure 3.26:** Application of the pseudo first order kinetic equation for the adsorption of chromium (VI) on DBTL at pH 2.0 for different temperatures.

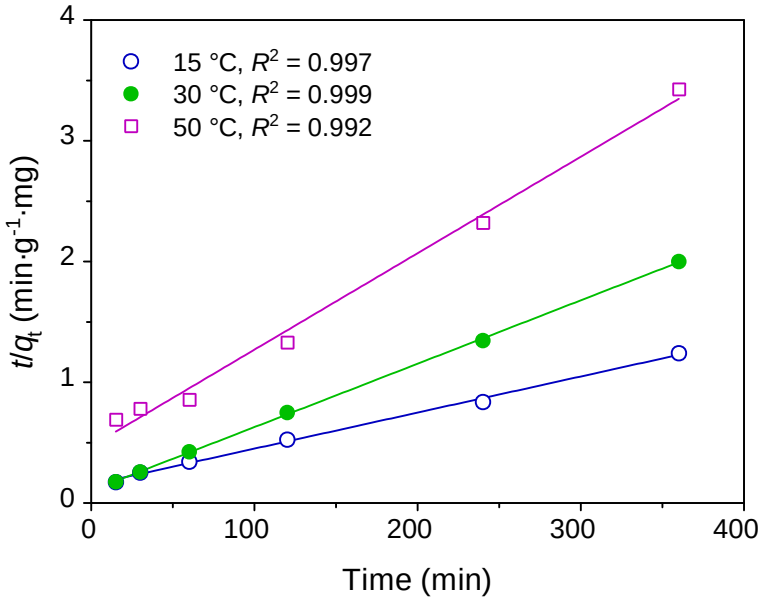


**Figure 3.27:** Application of the pseudo second order kinetic equation for the adsorption of chromium (VI) on DBTL at pH 2.0 for different temperatures.

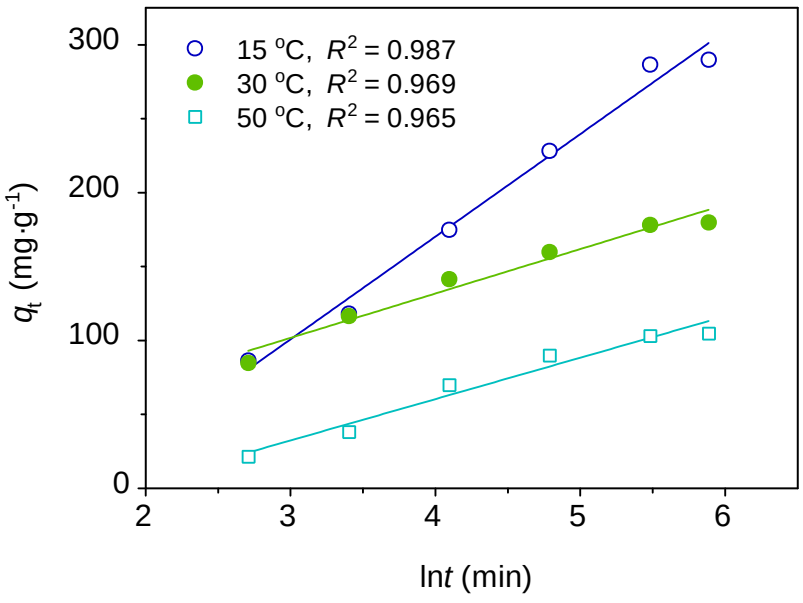


**Figure 3.28**: Application of the Elovich equation for the adsorption of chromium (VI) on DBTL with time from aqueous solution at pH 2.0 and 30.0 ± 0.2 °C.

**Table 3.17** Comparison of the regression co-efficient ($R^2$) to justify the fitness of different kinetic equations for adsorption of chromium (VI) on DBTL at different temperatures and pH 2.0.

| Temperature ± 0.2° (°C) | $R^2$ First order kinetic Equation (a.u.) | $R^2$ Second order kinetic Equation (a.u.) | $R^2$ Pseudo first order kinetic Equation (a.u.) | $R^2$ Pseudo second order kinetic Equation (a.u.) | $R^2$ Elovich equation (a.u.) |
|---|---|---|---|---|---|
| 15 | 0.877 | 0.897 | 0.967 | 0.997 | 0.987 |
| 30 | 0.789 | 0.804 | 0.988 | 0.999 | 0.968 |
| 50 | 0.785 | 0.797 | 0.998 | 0.992 | 0.965 |

**Table 3.18** Comparison of the rate constants of different kinetic equations for adsorption of chromium (VI) at different temperatures and pH 2.0.

| Temp. ± 0.2 (°C) | $k_1$ First order kinetic equation ($g.mg^{-1}\cdot min^{-1}$) | $k_2$ Second order kinetic equation ($g\cdot mg^{-1}\cdot min^{-1}$) | $k_{1p}$ Pseudo first order kinetic equation ($min^{-1}$) | $k_{2p}\times 10^{4}$ Pseudo second order kinetic equation ($g\cdot mg^{-1}\cdot min^{-1}$) | $\alpha$ Elovich equation ($mg\cdot g^{-1}\cdot min^{-1}$) |
|---|---|---|---|---|---|
| 15 | - | $1.0\times10^{-5}$ | 0.016 | 0.596 | 15.88 |
| 30 | - | - | 0.016 | 2.427 | 44.31 |
| 50 | - | - | 0.016 | 1.362 | 4.437 |

**Table 3.19** Parameters of different kinetic equations for adsorption of chromium (VI) at different temperatures and pH 2.0.

| Temperature (± 0.2) °C | $q_e$ Pseudo first order kinetics ($mg\cdot g^{-1}$) | Pseudo second order kinetics | | $\beta$ Elovich equation ($g\cdot mg^{-1}$) |
|---|---|---|---|---|
| | | $C_e$ ($mg\cdot L^{-1}$) | $q_e$ ($mg\cdot g^{-1}$) | |
| 15 | 327.34 | 68.000 | 333.33 | 0.014 |
| 30 | 119.67 | 81.333 | 200.00 | 0.033 |
| 50 | 108.39 | 88.833 | 125.00 | 0.036 |

**Table 3.20:** Variation of equilibrium amount adsorbed and pseudo second order rate constant of 101.333 mg·L$^{-1}$ chromium (VI) adsorbed on DBTL with temperature at pH 2.0.

| $T$ ($^{o}$C) | $1/T \times 10^{3}$ (K$^{-1}$) | $q_e$ (mg·g$^{-1}$) | $k_{2p} \times 10^{4}$ (g·mg$^{-1}$min$^{-1}$) | $k_{2p}$ (g·mol$^{-1}$min$^{-1}$) | log$k_{2p}$ log(g·mol$^{-1}$min$^{-1}$) | $R^2$ (a.u.) |
|---|---|---|---|---|---|---|
| 15 | 3.472 | 333.33 | 0.596 | 3.078 | 0.488 | 0.997 |
| 30 | 3.300 | 200.00 | 2.427 | 13.839 | 1.141 | 0.999 |
| 50 | 3.096 | 125.00 | 1.362 | 7.060 | 0.849 | 0.992 |

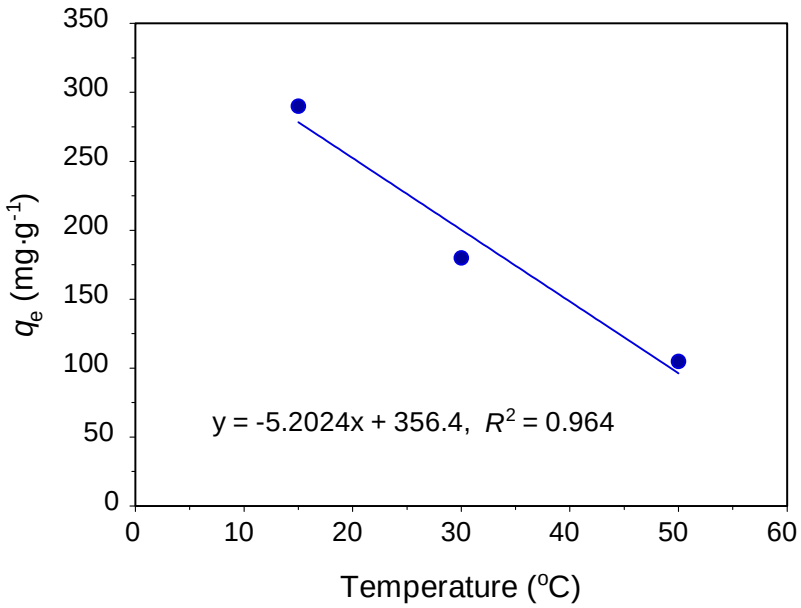


**Figure 3.29:** Variation of equilibrium amount adsorbed (from pseudo second order plot) with temperature for the adsorption of chromium (VI) on DBTL at pH 2.0.

### 3.6.2.1 Adsorption thermodynamics

***The apparent activation energy***

The apparent activation energy of adsorption, $E_a$ was calculated from the slope of the plot of natural logarithm of pseudo second order rate constant, log$k_{2p}$ values at different temperatures against the reciprocal of absolute temperature as shown in Figure 3.30, according to the Arrhenius type relationship, Eq. (3.22) (Bayramoglu *et al*., 2009),

$$\log k_{2p} = -\frac{Ea}{RT} + \log A \qquad (3.22)$$

where, $A$ is Arrhenius factor, $R$ is the molar gas constant (8.314 J·K$^{-1}$·mol$^{-1}$) and $T$ is the absolute temperature (K). The estimated apparent activation energy of chromium (VI) adsorption on DBTL, $E_a$ = + 7.37 kJ·mol$^{-1}$ suggested that the process is physical in nature ($E_a$ = 65 - 250 kJ·mol$^{-1}$) (Yu *et al.*, 2001).

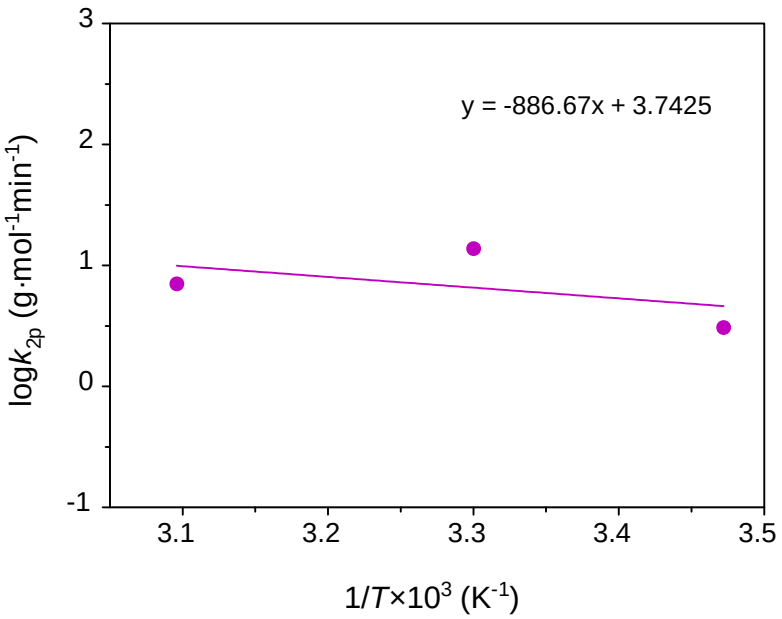


**Figure 3.30:** Arrhenius plot of log$k_{2p}$ vs 1/$T$ for the adsorption of chromium (VI) on DBTL at pH 2.0.

***The equilibrium adsorption constant***

The equilibrium adsorption constant values, $K_C$ for chromium, on DBTL were calculated at different temperatures by the following equation (3.23) (Hossain and Hassan, 2013; Singha and Das, 2012).

$$K_C = \frac{C_{ad}}{C_e} \tag{3.23}$$

where, $C_{ad}$ is the equilibrium concentration of the adsorbate on adsorbent ($mg \cdot L^{-1}$), $C_e$ is the equilibrium concentration of the adsorbate in solution ($mg \cdot L^{-1}$) and $K_C$ is the equilibrium adsorption constant (a.u.). The equilibrium adsorption constant values increase with increasing the initial concentration of chromium (VI) solution as shown in Table 3.21.

**Table 3.21:** Determination of equilibrium adsorption constant, $K_c$ from data derived from experimental results of the adsorption study at different temperatures.

| $1/T \times 10^3$ ($K^{-1}$) | $C_o$ ($mg \cdot L^{-1}$) | $C_e$ ($mg \cdot L^{-1}$) | $C_e \times 10^3$ ($mol \cdot L^{-1}$) | $C_R$ ($mg \cdot L^{-1}$) | $C_{ad}$ $\{C_o - (C_e + C_R)\}$ ($mg \cdot L^{-1}$) | $C_{ad} \times 10^3$ ($mol \cdot L^{-1}$) | $K_c$ (a.u.) | $\ln K_c$ (a.u) |
|---|---|---|---|---|---|---|---|---|
| 3.472 | 101.333 | 67.667 | 1.301 | 4.666 | 29.00 | 0.558 | 0.429 | -0.846 |
| 3.000 | | 77.667 | 1.494 | 5.666 | 18.00 | 0.346 | 0.232 | -1.461 |
| 3.096 | | 85.000 | 1.635 | 5.833 | 10.50 | 0.202 | 0.124 | -2.087 |

***Thermodynamic parameters***

The values of equilibrium adsorption constant, $K_C$ were used to calculate the thermodynamic parameters, $\Delta G^o$ and $\Delta H^o$ by using equations (3.24 and 3.25) (Hossain *et al*., 2013; Ada *et al*., 2009; Nandi *et al*., 2009),

$$\Delta G^o = -RT \ln K_C \tag{3.24}$$

$$\ln K_C = \frac{\Delta S^o}{R} - \frac{\Delta H^o}{RT} \tag{3.25}$$

where, $\Delta G^o$ is the standard free energy ($kJ \cdot mol^{-1}$) and $\Delta H^o$ is the standard enthalpy ($kJ \cdot mol^{-1}$), $\Delta S^o$ is the change in standard entropy ($kJ \cdot mol^{-1} \cdot K^{-1}$), $R$ is the gas constant

(8.314 J·mol$^{-1}$·K$^{-1}$) and $T$ is the absolute temperature (K). The values of $\Delta H^o$ and $\Delta S^o$ were calculated from the slope and intercept of the linear plot of ln$K_c$ *vs* 1/$T$ as shown in Figure 3.31. The standard entropy change, $\Delta S^o$ was also calculated by using equation (3.26),

$$\Delta S^o = \frac{\Delta H^o - \Delta G^o}{T} \qquad (3.26)$$

The values of $\Delta G^o$, $\Delta H^o$ and $\Delta S^o$ for chromium (VI) adsorption on DBTL at different temperatures are presented in Table 3.22. The negative value of $\Delta H^o$ indicated the adsorption chromium (VI) on DBTL was exothermic, physorption in nature and spontaneous. The positive value of $\Delta G^o$ increased with increase of temperature which indicated the process was slow and less feasible. The negative value of $\Delta S^o$ predicted the decreased randomness through the adsorption of chromium (VI) on DBTL.

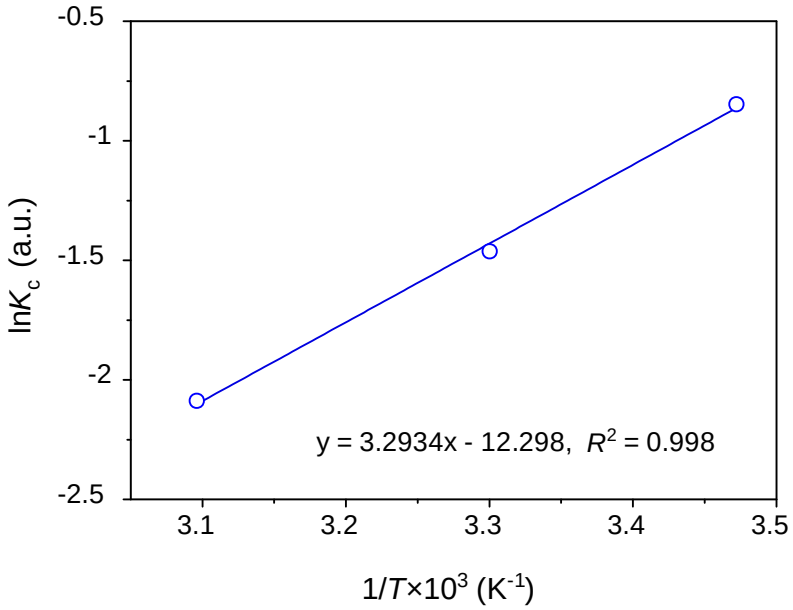


**Figure 3.31:** A plot of ln$K_c$ versus 1/$T$ for determination of change in enthalpy of chromium (VI) adsorption on DBTL at pH 2.0.

**Table 3.22** Thermodynamic parameters of chromium (VI) adsorption on DBTL at different temperatures.

| Temperature ± 0.2 (°C) | $\Delta H^o$ (kJ·mol$^{-1}$) | $\Delta G^o$ (kJ·mol$^{-1}$) | $\Delta S^o$ (kJ·mol$^{-1}$·K$^{-1}$) |
|---|---|---|---|
| 15 | - 27.38 | 2.026 | -0.102 |
| 30 | | 3.680 | |
| 50 | | 5.604 | |

### 3.6.2.2 Effect of temperature on diffusion mechanism

To evaluate the transfer mechanism, intra-particle diffusion model (3.20) was applied to the adsorption kinetics of a constant concentration of chromium (VI) on DBTL at different temperatures. The amount adsorbed ($q_t$) at time $t$ for different temperatures were plotted against the square root of time ($t^{1/2}$) to verify the applicability of intra-particle diffusion model at different temperatures as shown in Figure 3.32. The plots for different temperatures have shown that the experimental data did not follow the intraparticle diffusion shown in Figure 3.33a and the values the coefficient of correlation ($R^2$) are presented in Figure 3.33b. Such observations indicated that the adsorption is dominated by film diffusion, other than intraparticle diffusion.

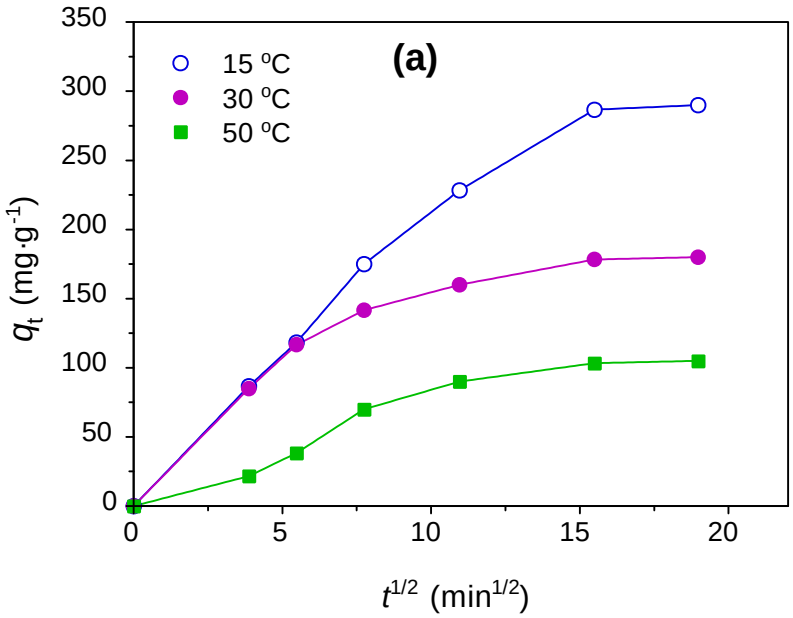


**Figure 3.32(a):** Application of the intra-particle diffusion equation to the adsorption of Cr (VI) on DBTL for different temperature at pH 2.0.

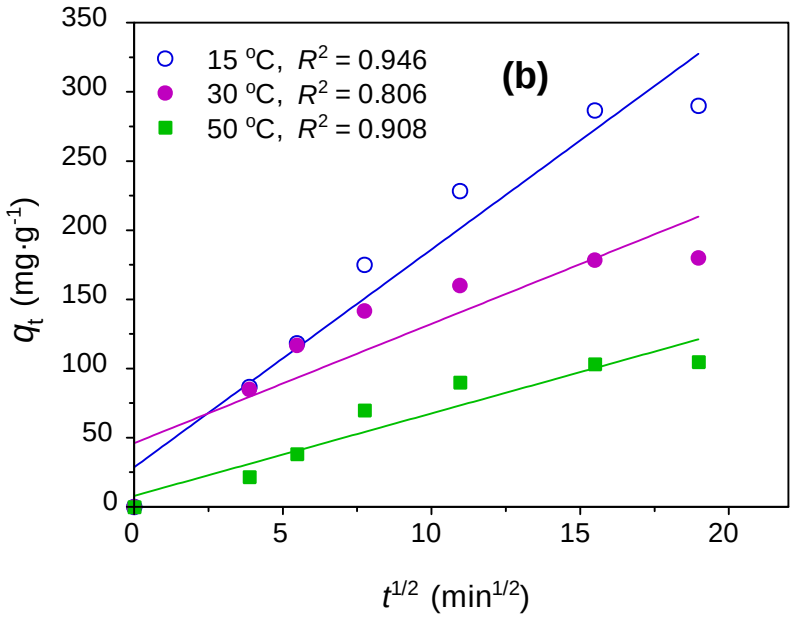


**Figure 3.32(b):** Application of the intra-particle diffusion equation to the adsorption of Cr (VI) on DBTL for different temperature at pH 2.0.

## 3.6.3 Effect of pH on Adsorption Kinetics

The effect of solution pH on the adsorption kinetic of chromium (VI) on DBTL was investigated using the following conditions:

**Experimental Conditions**

| | |
|---|---|
| Volume of chromium (VI) solution | : 25 mL |
| Concentration of chromium (VI) solution | : ≈100 $mg \cdot L^{-1}$ |
| Solution pH | : 2.0 – 8.0 |
| Amount of DBTL ($W_{DBTL}$) | : 0.0025 g |
| Particle size of DBTL | : < 106 µm |
| Adsorption temperature | : 30 ± 0.2 °C |
| Agitation rate | : 150 rpm |
| Agitation time ($t$) | : 0 to 6 hrs |

The amounts of chromium (VI) adsorbed on DBTL at different times for different pH of solution, were calculated using equation (3.9) and presented in Table 3.23 and 3.24. The amounts of chromium (VI) adsorbed on DBTL as a function of time for different pH were shown in Figure 3.33. The adsorption kinetic data for different pH were evaluated using different kinetic equations such as first order (Eq. 3.10), second order (Eq. 3.11), pseudo-first order (Eq. 3.12), pseudo-second order kinetic equations (Eq. 3.13), and Elovich equation (Eq. 3.15), and presented in Figures 3.34-3.38, respectively. Applicability of the equations was justified based on the value of coefficient corelation ($R^2 > 0.99$) of data fitness given in Table 3.26. Perameters of different kinetic equations are presented in Tables 3.27 and 3.28. Based on the values of coefficient of determination ($R^2$), experimental data for adsorption is well expressed by pseudo-second order kinetic equation. The equilibrium amount adsorbed and rate constants for different pH of solution were determined from the well fitted plot of pseudo second order kinetics and given in Table 3.28. The Figure 3.39 shows that the equilibrium amount of chromium (VI) adsorbed on DBTL linearly decreased with increase the initial pH of solution suggesting electrostatic interaction of Cr(VI) with DBTL at low pH.

**Table 3.23** Effect of solution pH on the adsorption kinetics of 101.333 mg·L$^{-1}$ chromium (VI) on DBTL at 30 ± 0.2 $^{o}$C.

| pH (-) | $t$ (min) | $C_t$ (mg·L$^{-1}$) | $C_T$ (mg·L$^{-1}$) | $C_R = C_T - C_t$ (mg·L$^{-1}$) | $q_t$ (mg·g$^{-1}$) |
|---|---|---|---|---|---|
| 2.0 | 15 | 90.500 | 92.833 | 2.333 | 85.00 |
| | 30 | 86.500 | 89.667 | 3.167 | 116.66 |
| | 60 | 83.500 | 87.167 | 3.667 | 141.66 |
| | 120 | 81.00 | 85.333 | 4.333 | 160.00 |
| | 240 | 79.000 | 83.500 | 4.500 | 178.33 |
| | 360 | 77.500 | 83.333 | 5.833 | 180.00 |
| 4.0 | 15 | 98.333 | 99.000 | 0.667 | 23.33 |
| | 30 | 97.000 | 98.000 | 1.000 | 33.33 |
| | 60 | 94.667 | 96.167 | 1.500 | 51.66 |
| | 120 | 91.000 | 93.833 | 2.833 | 75.00 |
| | 240 | 86.667 | 91.000 | 4.333 | 103.33 |
| | 360 | 85.167 | 90.667 | 5.500 | 106.66 |
| 6.0 | 15 | 100.000 | 101.167 | 0.167 | 11.66 |
| | 30 | 98.833 | 99.333 | 0.500 | 20.00 |
| | 60 | 97.500 | 98.667 | 1.167 | 26.66 |
| | 120 | 95.333 | 97.833 | 2.500 | 35.00 |
| | 240 | 92.833 | 97.000 | 4.167 | 43.33 |
| | 360 | 91.167 | 96.833 | 5.666 | 45.00 |
| 8.0 | 15 | 100.500 | 100.833 | 0.333 | 5.00 |
| | 30 | 99.833 | 100.500 | 0.667 | 8.33 |
| | 60 | 98.667 | 100.167 | 1.500 | 11.66 |
| | 120 | 96.667 | 99.500 | 2.833 | 18.33 |
| | 240 | 94.000 | 98.667 | 4.667 | 26.66 |
| | 360 | 93.333 | 98.500 | 5.167 | 28.33 |

**Table 3.24** Derived data for the application of first order, second order, pseudo-first order, pseudo-second order and Elovich equations to the adsorption chromium (VI) on DBTL at different pH of chromium (VI) solution.

| $C_o$ (mg·L-$^{1}$) | $t$ (min) | ln $t$ (a.u.) | $C_t$ (mg·L$^{-1}$) | $t/q_t$ (min·g·mg$^{-1}$) | ln$C_t$ (a.u.) | $1/C_t \times 10^2$ (L.mg$^{-1}$) | log $(q_e - q_t)$ (a.u.) |
|---|---|---|---|---|---|---|---|
| 2.0 | 15 | 2.708 | 90.500 | 0.176 | 4.505 | 1.105 | 1.978 |
| | 30 | 3.401 | 86.500 | 0.257 | 4.460 | 1.156 | 1.802 |
| | 60 | 4.094 | 83.500 | 0.424 | 4.425 | 1.198 | 1.584 |
| | 120 | 4.787 | 81.00 | 0.750 | 4.394 | 1.235 | 1.301 |
| | 240 | 5.481 | 79.00 | 1.346 | 4.369 | 1.266 | 0.223 |
| | 360 | 5.886 | 77.500 | 2.000 | 4.350 | 1.290 | - |
| 4.0 | 15 | 2.708 | 98.333 | 0.643 | 4.588 | 1.017 | 1.921 |
| | 30 | 3.401 | 97.000 | 0.900 | 4.575 | 1.031 | 1.865 |
| | 60 | 4.094 | 94.667 | 1.161 | 4.550 | 1.056 | 1.740 |
| | 120 | 4.787 | 91.00 | 1.600 | 4.511 | 1.099 | 1.501 |
| | 240 | 5.481 | 86.667 | 2.323 | 4.462 | 1.154 | 0.522 |
| | 360 | 5.886 | 85.167 | 3.375 | 4.445 | 1.174 | - |
| 6.0 | 15 | 2.708 | 100.00 | 1.286 | 4.605 | 1.000 | 1.523 |
| | 30 | 3.401 | 98.833 | 1.500 | 4.593 | 1.012 | 1.398 |
| | 60 | 4.094 | 97.500 | 2.251 | 4.580 | 1.023 | 1.263 |
| | 120 | 4.787 | 95.333 | 3.429 | 4.557 | 1.049 | 1.000 |
| | 240 | 5.481 | 92.833 | 5.539 | 4.531 | 1.077 | 0.223 |
| | 360 | 5.886 | 91.167 | 8.000 | 4.513 | 1.097 | - |
| 8.0 | 15 | 2.708 | 100.500 | 3.000 | 4.610 | 0.995 | 1.368 |
| | 30 | 3.401 | 99.833 | 3.601 | 4.603 | 1.002 | 1.301 |
| | 60 | 4.094 | 98.667 | 5.146 | 4.592 | 1.014 | 1.222 |
| | 120 | 4.787 | 96.667 | 6.547 | 4.571 | 1.034 | 1.000 |
| | 240 | 5.481 | 94.000 | 9.002 | 4.543 | 1.064 | 0.223 |
| | 360 | 5.886 | 93.333 | 12.707 | 4.536 | 1.071 | - |

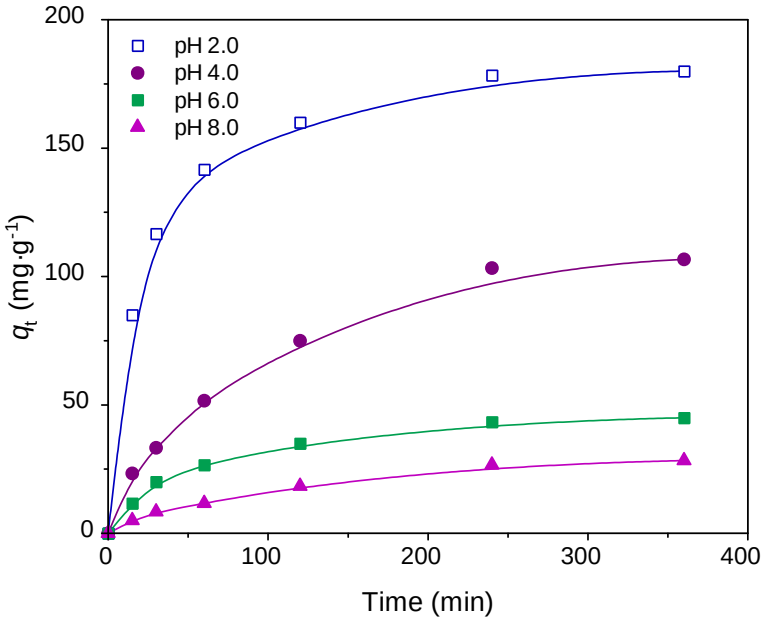


**Figure 3.33:** Variation of amount adsorbed of chromium (VI) on DBTL with time from aqueous solution of different pH at 30 $^{o}$C.

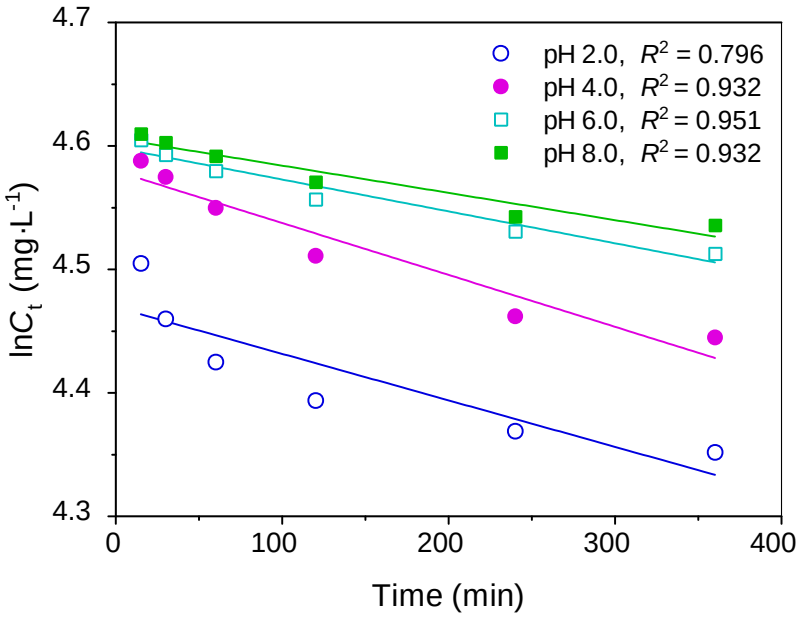


**Figure 3.34:** Application of the simple first order kinetic equation for the adsorption of chromium (VI) on DBTL from aqueous solution of different pH at 30 ± 0.2 $^{o}$C.

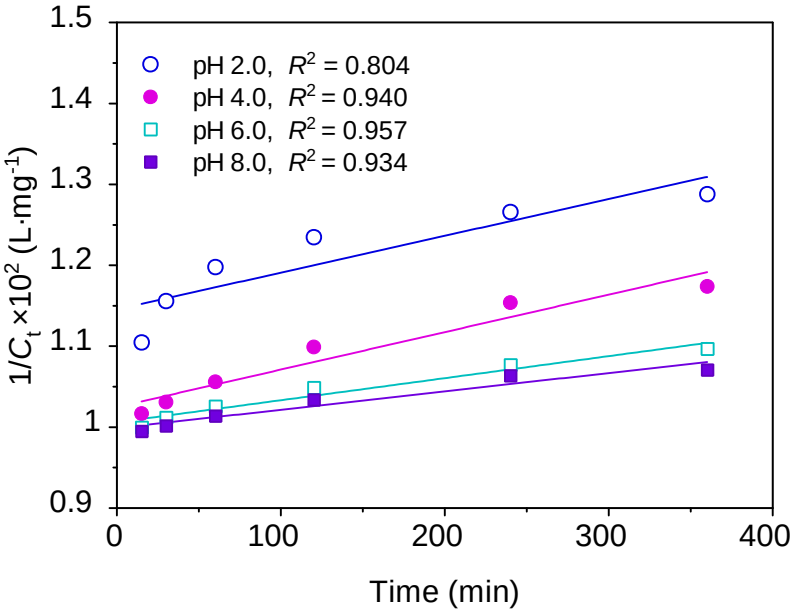


**Figure 3.35:** Application of the simple second order kinetic equation for the adsorption of chromium (VI) on DBTL from aqueous solution of different pH at 30 $^{o}$C.

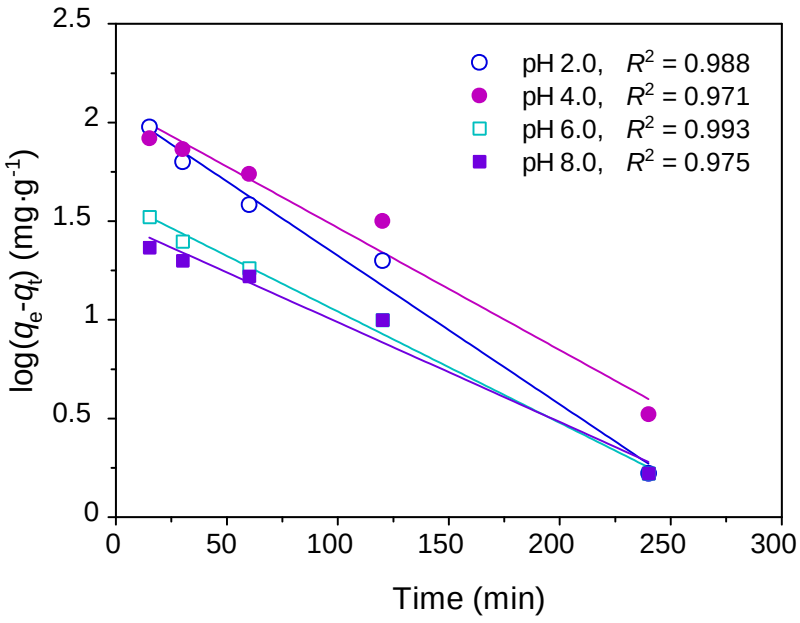


**Figure 3.36:** Application of the pseudo first order kinetic equation for the adsorption of chromium (VI) on DBTL from aqueous solution of different pH at 30 ± 0.2 $^{o}$C.

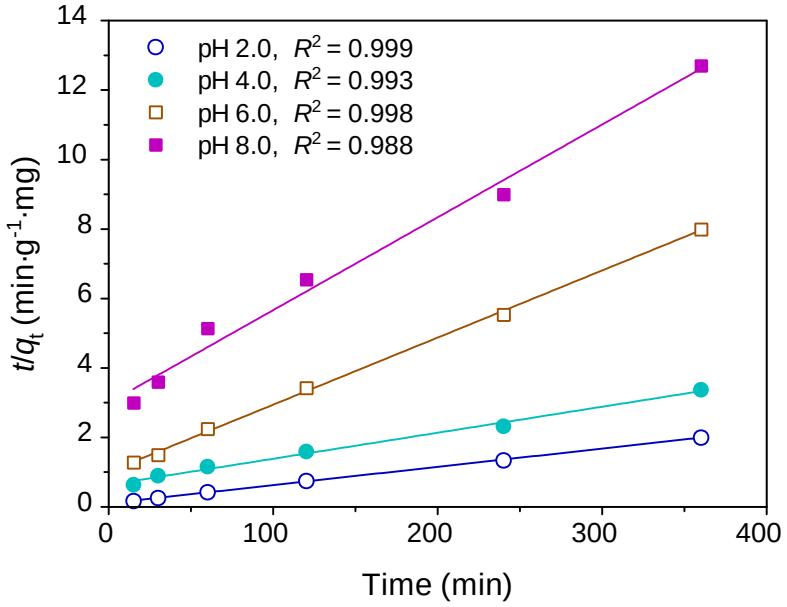


**Figure 3.37:** Application of the pseudo second order kinetic equation for the adsorption of chromium (VI) on DBTL from aqueous solution of different pH at 30 $^{o}$C.

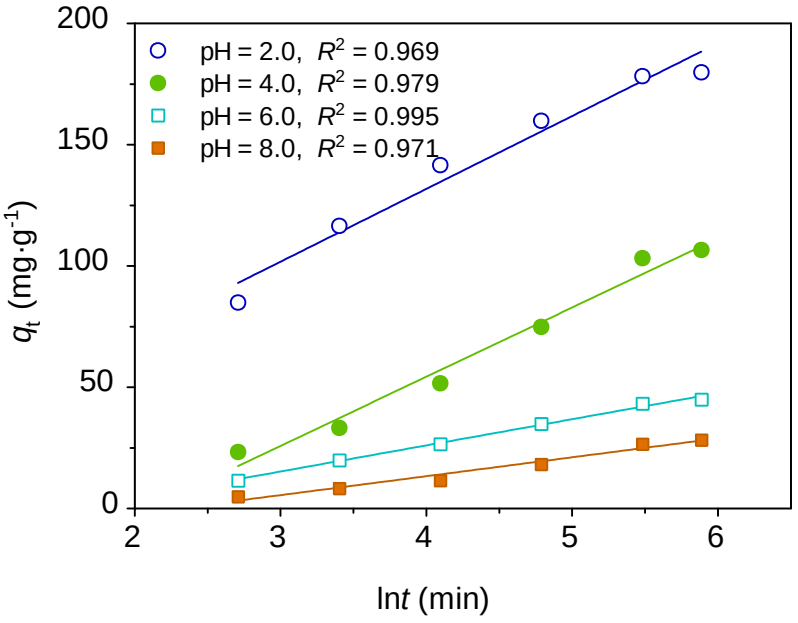


**Figure 3.38:** Application of the Elovich equation for the adsorption of chromium (VI) on DBTL from aqueous solution of different pH at 30 ± 0.2 $^{o}$C.

.

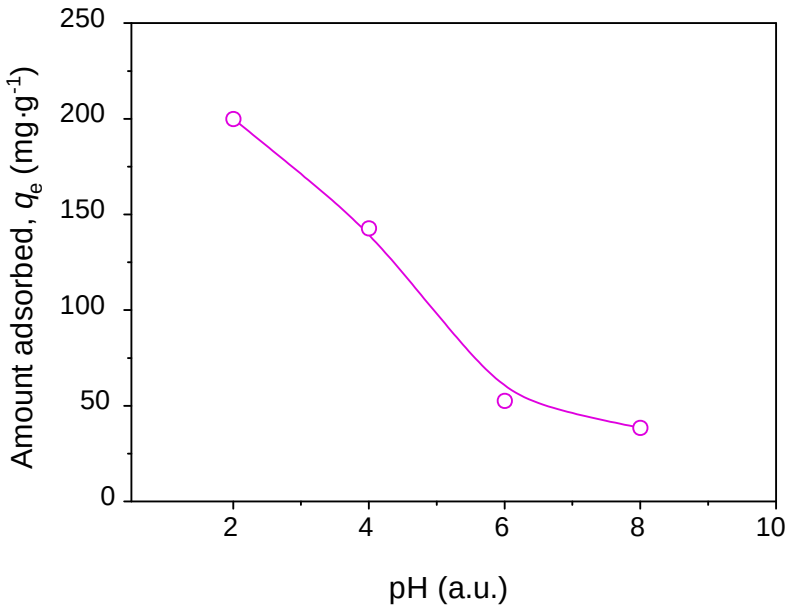


**Figure 3.39:** Variation of amount adsorbed with initial pH for the adsorption of chromium (VI) on DBTL from aqueous solution at 30 ± 0.2 $^{o}$C.

### 3.6.3.1 Effect of pH on adsorption mechanism

The pH of adsorbate solution is one of the most important parameters for adsorption of a metal-adsorbate from its aqueous solution, because it affects the solubility of metal-adsorbate ions, Concentration of counter ions on the functional groups of the adsorbent and the degree of ionization of the metal-adsorbate solution during reaction. The variation in pH of the adsorbate solution not only affects the charge profile of the adsorbent, it also adds extra $H^+$ or $OH^-$ ions to the adsorption system. These ions may compete with the ions of the adsorbate solution. It was evident in Figure 3.39 that equilibrium amount of chromium (VI) adsorbed on DBTL was the highest at initial pH 2.0 in comparison with that at initial pH 4, pH 6 and pH 8. The amount of chromium (VI) adsorbed decreased gradually with increase in initial pH from 2 to 8 of chromium (VI) solution. The observed findings may be interpreted as follows:

When pH of the chromium (VI) solution was lowest i.e. pH 2.0 in comparison with other pH values (pH 4, pH 6 and pH 8) of the solution, there is excess of protons ($H^+$ ions) in the adsorbate solution It was documented (Rumpa Saha *et al.,* 2011) that

chromium (VI) can mainly exists as an anionic species in the following forms and at three pH regions:

(i) $HCrO_4^-$ and $Cr_2O_7^{2-}$ ( pH 2-6)

(ii) $CrO_4^{2-}$ ( pH more than 6)

At pH 2, there is an excess $H^+$ ions in the solution of chromium (VI) which is attracted towards the oxygen-enriched hydroxyl groups of cellulose, phenolic groups of polyphenols and amino groups of proteins of tea leaves. These groups are coordinated by the unshared electrons of oxygen atoms of the groups. As a result, adsorption of chromium (VI) on DBTL at pH 2.0 was mostly favored due to electrostatic interaction among $HCrO_4^-$ and $Cr_2O_7^{2-}$ ions and protonated hydroxyl groups, phenolic groups and amino groups at the pH 2.0.

Tendency of adsorption of chromium (VI) gradually decreased with increase of pH of the solution because of gradual increase in repulsive interaction between dichromate, $Cr_2O_7^{2-}$ ions and deprotonated hydroxyl groups, phenolic groups and amino groups. Rather tendency for reduction of chromium (VI) to chromium (III) increased to significant extent due deprotonation of these groups with increase of pH. From such observation of the effect of solution pH, a possible mechanism for the removal of Cr(VI) by DBTL is schematically presented in Figure 3.40.

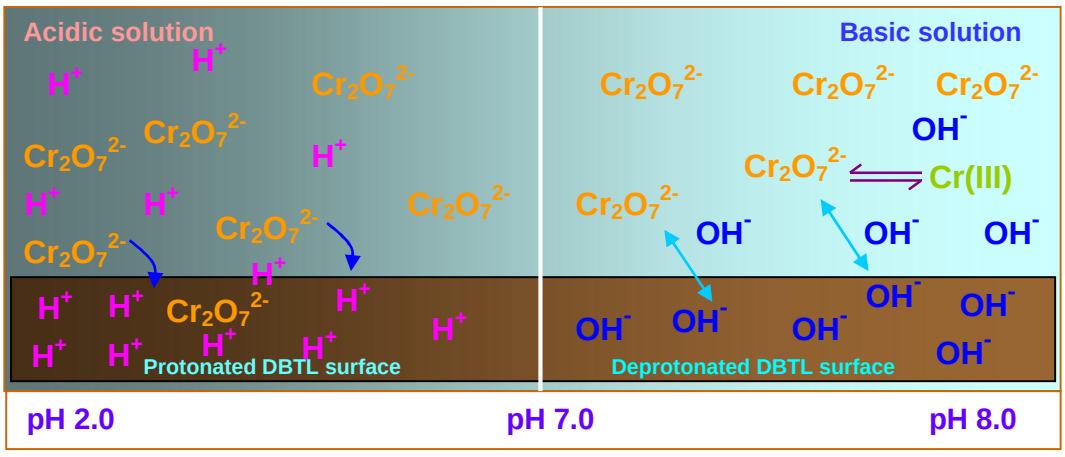


**Figure 3.40:** Schematic presentation of the removal mechanism of chromium (VI) by DBTL.

### 3.6.3.2 Effect of pH on diffusion mechanism

Intra-particle diffusion model equation (Eq. 3.20) was applied to the adsorption kinetics of a constant concentration of chromium (VI) on DBTL at different pH of solution to evaluate the effect of pH on diffusion mechanism. The amount adsorbed ($q_t$) at time $t$ for different pH of solution were plotted against the square root of time ($t^{1/2}$) as shown in Figure 3.41. The plots for different initial pH of solution have shown that the experimental data follow the intraparticle diffusion at higher pH of solution, but at low pH the lines became curvature (Figure 3.41a) which indicated that the adsorption is dominated by film diffusion at low pH of solution. The values the coefficients of correlation ($R^2$) of the plots are presented in Figure 3.41b. Such type of observation might be due to the electrostatic interaction between the protonated DBTL surface with the negatively charged ions of Cr(VI) at low pH.

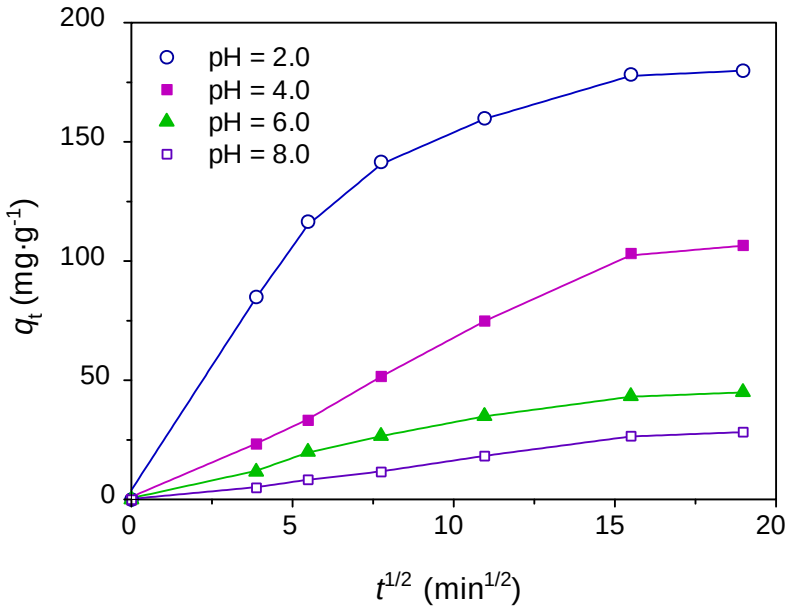


**Figure 3.41(a):** Application of the intra particle diffusion equation for the adsorption of Cr (VI) on DBTL at different pH of solution at 30 ± 0.2°C.

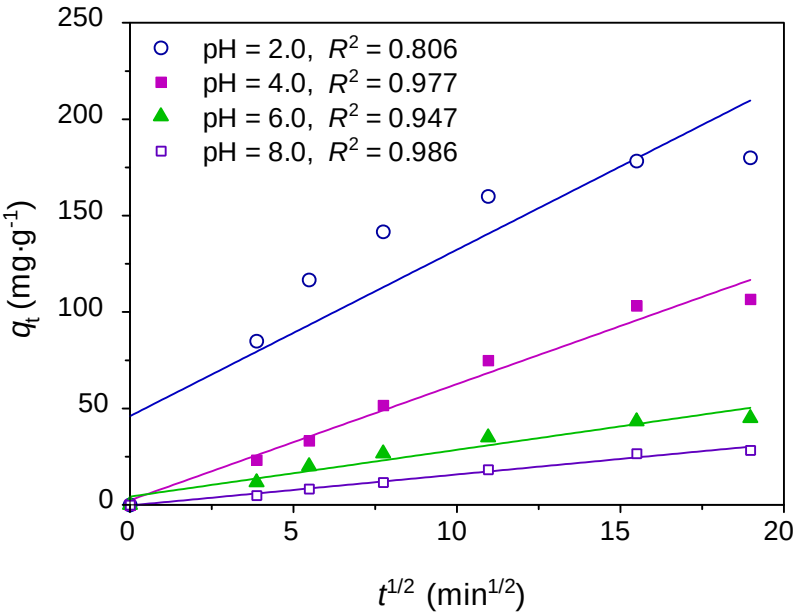


**Figure 3.41(b):** Application of the intra particle diffusion equation for the adsorption of Cr (VI) on DBTL at different pH of solution at 30 ± 0.2°C.

## 3.6.4 Effect of Particle Size on Adsorption Kinetics

The effect of particle size of DBTL on the adsorption kinetic of chromium (VI) on DBTL was investigated using the following conditions:

**Experimental Conditions**

| | |
|---|---|
| Volume of chromium (VI) solution | : 25 mL |
| Concentration of chromium (VI) solution | : ≈100 $mg \cdot L^{-1}$ |
| Solution pH | : 2.0 |
| Amount of DBTL ($W_{DBTL}$) | : 0.0025 g |
| Particle size of DBTL | : < 106, 150, 212 and 450 µm |
| Adsorption temperature | : 30 ± 0.2 °C |
| Agitation rate | : 150 rpm |
| Agitation time ($t$) | : 0 to 6 hrs |

The amounts of chromium (VI) adsorbed on DBTL at different times for different sizes of DBTL, were calculated using equation (3.9) and presented in Table 3.25 and 3.26. The amounts of chromium (VI) adsorbed on DBTL as a function of time for different sizes of DBTL were shown in Figure 3.42. The adsorption kinetic data for different sizes of DBTL were evaluated using different kinetic equations such as first order (Eq. 3.10), second order (Eq. 3.11), pseudo-first order (Eq. 3.12), pseudo-second order kinetic equations (Eq. 3.13) and Elovich equation (Eq. 3.15), and presented in Figures 3.43-3.47, respectively. Applicability of the equations was justified based on the value of coefficient corelation ($R^2 > 0.99$) of data fitness given in Table 3.27-3.28. Based on the values of coefficient of determination ($R^2$), experimental data for adsorption are well expressed by pseudo-second order kinetic equation for different particle sizes of DBTL. The equilibrium amount adsorbed and rate constants for different sizes of DBTL were determined from the well fitted plot of pseudo second order kinetics and given in Tables 3.29 and 3.30. The Figure 3.48 shows that the equilibrium amount of chromium (VI) adsorbed on DBTL decreased with increase of particle sizes of DBTL. The adsorption of Cr(VI) on DBTL also shows that the rate of adsorption decreased with the increase in particle size of DBTL from 106 to 450 µm. The higher rate of chromium (VI) uptake

by smaller particle is due to the greater accessibility to pores and greater surface area per unit mass of small sizes DBTL.

**Table 3.25** Effect of particle size of DBTL on the adsorption kinetics of about 101.333 $mg \cdot L^{-1}$ chromium (VI) on DBTL at pH 2.0 and 30 ± 0.2 $^{o}$C.

| Particle-size (µm) | *t* (min) | $C_t$ ($mg \cdot L^{-1}$) | $C_T$ ($mg \cdot L^{-1}$) | $C_R = C_T - C_t$ ($mg \cdot L^{-1}$) | $q_t$ ($mg \cdot g^{-1}$) |
|---|---|---|---|---|---|
| 106 | 15 | 90.500 | 92.833 | 2.333 | 85.00 |
| | 30 | 86.500 | 89.667 | 3.167 | 116.66 |
| | 60 | 83.500 | 87.167 | 3.667 | 141.66 |
| | 120 | 81.000 | 85.333 | 4.333 | 160.00 |
| | 240 | 79.000 | 83.500 | 4.500 | 178.33 |
| | 360 | 77.500 | 83.333 | 5.833 | 180.00 |
| 150 | 15 | 92.500 | 94.333 | 1.833 | 70.00 |
| | 30 | 90.167 | 92.667 | 2.500 | 86.66 |
| | 60 | 86.500 | 89.667 | 3.167 | 116.66 |
| | 120 | 84.833 | 88.500 | 3.666 | 128.33 |
| | 240 | 82.667 | 87.500 | 4.833 | 138.33 |
| | 360 | 81.167 | 87.167 | 6.000 | 141.66 |
| 212 | 15 | 94.500 | 95.667 | 1.167 | 56.66 |
| | 30 | 93.167 | 94.833 | 1.666 | 65.00 |
| | 60 | 91.000 | 93.667 | 2.667 | 76.66 |
| | 120 | 89.500 | 92.833 | 3.333 | 85.00 |
| | 240 | 85.000 | 89.333 | 4.333 | 120.00 |
| | 360 | 82.500 | 89.000 | 6.500 | 123.33 |
| 450 | 15 | 98.500 | 99.500 | 1.000 | 18.33 |
| | 30 | 97.333 | 98.667 | 1.334 | 26.66 |
| | 60 | 95.167 | 97.000 | 1.833 | 43.33 |
| | 20 | 91.000 | 94.333 | 3.833 | 65.00 |
| | 240 | 89.000 | 93.500 | 4.500 | 78.33 |
| | 360 | 86.667 | 93.167 | 6.500 | 81.66 |

**Table 3.26** Derived data for the application of first order, second order, pseudo-first order, pseudo-second order and Elovich equations to the adsorption chromium (VI) on different sizes of DBTL at pH 2.0 and 30 ± 0.2 °C.

| Particle-size (µm) | $t$ (min) | ln $t$ (a.u.) | $C_t$ (mg·L$^{-1}$) | $t/q_t$ (min·g·mg$^{-1}$)} | ln $C_t$ (a.u.) | $1/C_t \times 10^2$ (L.mg$^{-1}$) | log ($q_e$- $q_t$) (a.u.) |
|---|---|---|---|---|---|---|---|
| < 106 | 15 | 2.708 | 90.500 | 0.176 | 4.505 | 1.105 | 1.978 |
| | 30 | 3.401 | 86.500 | 0.257 | 4.460 | 1.156 | 1.802 |
| | 60 | 4.094 | 83.500 | 0.424 | 4.425 | 1.198 | 1.584 |
| | 120 | 4.787 | 81.000 | 0.750 | 4.394 | 1.235 | 1.301 |
| | 240 | 5.481 | 79.000 | 1.346 | 4.369 | 1.266 | 0.223 |
| | 360 | 5.886 | 77.500 | 2.000 | 4.350 | 1.290 | - |
| 106-150 | 15 | 2.708 | 92.500 | 0.214 | 4.527 | 1.081 | 1.855 |
| | 30 | 3.401 | 90.167 | 0.346 | 4.502 | 1.109 | 1.740 |
| | 60 | 4.094 | 86.500 | 0.514 | 4.460 | 1.156 | 1.398 |
| | 120 | 4.787 | 84.833 | 0.935 | 4.441 | 1.179 | 1.125 |
| | 240 | 5.481 | 82.667 | 1.735 | 4.415 | 1.210 | 0.522 |
| | 360 | 5.886 | 81.167 | 2.541 | 4.397 | 1.232 | - |
| 150-212 | 15 | 2.708 | 94.500 | 0.265 | 4.549 | 1.058 | 1.824 |
| | 30 | 3.401 | 93.167 | 0.462 | 4.534 | 1.073 | 1.766 |
| | 60 | 4.094 | 91.000 | 0.783 | 4.511 | 1.099 | 1.669 |
| | 120 | 4.787 | 89.500 | 1.412 | 4.494 | 1.117 | 1.584 |
| | 240 | 5.481 | 85.000 | 2.000 | 4.443 | 1.176 | 0.522 |
| | 360 | 5.886 | 82.500 | 2.919 | 4.413 | 1.212 | - |
| 212-450 | 15 | 2.708 | 98.500 | 0.818 | 4.590 | 1.015 | 1.802 |
| | 30 | 3.401 | 97.333 | 1.125 | 4.578 | 1.027 | 1.740 |
| | 60 | 4.094 | 95.167 | 1.385 | 4.556 | 1.051 | 1.584 |
| | 120 | 4.787 | 91.000 | 1.846 | 4.511 | 1.099 | 1.222 |
| | 240 | 5.481 | 89.000 | 3.064 | 4.489 | 1.124 | 0.522 |
| | 360 | 5.886 | 86.667 | 4.409 | 4.462 | 1.154 | - |

**Table 3.27** Comparison of the regression co-efficient ($R^2$) to justify the fitness of different kinetic equations for the adsorption of chromium (VI) on DBTL for different particle sizes at pH 2.0 and 30 ± 0.2 °C.

| Particle-size (µm) | $R^2$ First order kinetics (a.u) | $R^2$ Second order kinetics (a.u) | $R^2$ Pseudo first order kinetics (a.u) | $R^2$ Pseudo second order kinetics (a.u) | $R^2$ Elovich equation (a.u) |
|---|---|---|---|---|---|
| < 106 | 0.789 | 0.804 | 0.988 | 0.999 | 0.968 |
| 106-150 | 0.825 | 0.838 | 0.976 | 0.999 | 0.950 |
| 150-212 | 0.974 | 0.979 | 0.917 | 0.983 | 0.932 |
| 212-450 | 0.913 | 0.920 | 0.999 | 0.996 | 0.982 |

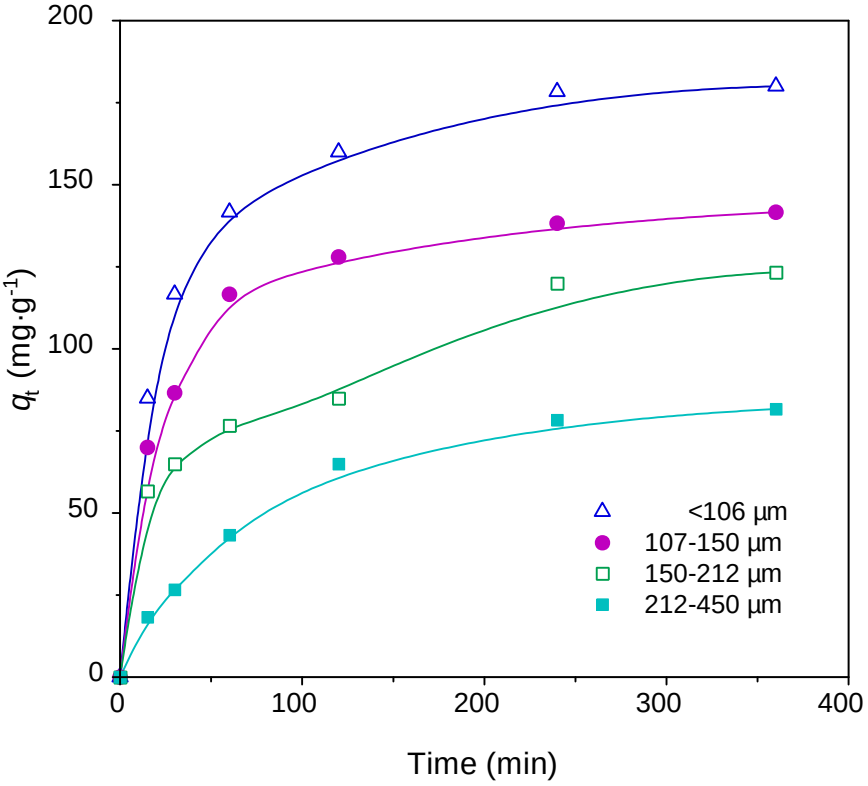


**Figure 3.42:** Variation of amount adsorbed of chromium (VI) on different sizes of DBTL with time from aqueous solution at pH 2.0 and 30 ± 0.2 $^{o}$C.

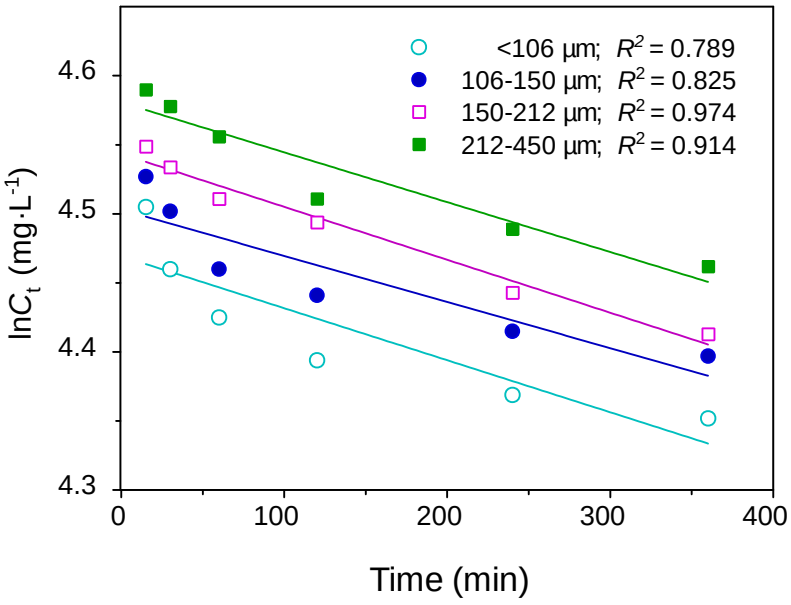


**Figure 3.43:** Application of the simple first order kinetic equation for the adsorption of chromium (VI) on different sizes of DBTL from aqueous solution at pH 2.0 and 30 ± 0.2 $^{o}$C.

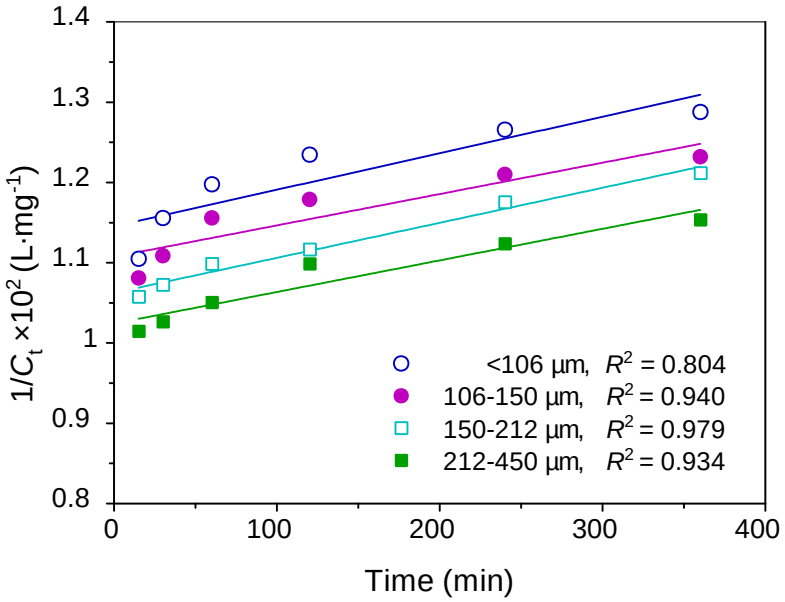


**Figure 3.44:** Application of the simple second order kinetic equation for the adsorption of chromium(VI) on different sizes of DBTL from aqueous solution at pH 2.0 and 30 $^{o}$C.

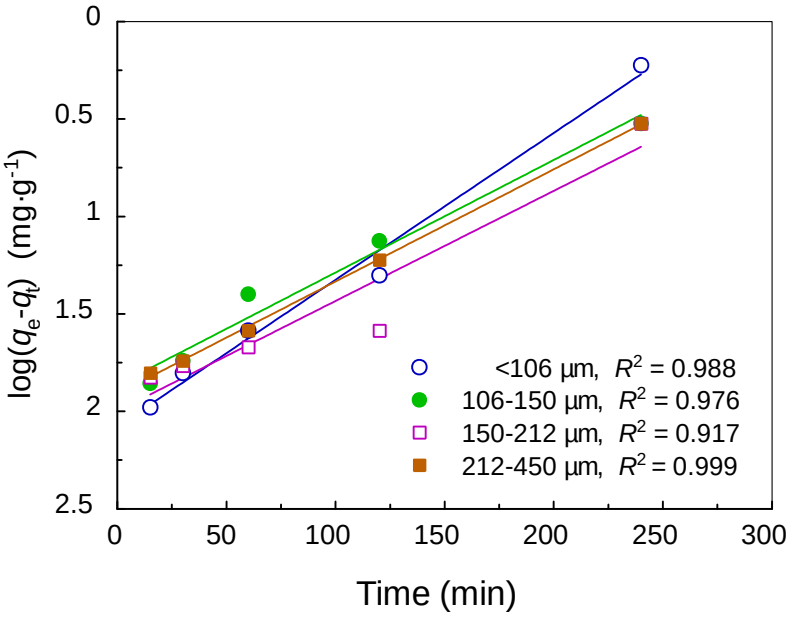


**Figure 3.45:** Application of the pseudo first order kinetic equation for the adsorption of chromium (VI) on different sizes of DBTL from aqueous solution at pH 2.0 and 30 ± 0.2 $^{o}$C

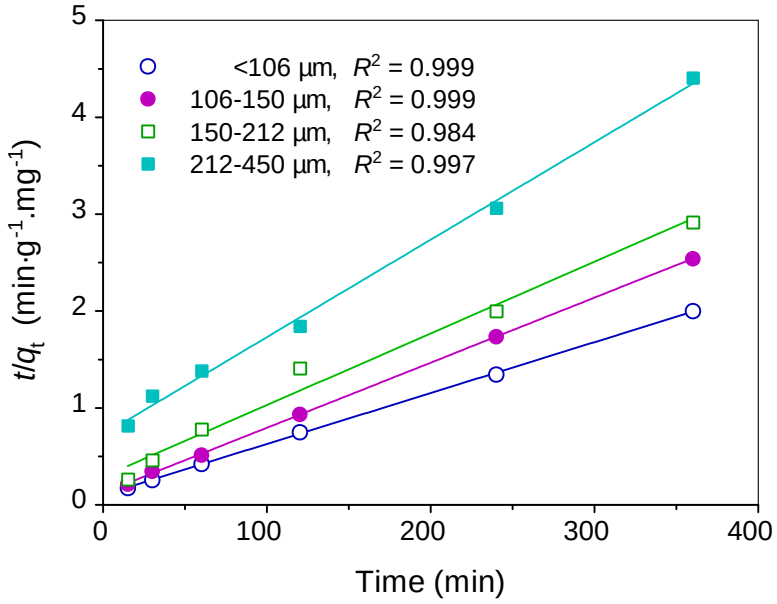


**Figure 3.46:** Application of the pseudo second order kinetic equation for the adsorption of chromium (VI) on different sizes of DBTL from aqueous solution at pH 2.0 and 30.0 ± 0.2°C.

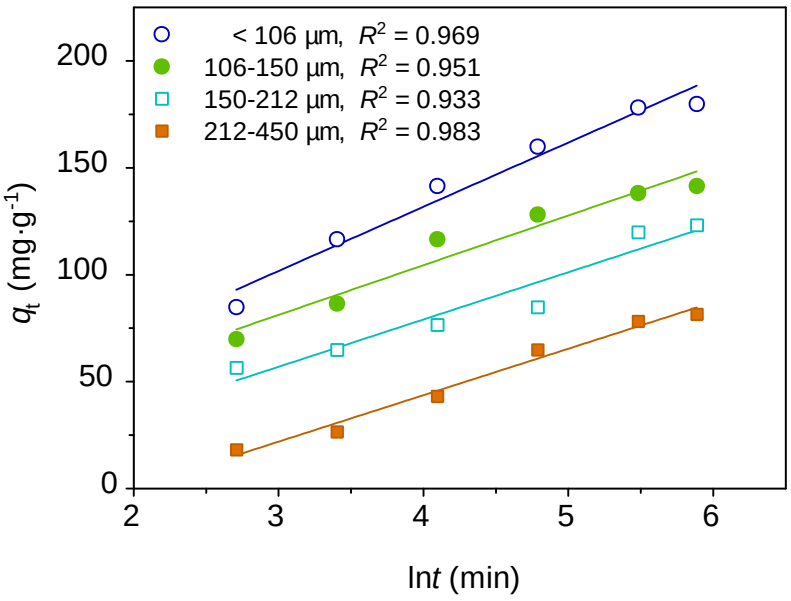


**Figure 3.47:** Application of the Elovih equation for the adsorption of Cr (VI) on different sizes of DBTL at pH 2.0 and 30.0 ± 0.2°C**.**

**Table 3.28** Comparison of the rate constants of different kinetic equations for adsorption of chromium (VI) at different particle sizes of DBTL at pH 2.0 and 30 ± 0.2 °C.

| Particle-size (μm) | $k_1$ First order kinetics equation ($min^{-1}$) | $k_2$ Second order kinetics ($g \cdot mg^{-1} \cdot min^{-1}$) | $k_{1p}$ Pseudo first order kinetics ($min^{-1}$) | $k_{2p} \times 10^4$ Pseudo second order kinetics ($g \cdot mg^{-1} \cdot min^{-1}$) | $\alpha$ Elovich equation ($mg \cdot g^{-1} \cdot min^{-1}$) |
|---|---|---|---|---|---|
| < 106 | 0 | 0 | 0.016 | 2.427 | 44.31 |
| 106-150 | 0 | 0 | 0.012 | 2.903 | 38.11 |
| 150-212 | 0 | 0 | 0.012 | 1.695 | 14.49 |
| 212-450 | 0 | 0 | 0.012 | 1.381 | 2.979 |

**Table 3.29** Parameters of different kinetic equations for adsorption of chromium (VI) at different particle sizes of DBTL at pH 2.0 and 30 ± 0.2 °C.

| Particle-size | $q_e$ Pseudo first order kinetics | Pseudo second order kinetics | | $\beta$ Elovich equation ($g \cdot mg^{-1}$) |
|---|---|---|---|---|
| | | $C_e$ ($mg \cdot L^{-1}$) | $q_e$ ($mg \cdot g^{-1}$) | |
| < 106 | 119.67 | 81.333 | 200.00 | 0.033 |
| 106-150 | 73.28 | 84.666 | 166.67 | 0.043 |
| 150-212 | 99.54 | 87.047 | 142.86 | 0.045 |
| 212-450 | 81.10 | 91.333 | 100.00 | 0.046 |

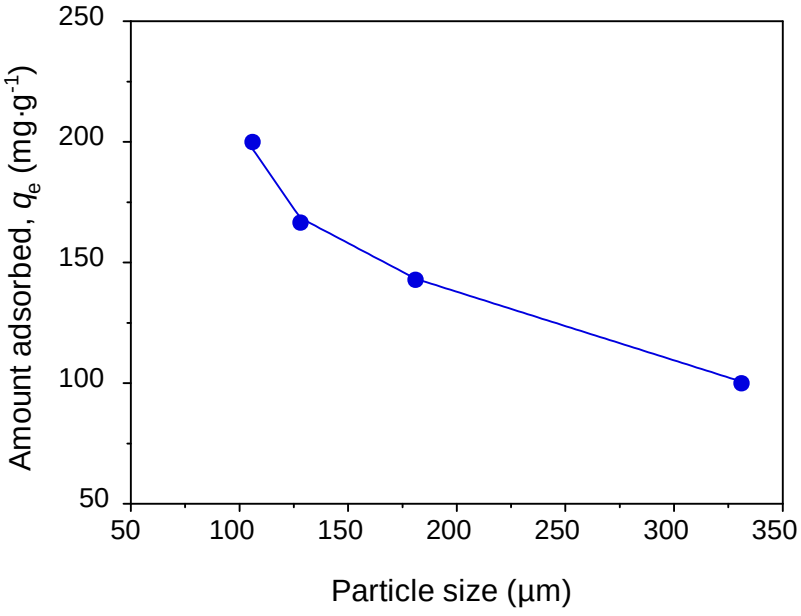


**Figure 3.48:** Variation of amount adsorbed (derived from pseudo second order kinetics) with particle sizes of DBTL for the adsorption of chromium (VI) on DBTL from aqueous solution at pH 2.0 and 30 ± 0.2 °C.

### 3.6.4.1 Effect of particle size on diffusion mechanism

The effect of particle size of DBTL on the intraparticle diffusion of chromium (VI) onto adsorbed on DBTL was investigated by performing kinetic experiments with four different particle size of DBTL using same concentration of chromium (VI) solution. The amount adsorbed ($q_t$) at time $t$ for different particle size of DBTL against square root of time ($t^{1/2}$) are shown in Figure 3.49. The plots for different particle sizes of DBTL have shown that the experimental data follow the intraparticle diffusion model equation for large size of particle, but for small size of DBTL the lines became curvature (Fig. 3.49a) which indicated that the adsorption is dominated by film diffusion for small size of particle. The values the coefficients of correlation ($R^2$) of the plots for different particle sizes are presented in Figure 3.49b. Such observation might be due to the existence of large size of cavity on the large size of DBTL particles resultant the retardation of the movement of adsorbed species from the cavity (Hossain, 2006). Thus both processes are observed for adsorption kinetics of Cr(VI) on DBTL– the external mass transfer from the solution to the liquid-solid interface and the diffusion of the adsorbed species inside the porous particle.

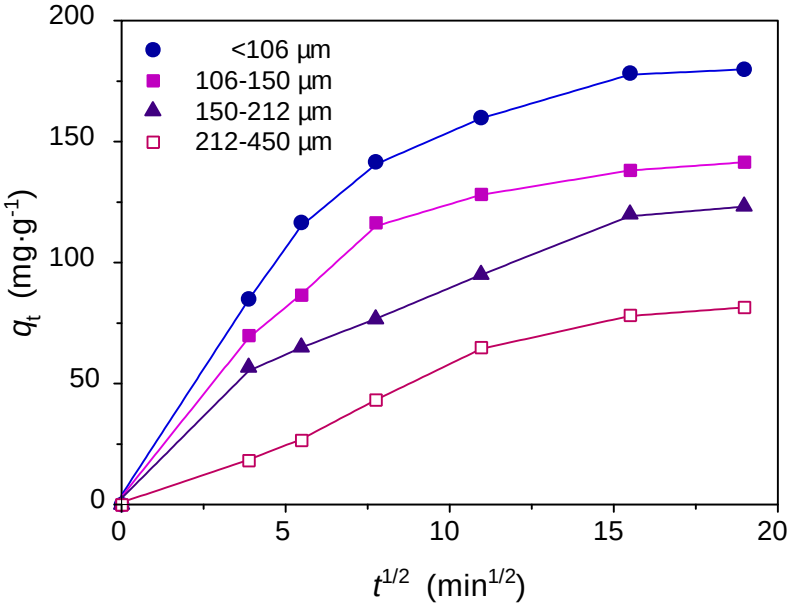


**Figure 3.49(a):** Application of the intra-particle diffusion equation for the adsorption of Cr (VI) on different sizes of DBTL (106 µm) at pH 2.0 and 30.0 ± 0.2°C**.**

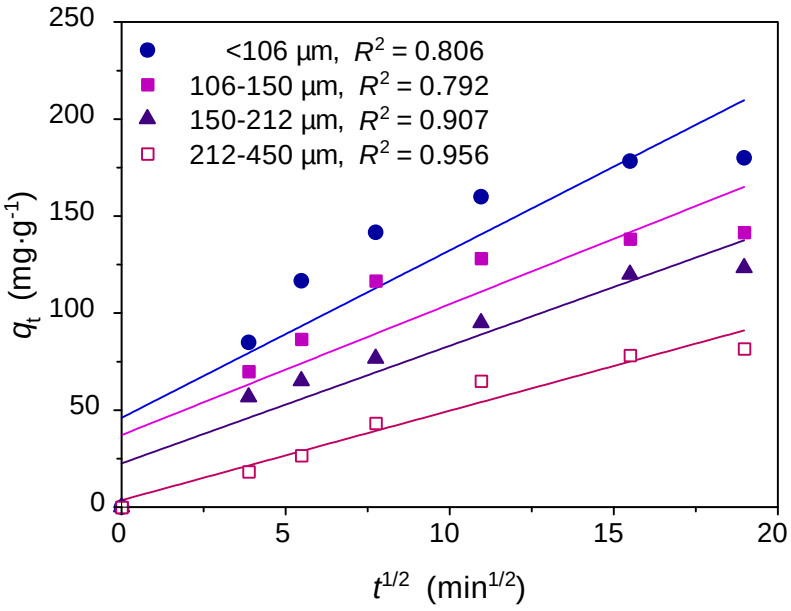


**Figure 3.49(b):** Application of the intra-particle diffusion equation for the adsorption of Cr (VI) on different sizes of DBTL (106 µm) at pH 2.0 and 30.0 ± 0.2°C**.**

# 3.7 Equilibrium Adsorption

## 3.7.1 Estimation of Equilibrium Time

Equilibrium time was estimated from the effect of time on the adsorption of chromium (VI) on DBTL using the following conditions:

**Experimental Conditions**

| | |
|---|---|
| Volume of chromium (VI) solution | : 25 mL |
| Concentration of chromium (VI) solution | : ≈100 $mg \cdot L^{-1}$ |
| Solution pH | : 2.0 |
| Amount of DBTL ($W_{DBTL}$) | : 0.0025 g |
| Particle size of DBTL | : < 106 µm |
| Adsorption temperature | : 30 ± 0.2 °C |
| Agitation rate | : 150 rpm |
| Agitation time (*t*) | : 0 to 6 hrs |

The amounts of chromium (VI) adsorbed on DBTL at different times was calculated using equation (3.9) and presented in Table 3.30. The amounts of chromium (VI) adsorbed on DBTL as a function of time are shown in Figure 3.50. The figure shows that the adsorption of chromium (VI) was rapid in the beginning and it became slower gradually with progress of time and became almost steady at 360 minutes (6 hours). This period of time was considered as equilibrium time in this study. The steadiness of adsorption at this stage may be interpreted due to the fact that the chromium (VI) ion occupied the active sites in a random manner because of maximum availability of sites.

**Table 3.30** Determination of equilibrium time for the adsorption isotherm of chromium (VI) on Dust Black Tea Leaves at .

| *t* (min) | $C_o$ ($mg \cdot L^{-1}$) | $C_t$ ($mg \cdot L^{-1}$) | $q_t$ ($mg \cdot g^{-1}$) |
|---|---|---|---|
| 15 | 101.333 | 90.50 | 85.00 |
| 30 | | 86.50 | 116.66 |
| 60 | | 83.50 | 141.66 |
| 120 | | 81.00 | 160.00 |
| 240 | | 78.50 | 178.33 |
| 360 | | 77.50 | 180.00 |

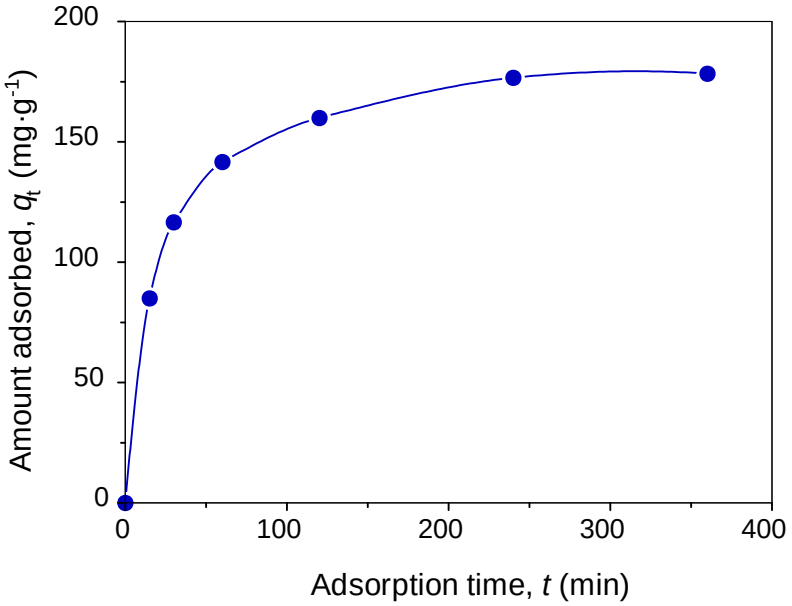


**Figure 3.50 :** Estimation of equilibrium time for purely adsorption of chromium (VI) on DBTL at pH 2.0 and 30.0 ± 0.2 $^{o}$C.

## 3.7.2 Adsorption Isotherms at Different Temperatures

The adsorption isotherms of chromium (VI) on DBTL at different temperatures were constructed using the following conditions:

**Experimental Conditions**

| | |
|---|---|
| Volume of chromium (VI) solution | : 25 mL |
| Concentration of chromium (VI) solution | : 25 – 250 mg·L$^{-1}$ |
| Solution pH | : 2.0 |
| Amount of DBTL ($W_{DBTL}$) | : 0.0025 g |
| Particle size of DBTL | : < 106 µm |
| Adsorption temperature | : 15, 30 and 50 (± 0.2) °C |
| Agitation rate | : 150 rpm |
| Agitation time ($t_e$) | : 6 hrs |

The equilibrium concentrations of chromium (VI), after adsorption, for different initial concentrations were determined from the analytical data and presented in Table 3.31. The equilibrium amounts of chromium (VI) adsorbed on DBTL for different initial concentrations were also calculated using equation (3.9) and presented in Table 3.31. The adsorption isotherms of chromium (VI) adsorbed on DBTL at different temperatures are presented in Figure 3.51. Derived-data are shown in Tables 3.32-3.34 to verify different isotherms model equations for the adsorption process at different temperatures.

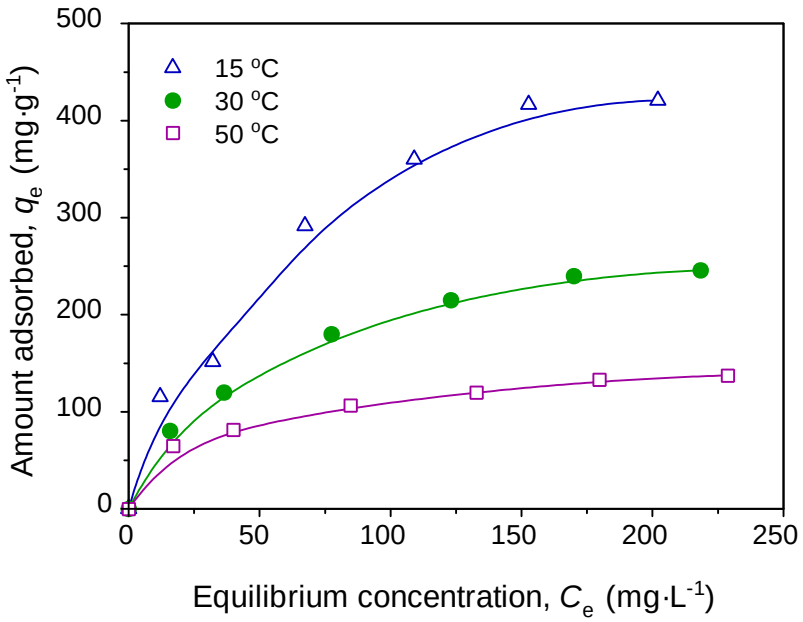


**Figure 3.51:** Adsorption isotherm of chromium (VI) on DBTL at different temperatures and at pH 2.0.

**Table 3.31** Estimation of adsorption isotherms of chromium (VI) on DBTL for different temperatures and at pH 2.0.

| Temp. ($^oC$) | $C_o$ ($mg{\cdot}L^{-1}$) | $C_e$ ($mg{\cdot}L^{-1}$) | $C_{oxidation}$ ($mg{\cdot}L^{-1}$) | $C_R = C_{oxidation} - C_e$ ($mg{\cdot}L^{-1}$) | $q_e$ $mg{\cdot}g^{-1}$ |
|---|---|---|---|---|---|
| 15 | 25.500 | 12.042 | 13.958 | 1.916 | 115.420 |
| | 50.083 | 32.830 | 34.917 | 2.834 | 151.660 |
| | 101.333 | 67.333 | 72.167 | 4.834 | 291.660 |
| | 150.750 | 109.000 | 114.750 | 5.750 | 360.000 |
| | 201.000 | 152.667 | 159.333 | 6.666 | 416.670 |
| | 251.250 | 202.083 | 209.167 | 7.084 | 420.830 |
| 30 | 25.833 | 15.750 | 17.792 | 2.042 | 80.410 |
| | 51.583 | 36.333 | 39.583 | 3.250 | 120.000 |
| | 101.333 | 77.500 | 83.333 | 5.833 | 180.000 |
| | 151.250 | 123.000 | 129.750 | 6.750 | 215.000 |
| | 201.333 | 170.000 | 177.333 | 7.333 | 240.000 |
| | 250.833 | 218.333 | 226.250 | 7.916 | 245.840 |
| 50 | 25.833 | 16.958 | 19.333 | 2.375 | 65.000 |
| | 52.333 | 39.917 | 44.167 | 4.250 | 81.660 |
| | 101.333 | 84.667 | 90.667 | 6.000 | 106.660 |
| | 151.750 | 132.750 | 139.750 | 7.000 | 120.000 |
| | 201.000 | 179.667 | 187.667 | 8.000 | 133.330 |
| | 250.833 | 228.750 | 237.083 | 8.333 | 137.500 |

**Table 3.32** Derived-data for investigation of Langmuir and Freundlich equations for adsorption of chromium (VI) on DBTL at different temperatures.

| Tempera-ture ± 0.2 (°C) | $C_o$ (mg·L$^{-1}$) | $C_e$ (mg·L$^{-1}$) | $C_e \times 10^3$ (mol·L$^{-1}$) | $q_e$ (mg·g$^{-1}$) | $q_e \times 10^3$ (mol·g$^{-1}$) | $C_e/q_e$ (g.L$^{-1}$) | log $C_e$ (a.u) | log $q_e$ (a.u) |
|---|---|---|---|---|---|---|---|---|
| 15 | 25.500 | 12.042 | 0.232 | 115.42 | 2.220 | 0.105 | 1.081 | 2.062 |
| | 50.083 | 32.083 | 0.617 | 151.66 | 2.917 | 0.212 | 1.506 | 2.181 |
| | 101.333 | 67.333 | 1.295 | 291.66 | 5.609 | 0.231 | 1.828 | 2.465 |
| | 150.750 | 109.000 | 2.096 | 360.00 | 6.923 | 0.303 | 2.037 | 2.556 |
| | 201.000 | 152.667 | 2.936 | 416.67 | 8.013 | 0.366 | 2.184 | 2.620 |
| | 251.250 | 202.083 | 3.886 | 420.83 | 8.093 | 0.480 | 2.306 | 2.624 |
| 30 | 25.833 | 15.750 | 0.303 | 80.410 | 1.546 | 0.196 | 1.197 | 1.905 |
| | 51.583 | 36.333 | 0.699 | 120.00 | 2.308 | 0.303 | 1.560 | 2.079 |
| | 101.333 | 77.500 | 1.490 | 180.00 | 3.462 | 0.430 | 1.889 | 2.255 |
| | 151.250 | 123.000 | 2.365 | 215.00 | 4.135 | 0.572 | 2.090 | 2.332 |
| | 201.333 | 170.000 | 3.269 | 240.00 | 4.615 | 0.708 | 2.230 | 2.380 |
| | 250.833 | 218.333 | 4.199 | 245.84 | 4.728 | 0.888 | 2.339 | 2.391 |
| 50 | 25.833 | 16.958 | 0.326 | 65.000 | 1.250 | 0.261 | 1.229 | 1.813 |
| | 52.333 | 39.917 | 0.768 | 81.660 | 1.570 | 0.489 | 1.601 | 1.912 |
| | 101.333 | 84.667 | 1.628 | 106.66 | 2.051 | 0.794 | 1.928 | 2.028 |
| | 151.750 | 132.750 | 2.553 | 120.00 | 2.308 | 1.106 | 2.123 | 2.079 |
| | 201.000 | 179.667 | 3.455 | 133.33 | 2.564 | 1.348 | 2.254 | 2.125 |
| | 250.833 | 228.750 | 4.399 | 137.50 | 2.644 | 1.664 | 2.359 | 2.138 |

**Table 3.33** Derived-data for investigation of Tempkin equation for adsorption of chromium (VI) on DBTL at different temperatures.

| Temperature ± 0.2 (°C) | $C_o$ ($mg \cdot L^{-1}$) | $C_e$ ($mg \cdot L^{-1}$) | $C_e \times 10^3$ ($mol \cdot L^{-1}$) | $q_e$ ($mg \cdot g^{-1}$) | $q_e \times 10^3$ ($mol \cdot g^{-1}$ | ln $C_e$ ($mol \cdot L^{-1}$l) |
|---|---|---|---|---|---|---|
| 15 | 25.500 | 12.042 | 0.232 | 115.420 | 2.220 | -8.371 |
| | 50.083 | 32.830 | 0.617 | 151.660 | 2.917 | -7.391 |
| | 101.333 | 67.333 | 1.295 | 291.660 | 5.609 | -6.649 |
| | 150.750 | 109.000 | 2.096 | 360.000 | 6.923 | -6.168 |
| | 201.000 | 152.667 | 2.936 | 416.670 | 8.013 | -5.831 |
| | 251.250 | 202.083 | 3.886 | 420.830 | 8.093 | -5.550 |
| 30 | 25.833 | 15.750 | 0.303 | 80.410 | 1.546 | - 8.102 |
| | 51.583 | 36.333 | 0.699 | 120.000 | 2.308 | -7.266 |
| | 101.333 | 77.500 | 1.490 | 180.000 | 3.462 | - 6.509 |
| | 151.250 | 123.000 | 2.365 | 215.000 | 4.135 | - 6.047 |
| | 201.333 | 170.000 | 3.269 | 240.000 | 4.615 | -5.723 |
| | 250.833 | 218.333 | 4.199 | 245.840 | 4.728 | -5.473 |
| 50 | 25.833 | 16.958 | 0.326 | 65.000 | 1.250 | -8.028 |
| | 52.333 | 39.917 | 0.768 | 81.660 | 1.570 | -7.172 |
| | 101.333 | 84.667 | 1.628 | 106.660 | 2.051 | -6.420 |
| | 151.750 | 132.750 | 2.553 | 120.000 | 2.308 | -5.970 |
| | 201.000 | 179.667 | 3.455 | 133.330 | 2.564 | -5.668 |
| | 250.833 | 228.750 | 4.399 | 137.500 | 2.644 | -5.426 |

**Table 3.34:** Derived-data for investigation of Dubinin-Radushkevich (D-R) isotherm of chromium (VI) adsorption on DBTL at different temperatures.

| Temp $^{o}$C | $C_o$ (mg·L$^{-1}$) | $C_e$ (mg·L$^{-1}$) | $C_e \times 10^3$ (mol.L$^{-1}$) | $\ln(1+1/C_e)$ (a.u) | $\{RT \ln(1+1/C_e)\}^2 \times 10^{-6}$ (a.u) | $q_e$ (mg·g$^{-1}$) | $\ln q_e$ (mol.g$^{-1}$) |
|---|---|---|---|---|---|---|---|
| 15 | 25.50 | 12.042 | 0.232 | 8.369 | 401.562 | 115.420 | -6.110 |
| | 50.083 | 32.830 | 0.617 | 7.391 | 313.193 | 151.660 | -5.837 |
| | 101.333 | 67.333 | 1.295 | 6.651 | 253.617 | 291.660 | - 5.183 |
| | 150.75 | 109.000 | 2.096 | 6.170 | 218.261 | 360.000 | -4.973 |
| | 201.00 | 152.667 | 2.936 | 5.834 | 195.136 | 416.670 | -4.827 |
| | 251.25 | 202.083 | 3.886 | 5.554 | 176.855 | 420.830 | -4.817 |
| 30 | 25.833 | 15.75 | 0.303 | 8.102 | 416.572 | 80.41 | - 6.472 |
| | 51.583 | 36.333 | 0.699 | 7.267 | 335.132 | 120.00 | - 6.071 |
| | 101.333 | 77.500 | 1.490 | 6.510 | 268.95 | 180.00 | - 5.666 |
| | 151.25 | 123.000 | 2.365 | 6.049 | 232.205 | 215.00 | -5.488 |
| | 201.333 | 170.000 | 3.269 | 5.727 | 208.142 | 240.00 | -5.378 |
| | 250.833 | 218.333 | 4.199 | 5.477 | 190.367 | 245.84 | -5.354 |
| 50 | 25.833 | 16.958 | 0.326 | 8.029 | 464.88 | 65.00 | - 6.685 |
| | 52.333 | 39.917 | 0.768 | 7.172 | 370.942 | 81.66 | - 6.456 |
| | 101.333 | 84.667 | 1.628 | 6.422 | 297.417 | 106.66 | - 6.189 |
| | 151.750 | 132.750 | 2.553 | 5.973 | 257.282 | 120.00 | - 6.072 |
| | 201.000 | 179.667 | 3.455 | 5.671 | 231.923 | 133.33 | -5.966 |
| | 250.833 | 228.750 | 4.399 | 5.431 | 212.708 | 137.50 | -5.935 |

## 3.7.3 Analysis of Adsorption Isotherm

Adsorption isotherm is an important characteristic to evaluate the adsorption behavior of a system. Different model equations for adsorption isotherm such as Langmuir, Freundlich, Temkin and Dubinin-Radushkevich **(**D-R) isotherms were used to evaluate feasibility of the adsorption process. The parameters obtain from these different models provide substantial information of adsorptive capacity of DBTL as well as its surface property and adsorption mechanism.

### 3.7.3.1 Langmuir isotherm

The Langmuir isotherm is successfully applied to many adsorbent in adsorption system for removal of hazardous materials from industrial effluents. The main focus of Langmuir assumption is that formation of monolayer at specific sites on adsorbent

surface containing single molecule per site in adsorption process (Langmuir 1916). The linear form of the Langmuir isotherm is expressed by the following equation (3.27).

$$\frac{C_e}{q_e} = \frac{1}{q_m b} + \frac{C_e}{q_m} \qquad (3.27)$$

where, $C_e$ (mg·L$^{-1}$) is the equilibrium concentration of Cr(VI), $q_e$ (mg·g$^{-1}$) is the equilibrium amount adsorbed of chromium (VI), $q_m$ (mg·g$^{-1}$) is the maximum adsorption capacity for complete monolayer formation and $b$ (L·mg$^{-1}$) is the Langmuir constant related to adsorption equilibrium constant. The values of $q_m$ and $b$ obtained from the slopes and intercepts of the linear plots of $C_e/q_e$ against $C_e$ at different temperatures as shown in Figure 3.52, are given in Table 3.35. The values of $R^2$ in the range of 0.983-0.992 suggested that the adsorption of chromium (VI) on DBTL is well expressed by Langmuir equation. The values of $q_m$ decreased with the increase of temperature (Table 3.35) suggested that the adsorption is exothermic.

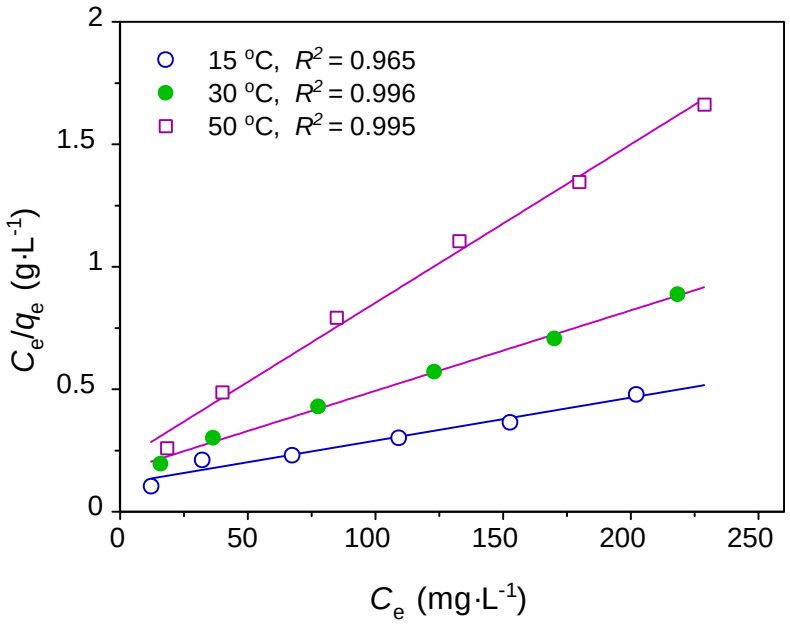


**Figure 3.52(a):** Langmuir isotherms for the adsorption of chromium (VI) (mg·g$^{-1}$) on DBTL at different temperatures and at pH 2.0.

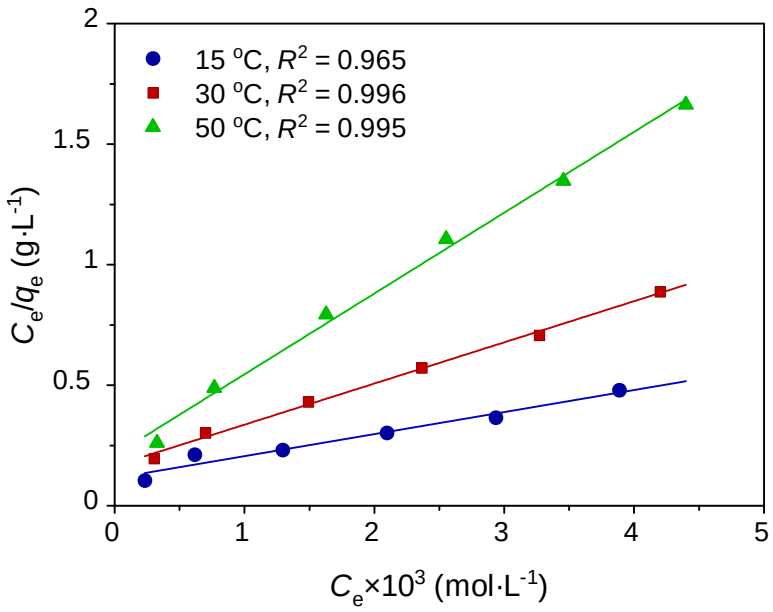


**Figure 3.52(b):** Langmuir isotherms for the adsorption of chromium (VI) (mol·g$^{-1}$) on DBTL at different temperatures and at pH 2.0.

### 3.7.3.2 Freundlich isotherm

The Freundlich isotherm equation is applicable where adsorption process takes place on a heterogeneous system with a multilayer adsorption mechanism (Freundlich, 1906). The linear form of Freundlich equation is mathematically given by equation (3.28).

$$\log q_e = \log k_F + \frac{1}{n}\log C_e \qquad (3.28)$$

where, $k_F$ is the proportionality constant and $n$ is considered as heterogeneity constant and the others parameters is previously described in Langmuir equation. The values of $n$ and $k_F$ were calculated from the slope and intercept of ln$q_e$ *vs* ln$C_e$ plot shown in Figure 3.53 and values are presented in Table 3.35. The values of $n$ for different temperatures were found in above 1.0 which indicated the adsorption process is favorable.

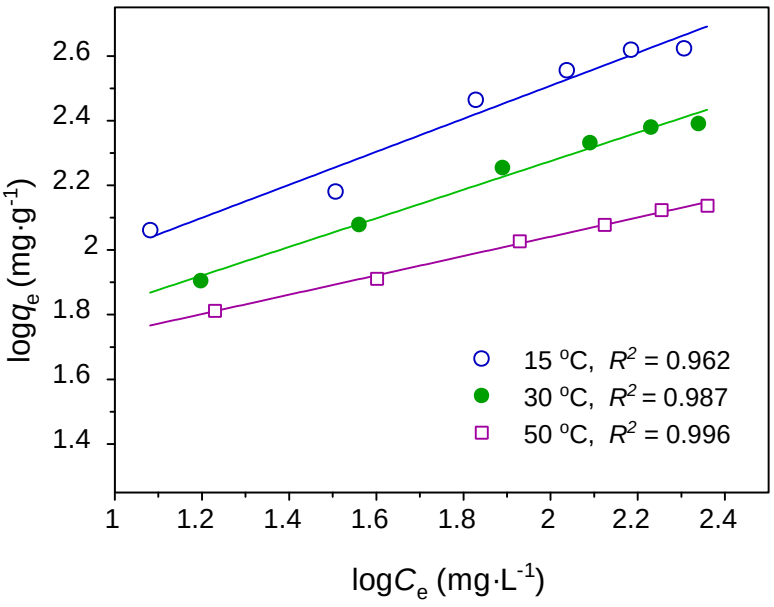


**Figure 3.53:** Freundlich isotherms of chromium (VI) adsorption on DBTL at different temperatures and at pH 2.0.

### 3.7.3.3 Temkin isotherm

The Temkin isotherm represents to investigate effective adsorption capacity of adsorbate on the adsorbent surface. The linear form of Temkin isotherm is given by equation (3.29).

$$q_e = B \ln A + B \ln C_e \qquad (3.29)$$

where, $B = RT/b$ (J·mol$^{-1}$) is the Temkin constant related to the heat of adsorption, $T$ (K) is the absolute temperature, $R$ (8.314 J·mol$^{-1}$·K$^{-1}$) is the molar gas constant, $A$ (L·g$^{-1}$) is the equilibrium binding constant related to the maximum binding energy. The constants of $A$ and $B$ were determined from the intercept and the slope of the plot of $q_e$ *vs* ln$C_e$, respectively as shown in Figure 3.54. Calculated parameters are presented in Table 3.35. This isotherm shows that the heat of adsorption of all the molecules in the layer of adsorbent decreases linearly by increase coverage layer of adsorbate onto the surface of adsorbent due to the interaction.

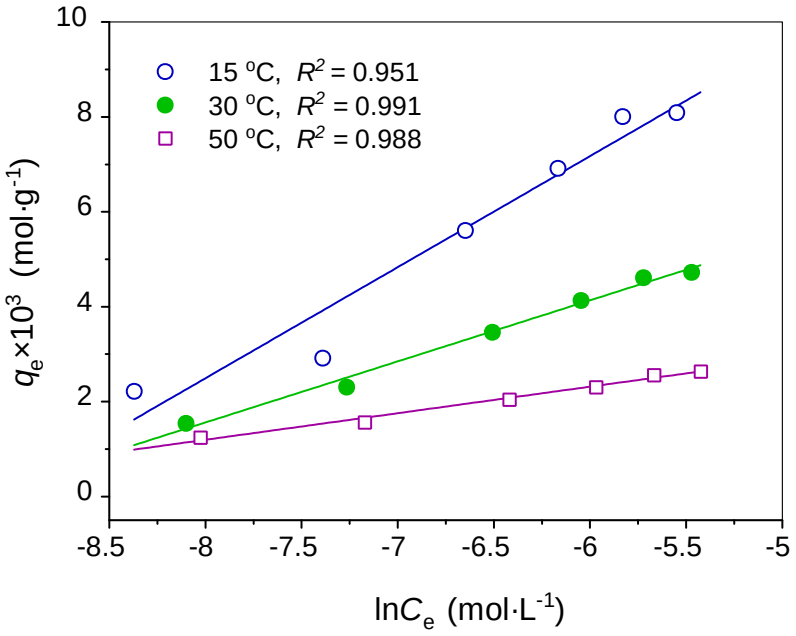


**Figure 3.54:** Temkin isotherms of chromium (VI) adsorption on DBTL at different Temperatures and at pH 2.0.

### 3.7.3.4 Dubinin-Radushkevich (D-R) isotherm

Dubinin-Radush-kevich (D-R) adsorption isotherm predicts whether the adsorption process is physical or chemical in nature. The Dubinin-Radushkevich (D-R) isotherm is expressed by equation (3.30) and (3.31) (Dubinin-Radush-kevich 1947).

$$\ln q_e = \ln q_{DR} - ¥£^2 \qquad (3.30)$$

$$\ln q_e = \ln q_{DR} - ¥\{RT \ln(1+\frac{1}{C_e})\}^2 \qquad (3.31)$$

where, $q_{DR}$ (mg·g$^{-1}$) is the maximum adsorption capacity of adsorbent, ¥ (mol$^2$·kJ$^{-2}$) is Dubinin-Radushkevich isotherm constant corresponding to the mean adsorption energy $E_a$ (kJ·mol$^{-1}$) as equation (3.22) and $\varepsilon$ (J·mol$^{-1}$) is the Polanyi potential that is determined by $RT\ln(1+1/C_e)$. Figure 3.55 represents the linear plot of ln$q_e$ *vs* £$^2$ for adsorption of chromium (VI) on DBTL which allowed estimating the Dubinin-Radushkevich isotherm parameters ¥ and $q_{DR}$ from the slope and the intercept, respectively. Based on the value

of Dubinin-Radushkevich isotherm constant, ¥ the mean adsorption energy, $E$ (kJ·mol$^{-1}$) was estimated from the following equation (3.32) (Ada *et al*., 2009 ),

$$E = -\frac{1}{\sqrt{2¥}} \qquad (3.32)$$

Calculated values are given in Table 3.35. The estimated value of equilibrium amount of chromium (VI) adsorbed on DBTL is high at 15 $^{o}$C and that was the low at 50 $^{o}$C. The results indicated that this adsorption system might be controlled by physisorption. The reason may be interpreted on the basis of the following facts: when temperature of the system increased, the kinetic energy of the dichromate, $Cr_2O_7^{2-}$ ions as well as DBTL particles increased and at the high temperature it became so high that chromium (VI) could not bind firmly in the active sites available on surface of DBTL. Similar types of results with the facts were also reported by other researchers (Papageorgiou *et al.*, 2008). The obtained values of adsorption energy, $E$ was limited within the range of – 8.8 to -12.7 kJ·mol$^{-1}$ which addresses chromium (VI)-DBTL adsorption process is physiosorption in nature.

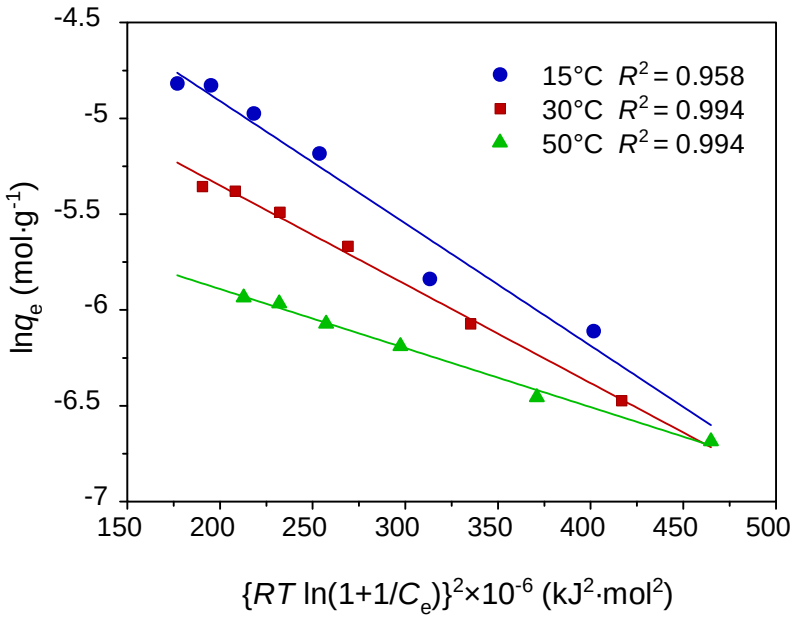


**Figure 3.55:** Dubinin-Radushkevich (D-R) isotherms of chromium (VI) adsorption on DBTL at different temperatures and at pH 2.0.

From the comparison of the values of regression coefficient ($R^2$) in Table 3.35, it is clear to understand that the adsorption isotherm of chromium (VI) on DBTL is well expressed by the Langmuir equation. Thus the Langmuir constant *b* was used to determine the separation factor and thermodynamic parameters to understand the mechanism of the process. Figures 3.56 and 3.57 represent the adsorption isobar and adsorption isoster, respectively for the adsorption of chromium (VI) on DBTL, suggested the endothermic nature of the process.

**Table 3.35** Parameters of different adsorption isotherms derived from equilibrium-study for the adsorption chromium (VI) on DBTL from aqueous solution at pH 2.0 and 30.0 ± 0.2 $^{o}$C.

| Isotherms | Parameter | Temperatures ($^{o}$C) | | |
|---|---|---|---|---|
| | | 15 | 30 | 50 |
| Langmuir isotherm | $q_m$ (mg·g$^{-1}$) | 555.56 | 303.03 | 156.25 |
| | $q_m$ (mol·g$^{-1}$) | 0.011 | 0.006 | 0.003 |
| | $b$ (L·mg$^{-1}$) | 0.016 | 0.02 | 0.03 |
| | $b$ (L·mol$^{-1}$) | 804.764 | 1008.268 | 1585.791 |
| | $R^2$ (a.u.) | 0.965 | 0.996 | 0.995 |
| Freundlich isotherm | $k_f$ (mg·g$^{-1}$) | 30.620 | 24.547 | 27.733 |
| | $n$ (a.u.) | 1.961 | 2.262 | 3.356 |
| | $R^2$ (a.u.) | 0.962 | 0.987 | 0.995 |
| Temkin isotherm | $A$ ×10$^{-3}$ (L·mol$^{-1}$) | 8.640 | 10.12 | 25.30 |
| | $B$ ×10$^{3}$ (a.u.) | 2.341 | 1.287 | 0.559 |
| | $R^2$ (a.u.) | 0.951 | 0.991 | 0.988 |
| Dubinin-Radushkevich | $q_{DR}$ (mol·g$^{-1}$) | 0.026 | 0.013 | 0.005 |
| | ¥ ×10$^{9}$ (mol$^2$·kJ$^{-2}$) | 6.40 | 5.20 | 5.20 |
| | $E$ (kJ· mol$^{-1}$) | -8.840 | -9.81 | -12.70 |
| | $R^2$ (a.u.) | 0.958 | 0.994 | 0.994 |

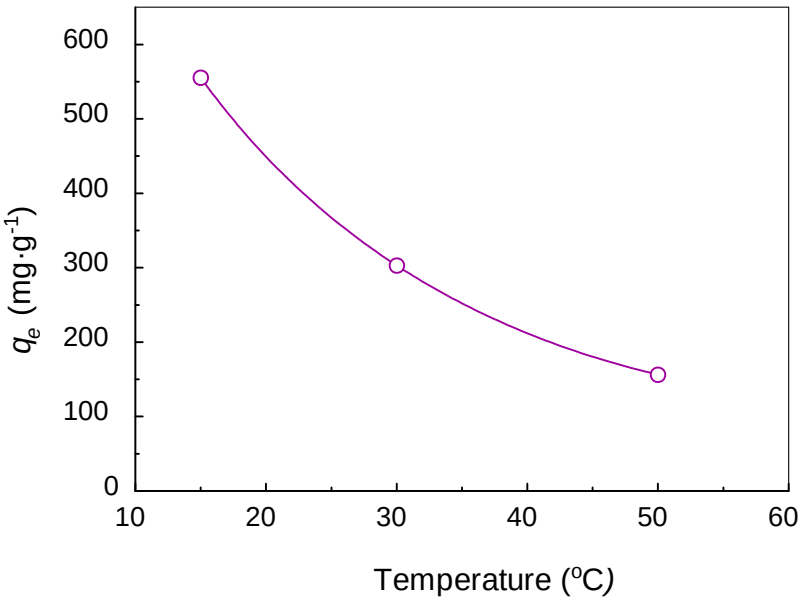


**Figure 3.56:** Adsorption isobar of Cr(VI) adsorption on DBTL at pH 2.0.

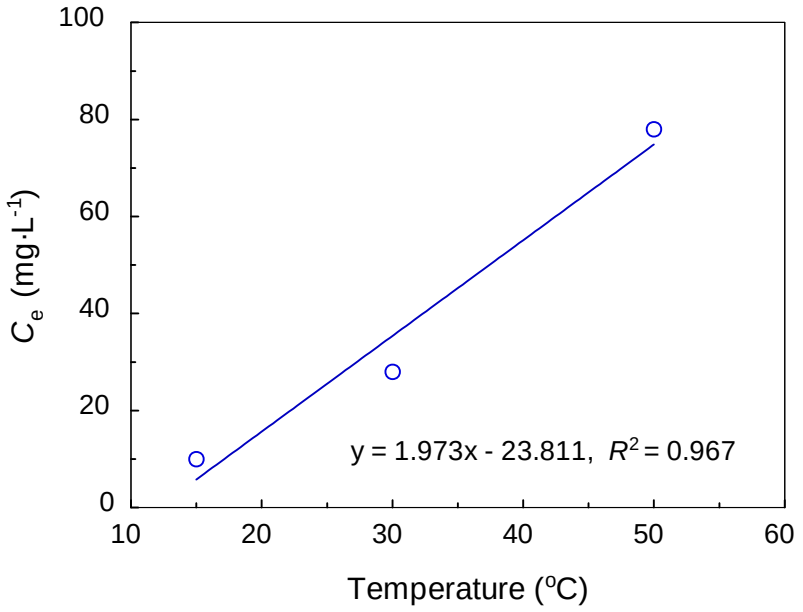


**Figure 3.57:** Adsorption isoster of Cr(VI) adsorption on DBTL at pH 2.0.

## 3.7.4 Separation Factor

Adsorption system is characterized whether it is favorable or not by determining the separation factor, ($R_b$) from Langmuir constant ($b$). Dimensionless constant, $R_b$ indicated isotherm acceptability to be favorable ($0 < R_b < 1$), unfavorable ($R_b > 1$), irreversible ($R_b = 0$) and linear ($R_b = 1$). The separation factor, $R_b$ was determined by the following equation (3.33) (Khezamia *et al*., 2016).

$$R_b = \left( \frac{1}{1 + bC_o} \right) \tag{3.33}$$

where $b$ is Langmuir constant and $C_o$ is the initial concentration of chromium (VI) in aqueous solution. The calculated value of $R_b$ decreases with increase in initial concentration of Cr(VI) for different temperatures are presented in Figure 3.58 and Table 3.36. At low concentration and low temperature, $R_b$ values were found near to 1 indicting that the adsorption is favorable at this condition (Vijayakumaran and Arivoli, 2012).

**Table 3.36(a)** Derived-data for determination of the values of Separation Factor, $R_b$ at different temperatures.

| 15 $^oC$ | | | 30 $^oC$ | | | 50 $^oC$ | | |
|---|---|---|---|---|---|---|---|---|
| $C_o \times 10^3$ ($mol \cdot L^{-1}$) | $b$ ($L \cdot mol^{-1}$) | $R_b$ (a.u.) | $C_o \times 10^3$ ($mol \cdot L^{-1}$) | $b$ ($L \cdot mol^{-1}$) | $R_b$ (a.u.) | $C_o \times 10^3$ ($mol \cdot L^{-1}$) | $b$ ($L \cdot mol^{-1}$) | $R_b$ (a.u.) |
| 0.490 | 797.448 | 0.719 | 0.497 | 1006.44 | 0.667 | 0.497 | 1585.79 | 0.559 |
| 0.963 | | 0.566 | 0.992 | | 0.500 | 1.006 | | 0.385 |
| 1.949 | | 0.392 | 1.949 | | 0.338 | 1.949 | | 0.244 |
| 2.899 | | 0.302 | 2.909 | | 0.255 | 2.918 | | 0.178 |
| 3.865 | | 0.245 | 3.872 | | 0.204 | 3.865 | | 0.140 |
| 4.832 | | 0.206 | 4.824 | | 0.171 | 4.824 | | 0.116 |

**Table 3.36(b)** Derived-data for determination of the values of Separation Factor, $R_b$ at different temperatures.

| Concentration of Chromium (VI) ($mg \cdot L^{-1}$) | Separation factor, $R_b$ (a.u.) | | |
|---|---|---|---|
| | 15 (°C) | 30 (°C) | 50 (°C) |
| 25.722 | 0.815 | 0.681 | 0.573 |
| 51.333 | 0.688 | 0.517 | 0.402 |
| 101.333 | 0.527 | 0.352 | 0.254 |
| 151.250 | 0.428 | 0.266 | 0.186 |
| 201.111 | 0.360 | 0.215 | 0.146 |
| 250.972 | 0.310 | 0.180 | 0.121 |

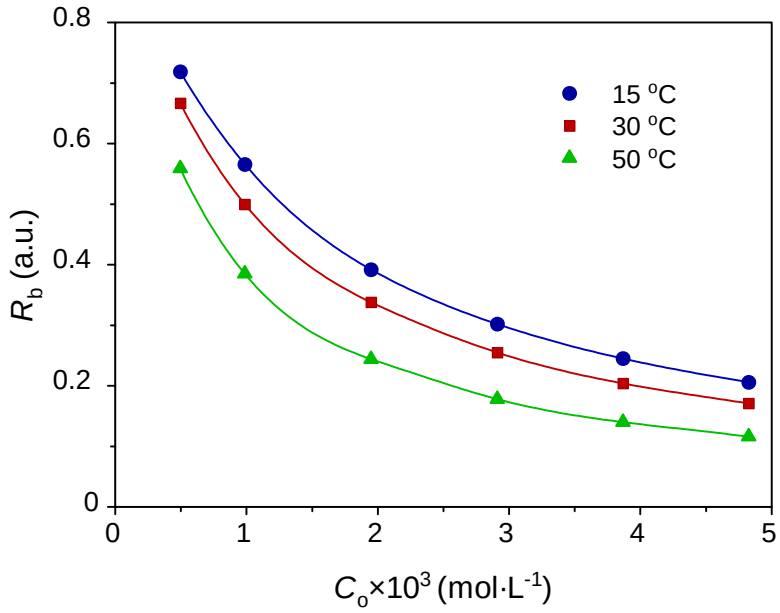


**Figure 3.58(a):** Effect of initial concentration ($mol \cdot L^{-1}$) of Cr(VI) on the dimensionless separation factor, $R_b$ of DBTL at different temperatures.

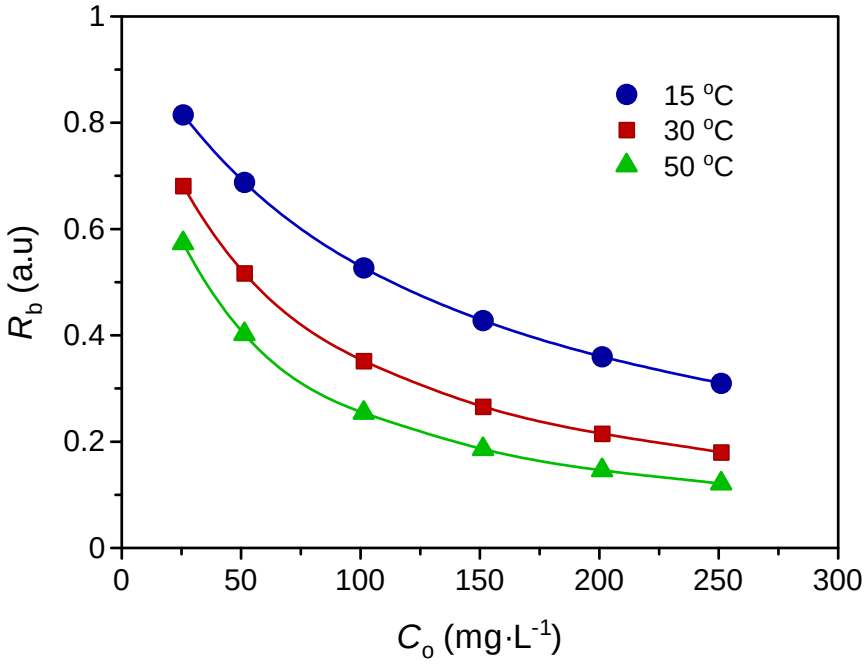


**Figure 3.58(b):** Effect of initial concentration (mg·L$^{-1}$) of chromium (VI) on the dimensionless separation factor, $R_b$ of DBTL at different temperatures.

## 3.7.5 Adsorption Thermodynamics

Thermodynamic parameters such as standard free energy ($\Delta G^o$), enthalpy ($\Delta H^o$) and entropy ($\Delta S^o$) were calculated by using values Langmuir constant, $b$ at different temperatures and equations (3.34) and (3.35).

$$\Delta G^o = -RT \ln b \qquad (3.34)$$

$$\ln b = \frac{\Delta S^o}{R} - \frac{\Delta H^o}{RT} \qquad (3.35)$$

where, $R$ is the molar gas constant (8.314 J·K$^{-1}$·mol$^{-1}$), $T$ is the absolute temperature (K), $b$ is Langmuir constant (L·g$^{-1}$) and $\Delta G^o$ is the change of standard free energy (kJ·mol$^{-1}$), $\Delta H^o$ is the change of standard enthalpy (kJ·mol$^{-1}$) and $\Delta S^o$ is the change of standard entropy (kJ·K$^{-1}$·mol$^{-1}$). Change of standard free energy, $\Delta G^o$ were calculated by using equation (3.34) and $\Delta H^o$ as well as $\Delta S^o$ values were calculated from the slope and intercept of the plot of ln$b$ *vs* 1/$T$ based on the van't Hoff equation (3.35) (Hossain 2006) which are presented in Figure 3.59 and Table 3.37. The negative value of $\Delta G^o$

indicated the uptake of chromium (VI) on DBTL is spontaneous and the positive values of $\Delta H^o$ (0.015 kJ·mol$^{-1}$, near to zero) and $\Delta S^o$ might be due to small amount of reduction of chromium (VI) to chromium (III), during the adsorption of chromium (VI) on DBTL.

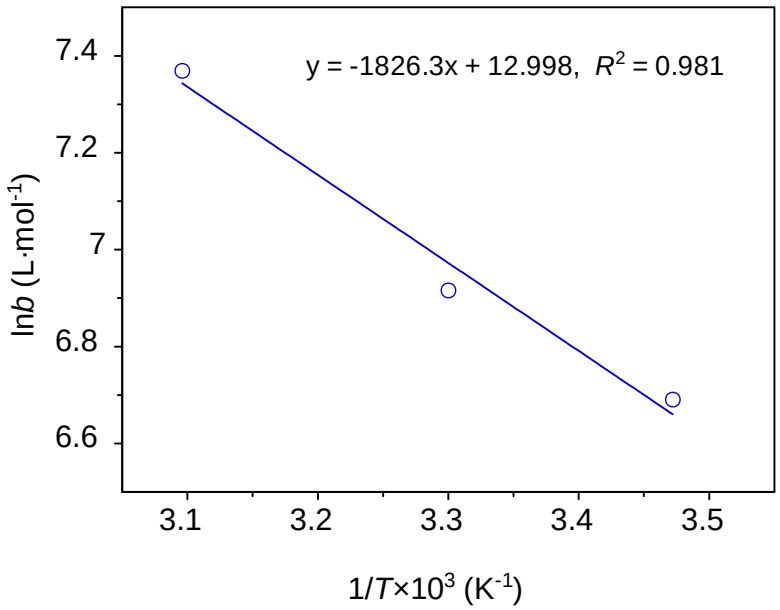


**Figure 3.59:** A plot of ln*b* *vs.* 1/*T* for determination of changes in enthalpy and entropy of adsorption for the uptake of chromium (VI) from aqueous solution on DBTL at pH 2.0.

**Table 3.37** Thermodynamic parameters of chromium (VI) adsorption on DBTL at different temperatures.

| *T* (° C) | *T* (K) | 1/*T* ×10$^3$ (K$^{-1}$) | *b* L·mol$^{-1}$ | ln*b* (L·mol$^{-1}$) | $\Delta H^o$ (kJ·mol$^{-1}$) | $\Delta S^o$ (kJ·mol$^{-1}$·K$^{-1}$) | $\Delta G^o$ (kJ·mol$^{-1}$) |
|---|---|---|---|---|---|---|---|
| 15 | 288 | 3.472 | 804.764 | 6.691 | 15.18 | 0.108 | - 16.02 |
| 30 | 303 | 3.300 | 1008.268 | 6.916 | | | - 17.42 |
| 50 | 323 | 3.096 | 1585.791 | 7.369 | | | - 19.79 |

### 3.7.6 Comparison of Adsorption Isotherms from Kinetic and Equilibrium Studies

A comparison of adsorption isotherms derived from kinetic and equilibrium studies are presented in Table 3.38 and Figure 3.60. Both isotherms are overlapping one to another within 3 % of deviation. The adsorption isotherm derived from kinetic study is superior to equilibrium study for long time equilibrium system (Hossain 2005).

**Table 3.38** Data for comparison of kinetic and equilibrium study to estimate the adsorption isotherm of chromium (VI) on DBTL at pH 2.0 and 30 ± 0.2 °C.

| Adsorption isotherm of chromium (VI) on DBTL obtained by adsorption kinetic study | | | Adsorption isotherm of chromium (VI) on DBTL obtained by adsorption equilibrium study | | |
|---|---|---|---|---|---|
| $C_o$ (mg·L$^{-1}$) | $C_e$ (mg·L$^{-1}$) | $q_e$ (mg·g$^{-1}$) | $C_o$ (mg·L$^{-1}$) | $C_e$ (mg·L$^{-1}$) | $q_e$ (mg·g$^{-1}$) |
| 25.417 | 15.625 | 79.17 | 25.833 | 15.750 | 80.41 |
| 51.167 | 36.250 | 117.50 | 51.583 | 36.333 | 120.00 |
| 101.333 | 77.500 | 180.00 | 100.667 | 77.500 | 180.00 |
| 150.750 | 122.500 | 212.50 | 151.250 | 123.000 | 215.00 |
| 201.667 | 170.333 | 236.67 | 201.333 | 170.000 | 240.00 |
| 251.250 | 218.750 | 241.67 | 250.833 | 218.333 | 245.84 |

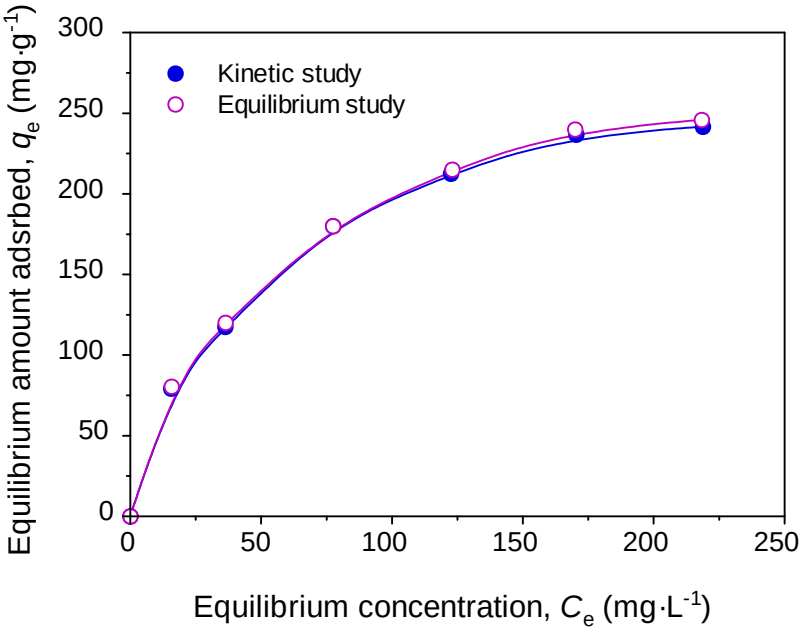


**Figure 3.60:** Comparison of adsorption isotherms constructed from kinetic and equilibrium studies for the adsorption of chromium (VI) on DBTL at pH 2.0 and 30 ± 0.2 °C.

## 3.7.2 Adsorption Isotherms at Different pH

The adsorption isotherms of chromium (VI) on DBTL at different pH of solution were constructed using the following conditions:

**Experimental Conditions**

| | |
|---|---|
| Volume of chromium (VI) solution | : 25 mL |
| Concentration of chromium (VI) solution | : 25 – 250 $mg \cdot L^{-1}$ |
| Solution pH | : 2.0, 4.0, 6.0 and 8.0 |
| Amount of DBTL ($W_{DBTL}$) | : 0.0025 g |
| Particle size of DBTL | : < 106 µm |
| Adsorption temperature | : 30 ± 0.2 °C |
| Agitation rate | : 150 rpm |
| Agitation time ($t_e$) | : 6 hrs |

The equilibrium concentrations of chromium (VI), after adsorption, for different initial concentrations were determined from the analytical data obtained at different pH of solution and presented in Table 3.39. The equilibrium amounts of chromium (VI) adsorbed on DBTL for different initial concentrations were calculated using equation (3.9) and presented in Table 3.39. The adsorption isotherms of chromium (VI) adsorbed on DBTL at different pH of solution is presented in Figure 3.61. Derived data are shown in Table 3.40 and 3.41 for the application of different isotherms model equations to the adsorption process at different pH of solution. Figures 3.62 to 3.65 show the verification of Langmuir, Freundlich, Temkin and Dubinin-Radushkevich (D-R) isotherm equations to the adsorption of chromium (VI) on DBTL for different pH of solution at 30 ± 0.2 °C. Different parameters of above isotherm equations are calculated, described previously and given in Table 3.42. Comparing the values of regression coefficient ($R^2$) in Table 3.42, it can be understood that the Langmuir equation is well fitted to the adsorption data of chromium (VI) on DBTL at different pH of solution. The equilibrium amount adsorbed, calculated from Langmuir equation, decreased exponentially with the increase of solution pH as shown in Figure 3.66. This observation might be due to the changing of DBTL surface from positive to negative with the increase of solution pH from 2.0 to 8.0, resultants the increase of repulsive force between negative species chromium (VI),

$Cr_2O_7^{2-}$ and negative surface of DBTL at high pH of solution. Such mechanism has been explained previously in Figure 3.40.

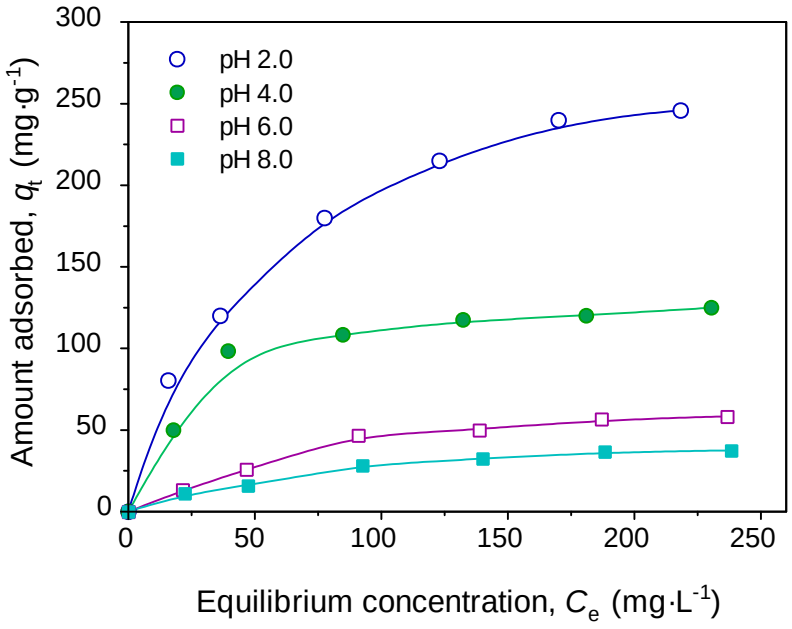


**Figure 3.61:** Adsorption isotherms of chromium (VI) on DBTL at different pH and 30 ± 0.2 °C.

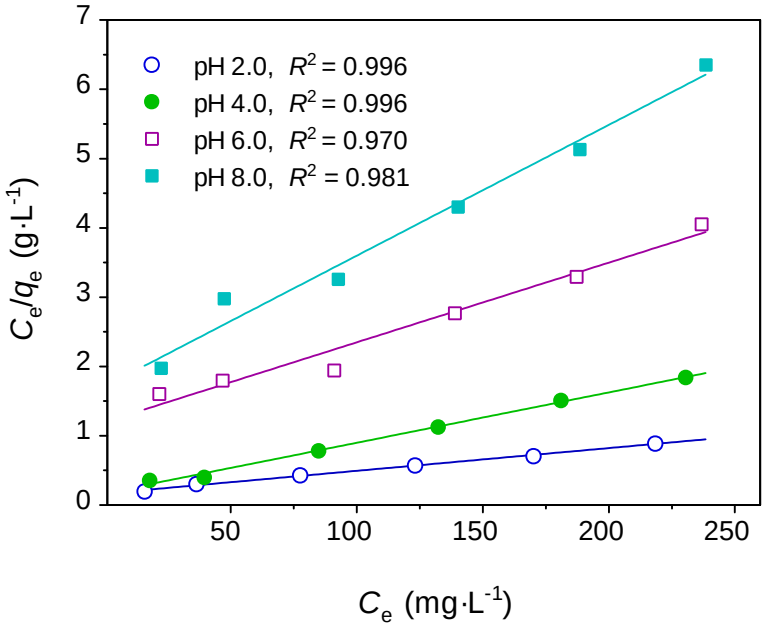


**Figure 3.62:** Langmuir adsorption isotherms of chromium (VI) on DBTL at different pH and 30 ± 0.2 °C.

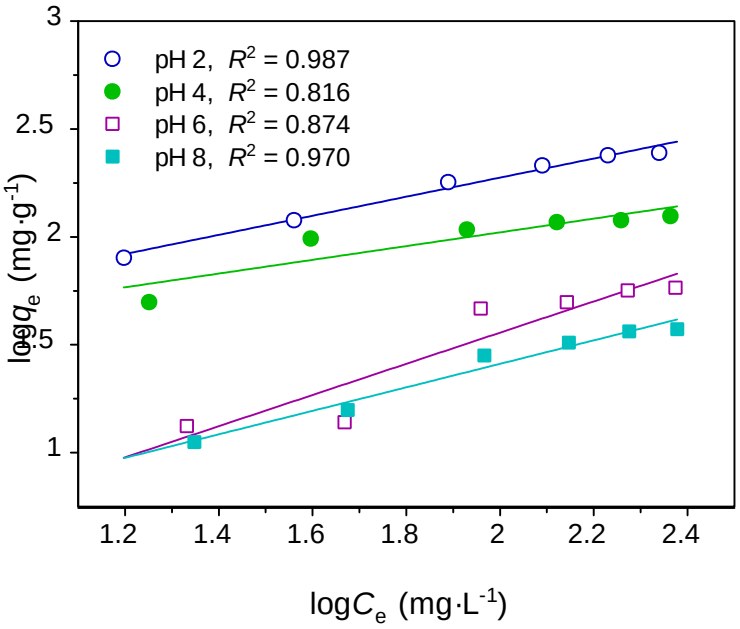


**Figure 3.63**: Freundlich adsorption isotherms of chromium (VI) on DBTL at different pH and 30 ± 0.2 °C.

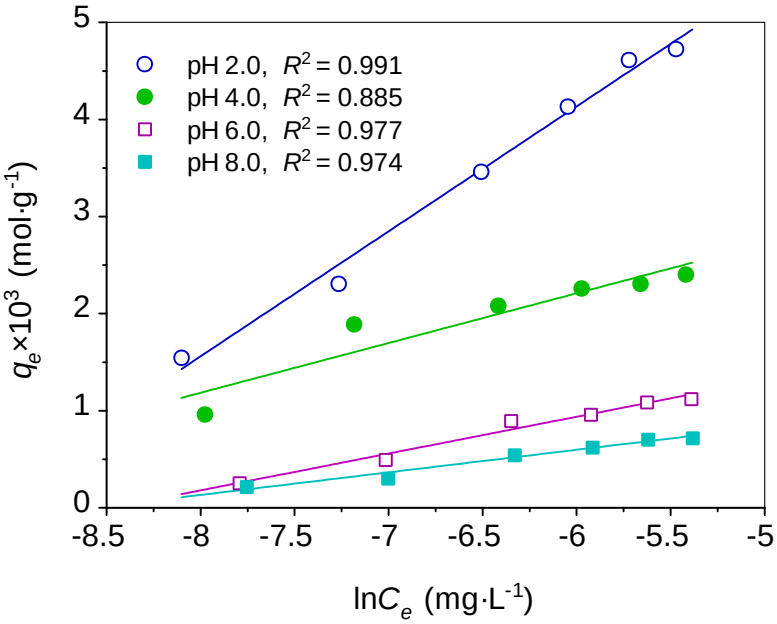


**Figure 3.64** : Temkin adsorption isotherms of chromium (VI) on DBTL at different pH and 30 ± 0.2 °C.

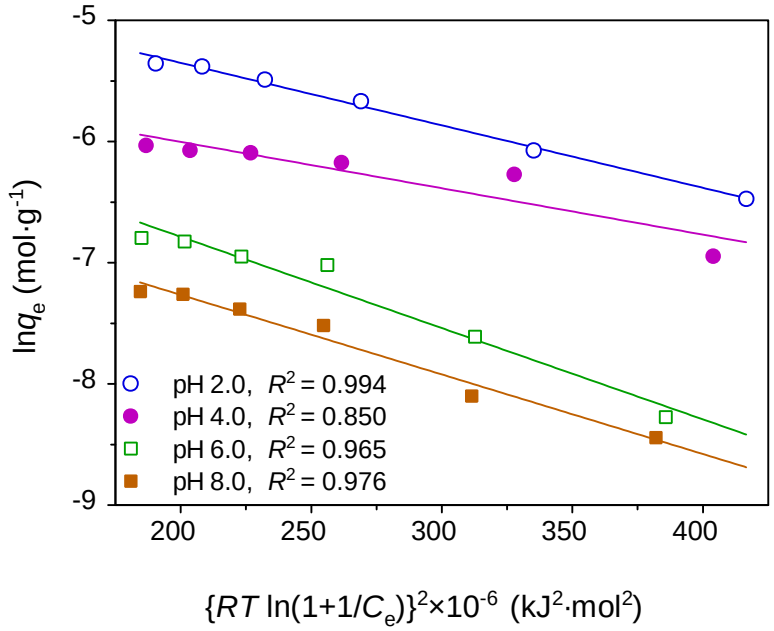


**Figure 3.65**: Dubinin-Radushkevich (D-R) isotherms of chromium (VI) on DBTL at different pH and 30 ± 0.2 °C.

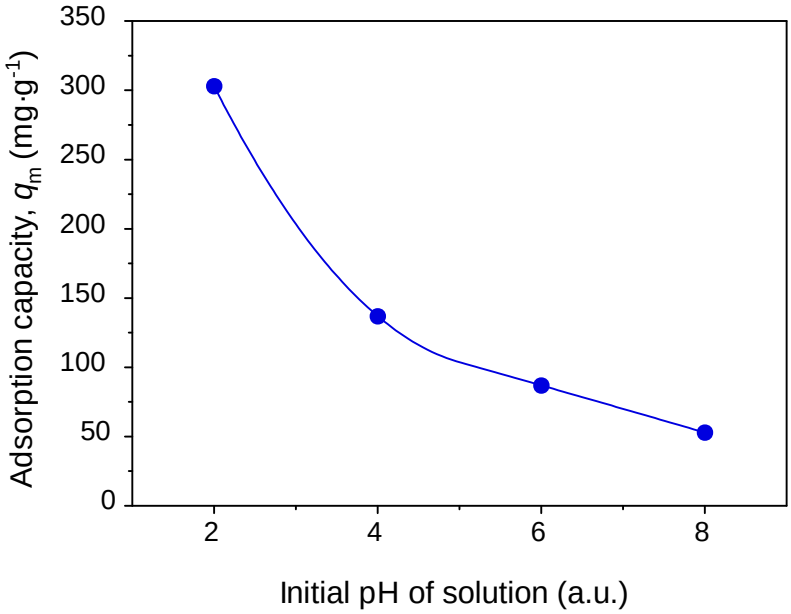


**Figure 3.66** : Variation of adsorption capacity with initial pH of solution at 30 ± 0.2 °C.

**Table 3.39** Effect of pH on the equilibrium adsorption isotherm of chromium (VI) on DBTL at 30 ± 0.2 °C.

| pH | $C_o$ (mg·L$^{-1}$) | $C_e$ (mg·L$^{-1}$) | $C_{oxidation}$ (mg·L$^{-1}$) | $C_R = C_{oxidation} - C_e$ (mg·L$^{-1}$) | $q_e$ (mg·g$^{-1}$) |
|---|---|---|---|---|---|
| 2.0 | 25.833 | 15.75 | 17.792 | 2.042 | 80.41 |
| | 51.583 | 36.333 | 39.583 | 3.250 | 120.00 |
| | 101.333 | 77.50 | 83.333 | 5.833 | 180.00 |
| | 151.25 | 123.00 | 129.75 | 6.750 | 215.00 |
| | 201.333 | 170.00 | 177.333 | 7.333 | 240.00 |
| | 250.833 | 218.333 | 226.25 | 7.916 | 245.84 |
| 4.0 | 25.333 | 17.833 | 20.333 | 2.50 | 50.00 |
| | 52.833 | 39.417 | 43.000 | 3.583 | 98.33 |
| | 101.333 | 84.833 | 90.500 | 5.667 | 108.33 |
| | 151.00 | 132.250 | 139.250 | 7.00 | 117.50 |
| | 200.667 | 181.000 | 188.667 | 7.667 | 120.00 |
| | 250.833 | 230.417 | 238.333 | 7.916 | 125.00 |
| 6.0 | 25.333 | 21.417 | 24.000 | 2.583 | 13.33 |
| | 52.833 | 46.583 | 50.250 | 3.667 | 25.83 |
| | 101.333 | 90.833 | 96.667 | 5.833 | 46.67 |
| | 151.000 | 138.750 | 146.000 | 7.250 | 50.00 |
| | 200.667 | 187.000 | 195.000 | 8.000 | 56.67 |
| | 250.833 | 236.667 | 245.000 | 8.333 | 58.33 |
| 8.0 | 26.000 | 22.250 | 24.875 | 2.625 | 11.25 |
| | 52.833 | 47.250 | 51.250 | 4.000 | 15.83 |
| | 101.333 | 92.500 | 98.500 | 6.000 | 28.33 |
| | 151.000 | 140.000 | 147.750 | 7.750 | 32.50 |
| | 200.667 | 188.333 | 197.000 | 8.667 | 36.67 |
| | 250.833 | 238.333 | 247.083 | 8.750 | 37.50 |

**Table 3.40** Derived-data for application of Langmuir, Freundlich and Temkin isotherms to the adsorption chromium (VI) on DBTL at 30 ± 0.2 °C.

| pH (a.u.) | $C_o$ (mg·L$^{-1}$) | $C_e$ (mg·L$^{-1}$) | $q_e$ (mg·g$^{-1}$) | $C_e/q_e$ (g·L$^{-1}$) | log $C_e$ (mg·L-$^{1}$) | log $q_e$ (-) | ln $C_e$ (-) |
|---|---|---|---|---|---|---|---|
| 2.0 | 25.833 | 15.75 | 80.41 | 0.196 | 1.197 | 1.905 | -8.102 |
| | 51.583 | 36.333 | 120.0 | 0.303 | 1.560 | 2.079 | -7.266 |
| | 101.333 | 77.50 | 180.0 | 0.431 | 1.889 | 2.255 | -6.509 |
| | 151.25 | 123.00 | 215.0 | 0.572 | 2.090 | 2.332 | -6.047 |
| | 201.333 | 170.00 | 240.0 | 0.708 | 2.230 | 2.380 | -5.723 |
| | 250.833 | 218.333 | 245.84 | 0.888 | 2.339 | 2.391 | -5.473 |
| 4.0 | 25.333 | 17.833 | 50.00 | 0.357 | 1.251 | 1.699 | -7.978 |
| | 52.833 | 39.417 | 98.33 | 0.401 | 1.596 | 1.993 | -7185 |
| | 101.333 | 84.833 | 108.33 | 0.783 | 1.929 | 2.035 | -6.418 |
| | 151.00 | 132.25 | 117.50 | 1.125 | 2.121 | 2.070 | -5.974 |
| | 201.667 | 181.00 | 120.00 | 1.508 | 2.258 | 2.079 | -5.661 |
| | 250.833 | 230.417 | 125.00 | 1.843 | 2.363 | 2.097 | -5.419 |
| 6.0 | 25.333 | 21.417 | 13.32 | 1.607 | 1.331 | 1.125 | -7.795 |
| | 52.833 | 46.583 | 25.83 | 1.803 | 1.668 | 1.412 | -7.018 |
| | 101.333 | 90.833 | 46.67 | 1.946 | 1.958 | 1.669 | -6.350 |
| | 151.00 | 138.750 | 50.00 | 2.775 | 2.142 | 1.699 | -5.926 |
| | 201.667 | 187.000 | 56.67 | 3.300 | 2.272 | 1.753 | -5.628 |
| | 250.833 | 236.667 | 58.32 | 4.057 | 2.374 | 1.766 | -5.392 |
| 8.0 | 26.000 | 22.250 | 11.25 | 1.978 | 1.347 | 1.051 | -7.757 |
| | 52.833 | 47.250 | 15.83 | 2.985 | 1.674 | 1.200 | -7.004 |
| | 101.333 | 92.500 | 28.33 | 3.265 | 1.966 | 1.452 | -6.332 |
| | 151.000 | 140.000 | 32.50 | 4.308 | 2.146 | 1.512 | -5.917 |
| | 200.667 | 188.333 | 36.67 | 5.136 | 2.275 | 1.564 | -5.621 |
| | 250.833 | 238.333 | 37.50 | 6.356 | 2.377 | 1.574 | -5.385 |

**Table 3.41** Derived-data for application of Dubinin-Radushkevich (D-R) isotherm to adsorption chromium (VI) on DBTL at 30 ± 0.2 °C.

| pH (a.u) | $C_o$ (mg·L-$^{1}$) | $C_e$ (mg·L$^{-1}$) | $C_e \times 10^{-3}$ (mol.L$^{-1}$) | ln $(1+1/C_e)$ (L·mol$^{-1}$) | {RT ln $1+1/C_e)\}^2 \times 10^{-6}$ (a.u.) | $q_e$ (mg·g$^{-}$ | *ln* $q_e$ (mol.g$^{-1}$) |
|---|---|---|---|---|---|---|---|
| 2.0 | 25.833 | 15.75 | 0.303 | 8.102 | 416.572 | 80.41 | -6.472 |
| | 51.583 | 36.333 | 0.699 | 7.267 | 335.132 | 120.00 | - 6.071 |
| | 101.333 | 77.500 | 1.490 | 6.510 | 268.950 | 180.00 | - 5.666 |
| | 151.25 | 123.000 | 2.365 | 6.049 | 232.205 | 215.00 | -5.488 |
| | 201.333 | 170.000 | 3.269 | 5.727 | 208.142 | 240.00 | -5.378 |
| | 250.833 | 218.333 | 4.199 | 5.477 | 190.367 | 245.84 | -5.354 |
| 4.0 | 25.333 | 17.833 | 0.343 | 7.988 | 403.918 | 50.00 | -6.946 |
| | 51.833 | 39.417 | 0.758 | 7.186 | 327.702 | 98.33 | - 6.271 |
| | 101.333 | 84.833 | 1.631 | 6.420 | 261.562 | 108.33 | - 6.174 |
| | 151.000 | 132.25 | 2.543 | 6.977 | 226.711 | 117.50 | -6.092 |
| | 200.667 | 181.000 | 3.480 | 5.664 | 203.588 | 120.00 | -6.071 |
| | 250.833 | 230.417 | 4.430 | 5.424 | 186.700 | 125.00 | -6.031 |
| 6.0 | 25.333 | 21.417 | 0.412 | 7.795 | 385.600 | 13.33 | -8.269 |
| | 52.833 | 46.583 | 0.896 | 7.018 | 312.559 | 25.83 | -7.607 |
| | 101.333 | 90.833 | 1.747 | 6.352 | 256.051 | 46.67 | -7.015 |
| | 151.000 | 138.75 | 2.668 | 5.929 | 223.084 | 50.00 | -6.946 |
| | 200.667 | 187.000 | 3.596 | 5.632 | 201.294 | 56.67 | -6.822 |
| | 250.833 | 236.667 | 4.551 | 5.397 | 184.846 | 58.33 | -6.793 |
| 8.0 | 26.00 | 22.250 | 0.428 | 7.757 | 381.850 | 11.250 | -8.440 |
| | 52.833 | 47.250 | 0.909 | 7.004 | 311.313 | 15.833 | -8.098 |
| | 101.333 | 92.500 | 1.779 | 6.333 | 254.521 | 28.333 | -7.515 |
| | 151.000 | 140.000 | 2.692 | 5.920 | 222.407 | 32.500 | -7.378 |
| | 200.667 | 188.333 | 3.622 | 5.624 | 200.722 | 36.670 | -7.257 |
| | 250.833 | 238.333 | 4.583 | 5.390 | 184.367 | 37.500 | -7.235 |

**Table 3.42** Parameters of different isotherms derived from equilibrium study for the adsorption Cr (VI) on DBTL from aqueous solution of different pH at 30.0 ± 0.2 $^{o}$C.

| Isotherms | Parameter | pH (a.u) | | | |
|---|---|---|---|---|---|
| | | 2.0 | 4.0 | 6.0 | 8.0 |
| Langmuir isotherm | $q_m$ (mg·g$^{-1}$) | 303.030 | 136.986 | 86.957 | 52.910 |
| | $b$ (L·mg$^{-1}$) | 0.020 | 0.042 | 0.010 | 0.011 |
| | $R^2$ (a.u.) | 0.996 | 0.996 | 0.970 | 0.981 |
| Freundlich isotherm | $k_f$ (mg·g$^{-1}$) | 24.564 | 24.227 | 1.291 | 2.102 |
| | $n$ (a.u.) | 2.261 | 3.141 | 1.384 | 1.836 |
| | $R^2$ (a.u.) | 0.987 | 0.816 | 0.874 | 0.970 |
| Temkin isotherm | $A$ ×10$^{-3}$ (L·mol$^{-1}$) | 10.02 | 30.35 | 4.790 | 5.390 |
| | $B$ ×10$^{3}$ (a.u.) | 1.287 | 0.512 | 0.379 | 0.232 |
| | $R^2$ (a.u.) | 0.991 | 0.885 | 0.977 | 0.974 |
| Dubinin-Radushkevich | $q_{DR}$ (mg·g$^{-1}$) | 0.013 | 0.005 | 0.005 | 0.003 |
| | ¥ ×10$^{9}$ (mol$^2$·$k$J$^{-2}$) | 5.20 | 3.80 | 7.50 | 6.60 |
| | $E$ (kJ·mol$^{-1}$) | -9.81 | -11.47 | -8.16 | -8.70 |
| | $R^2$ (a.u.) | 0.994 | 0.850 | 0.965 | 0.976 |

### 3.7.3 Adsorption Isotherms with Different Particle Sizes

The adsorption isotherms of chromium (VI) on DBTL at different pH of solution were constructed using the following conditions:

**Experimental Conditions**

| | |
|---|---|
| Volume of chromium (VI) solution | : 25 mL |
| Concentration of chromium (VI) solution | : 25 – 250 $mg \cdot L^{-1}$ |
| Solution pH | : 2.0 |
| Amount of DBTL ($W_{DBTL}$) | : 0.0025 g |
| Particle size of DBTL | : < 106, 150, 212, 450 µm |
| Adsorption temperature | : 30 ± 0.2 °C |
| Agitation rate | : 150 rpm |
| Agitation time ($t_e$) | : 6 hrs |

The equilibrium concentrations of Cr(VI), after adsorption, for different initial concentrations were determined from the analytical data obtained for different sizes of DBTL particles and presented in Table 3.43. The equilibrium amounts of chromium (VI) adsorbed on DBTL for different initial concentrations were calculated using equation (3.9) and presented in Table 3.43. The adsorption isotherms of chromium (VI) adsorbed on different sizes of DBTL particles at pH 2.0 are presented in Figure 3.67. Derived data are shown in Table 3.44 and 3.45 for the application of different isotherms model equations to the adsorption on different sizes of DBTL particles. Figures 3.68 to 3.71 show the verification of Langmuir, Freundlich, Temkin and Dubinin-Radushkevich (D-R) isotherm equations to the adsorption of chromium (VI) on different sizes of DBTL particles at pH 2.0 and 30 ± 0.2 °C. Different parameters of above isotherm equations are calculated, described previously and given in Table 3.46. Comparing the values of regression coefficient ($R^2$) in Table 3.46, it can be understood that the Langmuir equation is well fitted to the adsorption data of chromium (VI) on different sizes of DBTL particles at pH 2.0. Variation of equilibrium amount adsorbed, calculated from Langmuir equation, on different sizes of DBTL particles is shown in Figure 3.72. The figure shows the equilibrium amount adsorbed of chromium (VI) on DBTL is decreased gradually with increase of particle size of DBTL. Such observation might be

due to the fact that the smaller particle size of the adsorbent with fixed dose, having larger surface area of the adsorbent leads to more active sites to adsorb. Identical trend was observed on adsorptive removal of removal of chromium (VI) from aqueous solutions using Mosambi fruit peelings powder (Krishna and Swamy, 2012).

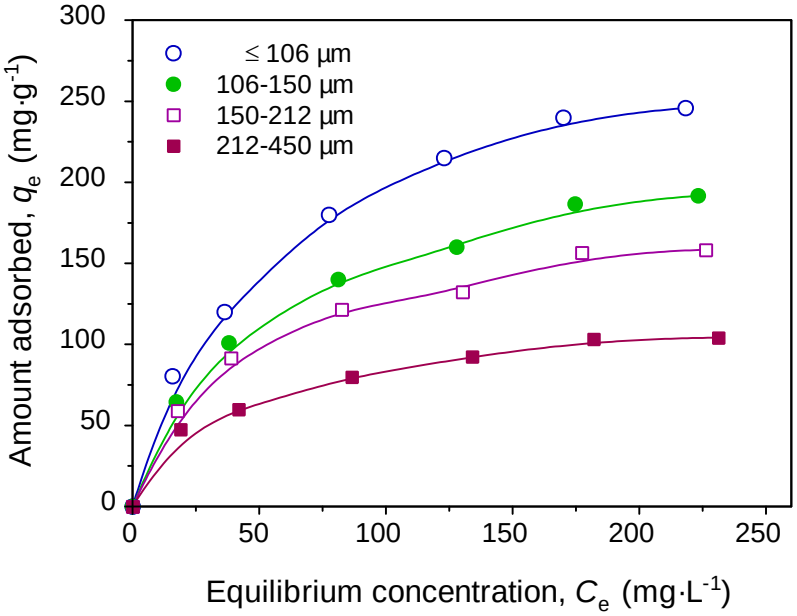


**Figure 3.67:** Adsorption isotherms of chromium (VI) adsorbed on different sizes of DBTL at pH 2.0 and 30 ± 0.2 $^{o}$C.

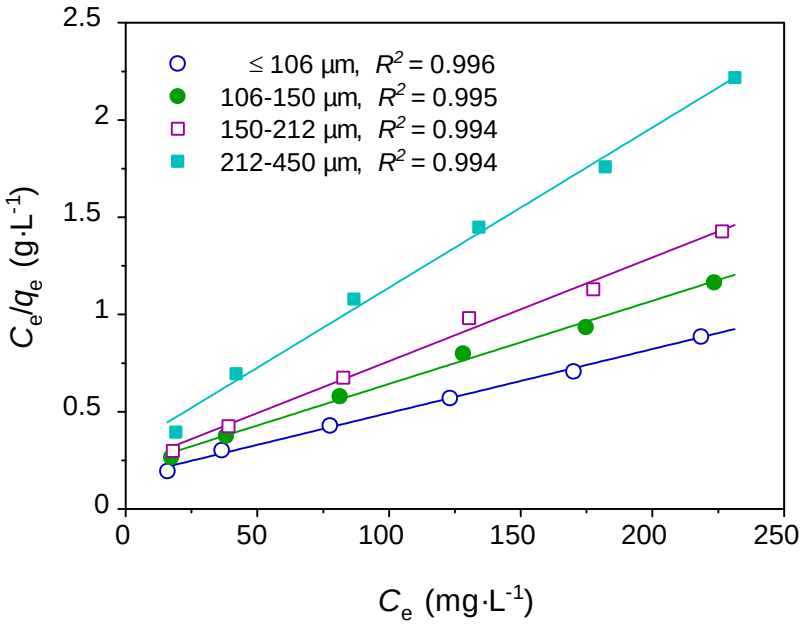


**Figure 3.68:** Langmuir isotherm of chromium (VI) adsorption on different sizes of DBTL at pH 2.0 and 30 ± 0.2 $^{o}$C.

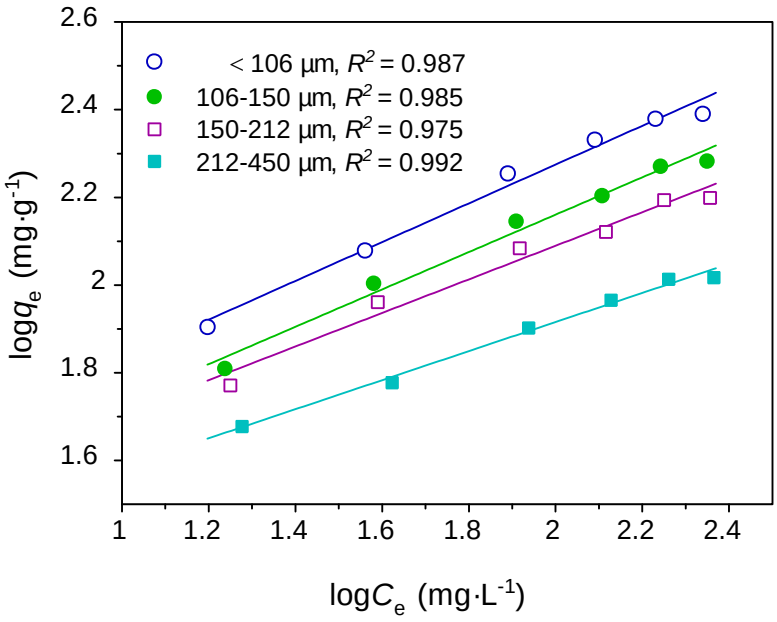


**Figure 3.69:** Freundlich isotherm of chromium (VI) adsorption on different sizes of DBTL at pH 2.0 and 30 ± 0.2 $^{o}$C.

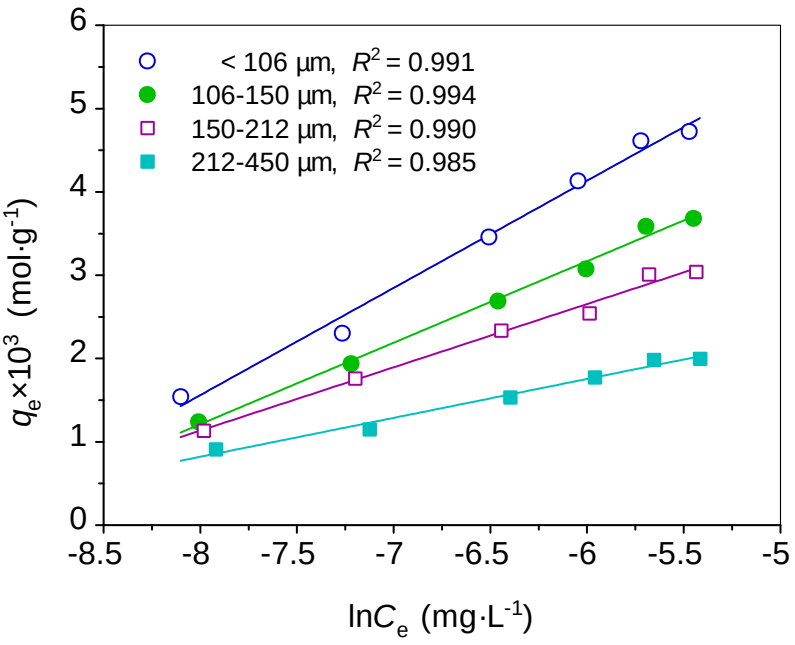


**Figure 3.70:** Temkin isotherm of chromium (VI) adsorption on different sizes of DBTL at pH 2.0 and 30 ± 0.2 $^{o}$C.

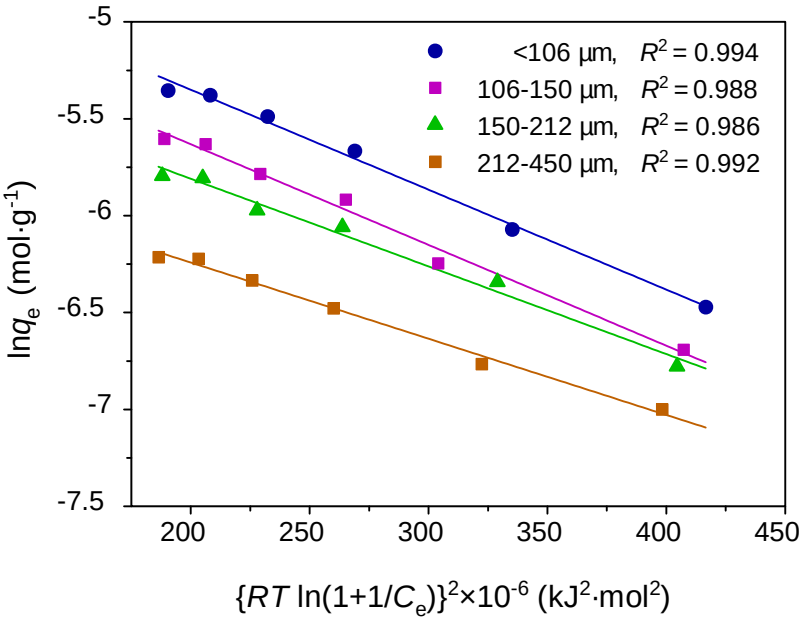


**Figure 3.71:** Dubinin-Radushkevich (D-R) isotherm of chromium (VI) adsorption on different sizes of DBTL at pH 2.0 and 30 ± 0.2 $^{o}$C.

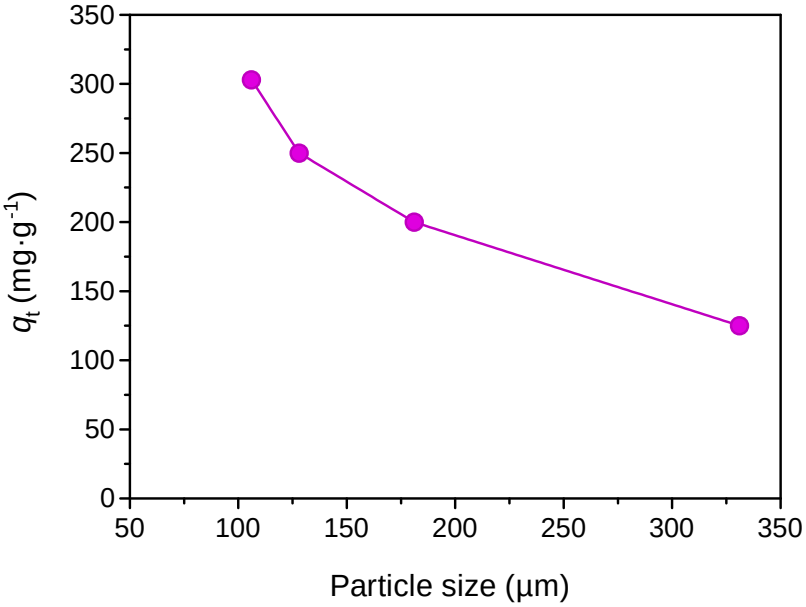


**Figure 3.72:** Variation of adsorption capacity with the particle sizes of DBTL for the adsorption of chromium (VI) on DBTL at pH 2.0 and at 30 ± 0.2 $^{o}$C.

**Table 3.43** Effect of particle size on the equilibrium adsorption isotherm of chromium (VI) on DBTL

| Particle size (µm) | $C_o$ (mg·L-$^1$) | $C_e$ (mg·L-$^1$) | $C_{oxidation}$ (mg·L-$^1$) | $C_R = C_{oxidation} - C_e$ (mg·L-$^1$) | $q_e = (C_o\text{-}C_e\text{-}C_R) \times V/W_{DBTL}$ (mg·g$^{-1}$) |
|---|---|---|---|---|---|
| < 106 | 25.833 | 15.75 | 17.792 | 2.042 | 80.41 |
| | 51.583 | 36.333 | 39.583 | 3.250 | 120.00 |
| | 101.333 | 77.50 | 83.333 | 5.833 | 180.00 |
| | 151.25 | 123.00 | 129.750 | 6.750 | 215.00 |
| | 201.333 | 170.00 | 177.333 | 7.333 | 240.00 |
| | 250.833 | 218.333 | 226.250 | 7.916 | 245.840 |
| 106-150 | 25.792 | 17.250 | 19.333 | 2.083 | 64.59 |
| | 51.417 | 38.000 | 41.333 | 3.333 | 100.84 |
| | 101.333 | 81.167 | 87.333 | 6.166 | 140.00 |
| | 150.750 | 128.000 | 134.750 | 6.750 | 160.00 |
| | 201.000 | 174.667 | 182.333 | 7.666 | 186.67 |
| | 250.417 | 223.333 | 231.250 | 7.917 | 191.67 |
| 150-212 | 25.792 | 17.750 | 19.875 | 2.125 | 59.17 |
| | 51.417 | 38.833 | 42.250 | 3.417 | 91.67 |
| | 101.333 | 82.500 | 89.167 | 6.667 | 121.66 |
| | 150.750 | 130.250 | 137.500 | 7.250 | 132.50 |
| | 201.00 | 177.333 | 185.333 | 8.000 | 156.67 |
| | 250.417 | 226.250 | 234.583 | 8.333 | 158.34 |
| 212-450 | 25.792 | 18.875 | 21.042 | 2.167 | 47.50 |
| | 51.417 | 41.833 | 45.417 | 3.584 | 60.00 |
| | 101.333 | 86.500 | 93.333 | 6.833 | 80.00 |
| | 150.750 | 134.000 | 141.500 | 7.500 | 92.40 |
| | 201.00 | 182.000 | 190.667 | 8.667 | 103.33 |
| | 250.417 | 231.250 | 240.000 | 8.750 | 104.17 |

**Table 3.44** Derived-data for application of Langmuir, Freundlich and Temkin isotherms to the adsorption chromium (VI) on different sizes of DBTL at pH 2.0 and 30 ± 0.2 °C.

| Particle size (µm) | $C_o$ ($mg \cdot L^{-1}$) | $C_e$ ($mg \cdot L^{-1}$) | $q_e$ ($mg \cdot g^{-1}$) | $C_e/q_e$ ($g.L^{-1}$) | log $C_e$ ($mg \cdot L^{-1}$) | log $q_e$ ($mg \cdot g^{-1}$) | ln$C_e$ ($mol \cdot L^{-1}$) |
|---|---|---|---|---|---|---|---|
| < 106 | 25.833 | 15.750 | 80.41 | 0.196 | 1.197 | 1.905 | - 8.102 |
| | 51.583 | 36.333 | 120.00 | 0.303 | 1.560 | 2.079 | -7.266 |
| | 101.333 | 77.500 | 180.00 | 0.431 | 1.889 | 2.255 | - 6.509 |
| | 151.25 | 123.000 | 215.00 | 0.572 | 2.090 | 2.332 | - 6.047 |
| | 201.333 | 170.000 | 240.00 | 0.708 | 2.230 | 2.380 | -5.723 |
| | 250.833 | 218.333 | 245.84 | 0.888 | 2.339 | 2.391 | -5.473 |
| 106-150 | 25.792 | 17.250 | 64.59 | 0.267 | 1.237 | 1.810 | - 8.010 |
| | 51.417 | 38.000 | 100.84 | 0.377 | 1.580 | 2.004 | -7.221 |
| | 101.333 | 81.167 | 140.00 | 0.580 | 1.909 | 2.146 | - 6.462 |
| | 150.750 | 128.000 | 160.00 | 0.800 | 2.107 | 2.204 | - 6.007 |
| | 201.000 | 174.667 | 186.67 | 0.936 | 2.242 | 2.271 | -5.696 |
| | 250.417 | 223.333 | 191.67 | 1.165 | 2.349 | 2.283 | -5.450 |
| 150-212 | 25.792 | 17.75 | 59.17 | 0.300 | 1.249 | 1.772 | -7.983 |
| | 51.417 | 38.833 | 91.67 | 0.424 | 1.589 | 1.962 | -7.200 |
| | 101.333 | 82.500 | 121.66 | 0.678 | 1.916 | 2.085 | - 6.446 |
| | 150.750 | 130.250 | 132.50 | 0.983 | 2.115 | 2.122 | -5.989 |
| | 201.000 | 177.333 | 156.67 | 1.132 | 2.249 | 2.195 | -5.681 |
| | 250.417 | 226.250 | 158.34 | 1.429 | 2.355 | 2.200 | -5.437 |
| 212-450 | 25.792 | 18.875 | 47.50 | 0.397 | 1.276 | 1.678 | -7.921 |
| | 51.417 | 41.833 | 60.00 | 0.697 | 1.622 | 1.778 | -7.126 |
| | 101.333 | 86.500 | 80.00 | 1.081 | 1.937 | 1.903 | - 6.399 |
| | 150.750 | 134.00 | 92.40 | 1.450 | 2.127 | 1.966 | -5.961 |
| | 201.000 | 182.000 | 103.33 | 1.761 | 2.260 | 2.014 | -5.655 |
| | 250.417 | 231.250 | 104.17 | 2.220 | 2.364 | 2.018 | -5.416 |

**Table 3.45** Derived-data for application of Dubinin- Radushkevich (R-D) isotherm to the adsorption chromium (VI) on different sizes of DBTL at pH 2.0 and 30.0± 0.2 °C.

| Particle size (μm) | $C_o$ (mg·L$^{-1}$) | $C_e$ (mg·L$^{-1}$) | $C_e \times 10^{-3}$ (mol·L$^{-1}$) | $\ln(1+1/C_e)$ (L·mol$^{-1}$) | $\{RT \ln 1+1/C_e)\}^2 \times 10^{-6}$ (a.u.) | $q_e$ (mg·g$^{-1}$) | $\ln q_e$ (mol·g$^{-1}$) |
|---|---|---|---|---|---|---|---|
| < 106 | 25.833 | 15.750 | 0.303 | 8.102 | 416.572 | 80.41 | -6.472 |
| | 51.583 | 36.333 | 0.699 | 7.267 | 335.132 | 120.00 | - 6.071 |
| | 101.333 | 77.500 | 1.490 | 6.510 | 268.950 | 180.00 | - 5.666 |
| | 151.250 | 123.000 | 2.365 | 6.049 | 232.205 | 215.00 | -5.488 |
| | 201.333 | 170.000 | 3.269 | 5.727 | 208.142 | 240.00 | -5.378 |
| | 250.833 | 218.333 | 4.199 | 5.477 | 190.367 | 245.84 | -5.354 |
| 106-150 | 25.792 | 17.750 | 0.332 | 8.011 | 407.270 | 64.59 | -6.691 |
| | 51.417 | 38.000 | 0.731 | 7.222 | 303.990 | 100.84 | - 6.245 |
| | 101.333 | 81.167 | 1.561 | 6.464 | 265.160 | 140.00 | - 5.917 |
| | 150.750 | 128.000 | 2.462 | 6.009 | 229.145 | 160.00 | -5.784 |
| | 201.000 | 174.667 | 3.359 | 5.699 | 206.112 | 186.67 | -5.630 |
| | 250.417 | 223.333 | 4.295 | 5.455 | 188.840 | 191.67 | -5.603 |
| 150-212 | 25.792 | 17.250 | 0.341 | 7.984 | 404.530 | 59.17 | - 6.779 |
| | 51.417 | 38.833 | 0.747 | 7.200 | 328.980 | 91.67 | - 6.341 |
| | 101.333 | 82.500 | 1.587 | 6.447 | 263.770 | 121.66 | - 6.058 |
| | 150.750 | 130.250 | 2.505 | 5.992 | 227.850 | 132.50 | -5.972 |
| | 201.000 | 177.333 | 3.410 | 5.684 | 205.030 | 156.67 | -5.805 |
| | 250.417 | 226.250 | 4.351 | 5.442 | 187.940 | 158.34 | -5.794 |
| 212-450 | 25.792 | 18.875 | 0.363 | 7.921 | 398.170 | 47.50 | - 6.999 |
| | 51.417 | 41.833 | 0.804 | 7.127 | 322.340 | 60.00 | - 6.765 |
| | 101.333 | 86.500 | 1.663 | 6.401 | 260.020 | 80.00 | - 6.477 |
| | 150.750 | 134.00 | 2.577 | 5.964 | 225.730 | 92.40 | - 6.337 |
| | 201.000 | 182.000 | 3.500 | 5.658 | 203.160 | 103.33 | - 6.221 |
| | 250.417 | 231.250 | 4.447 | 5.420 | 186.420 | 104.17 | - 6.213 |

**Table 3.46** Parameters of different isotherms derived from equilibrium study for the adsorption chromium (VI) on different sizes of DBTL from aqueous solution at pH 2.0 and 30.0 ± 0.2 $^{o}$C.

| Isotherms | Parameter | Particle size (μm) | | | |
|---|---|---|---|---|---|
| | | < 106 | 106-150 | 150-212 | 212-450 |
| Langmuir isotherm | $q_m$ (mg·g$^{-1}$) | 303.030 | 250.00 | 200.00 | 125.00 |
| | $b$ (L·mg$^{-1}$) | 0.020 | 0.019 | 0.022 | 0.025 |
| | $R^2$ (a.u.) | 0.996 | 0.996 | 0.993 | 0.994 |
| Freundlich isotherm | $k_f$ (mg·g$^{-1}$) | 24.564 | 20.323 | 21.038 | 17.865 |
| | $n$ (a.u.) | 2.261 | 2.347 | 2.611 | 3.021 |
| | $R^2$ (a.u.) | 0.987 | 0.988 | 0.975 | 0.992 |
| Temkin isotherm | $A$ ×10$^{-3}$ (L·mol$^{-1}$) | 10.033 | 10.324 | 13.202 | 17.330 |
| | $B$ ×10$^{3}$ (a.u.) | 1.287 | 0.978 | 0.760 | 0.467 |
| | $R^2$ (a.u.) | 0.991 | 0.994 | 0.990 | 0.985 |
| Dubinin-Radushkevich | $q_{DR}$ (mol·g$^{-1}$) | 0.013 | 0.01 | 0.0074 | 0.0043 |
| | ¥ ×10$^{9}$ (mol$^2$·$k$J$^{-2}$) | 5.20 | 5.20 | 4.50 | 3.90 |
| | $E$ (kJ·mol$^{-1}$) | -9.81 | -9.81 | -10.541 | -11.323 |
| | $R^2$ (a.u.) | 0.994 | 0.988 | 0.986 | 0.992 |

# 3.8 Analysis of Adsorbed Surface

## 3.8.1 ATR-IR study on Cr(VI) adsorbed DBTL

Attenuated Total Reflectance Infra-red (ATR-IR) spectroscopic study on Cr(VI) adsorbed DBTL was carried out to identify the possible interaction of adsorbed Cr with the composition of DBTL. Figure 3.73 shows the ATR-IR spectrum (ATR-IR, Shimadzu, Japan) of Cr(VI) adsorbed DBTL. The characteristic peaks with their positions are given in Table 3.47. The broad peak at 3342.64 $cm^{-1}$ indicates the presence of – OH groups in DBTL. Other peaks at 1624.06, 1379.10, 1265.30 and 1045.42 $cm^{-1}$ for C=C, -C-H, C-O-H and C-O, respectively shown in Table 3.47 with reference peaks of functional groups. A comparison of analytical data of different spectra is given Table-3.47. A combination of ATR-IR spectra of above mentioned is shown in Figure 3.74. Comparing the shifting of peak positions of different functional groups for above spectra of un-adsorbed and Cr(VI) adsorbed UBTL, it can be suggested that OH and C=C groups (peak positions shifted towards the shorter wave number due to hydrogen bonding), and C-O (peak positions shifted towards the longer wave number due delocalization of loon pair electrons), of UBTL are interacted with Cr through aromatic =C-H (peak positions shifted towards the longer wave number due delocalization of aromatic electrons) and other parts of positive centers of the molecules depending on the pH value of solution. A new peak appears at 717.52 $cm^{-1}$ for **–C-Cr** interaction.

**Table 3.47** Peak position of AT-FTIR spectra of prepared DBTL and Cr(VI) adsorbed DBTL.

| **Peak positions ($cm^{-1}$)** | | **Reference values** | **Characteristics Gr.** |
|---|---|---|---|
| **Un-adsorbed DBTL** | **Cr-adsorbed DBTL** | | |
| 3342.64 | ↓ 3338.78 | 3400-3200 | -O-H (str) (H-bonded) |
| 2916.37 | 2920.23 | 3000-2850 | -C-H (str) |
| 2708.06 | ------- | 2850.79 | -O-C-H (def) |
| 1624.06 | ↓ 1620.21 | 1680-1620 | >C=C (aromatic) |
| 1379.10 | 1382.96 | 1375 | -C-H (bending) |
| 1265.30 | 1276.88 | 1440-1220 | C-O-H (bending) |
| 1045.42 | 1047.35 | 1300-1000 | C-O-C (def) |
| -------- | **717.52** | 719 | **-C-Cr** |
| 686.66 | 671.23 | 667 | =C-H |

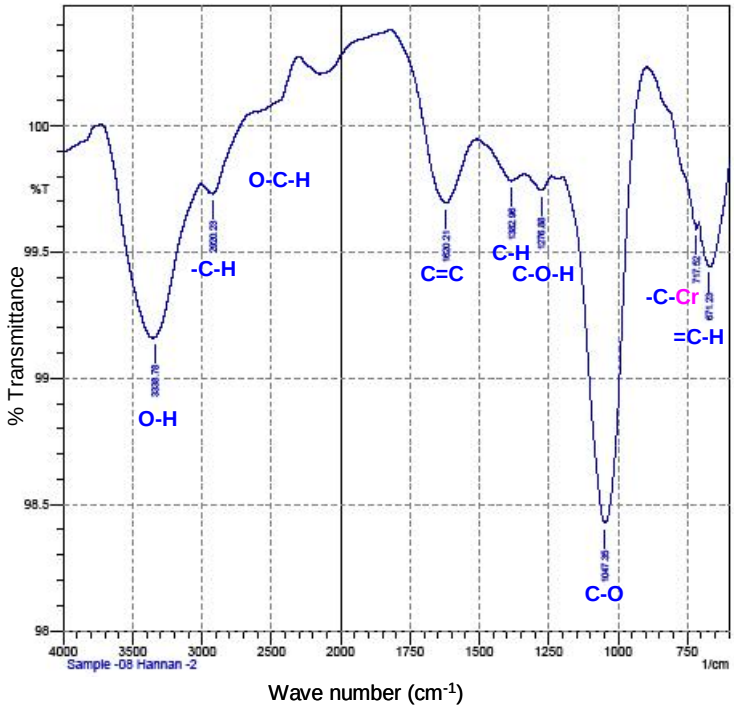


FTIR spectrum of Cr(VI) adsorbed DBTL

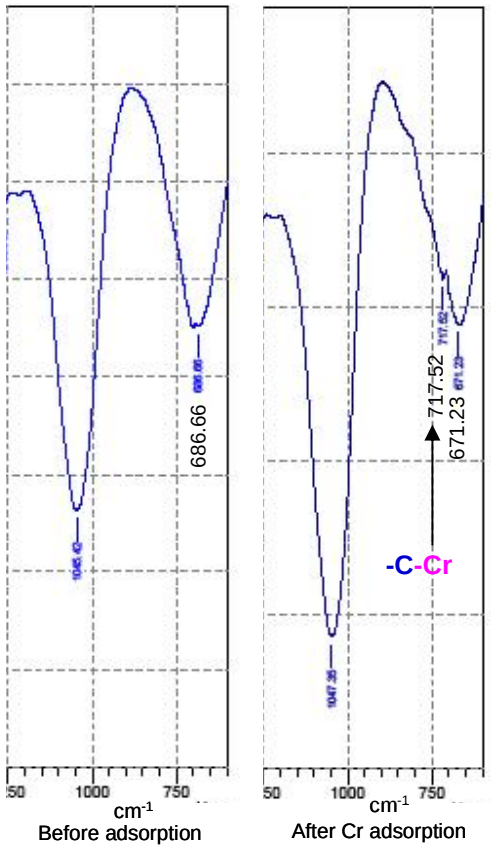


**Figure 3.73:** Comparison of ATR-IR spectra of before and after Cr(VI) adsorbed DBTL.

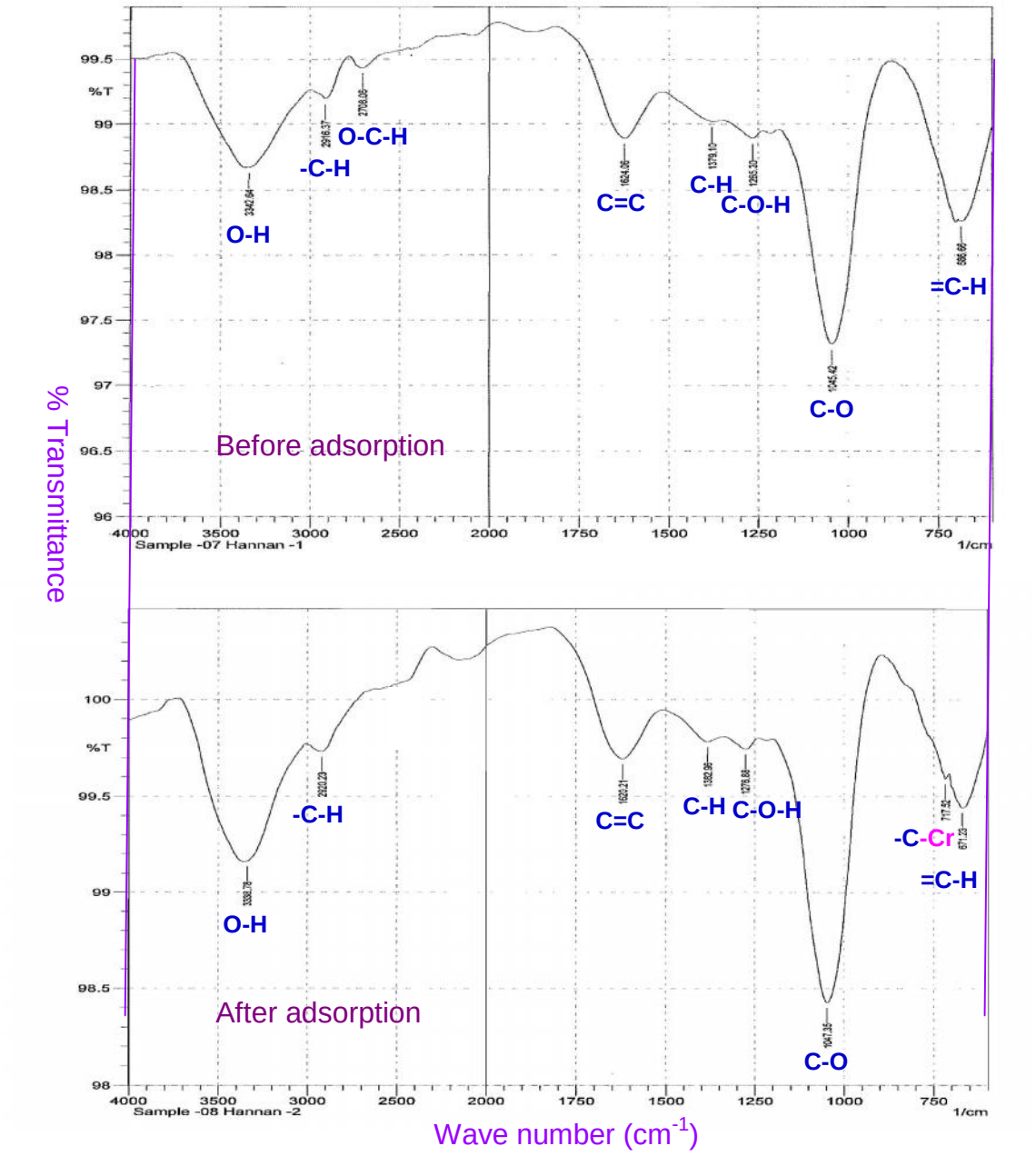


**Figure 3.74:** Comparison of FTIR spectra of WBTL before and after adsorption of Cr(VI); (Top is for before adsorption and the Bottom one is for after adsorption).

## 3.8.2 SEM and EDX Analysis of Cr(VI) adsorbed DBTL

The Scanning Electron Microscope (SEM) (JSEM-6490LA, JEOL, Japan) was used to analyze the surface morphology of Cr(VI) adsorbed DBTL surfaces. Figure 3.75 presents the SEM micrograph Cr(VI) adsorbed DBTL surfaces at which shows the existence of some foreign materials (spherical shape) on the DBTL surface at high magnifying (×5000 and ×20,000) micrograms in Figure 3.75(b) and 3.75(c). The existence of such foreign material of Cr was confirmed by Energy Dispersive X-ray (EDX, JED 2300) analysis as shown in Figure 3.75(d). An enlarge sized EDX spectrum of Cr(VI) adsorbed DBTL surface in Figure 3.76 shows three signals at 0.573, 5.411 and 6.1204 keV for $Cr_{L\alpha}$, $Cr_{K\alpha}$ and $Cr_{K\beta}$, respectively. These observations confirmed the adsorption of Cr on DBTL and the percent amount chromium and other elements of DBTL constituent are given in Table 3.48. A comparison of the composition of un-adsorbed (Table 3.3) and Cr adsorbed DBTL surface is presented in Table 3.49. The EDX analytical data show that the un-adsorbed DBTL contained less (0.98 % mass) amount of calcium (Ca) at 3.690 and 4.00 keV in Figure 3.8 which is disappeared on surface after adsorption of chromium, Cr (4% mass) on DBTL surface found in Figure 3.77 at 5.411 and 6.120 keV.

The amount of carbon contained (45.99 % mass and 53.42 % Atom) in un-adsorbed DBTL is decreased in Cr(VI) adsorbed DBTL surface (42.79 % mass and 51.15) due to the covered of DBTL surface by Cr(VI). Again, the amount of oxygen contained (53.03 % mass and 46.24 % Atom) in un-adsorbed DBTL is increased in Cr(VI) adsorbed DBTL surface (53.19 % mass and 47.74 % Atom) due to the addition of oxygen in the form of $Cr_2O_7^{2-}$ and $HCrO_4^-$ of Cr(VI). These observations are presented in Figures 3.78.

Since the DBTL surface is heterogeneous, distribution of the amount of chromium adsorbed on DBTL surface was investigated using EDX analysis at 7 different points (A-G) on DBTL surface shown in Figure 3.79. The analytical data in Table 3.50 shows that the amount of chromium adsorbed on DBTL surface (Figure 3.79) at cavity (E and F) is higher than at top position on the surface presented in Figure 3.80. Thus the heterogeneity of DBTL surface enhanced its adsorption capacity.

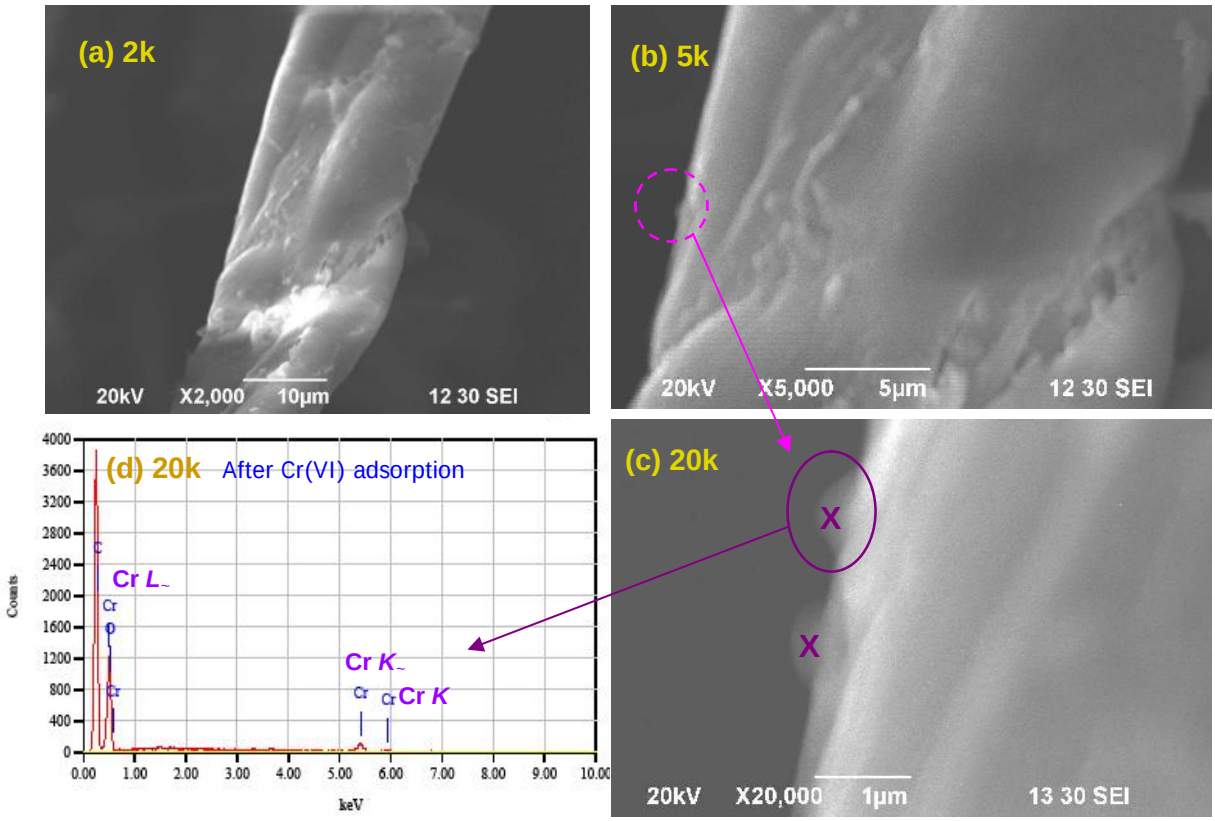


**Figure 3.75:** SEM and EDX analysis of Cr adsorbed DBTL surface at different magnifications.

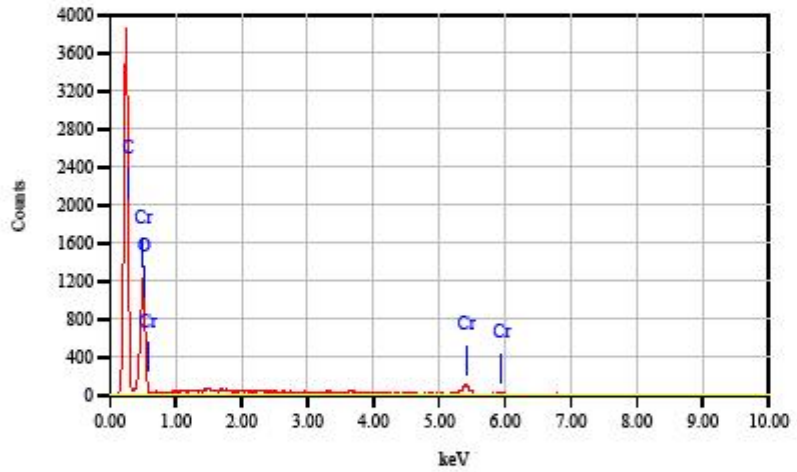


**Figure 3.76:** EDX spectrum of Cr adsorbed DBTL surface (×20,000).

**Table 3.48** Composition of Cr(VI) adsorbed DBTL surface by EDX analysis.

| Elements | Mass (%) | Atom (%) |
|---|---|---|
| **C** | 42.79 | 51.15 |
| **O** | 53.19 | 47.74 |
| **Cr** | 4.02 | 1.11 |

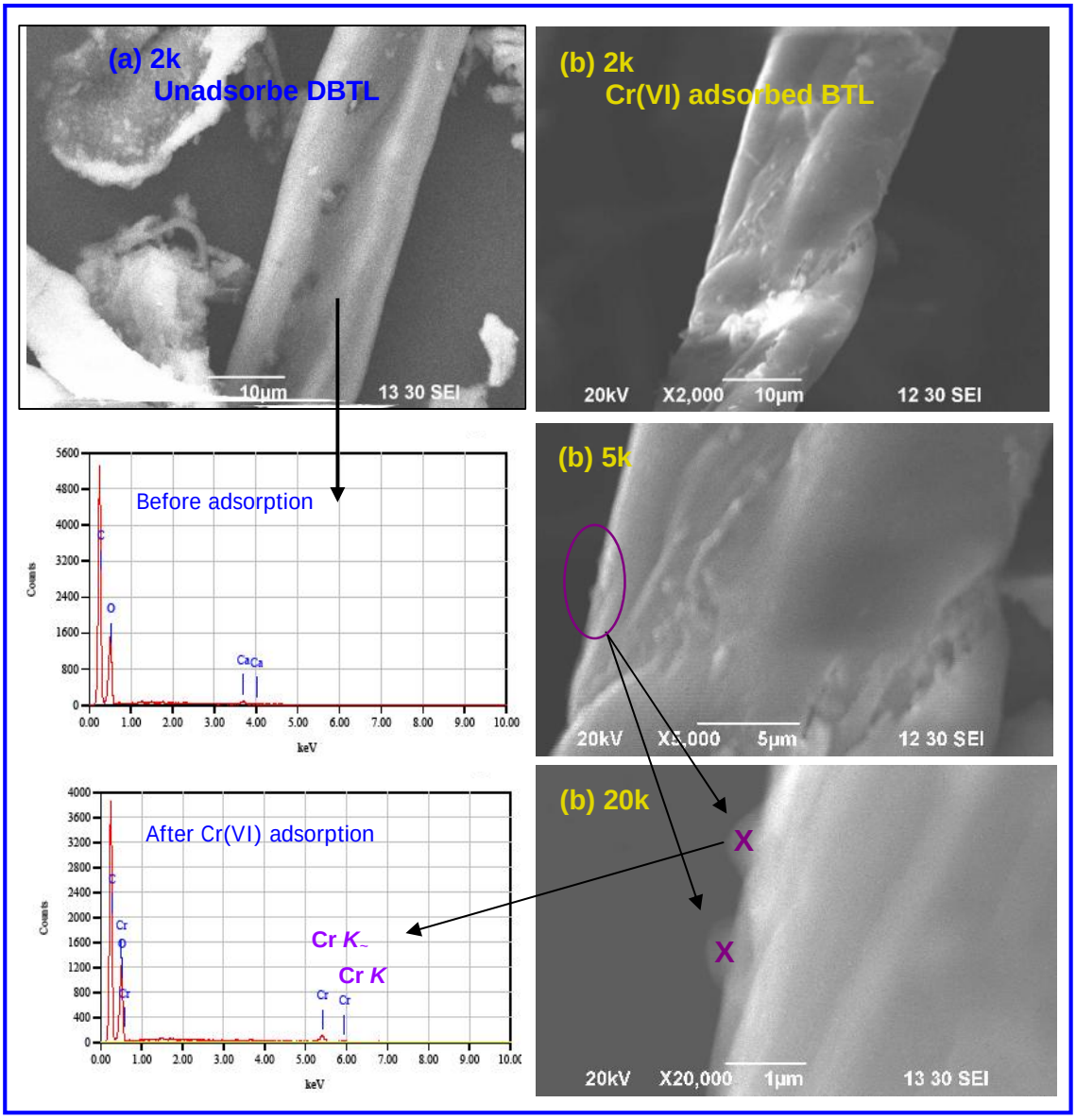


**Figure 3.77:** A comparison of the SEM and EDX analysis of un-adsorbed and Cr(VI) adsorbed DBTL surface.

**Table 3.49** Composition of DBTL estimated by energy dispersive X-ray (EDX).

| Elements | Un-adsorbed DBTL | | Cr(VI) adsorbed DBTL | |
|---|---|---|---|---|
| | Mass (%) | Atom (%) | Mass (%) | Atom (%) |
| **C** | 45.99 | 53.42 | 42.79 | 51.15 |
| **O** | 53.03 | 46.24 | 53.19 | 47.74 |
| **Ca** | 0.98 | 0.34 | --- | --- |
| **Cr** | --- | --- | 4.02 | 1.11 |

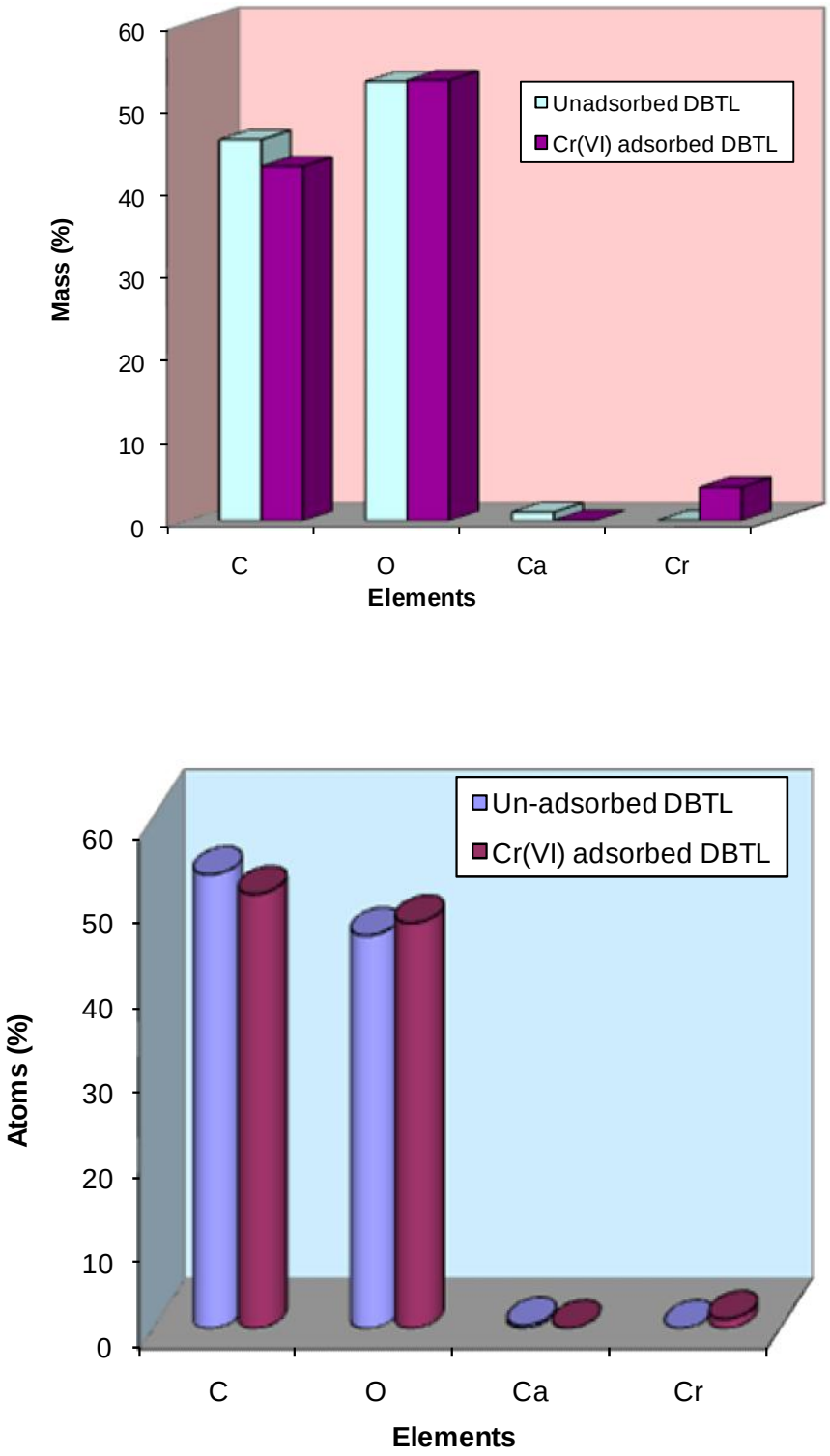


**Figure 3.78:** A comparison of the elemental composition of un-adsorbed and Cr(VI) adsorbed DBTL.

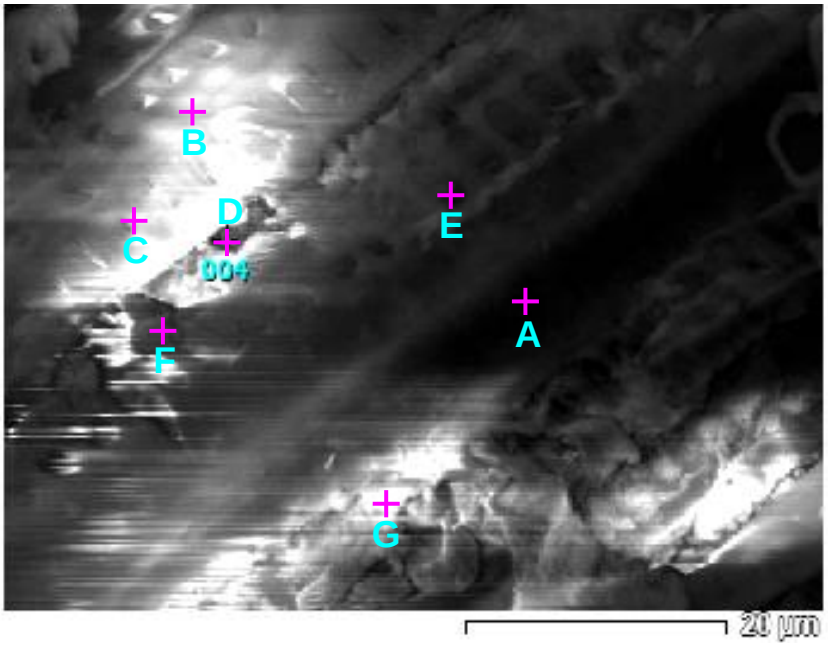


**Figure 3.79:** EDX point analysis in SEM microgram of Cr adsorbed DBTL surface.

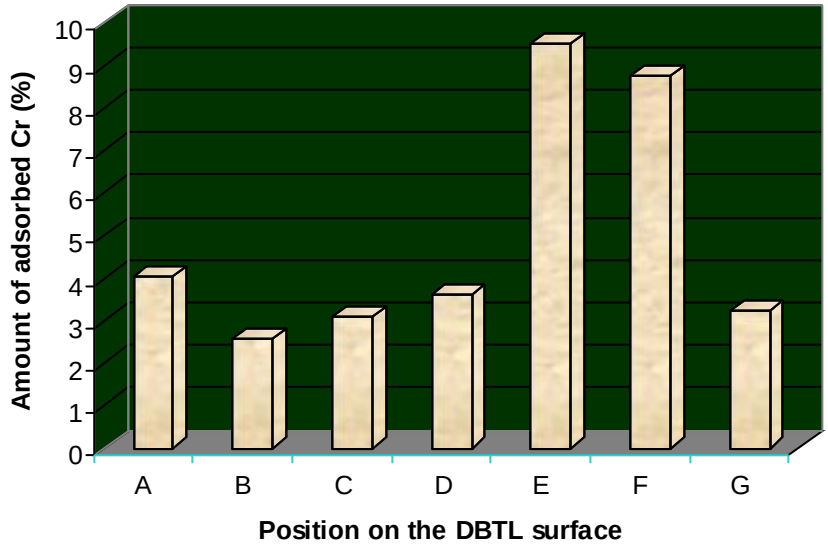


**Figure 3.80** Variation of the amount adsorbed Cr at different points on DBTL surface after adsorption of Cr(VI) at pH 2.0.

**Table 3.50** Composition of DBTL estimated by energy dispersive X-ray (EDX).

| Positions in Figure 3.74 | Mass of adsorbed Cr (%) | Mass of Carbon (%) | Mass of Oxygen (%) |
|---|---|---|---|
| **A** | 4.02 | 42.79 | 53.19 |
| **B** | 2.58 | 49.94 | 47.48 |
| **C** | 3.10 | 50.05 | 46.85 |
| **D** | 3.59 | 51.60 | 44.81 |
| **E** | 9.50 | 62.51 | 27.98 |
| **F** | 8.76 | 65.86 | 25.38 |
| **G** | 3.22 | 60.09 | 36.68 |

# 3.9 Desorption and Recovery of Cr

After adsorption, recovery of adsorbed chromium is necessary for further use. For this, desorption process was studied. But in the present study, within 1-2 hours, chromium was fully recovered from DBTL surface by chemical decomposition of DBTL with 2M sodium hydroxide (NaOH) solution which was collected from the sodium hydroxide solution by precipitation process. Recovery system is schematically presented in Figure 3.81.

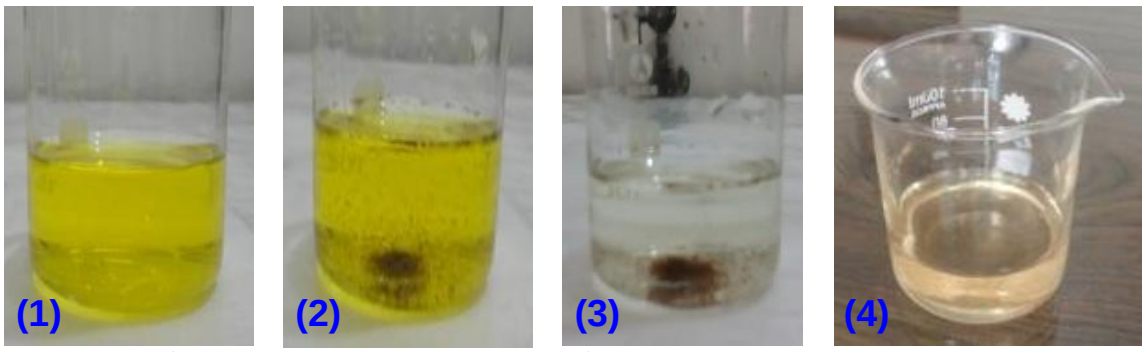


(1) 100 mg·$L^{-1}$ solution, (2) DBTL with 100 mg·$L^{-1}$ solution, (3) Aqueous media after adsorption of Cr (VI) on DBTL and (4) Cr (VI)-adsorbed DBTL completely decomposed with 2M NaOH

**Figure 3.81:** Cr (VI) adsorbed on DBTL decomposes easily with 2M NaOH solution which leads to the complete recovery of Cr from DBTL.

# *Chapter 4*

# CONCLUSIONS

# 4. CONCLUSIONS

The research findings revealed the following information:

1. Dust Black Tea Leaves (DBTL) are heterogeneous surface with small surface area (1.7 $m^2 \cdot g^{-1}$) and pore volume ($1.9 \times 10^{-2}$ $cm^3 \cdot g^{-1}$).

2. Both adsorption and reduction of Cr (VI) involved in the removal of Cr (VI) by DBTL but adsorption is dominating over reduction at low pH of solution. At pH 2.0, of total removal of Cr(VI), about 80% of Cr (VI) adsorbed on DBTL and about 20% reduced to Cr (III), exists in solution which is less harmful for living system..

3. The adsorption kinetics of Cr(VI) on DBTL has significantly been affected by initial concentration of Cr(VI), solution pH, temperature and particle-size of DBTL, and all data were well-expressed by pseudo second order kinetic equation.

4. The equilibrium adsorption has also been affected by the solution pH, temperature and particle-size of DBTL. The maximum monolayer adsorption capacity, $q_m$ = 303.03 $mg \cdot g^{-1}$ at 30 $^oC$ has been calculated using the best-fitted Langmuir isotherm equation other than Freundlich, Tempkin and Dominin-Radushkevich equations, which value is decreased with increase of temperature.

5. The values of thermodynamic parameters ($\Delta H$ = - 27.38 $kJ \cdot mol^{-1}$, $\Delta G^o$ = -17.42 $kJ \cdot mol^{-1}$, $\Delta S$ = - 0.102 $kJ \cdot mol^{-1} \cdot K^{-1}$ and $E_a$ = + 7.37 $kJ \cdot mol^{-1}$) suggested that the adsorption of Cr(VI) on DBTL is exothermic, spontaneous and physical in nature.

6. SEM and EDX analyses of Cr(VI) adsorbed DBTL surface indicated the existence of heterogeneous distribution of chromium on DBTL surface.

7. ATR-IR investigation of DBTL showed the presence of -O-H, -CH, -OCH, -COH, =C-H and C=C groups in DBTL and these groups has been affected by the adsorption of Cr(VI).

8. 100 % chromium can be recovered from Cr-adsorbed DBTL loaded with Cr (VI) by chemical decomposition.

Considering the findings of this study, it is concluded that Dust Black Tea Leaves (DBTL), a waste of tea process plants, could be utilized as an inexpensive adsorbent to remove toxic chromium (VI) from aquatic environment and the potential of this bio-material may be used for adsorptive removal of other toxic heavy metal ions from aquatic system.

# REFERENCES

# REFERENCES

Ada, K., Ergene, A., Tan, S. and Yalcin, E.: Adsorption of Remazol Brilliant Blue R Using ZnO Fine Powder: Equilibrium, Kinetic and Thermodynamic Modeling Studies, *J. Hazard. Matter*, **165(1-3),** 637-644, 2009.

Agegnehu, A., Lemma, B., Gabbiye,N., Alula, M. T. and Desta, M. T.: Removal of Chromium (VI) from Aqueous Solution Using Vesicular Basalt: A Potential Low-Cost Wastewater Treatment System, *Environ. Sci*., **4(7),** e 00682, 2018.

Alam, S.: Equilibrium and Continuous Column Adsorption of Rhodamine B on Used Black Tea Leaves, *MS. Thesis*, Department of Chemistry, University of Dhaka, Bangladesh, 2010.

Allen, S. J. and Koumanova, B.: Decolourisation of Water/Wastewater Using Adsorption (Review). *J. Univ. Chem. Technol. and Metal*, **3**, 175 -192, 2005.

Altun, T. and Kar, Y.: Removal of Cr(VI) from Aqueous Solution by Pyrolytic Charcoals, **31(5)**, 501-509, 2016.

Alves, M., Margarida, C. G., González Beça, R., Guedes de Carvalho, J. M., Castanheira, M. C., Sol Pereira, L. A. T. and Vasconcelos: Chromium Removal in Tannery Wastewaters "polishing" by Pinus Sylvestris Bark, *Water Res*., **27(8)**,1333-1338, 1993.

Alzaydien, A. S., Manasreh, W.: Equilibrium, Kinetic and Thermodynamic Studies on the Adsorption of Phenol onto Activated Phosphate Rock, *J. Phy. Sci.*, **4(4),** 172-181, 2009.

Alzaydien, A. S.: Adsorption of Methylene Blue from Aqueous Solution onto a Low-Cost Natural Jordanian Tripoli, *Am. J. Appl. Sci*., **5(1),** 197-208, 2009.

American Public Health Association (APHA): Standard Method for the Examination of Water and Waste Water, 16th Edition, Washington DC, 1985.

Amin, N. K.: Removal of Reactive Dye from Aqueous Solutions by Adsorption onto Activated Carbons Prepared from Sugarcane Bagasse Pith, *Desalination*, **223**, 152–161, 2008.

Ansari, T., Sundaramoorthy, N. and Kavitha, M.: Adsorption, Biosorption and Discolourisation of Rhodamine-B and Basic Violet-2 Using Fungi Isolated form Soil Sample Collected Near Textile Dye Industry; *Int. J. Res. Pharm. and Biomedi. Sci.*, **2(4)**, 1706-1710, 2011.

Arami, M., Limaee, N. Y., Mahmoodi, N. M. and Tabrizi, N. S.: Removal of Dyes from Colored Textile Wastewater by Orange Peel Adsorbent: Equilibrium and Kinetic Studies, *J. Colloid Interf. Sci*., **288**, 371-376, 2005.

Attia, A. A., El-Hendawy, A. A, Khedr, S. A., El-Nabarawy, T. H.: Textural Properties and Adsorption of Dyes onto Carbons Derived from Cotton Salks, *Adv. Sci. Technol.*, **22,** 411-426, 2004.

Awala, H. A. El. and Jamal, M. M.: Equilibrium and Kinetics Study of Adsorption of Some Dyes onto Feldspar. *J. Univ. Chem. Tech. and Metallurgy*, **46 (1)**, 45-52, 2011.

Babu, B. V. and Gupta, S.: Removal of Cr(VI) from Wastewater Using Activated Tamarind Seeds as an Adsorbent, *J. Environ. Eng. and Sci.*, 7(5), 553-557, 2008.

Barceloux, B. and Doland, G.: Chromium, *J. Toxicol. Clin. Toxicol.*, **37(2)**, 173-194, 1999.

Barrett, E. P., Joyner, L. G. and Halenda, P. P.: The Determination of Pore Volume and Area Distributions in Porous Substances. I. Computations from Nitrogen Isotherms, *J. Am. Chem. Soc*., **73**, 373-380, 1951.

Bayramoglu, G., Altintas. B, Arica, M. Y.: Adsorption Kinetics and Thermodynamic Parameters of Cationic Dyes from Aqueous Solutions by Using a New strong Cation-exchange Resin, *J. Chem. Eng.*, **152**, 339-346, 2009.

Benjamin, M. M., Sletten, R. S., Bailey, R. P. and Bennett, T.: Sorption and Filtration of Metals Using Iron-Oxide-coated Sand, *Water Res.*, **30(11),** 2609-2620, 1996.

Brunauer, S., Emmet, P. H. and Teller, E.: Adsorption of Gases in Multimolecular Layers, *J. Am. Chem. Soc*. **60(2)**, 309-3019, 1938.

Chien, S. H. and Clayton, W. R.: Application of Elovich Equation to the Kinetics of Phosphate Release and Sorption in Soils. *Soil Sci. Soc. Am. J*., **44**, 265-268, 1980.

Cimino, G., Passerine, A. and Toscno, G.: Removal of Toxic Cation and Cr(VI) from Aqueous Solution by Hazelnut shell, *Water Res*. **34**, 2955-2962, 2000.

Cohen, M. D., Kargachin, B. and Klein, C. B., Costa, M.: Mechanism of Chromium Carcinogenicity and Toxicity, *Crtical Reviews on Toxicology*, **23(3)**, 255-81, 1993.

Colella, C.: Ion Exchange Equilibria in Zeolite Minerals, *Mineral. Dcposita*., **31**, 554-562, 1996.

Cotton, F. A. and Wilkinson, G.: Advance Inorganic Chemistry, 5th Edition, 297-298, John Wiley and Sons, 1998.

Dakiky, M., Khamis, M., Manassara, A. and Mereb, M.: Selective Adsorption of Chromium (VI) in Industrial Wastewater Using Low-cost Abundantly Available Adsorbents, *Adv. Environ. Res*., **6**, 533-540, 2002.

Dehghani, M. H., Sanaei, D., Ali, I., Bhatnagar, A.: Removal of Chromium (VI) from Aqueous Solution Using Treated Waste Newspaper as a Low-Cost Adsorbent: Kinetic Modeling and Isotherm Studies, Journal of Molecular Liquids **215**, 671-679, 2016.

Dhanakumar, S., Solaraj, G., Mohonraj, R. and Pattabhi, S.: Removal of Cr(VI) from Aqueous Solution by Adsorption Using Cooked Tea Dust, *Indian J. Sci. and Technol.*, **1(2)**, 1-6, 2007.

Dubinin, M. M. and Radushkevich, L. V.: The Equation of the Characteristic Curve of Activated Charcoal, *Proceedings of the Academy of Sciences, Physical Chemistry Section*, **55,** 331-333, 1947.

Ecolological, Analysts, Inc., E. A. I.: The Sources, Chemistry, Fate and Effect of Chromium in Aquatic Environments, Available from American Petroleum Institute, Washington, DC 20037, **207**, 1981.

EPA, Environment Protection Agency, United State of American, Proposed Rules, Federal Register 50, No. **219**, 46966-46967, 1985.

Espinola, A., Adamian, R. and Gomes, L. M. P.: An Innovative Technology: Natural Coconut Fibre as Adsorptive Medium in Industrial Wastewater Cleanup. In Proceedings of the TMS Fall Extraction and Processing Conference, **3**, 2057-2066, 1999.

Freundlich, H.: Adsorption in Solution, *Phys. Chem. Soc*., **40**, 1361-1368, 1906.

Ghani, A.: Effect of Chromium Toxicity on Growth, Chlorophyll and Some Mineral Nutrients of Brassica Juncea L, *Egypt. Acad. J. Biolo. Sci.* **2(1)**, 9-15, 2011.

Gholami-Borujeni, F., Mahvi, A. H., Nasseri, S., Faramarzi, M. A., Nabizadeh, R. and Alimohammadi, M.: Enzymatic Treatment and Detoxification of Acid Orange 7 from Textile Wastewater, *Appl. Biochem. and Biotech.*, **165(5-6),** 1274-1284, 2011.

Goldstein, J., Newbury, D. E., Joy, D. C., Lyman, C. E., Echlin, P., Lifshin, E. and Sawyer, L.: Scanning Electron Microscopy and X-ray Micronalysis, 3rd ed, XIX, **689**, Plenum Press, New York, 2003.

Gupta, S. and Babu, B. V.: Utilization of Waste Product (Tamarind Seeds) for the Removal of Cr(VI) from aqueous solutions: Equilibrium, Kinetics, and Regeneration Studies, *J. Environ. Management*, **90(10)**, 3013-3022, 2009.

Gupta, V. K., Gupta, M. and Sharma, S.: Process Development for the Removal of Lead and Chromium from Aqueous Solutions Using Red Mud, an Aluminium Industry Waste, *Water Res*., **34**, 735-742, 2001.

Gupta, V. K., Shrivastava, A. K. and Jain, N.: Biosorption of Chromium (VI) from Aqueous Solution by Green Algae Spirogyra Species, *Wat. Res*., **35**, 4079-4085, 2001.

Hajira, T., Sultan, M. and Jahanzeb, Q.: Remedial of Azo Dyes by Using Household Used Black Tea as an Adsorbent, *African J. Biotechnol.*, **8(15)**, 3584-3589, 2009.

Harler, C. R.: Tea Manufacture, Oxford University Press, New York, 108, 1972.

Ho, Y. S. and McKay, G.: Kinetics of Sorption of Divalent Metal Ions onto Sphagnum Moss Peat, *Water Res*., **34**, 735-742, 2000.

Ho, Y. S. and McKay, G.: The Sorption of Lead (II) on Peat, *Water Res.*, **33(2),** 578-584, 1999.

Hossain, M. A. and Alam, M. S.: Adsorption Kinetics of Rhodamine-B on Used Black Tea Leaves, *Iran. J. Environ. Health. Sci. Eng.*, **9**, 2-15, 2012.

Hossain, M. A. and Hassan, M. T.: Kinetic and Thermodynamic Studies of Adsorption of Crystal Violet onto Used Black Tea Leaves, **5(3),** 148-156, 2013.

Hossain, M. A. and Hassan, T. M.: Adsorption of Crystal Violet on Used Black Tea Leaves from Aquatic Solution: Equilibrium, Thermodynamic and Mechanism Studies, *Int. J. Sci,* **4(10)**, 31-139, 2015.

Hossain, M. A. and Hossain, L. M.: Kinetic Study of Malacite Green Adsorption on Used Black Tea Leaves from Aqueous Solution, *Int. J. Adv. Res*., **2(4**), 360-374, 2014.

Hossain, M. A. and Hossain, M. L.: Dynamic Modeling of the Transport Mechanism of Malachite Green to Adsorb on Used Black Tea Leaves, *Int. J. Recent Sci. Res*., **4(10**), 1575-1579, 2013.

Hossain, M. A., Hasan, Z. and Islam, T. S. A.: Kinetic Evaluation on the Adsorption of Reactive Black 5 on Used Black Tea Leaves, *Dhaka Univ. J. Sci.*, **59(2)**, 193–197, 2011.

Hossain, M. A., Kumita, M., Michigami, Y. and Mori, S.: Kinetics of Cr(VI) Adsorption on Used Black Tea Laves, *J. Chem. Eng. Jpn.*, **38(6**): 402-406, 2005.

Hossain, M. A., Mikio, K., Yoshimasa, M. and Shigeru, M.: Optimization of Parameters for Cr (VI) Adsorption on Used Black Tea Leaves, *Adsorption*, **11,** 561-568, 2005.

Hossain, M. A.: Removal of Cr(VI) from Environment by Adsorption on Used Tea Leaves- *M. Sc. Thesis*, Department of Chemistry, University of Dhaka, Bangladesh, 1997.

Hossain, M. A.: Study on Process Development for Removal of Cr(VI) from Wastewater by Sorption on Used Black Tea Leaves, *Ph. D Thesis*, Kanazawa University, Kanazawa, Japan, 2006.

Hossain, M. A.: Treatment of Wastewater Containing Toxic Heavy Metal Cr(VI) with Used Black Tea Leaves, *MS. Thesis*, Kanazawa University, Kanazawa, Japan, 2003.

Iqbal, M., Sayeed, A. and Akhtar, N.: Petiolar Feltsheath of Palm: A New Biosorbent for Removal of Heavy Metals from Contaminated Water, *Bioresour. Technol*., **81**, 153-155, 2002.

Jeyaseelan, C. and Gupta, A.: Green Tea Leaves as a Natural Adsorbent for the Removal of Cr(VI) from Aqueous Solutions, *Air, Soil and Water Res*., **9**, 13-19, 2016.

John, H. Duffus: Heavy Metals-A Meaningless Term, *Pure Appl. Chem.*, **74(5)**,793-807, 2002.

Khan, A. R.: Adsorption Studies of Tartaric Acid from Aqueous Solutions on Charcoal, *Pak. J. Sci. Ind. Res*., **37**, 40-42, 1994.

Khan, T. A., Sharma, S. and Ali, I.: Adsorption of Rhodamine B dye from Aqueous Solution onto Acid Activated Mango (Magnifera indica) Leaf Powder:

Equilibrium, Kinetic and Thermodynamic Studies, *J. Toxicol. and Environ. Health Sci.*, **3(10)**, 286-297, 2011.

Khezamia, L. K., Tahaa, K. B., Ezzeddinne, A. E., Imed G. I., Mird, L. E.: Removal of Cadmium (II) from Aqueous Solution by Zincoxide Nanoparticles: Kinetic and Thermodynamic Studies, *Desalination and Water Treatment*, **20**, 1-9, 2016.

Krishna, R. H. and Swamy, A. V. V. S.: Studies on Removal of Cr (VI) From Aqueous Solutions Using Powder of Mosambi Fruit Peelings (PMFP) As a Low Cost Sorbent, *E-J. Chem.*, **9(3),** 1389-1399, 2012.

Ksakas, A., Loqman, A., EI Bali, B., Taleb,M. and Kherbeche, A.:The Adsorption of Cr(VI) from Aqueous Solution by Natural Materials, *J. Mater. Environ. Sci*., **6(7)** 2003-2012, 2015**.**

Lagergren, S.: About the Theory of So-called Dsorption of Soluble Substances. Kungliga Svenska Vertenskapsakademiens, *Handlinger*, **24(4**),1-39, 1898.

Langmuir, I.: The Adsorption of Gases on Plane Surface of Glass, Mica and Platinum. *J. Am. Chem. Soc*., **40,** 1361-1403, 1918.

Langmuir, I.: The Constitution and Fundamental Properties of Solid and Liquids. Part I. Solids, *J. Am. Chem. Soc.*, **38(11)**, 2221–2295, 1916.

Lanids, W. G., Sofield, R. M., Ming, Y.: Hand Book on Introduction to Environmental Toxicology*:* Molecular Substructures to Ecological Landscapes, 1 – 200, 2010.

Lim, J., Hee-Man, K., Lee-Hyung, K. and Seok, K.: Removal of Heavy Metals Sawdust Adsorption: Equilibrium and Kinetic Studies, *Environ Eng. Res*., **13 (2),** 79-84, 2008.

Maximova, A. and Koumanova, B.: Equilibrium and Kinetics Study of Adsorption of Basic Dyes onto Perfit from Aqueous Solutions, *J. Univ. Chem. Technol. and Metallur.,* **43**, 101-108, 2008.

Mishra, A.: Biosorption of Chromium (VI) from aqueous solutions using waste plant biomass, *Int. J. Environ. Sci. and Technol*., **12(4)**, 1415-1426, 2015.

Mohan, D., Kunwar, P. Singh and Singh, Vinod, K.: Removal of Hexavalent Chromium from Aqueous Solution Using Low-Cost Activated Carbons Derived from Agricultural Waste Materials and Activated Carbon Fabric Cloth. *Ind Eng. Chem. Res*., *I & EC research*, **44(4),** 1027-1042, 2005.

Mohon, S. V. and Karthikeyan, J.: Removal of Lignin and Tannin Color from Aqueous Solution by Adsorption onto Activated Carbon Solution by Adsorption onto Activated Charcoal, *Environ, Pollut.*, **97**, 183-187, 1997.

Mokgalaka, N.S.,Mccrindle, R.I. and Botha, B.M.: Multi-element Analyses of Tea Leaves by Inductively Coupled Plasma Optical Emission Spectrometry Using Slurry Nebulization, *J. Anal. Atomic Spectrum*, **19(10)**, 1375-1378, 2004.

Monisha, J., Tenzin, T., Naresh, A., Blessy, B. Mathew and Krishnamurthy and N., Beeregowda: Toxicity, Mechanism and Health Effects of Some Heavy Metals, *Interdiscip Toxicol.*, **7(2)**, 60–72, 2014.

Mozumder, M. S. I., Khan, M. M. R. and Islam, M. A..: Kinetics and Mechanism of Cr(VI) Adsorption onto Tea-leaves Waste, *Asia-Pac. J. Chem. Eng*., **3(4)**, 452 – 458, 2008.

Mutongo, F., Kuipa, O., Kuipa, Pardom, K.: Removal of Cr (VI) from Aqueous Solutions Using Powder of Potato Peelings as a Low-Cost Sorbent, *Bioinorg. Chem. Appl.*, ID 973153, 1-7, 2014.

Namasivayam, C. and K. Ranganathan, K.: Removal of Cd(II) from Wastewater by Adsorption on Waste Fe(III)Cr(III) Hydroxide, *Wat. Resour*., **29**, 1737-1744, 1995.

Nandi, B. K., Goswami, A., Purkait, M. K.: Removal of Cationic Dyes from Aqueous Solutions by Kaolin: Kinetic and Equilibrium Studies, *Appl. Clay. Sci*., **42**, 583-590, 2009.

Nevine, K. A.: Removal of Reactive Dye from Aqueous Solutions by Adsorption onto Activated Carbons Prepared from Sugarcane Bagasse Pith, *Desalination*., **223**, 152–161. 2008.

Ozlen, M., Rozada, F., Calvo, L. F., Garcia, A. I. and Moran, A.; Kinetic and Equilibrium Modelling of the Methylene Blue Removal from Solution by Adsorbent Materials Produced from Sewage Sludges, *Biochem. Eng. J*., **15,** 59-68, 2003.

Papageorgiou, S. K., Kouvelos, E. P.: Calcium Alginate Beads from Laminaria Digitata for the Removal of $Cu^{+2}$ and $Cd^{+2}$ from Dilute Aqueous Metal Solutions, *Desalination*, **224,** 293–306, 2008.

Parfitt, G. D. and Rochester, C. H.: Adsorption from Solution at the Solid-liquid Interface, Academic press, London, USA, 223-331, 1983.

Park, S. and Jung, W. Y.: Removal of Chromium by Activated Carbon Fibers Plated with Copper Metal, *Carbon Sc*i., **2**, 15-21, 2001.

Park, Hyung-Jun and Tavlarides, Lawrence L.: Adsorption of Chromium (VI) from Aqueous Solutions Using an Imidazole Functinalized Adsorbent,Ind. *Eng. Chem. Res..*,**47(10)** 3401-3409, 2008.

Park, K. T., Gupta, V. K., Mohan, D. and Sharma, S.: Removal of Chromium (VI) from Eletroplating Industry Wastewater Using Bagasse Fly ash- A Sugar Industry Waste Material, *The Environmentalist*, **19,** 129-136, 1999.

Poots, V. J. P., McKay, G. and Healy, J. J.: Removal of Basic Dye from Effluent Using Wood as an Adsorbent. *J. Water Pollut. Contr. Fed*., **50**, 926-939, 1978.

Richard, F. C. and Bourg, A. C.: Aqueous Geochemistry of Chromium: A Review. *Water Res.*, **25**, 807-816, 1991.

Saeed, A., Iqbal, M. and Akhtar, M. W.: Application of Biowaste Materials for the Sorption of Heavy Metals in Contaminated Aqueous Medium, *Pakistan J. Sci. and Industrial Res*., **45(3)**, 206-211, 2002.

Saha, R., Nandi, R. and Saha, B.: Sources and Toxicity of Hexavalent Chromium, *J. Co. Chem.* **64(10),** 1782-1806, 2011.

Sarkar, K. T.: Theory Particle Leather Manufacture, United Nations, 1994.

Selvi, K., Pattabhi, S. and Kadirvelu, K.: Removal of Cr (VI) from Aqueous Solution by Adsorption onto Activated Carbon, *Bioresour. Technol.,* **80(1),** 87-89, 2001.

Singha B, Das S. K: Removal of Pb(II) ions from Aqueous Solution and Industrial Effluent Using Natural Biosorbents, *Environ Sci. Pollut. Res.,* **19**, 2212-2226., 2012.

Steven, J. D., Davies, L. J., Stanley E. K., Abbott, R. A., Ihnat, M., Bidstrup, L., Jaworski ,J. F.: Effects of Chromium in the Canadian Environment. *Nat. Res. Coun. Canada*, 168, 1976.

Sultana, A.: Equilibrium and Kinetic Evaluation of the Adsorption of Commercial Brilliant Red on Used Black Tea Leaves, *MS Thesis*, Department of Chemistry, University of Dhaka, Bangladesh, 2009.

Sultana, N.: Equilibrium and Kinetic Evaluation of the Adsorption of Commercial Brilliant Red on Used Black Tea Leaves, *MS. Thesis*, Department of Chemistry, University of Dhaka, Bangladesh, 2009.

Sun, G. and Xu X: Sunflower Stalks as Adsorbents for Color Removal from Textile Wastewater, *Indian Eng. Chem. Res*., **36**, 808-812, 1997.

Suyamboo, B. K. and Perumal, R. S.: Equilibrium, Thermodynamic and Kinetic Studies on Adsorption of a Basic Dye by Citrullus Lanatus Rind, *Iran. J. Energy & Environ.,* **3(1)**, 23-34, 2012.

Tajmeri, S. A. Islam, Begum, H. A., Hossain, M. A. and Rahman, M. T.: Removal of Pb (II) From Aqueous Solution by Adsorption and Used Tea Leaves, *J. Bangla Acad.* Sc., **33(2),** 167-178, 2009.

Tarley, T., Ricardo C., Arruda, Z. and Macro, A.: Biosorption of Heavy Metals Using Rich Milling By-products. Characterisation and Application for Removal of Metals from Aqueous Solutions, *Chemospher,* **54**, 905-915, 2004.

Tejada-Tover, C., Villabona-Ortiz, A., Herrera-Barros, Gonzalez-Delgado, A. D. and Garces, L.:Aadsorption Kinetics of Cr (VI) Using Modified Residual Biomass in Batch and Continuous System, **11(14),** 2018.

Temkin, M. I. and Pyzhev, V.: Kinetic of Ammonia Synthesis on Promoted Iron Catalyst, *Acta. Phy. Chem*, **12**, 327-356, 1940.

Theivarasu, C. and Mylsamy, S.: Equilibrium and Kinetic Adsorption Studies of Rhodamine-B from Aqueous Solutions Using Cocoa (Theobroma Cacao) Shell as a New Adsorbent, *J. Eng. Sci. and Tech.,* **2(11),** 6284-6292, 2010.

Timbo, C. C., Kandawa-Schulz, M., Amuanyena, M., Kwaambwa, H. M.: Adsorptive Removal from Aqueous Solution of Cr(VI) by Green Moringa Tea Leaves Biomass, *J. Encapsulation and Adsorption Sci.*, 7, 108-119, 2017.

Towill, L. E., Shriner, C. R., Drury, J. S., Hammoons, A. S., and Holleman, J. W.: Reviews of the Environmental Effects of Pollutants: III Chromium. *U.S. Environ. Protection Agency Rep.*, **600**/1-78-023, 287, 1978.

Tsibranska, I. and Hristova, E.: Comparison of Different Kinetic Models for Adsorption of Heavy Metals onto Activated Carbon from Apricot Stones, Bulgarian Chem. Comm., **43( 3)**, 370-377, 2011.

Uosaki, K., and Kokai, J.: Scavengers of Heavy Metal Ions Mainly Cr(VI) and Cr(III), **75(16)**, 357-359, 1975.

Vasu, A. E.: Studies on the Removal of Rhodamine B and Malachite Green from Aqueous Solutions by Activated Carbon, *E-J. Chemistry*, **5(4)**, 844-852, 2008.

Vijayakumaran, V and Arivoli, S., Equilibrium and Kinetic Modeling on the Removal of Malachite Green from Aqueous Solution Using Odina Wodier Bark Carbon, *J. Mater. Environ. Sci*., **33,** 525-536, 2012.

Voudrias1, E., Fytianos, K, Bozani, E. and Bozani, E.: Sorption Description Isotherm of Dyes from Aqueous Solution and Waste Water with Different Sorbent Materials, *The Int, J. Global Nest*., **4(1),** 75-83, 2002.

Weber, W. J., Morris, J. C.: Kinetics of Adsorption on Carbon from Solution, *J. Sanit. Eng. Div. Am. Soc. Civ. Eng.*, **89(1)**, 31-60, 1963.

Xiu-Yan, P. and Gong, F.: Study on the Adsorption Kinetics of Acid Red 3B on Expanded Gaphite, *E-J. Chem.*, **5,** 802-809, 2008.

Xiu-Yan, P. and Gong, F.; Study on the Adsorption Kinetics of Acid red 3B on Expanded Graphite, *E-J. Chem.*, **5**, 802-809, 2008.

Yeddou, N., Bensmaili, A.: Kinetic Models for the Sorption of Dye from Aqueous Solution by Clay-wood Saw Dust Mixture, *Dessalination*, **185**, 499-508, 2005.

Yu, Q., Matheikal, J. T., Kaewsarn, P.: Heavy Metal Uptake Capacities of Common Marine Macro Algal Biomass, *Wat. Res.*, **33**, 1534-1537, 1999.

Yu, Y., Zhuang, Y. Y. and Wang, Z. H.: Adsorption of Water-soluble Dye onto Functionalized Resin, *J. Colloid Interf. Sci*., **242**, 288-293, 2001.

Zhan , X., Miazanki, A. and Nakano, Y.: Mechanisms of Lead Removal from Aqueous Solutions Using a Novel Tannin Gel Adsorbent Synthesized from Natural Condensed Tannin, *J. Chem. Eng. Jpn*, **34(10)**, 1204-1210, 2001.

Zhang, W., Li XM, Wang, F., Yang, Q., Deng, P. and Zeng, G. M.: Adsorption Removal of Cadmium and Copper from Aqueous Solution by Areca -*A food Waste*, *J. Hazard. Mater.*, **157(2-3)**, 490-495, 2008.

Zheng, G., Xijin, X., Bin, L., Kusheng, W., Taofeek, A. Y., and Xia, H.: Association Between Lung Function in School Children and Exposure to Three Transition Metals from an e-waste Recycling Area, *J. Expo. Sci. and Environ. Epid.*, **23**, 67–72, 2013.

Zhonghua, Y., Fang, Y. and Zhi, X. Z.: Chromium Pollution of Soil and Water in Jinzhou, *J. Chinese Preventive Medicine.*, **21(5)**, 262-264,1987.